



GEOSCIENCE BC SUMMARY OF ACTIVITIES 2012





GEOSCIENCE BC SUMMARY OF ACTIVITIES 2012



© 2013 by Geoscience BC.

All rights reserved. Electronic edition published 2013.

This publication is also available, free of charge, as colour digital files in Adobe Acrobat® PDF format from the Geoscience BC website: <http://www.geosciencebc.com/s/DataReleases.asp>.

Every reasonable effort is made to ensure the accuracy of the information contained in this report, but Geoscience BC does not assume any liability for errors that may occur. Source references are included in the report and the user should verify critical information.

When using information from this publication in other publications or presentations, due acknowledgment should be given to Geoscience BC. The recommended reference is included on the title page of each paper. The complete volume should be referenced as follows:

Geoscience BC (2013): Geoscience BC Summary of Activities 2012; Geoscience BC, Report 2013-1, 148 p.

ISSN 1916-2960 Summary of Activities (Geoscience BC)

Cover photo: Blackdome mine road, Chilcotin Plateau, British Columbia

Photo credit: Esther Bordet, Mineral Deposit Research Unit, University of British Columbia, 2012

Foreword

Geoscience BC is pleased to present results from many of our ongoing geoscience projects and surveys in this, our sixth edition of the *Geoscience BC Summary of Activities*. The volume is divided into two sections, 'Minerals' and 'Oil and Gas', and contains a total of 15 papers.

The first section contains 12 papers from Geoscience BC minerals projects throughout the province. The first three papers provide updates on Geoscience BC's most recent major projects: QUEST-Northwest and the Northern Vancouver Island Exploration Geoscience projects. Simpson et al. provide details on the new airborne magnetic surveys flown in both project areas during the summer and fall of 2012. Jackaman and Lett describe regional geochemical work undertaken as part of the Northern Vancouver Island Exploration Geoscience Project (as well as geochemical reanalysis work done in central and southeastern BC). Finally, Logan and Iverson summarize geochemical characteristics of volcanic rocks in the QUEST-Northwest Project area.

The rest of the papers in the 'Minerals' section present interim results from smaller Geoscience BC partnership projects across the province. Lewis et al. highlights work undertaken to re-release the Mineral Deposit Research Unit's Iskut River area maps in a modern GIS format. Celis et al. describe new work on porphyry indicator minerals from alkalic porphyry Cu-Au deposits, which builds on a Mineral Deposit Research Unit-Geoscience BC project on porphyry indicator minerals initiated in 2009.

Three papers in the volume describe field activities undertaken in the Woodjam property area. Heberlein et al. discuss a new study aimed at using organic media (e.g., plant vegetation and exudates) in the geochemical detection of blind porphyry deposits. A companion study (Bissig et al.) discusses whether a geochemical signal of mineralization under basalt cover can be detected in a near-surface environment using soil and plant samples. Both these projects are using the Woodjam area as a test site. del Real et al. discuss the paragenesis and alteration at two of the discrete porphyry deposits on the Woodjam property.

Three papers in the 'Minerals' section discuss projects in southeastern BC. Höy discusses new mapping and compilation work in the Burrell Creek map area, an extension of a previous Geoscience BC-sponsored mapping project in the Deer Park map area (completed in 2010). Webster and Pattison describe ongoing work on the metamorphism and structure of the southern Kootenay Arc and Purcell Anticlinorium, and Hartlaub describes the 2012 activities of the SEEK (Stimulating Exploration in the East Kootenays) Project.

Finally, Reichheld outlines his planned methodologies for a study aimed at documenting and assessing exploration activities generated by the Geoscience BC QUEST Project.

The second section discusses some of Geoscience BC's oil and gas projects, all of which are focused on northeastern BC. Salas et al. discuss the creation of a seismographic network in northeastern BC to monitor the effects of induced seismicity from unconventional gas completions. Surface-water studies are the focus of the last two papers, with Salas and Murray discussing a three-year water-monitoring program in the Horn River Basin, and Saha et al. discussing their work in the Kiskatinaw River watershed near Dawson Creek.

Readers are encouraged to visit our website for additional information on all Geoscience BC-funded projects, including project descriptions, posters and presentations, previous *Summary of Activities* or *Geological Fieldwork* papers, and final datasets and reports. The website also contains information on many of Geoscience BC's other activities, including workshops and student scholarships. All papers in this and past volumes are available for download through Geoscience BC's website (www.geosciencebc.com). Limited print copies of past volumes are also available from the Geoscience BC office.

Geoscience BC Publications 2012

In addition to this *Summary of Activities* volume, Geoscience BC releases interim and final products from our projects as Geoscience BC Reports. All Geoscience BC data and reports can be accessed through our website at www.geosciencebc.com/s/DataReleases.asp. Geoscience BC datasets and reports released in 2012 include the following:

- 16 technical papers in the *Geoscience BC Summary of Activities 2011* volume
- **QUEST-Northwest Block 1 Airborne Magnetic Survey, British Columbia**, by Aeroquest Airborne (Geoscience BC Report 2012-02)

- **QUEST-Northwest Block 2 Airborne Magnetic Survey, British Columbia**, by Geo Data Solutions (Geoscience BC Report 2012-03)
- **Results from a Pilot Airborne Electromagnetic Survey, Horn River Basin, British Columbia**, by SkyTEM Canada Inc. (Geoscience BC Report 2012-04)
- **QUEST-Northwest Sample Reanalysis (ICP-MS)**, by W. Jackaman (Geoscience BC Report 2012-05)
- **QUEST-Northwest Sample Reanalysis (INAA)**, by W. Jackaman (Geoscience BC Report 2012-06)
- **QUEST-Northwest Regional Geochemical Data, Northwest British Columbia**, by W. Jackaman (Geoscience BC Report 2012-07)
- **Dease Lake – Little Tuya River Geology, NTS 104J/08 & 07E**, by J.M. Logan, D.P. Moynihan, L.J. Diakow and B.I. van Straaten (Geoscience BC Map 2012-08-1 / BC Ministry of Energy, Mines and Natural Gas, BC Geological Survey Open File 2012-04)
- **Horn River Basin Aquifer Characterization Project Phase 2: Geological Report**, by Petrel Robertson Consulting Ltd. (Geoscience BC Report 2012-09)
- **Mesozoic Magmatism and Metallogeny of the Hotailuh Batholith, Northwestern British Columbia**, by B.I. van Straaten, J.M. Logan and L.J. Diakow (Geoscience BC Report 2012-10 / BC Ministry of Energy, Mines and Natural Gas, BC Geological Survey Open File 2012-06)
- **Till Geochemistry and Clast Lithology Studies of the Bulkley River Valley, West-Central British Columbia**, by A.J. Stumpf (Geoscience BC Report 2012-11)
- **Stimulating Exploration in the East Kootenays (SEEK Project): East Kootenay Gravity Database**, by T. Sanders (Geoscience BC Report 2012-12)
- **Subsurface Structure of the Eastern Nechako Basin from Coincident Three-dimensional Tomographic Velocity and Reflection Data**, by D.A. Talinga and A.J. Calvert (Geoscience BC Report 2012-13)
- **Modelling and Investigation of Airborne Electromagnetic Data, and Reprocessing of Vibroseis Data, from Nechako Basin, B.C., Guided by Magnetotelluric Results**, by J. Spratt, J.K. Welford, C. Farquharson and J. Craven (Geoscience BC Report 2012-14)

All releases of Geoscience BC reports and data are announced through our website and e-mail list. If you are interested in receiving e-mail regarding these reports and other Geoscience BC news, please contact info@geosciencebc.com.

Acknowledgments

Geoscience BC would like to thank all authors of the *Summary of Activities* papers, including project proponents, graduate students, consultants and staff, for their contributions to this volume. RnD Technical is also thanked for their work in editing and assembling this volume.

Christa Sluggett, M.Sc.
Project Geologist and Communications Co-ordinator
Geoscience BC
www.geosciencebc.com

Contents

Minerals Projects

- Simpson, K.A., Kowalczyk, P.L. and Kirkham, G.D.:** Update on Geoscience BC's 2012 geophysical programs 1
- Jackaman, W. and Lett, R.E.W.:** Updating the British Columbia Regional Geochemical Survey database with new field survey and sample reanalysis data to support mineral exploration 5
- Logan, J.M. and Iverson, O.:** Dease Lake Geoscience Project: geochemical characteristics of Tsaybahe, Stuhini and Hazelton volcanic rocks, northwestern British Columbia. 11
- Lewis, P.D., Hart, C.J.R. and Simpson, K.A.:** Re-release of the Mineral Deposit Research Unit's Iskut River area maps (1989–1993), northwestern British Columbia ... 33
- Celis, M.A., Hart, C.J.R., Bouzari, F., Bissig, T. and Ferbey, T.:** Porphyry indicator minerals (PIMs) from alkalic porphyry copper-gold deposits in south-central British Columbia 37
- Heberlein, D.R., Dunn, C.E. and Macfarlane, W.:** Use of organic media in the geochemical detection of blind porphyry copper-gold mineralization in the Woodjam property area, south-central British Columbia 47
- Bissig, T., Heberlein, D.R. and Dunn, C.E.:** Geochemical techniques for detection of blind porphyry copper-gold mineralization under basalt cover, Woodjam prospect, south-central British Columbia 63
- del Real, I., Hart, C.J.R., Bouzari, F., Blackwell, J.L., Rainbow, A., Sherlock, R. and Skinner, T.:** Paragenesis and alteration of the Southeast Zone and Deerhorn porphyry deposits, Woodjam property, central British Columbia. 79
- Höy, T.:** Burrell Creek map area: setting of the Franklin mining camp, southeastern British Columbia 91
- Webster, E.R. and Pattison, D.R.M.:** Metamorphism and structure of the southern Kootenay Arc and Purcell Anticlinorium, southeastern British Columbia 103
- Hartlaub, R.P.:** The SEEK Project: Stimulating Exploration in the East Kootenays, southeastern British Columbia .. 119
- Reichheld, S.A.:** Documentation and assessment of exploration activities generated by Geoscience BC data publications 125

Oil and Gas Projects

- Salas, C.J., Walker, D. and Kao, H.:** Creating a regional seismographic network in northeastern British Columbia to study the effect of induced seismicity from unconventional gas completions 131
- Salas, C.J. and Murray, D.:** Developing a water monitoring network in the Horn River Basin, northeastern British Columbia. 135
- Saha, G.C., Paul, S.S., Li, J., Hirshfield, F. and Sui, J.:** Investigation of land-use change and groundwater–surface water interaction in the Kiskatinaw River watershed, northeastern British Columbia. 139

Update on Geoscience BC's 2012 Geophysical Programs

K.A. Simpson, Geoscience BC, Vancouver, BC, simpson@geosciencebc.com

P.L. Kowalczyk, PK Geophysics Inc., Vancouver, BC

G.D. Kirkham, Kirkham Geosystems Ltd., Burnaby, BC

Simpson, K.A., Kowalczyk, P.L. and Kirkham, G.D. (2013): Update on Geoscience BC's 2012 geophysical programs; *in* Geoscience BC Summary of Activities 2012, Geoscience BC, Report 2013-1, p. 1–4.

Introduction

Geoscience BC continued to fly new geophysical surveys in 2012 with the acquisition of aeromagnetic data at a line spacing of 250 m in northwestern British Columbia and on northern Vancouver Island. These new, regional, tightly spaced and high-quality aeromagnetic datasets are a game-changer for exploration in BC. The quality of these new datasets allows them to be used for district-scale to property-scale targeting and mapping. In addition to the acquisition of new data, Geoscience BC is implementing a new program to purchase proprietary industry geophysical data that will then be released to the public.

QUEST-Northwest

Geoscience BC launched the QUEST-Northwest Project in April 2011. The QUEST-Northwest Project aims to compile and update existing datasets, as well as provide new geoscience data, to help focus exploration in this highly prospective region of the province. The main activities include bedrock geological mapping, a regional ground geochemical program and a compilation of existing high-quality industry aeromagnetic data (Simpson, 2012; Jackaman, 2012).

The QUEST-Northwest geophysical program has flown three aeromagnetic surveys. Two of these surveys were flown in 2011 (Block 1 and Block 2; Figure 1) and the most recent survey (part of Block 3) was flown in the summer of 2012 (Figure 1). All surveys were flown at 250 m line spacing, in an east-west orientation with 2500 m spaced tie lines. They were flown using a controlled drape over the terrain with a nominal ground clearance of 80 m. The terrain is rugged and varied, ranging in elevation from 400 m to more than 2000 m. The details of the 2011 surveys were published in Simpson (2012) and the data were released at

Mineral Exploration Roundup 2012. The 2012 survey (part of Block 3) was flown by Geo Data Solutions (Laval, Quebec) in July and August 2012. The survey was flown using the same specifications and the same HeliMAG stinger system used to survey Block 2 (Simpson, 2012). The survey area comprised approximately 1198 km². The planned release date is late 2012.

During the survey planning stage of Block 3, Geoscience BC learned that a portion of the planned survey had recently been flown (in late 2011 and early 2012) by a private mineral exploration company. Rather than re-fly the area, Geoscience BC agreed to purchase the data at a reduced rate from the company. The company survey was flown at 100 m line spacing in a northeast-southwest orientation and has been fully integrated into the new Geoscience BC dataset. The combined surveys are being released as one seamless dataset. The total area of the new combined dataset for Block 3 being released by Geoscience BC is 1398 km².

Historical coverage in the QUEST-Northwest area is fairly typical, district-scale, fixed-wing aeromagnetics with approximately 1.6 km line spacing. The new 250 m line-spaced, low-level helicopter-borne aeromagnetic survey provides a step-change in the quality of data and is a game-changer for exploration companies working in this highly prospective region of the province (Figure 2). These new datasets should stand the test of time and provide the exploration geologist with the opportunity for district-scale to property-scale targeting and mapping.

Northern Vancouver Island

The Northern Vancouver Island (NVI) Exploration Geoscience Project is a partnership between Geoscience BC and the Island Coastal Economic Trust (ICET). In addition, the Ministry of Jobs, Tourism and Skills Training has provided generous support for stakeholder engagement in the project-development phase, through the Campbell River Regional Economic Pilot initiative.

The NVI Exploration Geoscience Project will generate new geoscience data for northern Vancouver Island, near the communities of Campbell River, Port Hardy, Port McNeill, Alert Bay, Port Alice and Zeballos (Figure 3).

Keywords: *airborne magnetics, aeromagnetic data, Quesnel Terrane, Stikine Terrane, QUEST-Northwest Project, Northern Vancouver Island Exploration Geoscience Project*

This publication is also available, free of charge, as colour digital files in Adobe Acrobat® PDF format from the Geoscience BC website: <http://www.geosciencebc.com/s/DataReleases.asp>.

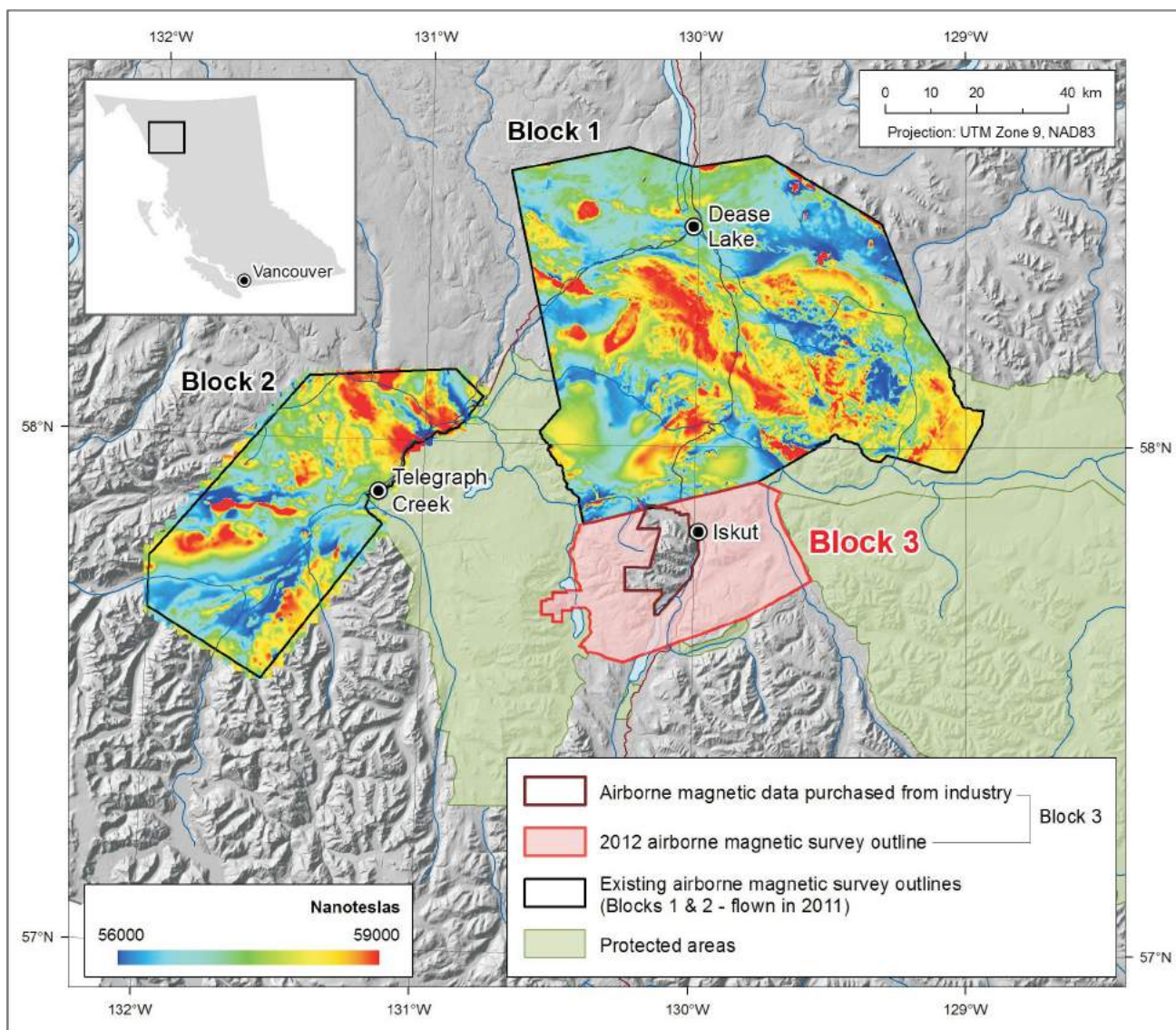


Figure 1. Geoscience BC's QUEST-Northwest Project area showing the three geophysical survey outlines flown in 2011 and 2012, as well as the data purchased from industry. Data from GeoBase® (2004), Natural Resources Canada (2007) and DataBC (2008).

This new regional information will help attract mineral exploration interest and investment, increase the understanding of the mineral potential, and provide local First Nations and communities with more information on the geology of the region.

The project activities include an aeromagnetic survey and a stream-sediment geochemical sampling and reanalysis program. Both of these programs were undertaken in the summer and fall of 2012 (Figure 3). In addition, the project to date has supported two community awareness sessions on geoscience, mineral exploration and mining. Details of the geochemical program are outlined in Jackaman and Lett (2013).

The geophysical survey was flown by Geo Data Solutions (Laval, Quebec), using the HeliMAG stinger system, at 250 m line spacing in a northeast-southwest orientation with 2500 m spaced tie lines. It was flown using a controlled drape over the terrain with a nominal ground clearance of 80 m. The survey area comprised approximately 4204 km² (Figure 3). Release of the geophysical data from the survey is planned for Mineral Exploration Roundup 2013.

Purchasing Proprietary Industry Geophysical Data

Geoscience BC is implementing a new program to purchase proprietary industry geophysical data, modelled after the successful Ontario Geological Survey (OGS) Request

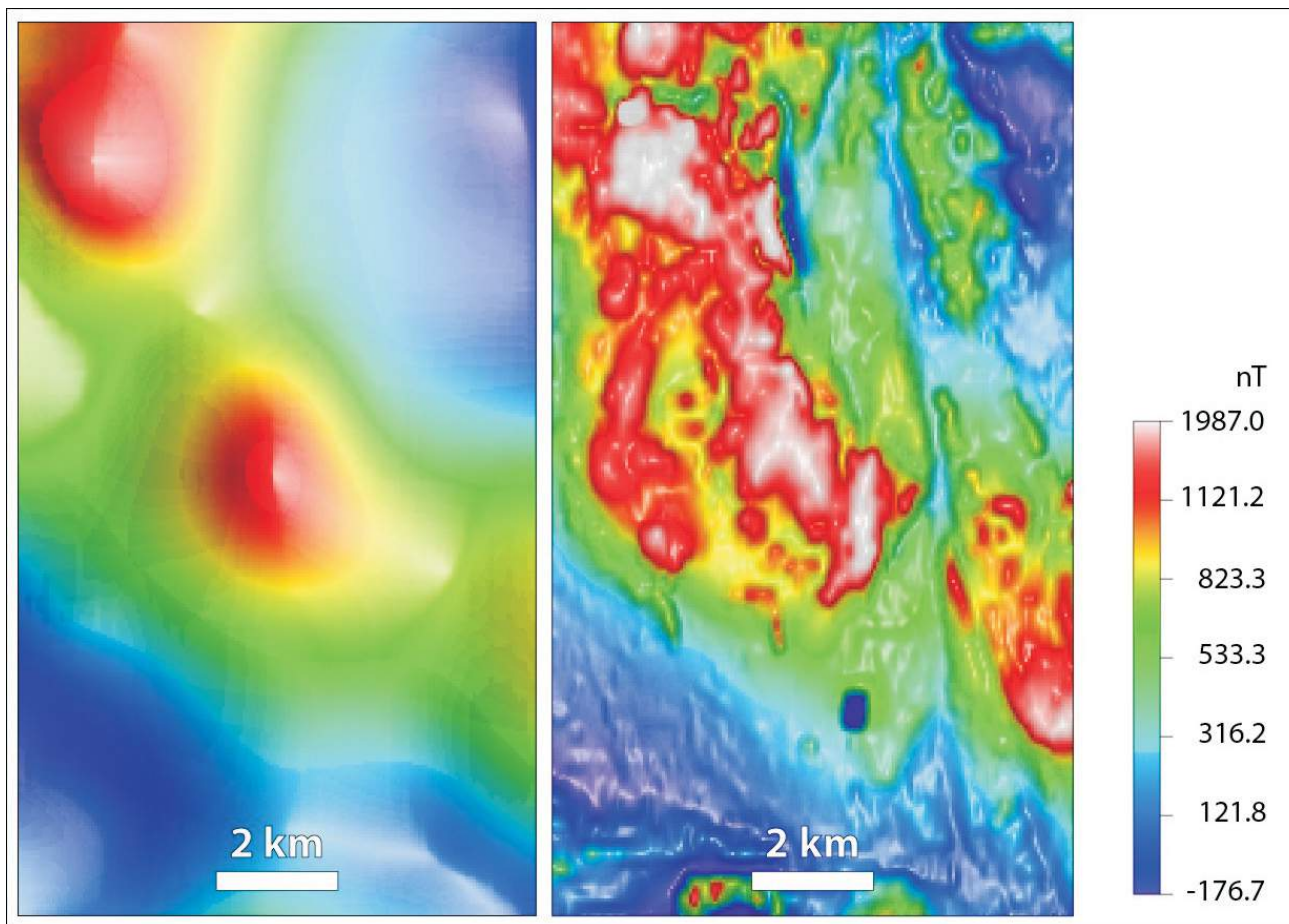


Figure 2. Example of the step-change in quality in the new aeromagnetic data from QUEST-Northwest. The image on the left shows the historical Geological Survey of Canada data and the image on the right shows the new Geoscience BC data for the same area. Data from Natural Resources Canada (2012). Abbreviation: nT, nanoteslas.

for Data for Purchase of Proprietary Airborne Geophysical Data. The OGS model uses a formula to evaluate industry data and determine a purchase price, which ensures a consistent, reproducible and fair process for determining price. Geoscience BC will initially focus on aeromagnetic data within selected areas of BC that complement Geoscience BC projects. Through this program, Geoscience BC hopes to encourage companies to see the value in sharing information while increasing the publically available high-resolution aeromagnetic coverage of the province.

Summary

Geoscience BC continues to prioritize high-quality, tightly spaced aeromagnetics as one of the key datasets for successful exploration in BC. Two new surveys were flown in 2012 in the QUEST-Northwest Project and Northern Vancouver Island Exploration Geoscience Project areas. Geoscience BC is also initiating a program to purchase proprietary industry aeromagnetic data in selected parts of the Province. All Geoscience BC data are released free to the public through the Geoscience BC website (<http://www.geosciencebc.com/s/DataReleases.asp>).

Acknowledgments

The digital-elevation model used in Figures 1 and 3 was prepared by K. Shimamura, and F. Ma created the final figures. F. Ma is also thanked for finalizing Figure 2 for the manuscript. The manuscript benefited from a review by C. Sluggett.

References

- DataBC (2008): TANTALIS—parks, ecological reserves and protected areas; BC Ministry of Forests, Lands and Natural Resource Operations, URL <<https://apps.gov.bc.ca/pub/geometadata/metadataDetail.do?recordUID=54259&recordSet=ISO19115>> [November 2012].
- GeoBase® (2004): Canadian digital elevation data; Natural Resources Canada, GeoBase®, URL <<http://www.geobase.ca/geobase/en/data/cded/description.html>> [November 2012].
- Jackaman, W. (2012): QUEST-Northwest Project: new regional geochemical survey and sample reanalysis data (NTS 104F, G, H, I, J, K), northern British Columbia; *in* Geoscience BC Summary of Activities 2011, Geoscience BC, Report 2012-1, p. 15–18, URL <http://www.geosciencebc.com/i/pdf/SummaryofActivities2011/SoA2011_Jackaman.pdf> [November 15, 2012].

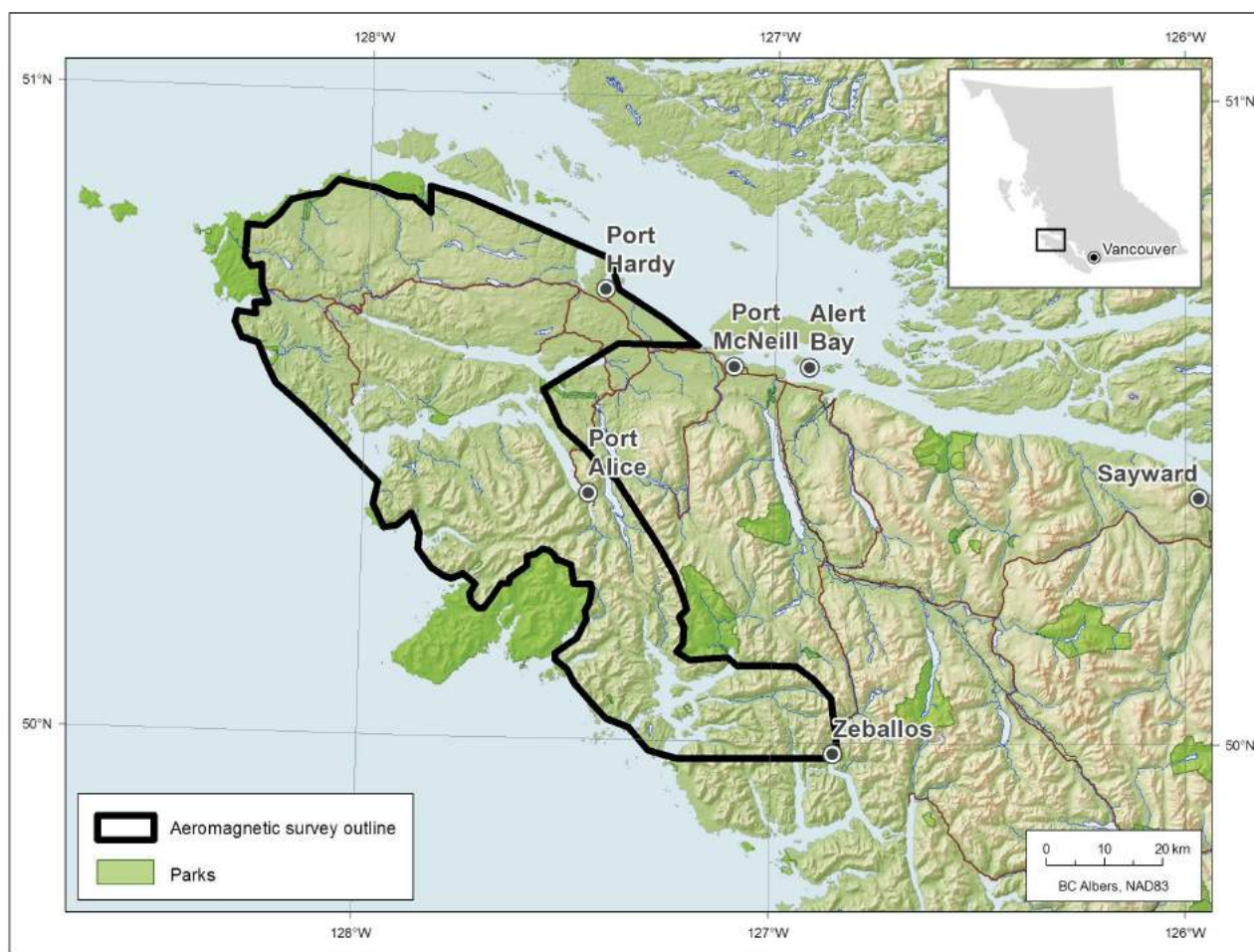


Figure 3. Geoscience BC's Northern Vancouver Island Exploration Geoscience Project area, showing the location of the geophysical survey. Data from GeoBase® (2004), Massey et al. (2005), Natural Resources Canada (2007) and DataBC (2008).

Jackaman, W. and Lett, R.E. (2013): Updating the British Columbia Regional Geochemical database with new field survey and sample reanalysis data to support mineral exploration; *in* Geoscience BC Summary of Activities 2012, Geoscience BC, Report 2013-1, p. 5–10.

Massey, N.W.D., MacIntyre, D.G., Desjardins, P.J. and Cooney, R.T. (2005): Digital geology map of British Columbia: whole province; BC Ministry of Energy, Mines and Natural Gas, GeoFile 2005-1, URL <<http://www.empr.gov.bc.ca/Mining/Geoscience/PublicationsCatalogue/GeoFiles/Pages/2005-1.aspx>> [November 2012].

Natural Resources Canada (2007): Atlas of Canada base maps; Natural Resources Canada, Earth Sciences Sector, URL <[http://geogratis.gc.ca/geogratis/en/option/select.do?id=](http://geogratis.gc.ca/geogratis/en/option/select.do?id=0BCF289A-0131-247B-FDBD-4CC70989CBCB)

[0BCF289A-0131-247B-FDBD-4CC70989CBCB](http://geogratis.gc.ca/geogratis/en/option/select.do?id=0BCF289A-0131-247B-FDBD-4CC70989CBCB)> [November 2012].

Natural Resources Canada (2012): Canadian Aeromagnetic Data Base; Natural Resources Canada, Earth Sciences Sector, URL <http://gdr.nrcan.gc.ca/aeromag/index_e.php> [November 2012].

Simpson, K.A. (2012): QUEST-Northwest: Geoscience BC's new minerals project in northwestern British Columbia (NTS 104G, J, parts of NTS 104A, B, F, H, I, K, 103O, P); *in* Geoscience BC Summary of Activities 2011, Geoscience BC, Report 2012-1, p. 1–4, URL <http://www.geosciencebc.com/i/pdf/SummaryofActivities2011/SoA2011_Simpson.pdf> [November 15, 2012].

Updating the British Columbia Regional Geochemical Survey Database with New Field Survey and Sample Reanalysis Data to Support Mineral Exploration (NTS 082F, K, 092K, L, 093J, 102I)

W. Jackaman, Noble Exploration Services Ltd., Sooke, BC, wjackaman@shaw.ca

R.E.W. Lett, Consultant, Victoria, BC

Jackaman, W. and Lett, R.E.W. (2013): Updating the British Columbia Regional Geochemical Survey database with new field survey and sample reanalysis data to support mineral exploration (NTS 082F, K, 092K, L, 093J, 102I); *in* Geoscience BC Summary of Activities 2012, Geoscience BC, Report 2013-1, p. 5–10.

Introduction

Results compiled from government-funded regional geochemical surveys are routinely used by the mining sector to focus and support mineral exploration projects throughout British Columbia. Introduced in 1976, efforts to develop and maintain survey results as a consistent and functional multi-element geochemical database have been ongoing. Currently, the BC Regional Geochemical Survey database has analytical results and site information for more than 63 000 sediment and water samples and sample locations that cover approximately 80% of BC at an average density of one site every 12 km².

For several years, Geoscience BC has advanced the utility of the provincial Regional Geochemical Survey database by supporting new field surveys and the reanalysis of sample material saved from previously completed programs. Since 2005, a total of 12 000 new drainage samples have been collected and more than 35 000 pulps from previous government programs, including the BC Geological Survey's Regional Geochemical Survey (RGS) and the Geological Survey of Canada's (GSC) National Geochemical Reconnaissance (NGR) programs have been analyzed using up-to-date laboratory techniques. In 2012, Geoscience BC supported the following upgrades to the BC RGS database (Figure 1):

- reanalysis of approximately 1150 stream sediment samples originally collected in 1985 from sites located in the McLeod Lake (NTS 093J) map area (W. Jackaman, unpublished data, 2012). The samples have been analyzed for 35 elements by instrumental neutron activation analysis (INAA);
- reanalysis of approximately 2690 stream sediment samples originally collected in 1977 from sites in the Nelson

(NTS 082F) and Lardeau (NTS 082K) map areas (W. Jackaman, unpublished data, 2012). The samples have been analyzed for 51 elements by aqua-regia digestion followed by inductively coupled plasma–mass spectrometry (ICP-MS); and

- new sample collection and till sample reanalysis covering parts of the Alert Bay (NTS 092L), Bute Inlet (NTS 092K) and Cape Scott (NTS 102I) map areas as part of the Northern Vancouver Island Exploration Geoscience Project (W. Jackaman, unpublished data, 2012).

Geoscience BC 2012 Projects

McLeod Lake Sample Reanalysis by INAA

Bedrock in the McLeod Lake map area has the potential to host different types of economically important mineral deposits. These include Cu-Au-porphyry-style mineralization in Triassic deposits, calcalkaline volcanic and sedimentary rocks similar to the Mount Milligan Cu-Au deposit northwest of the map area and Pb-Zn sulphide mineralization in Paleozoic sedimentary rocks in the eastern part of the map area. However, successful exploration for new deposits is challenged by the thick, extensive glacial sediments that cover much of the bedrock. Stream sediment, lake sediment, heavy mineral concentrate and glacial sediment sampling have all been used to detect the existence of new sulphide mineralization. The first regional geochemical survey of the McLeod Lake map area carried out in 1986 was jointly managed by the then BC Ministry of Energy, Mines and Petroleum Resources and the GSC. At that time, a total of 1152 stream samples were collected and the sediment material was analyzed for 18 metals (Ag, As, Ba, Cd, Co, Cu, Fe, Hg, Mn, Mo, Ni, Pb, Sb, Sn, U, V, W and Zn). In 2006, the sediment samples were recovered from storage and a 0.5 g portion of each pulp was analyzed by an aqua-regia digestion followed by ICP-MS for 37 elements (Lett and Bluemel, 2006). Unfortunately, the samples were not included in recent INAA reanalysis initiatives and remained the only area surveyed prior to 1989 that did not include this important analytical information. To close this

Keywords: *Vancouver Island, Nelson, Lardeau, McLeod Lake, mineral exploration, geochemistry, Regional Geochemical Survey, RGS, multi-element, reanalysis, stream sediment, moss mat*

This publication is also available, free of charge, as colour digital files in Adobe Acrobat® PDF format from the Geoscience BC website: <http://www.geosciencebc.com/s/DataReleases.asp>.

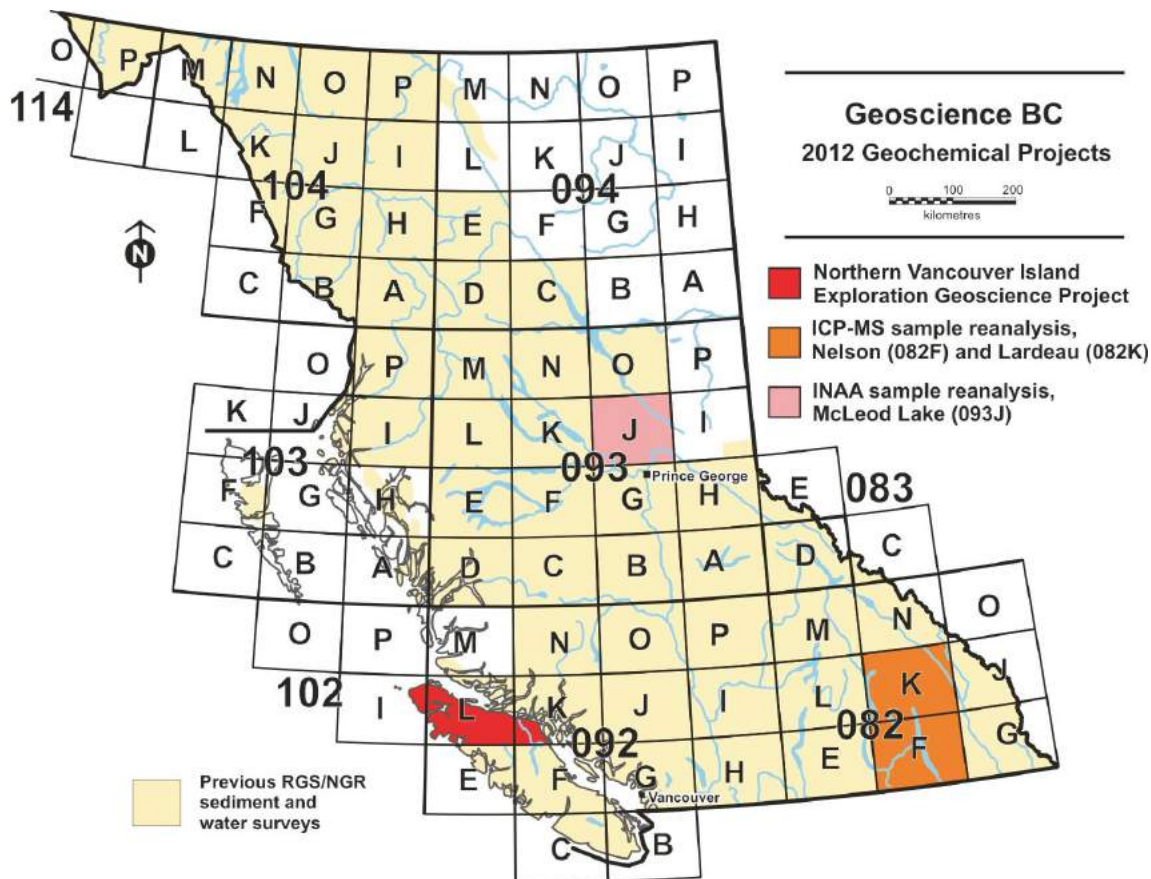


Figure 1. Location of the Geoscience BC 2012 sample reanalysis programs and the Northern Vancouver Island Exploration Geoscience Project in British Columbia. Abbreviations: ICP-MS, inductively coupled plasma–mass spectrometry; INAA, instrumental neutron activation analysis; NGR, National Geochemical Reconnaissance; RGS, Regional Geochemical Survey.

gap in the database, the samples and quality-control materials are being analyzed by INAA for 35 elements. These INAA results will significantly upgrade the Au values because of the larger sample analyzed and will report a range of other valuable metals such as pathfinder and rare earth elements. Near-total INAA element data will further refine the neural network approach to mapping bedrock geology developed by Barnett and Williams (2009) using the McLeod Lake stream sediment geochemical data. The INAA data will also offer greater survey continuity with previous geochemical survey work completed in adjacent map areas and will complement various Geoscience BC-supported and other exploration research conducted in the region, including lake sediment and till geochemical surveys (Jackaman, 2008a; Ward et al., 2012). The new INAA data is scheduled to be publicly released in early 2013.

Nelson and Lardeau Sample Reanalysis by ICP-MS

The Nelson and Lardeau geochemical surveys were conducted 35 years ago as part of the original NGR program.

During the 1977 surveys, a total of 2691 stream sediment samples were collected and analyzed for Ag, Co, Cu, Fe, Hg, Mn, Mo, Ni, Pb, V, W and Zn by an aqua-regia digestion followed by atomic absorption spectrometry (AAS) and for U by neutron activation and delayed neutron counting. Subsequent analyses of the archived pulps by INAA in the early 1990s provided additional analytical information to the geochemical database (Jackaman et al., 1991). As host to a number of important mining camps and exploration areas (Figure 2), the region has been identified as an important candidate for further upgrades to the related geochemical information by recovering and analyzing sediment pulps saved from the original survey work. These samples, with quality-control materials, have now been analyzed by an ultratrace aqua-regia digestion (0.5 g) ICP-MS package for 53 elements. This work is a continuation of a series of large-scale reanalysis initiatives that have been sponsored by Geoscience BC since 2007 and are recognized as a cost-effective means of updating older NGR and RGS information with a range of new analytical information at significantly improved detection levels (Jackaman, 2008b, c, 2009, 2010, 2011a). The new ICP-MS data is scheduled to be released in early 2013.

Northern Vancouver Island Exploration Geoscience Project

Regional Geochemical Survey and Till Reanalysis

The Northern Vancouver Island Exploration Geoscience Project includes new stream-based sampling and the reanalysis of approximately 480 till samples (Figure 3) collected during surveys conducted in the early to mid-1990s (Bobrowsky and Sibbick, 1996). The work will generate new geochemical information that will help stimulate mineral exploration in the region and complement other components of the initiative such as a high-resolution airborne geophysical survey and community workshops (Simpson,

2013) as well as earlier geochemical survey work and geological mapping.

The BC Ministry of Energy, Mines and Natural Gas (BCMEMNG) originally conducted stream-based RGS on northern Vancouver Island and the adjacent mainland in 1988 (Gravel and Matysek, 1989). The northern Vancouver Island portion of these surveys included the collection of moss-mat sediment and water samples. Moss-mat sediment has been collected in areas such as Vancouver Island where conventional stream sediment is scarce because of high-energy water flow. Living mosses found in the stream channel below the high water level have been found to capture sus-

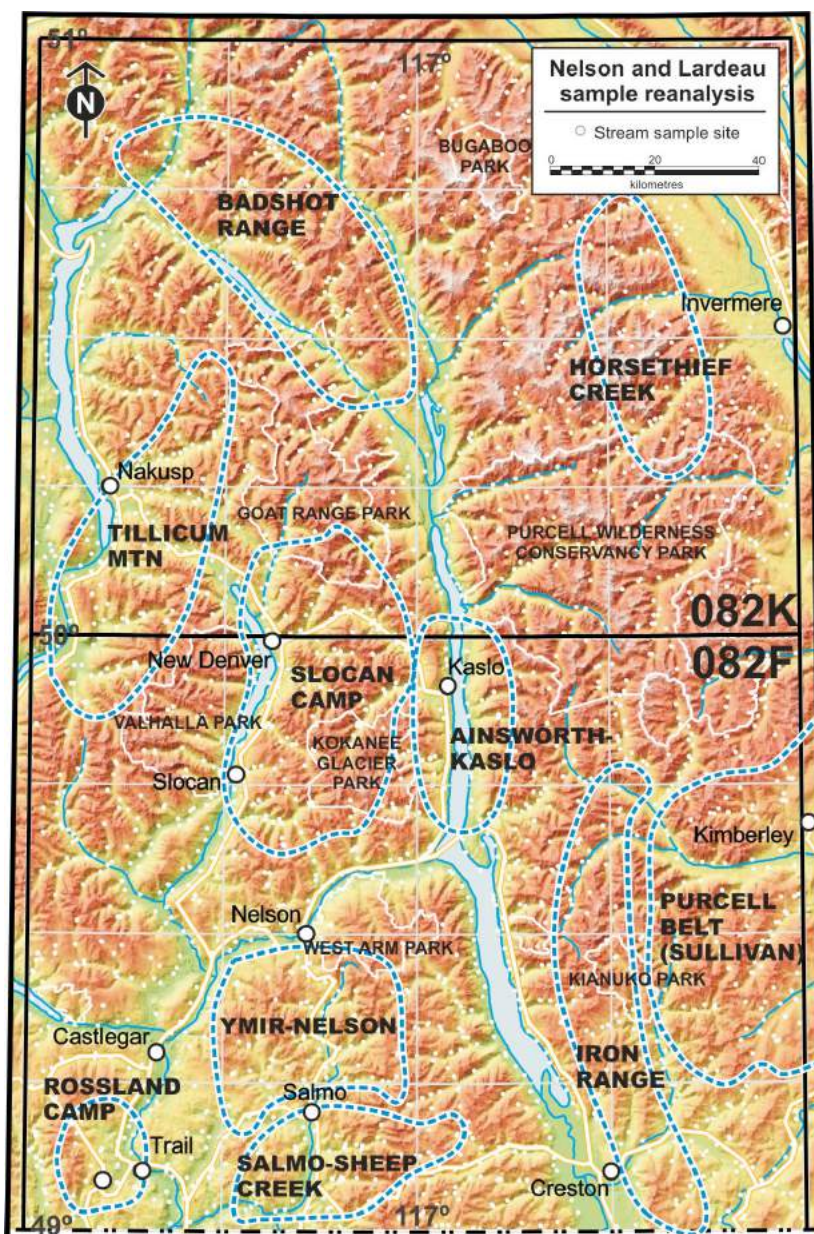


Figure 2. Location of the southeastern British Columbia study area, the stream sample site locations and the distribution of historical mining camps and exploration areas, indicated by the dashed lines.

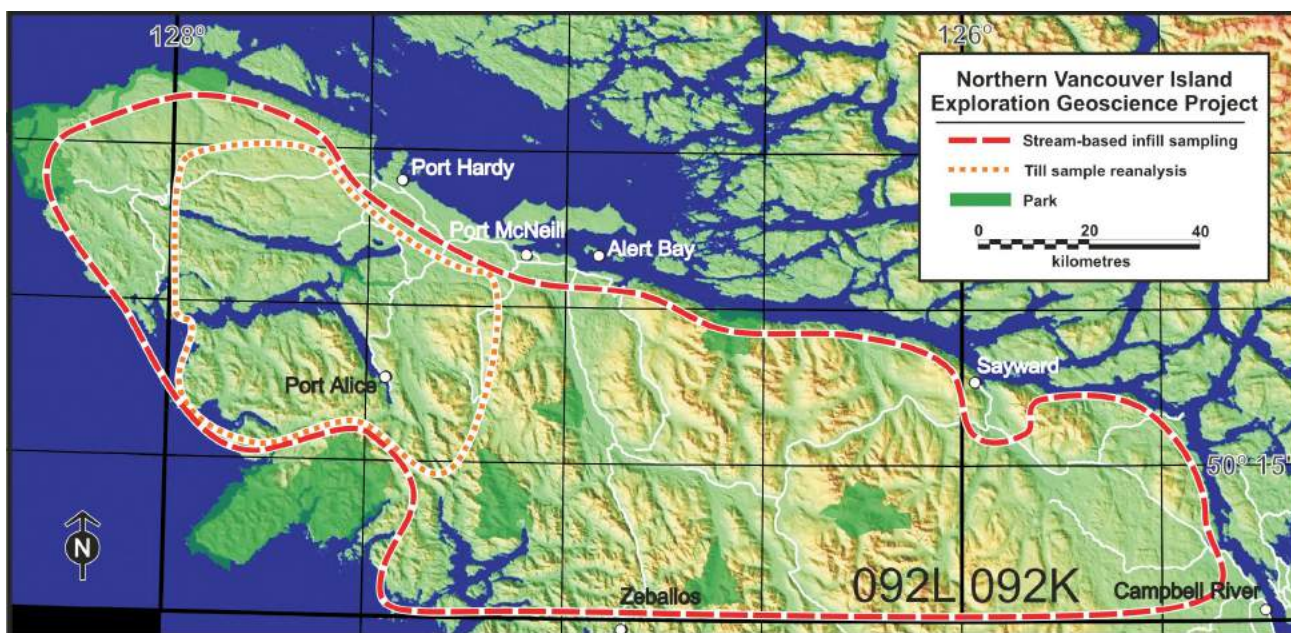


Figure 3. Location of the Northern Vancouver Island Exploration Geoscience Project study area.

pendent fine-grained sediment from the streamwater (Figure 4). When the original data was published, the sediment analytical package included Ag, As, Bi, Cd, Cu, Co, Cr, Fe, Hg, Mn, Mo, Ni, Pb, Sb, Sn, U, V, W and Zn by aqua-regia digestion–AAS finish and Au by lead-collection fire assay. In 2010, as part of a Geoscience BC–supported initiative, the Vancouver Island moss-mat sediment with quality-control samples were reanalyzed for 51 elements by aqua-regia digestion (0.5 g) The inductively coupled plasma–mass spectrometry/inductively coupled plasma–atomic emission spectroscopy (ICP-AES) analysis and Pt and Pd by lead-collection fire assay (30 g) with an ICP-MS finish (Jackaman, 2011b).

In September and October 2012, infill sampling involving the collection of approximately 700 moss-mat sediment



Figure 4. A typical moss-mat sediment sample, British Columbia, 3.8 cm (1.5 in) plastic putty knife for scale.

and water samples was conducted on parts of northern Vancouver Island (NTS map areas 092L, 092K and 102I). The new sampling has been designed to increase geochemical coverage by targeting primary drainages not previously sampled and adding more sample sites upstream from existing locations in secondary or larger drainages. To maintain continuity with the original surveys, 1–2 kg moss-mat sediment samples were collected from each site when available. In some cases, often due to stream channel disruptions associated with logging, conventional sediment (recently deposited, fine-grained material found within the active channel) was collected. Water samples were also collected, but due to the unusually dry weather, many of the sites were dry.

At the completion of the field program, moss-mat sediment and stream samples were dried and sieved to –80 mesh (<177 µm). Once processed, splits of the sediment samples were forwarded to commercial laboratories and analyzed for 53 analytes by ICP-MS using aqua-regia digestion and INAA for 35 elements. Loss-on-ignition and F content will also be determined for moss-mat and stream sediment samples. Streamwater was measured for pH and conductivity at each site and fluoride was determined in the laboratory from the raw streamwater samples.

To further augment the region’s geochemical database, the –230 mesh (<63 µm) fraction of till samples collected in the 1990s as part of the northern Vancouver Island drift prospecting program (Bobrowsky and Sibbick, 1996) was retrieved from a storage facility in Victoria and a portion of each sample was recovered for analysis by an ultratrace aqua-regia digestion (0.5 g) ICP-MS package for 53 elements. Blind duplicate and control reference materials

were included with the submitted samples to monitor the quality of the analysis.

There is a high probability for new metal deposit discoveries on Vancouver Island because bedrock geology reflects periodic accretion of island arc-related volcanic rocks and related intrusive bodies and most of the area has considerably improved access by an extensive logging road network. There are numerous mineral occurrences, ranging from porphyry Cu-Mo to volcanogenic massive sulphides to skarn-type mineralization. Bedrock mapping by Nixon et al. (2008) has significantly improved an appreciation of northern Vancouver Island geology and has complementary litho-geochemical studies that suggest the volcanic rocks may also host Pt-Pd mineralization (Nixon et al., 2008). Geochemical information compiled from the Northern Vancouver Island Exploration Geoscience Project will be released in 2013.

Summary

Ongoing efforts by government-funded agencies such as the GSC, the BCMEMNG and Geoscience BC to update and maintain the provincial Regional Geochemical Survey database has helped produce one of the most comprehensive collections of field information and multi-element analytical data in Canada. The collection remains an important instrument for focusing and directing mineral exploration activities in the province and has been credited with locating many prospective areas as well as the discovery of new sources of metals. Its value is sustained by the fact that data has been acquired and maintained according to strict operational standards (Ballantyne, 1991; Friske and Hornbrook, 1991) and is provided to the public free of charge and in usable formats. With ongoing development and maintenance, the information will remain relevant and will contribute to the success of mineral exploration and mining initiatives.

Acknowledgments

The authors greatly appreciate contributions from E. Jackaman, S. Reichheld, J. Dimock, J. Constable and B. Elder to the field programs. A. Rukhlov of the BCMEMNG and M. McCurdy and A. Therriault of Natural Resources Canada are acknowledged for their ongoing support of the development and maintenance of the BC Regional Geochemical Survey database and archive storage facilities. The Northern Vancouver Island Exploration Geoscience Project is jointly funded by Geoscience BC and the Island Coastal Economic Trust. T. Höy's editorial comments are greatly appreciated.

References

Ballantyne, S.B. (1991): Stream geochemistry in the Canadian Cordillera: conventional and future applications for exploration; *in* Exploration Geochemistry Workshop, Geological Survey of Canada, Open File 2390, p. 6.1–6.7, URL <<http://geoscan.ess.nrcan.gc.ca/cgi-bin/starfinder/0?path=geoscan.fl&id=fastlink&pass=&format=FLFULL&search=R=132388>> [October 2012].

Barnett, C.T. and Williams, P.M. (2009): Using geochemistry and neural networks to map geology under glacial cover; Geoscience BC, Report 2009-3, 27 p., URL <<http://www.geosciencebc.com/s/2009-03.asp>> [November 2012].

Bobrowsky, P.T. and Sibbick, S.J. (1996): Till geochemistry of northern Vancouver Island area, (NTS 92L/5, 6W, 11W, 12); BC Ministry of Energy, Mines and Natural Gas Open File 1996-07, 26 p., URL <<http://www.empr.gov.bc.ca/Mining/Geoscience/PublicationsCatalogue/OpenFiles/1996/Pages/1996-7.aspx>> [October 2012].

Friske, P.W.B. and Hornbrook, E.H.W. (1991): Canada's National Geochemical Reconnaissance programme; *in* Transactions of the Institution of Mining and Metallurgy, Section B, v. 100, p. 47–56, URL <http://geochem.cgkn.net/cdogs/metadata_pub_e.php?id=01454> [October 2012].

Gravel, J.L. and Matysek, P.F. (1989): 1988 regional geochemical survey, northern Vancouver Island and adjacent mainland (092E, 092K, 092L); BC Ministry of Energy, Mines and Natural Gas, Paper 1989-1, p. 585–591, URL <<http://www.empr.gov.bc.ca/Mining/Geoscience/PublicationsCatalogue/Fieldwork/Pages/GeologicalFieldwork1988.aspx>> [October 2012].

Jackaman, W. (2008a): Regional lake sediment and water geochemical data, northern Fraser Basin, Central BC (parts of NTS 93G, H, J, K, N & O); Geoscience BC, Report 2008-5, 4 p., URL <<http://www.geosciencebc.com/s/2008-05.asp>> [October 2012].

Jackaman, W. (2008b): QUEST Project sample reanalysis; Geoscience BC, Report 2008-3, 4 p., URL <<http://www.geosciencebc.com/s/2008-03.asp>> [October 2012].

Jackaman, W. (2008c): Regional stream sediment and water geochemical data: Terrace & Prince Rupert (NTS 103I & 103J), British Columbia; Geoscience BC, Report 2008-11, 4 p., URL <<http://www.geosciencebc.com/s/2008-11.asp>> [October 2012].

Jackaman, W. (2009): QUEST-West Project sample reanalysis; Geoscience BC, Report 2009-5, 4 p., URL <<http://www.geosciencebc.com/s/2009-05.asp>> [October 2012].

Jackaman, W. (2010): QUEST-South Project sample reanalysis; Geoscience BC, Report 2010-4, 4 p., URL <<http://www.geosciencebc.com/s/2010-004.asp>> [October 2012].

Jackaman, W. (2011a): Northern BC sample reanalysis project; Geoscience BC, Report 2011-2, 11 p., URL <<http://www.geosciencebc.com/s/2011-02.asp>> [October 2012].

Jackaman, W. (2011b): Regional stream sediment and water geochemical data, Vancouver Island, British Columbia; Geoscience BC, Report 2011-4, 5 p., URL <<http://www.geosciencebc.com/s/2011-04.asp>> [October 2012].

Jackaman, W., Matysek, P.F. and Cook, S.J. (1991): The regional geochemical survey program: summary of activities; *in* Geological Fieldwork 1991, BC Ministry of Energy, Mines and Natural Gas, Paper 1992-1, p. 307–318, URL <<http://www.empr.gov.bc.ca/Mining/Geoscience/PublicationsCatalogue/Fieldwork/Pages/GeologicalFieldwork1991.aspx>> [October 2012].

Lett, R.E.W. and Bluemel, B. (2006): Re-analysis of Regional Geochemical Survey stream sediment samples from the McLeod Lake area (NTS map sheet 093J); BC Ministry of Energy, Mines and Natural Gas, GeoFile 2006-09, 220 p.,

URL <<http://www.empr.gov.bc.ca/Mining/Geoscience/PublicationsCatalogue/GeoFiles/Pages/2006-9.aspx>> [October 2012].

- Nixon, G.T., Larocque, J., Pals, A., Styan, J., Greene, A.R. and Scoates, J.S. (2008): High-Mg lavas in the Karmutsen flood basalts, northern Vancouver Island (NTS 092L): stratigraphic setting and metallogenic significance; *in* Geological Fieldwork 2007; BC Ministry of Energy, Mines and Natural Gas, Paper 2008-1, p. 175–190, URL <<http://www.empr.gov.bc.ca/Mining/Geoscience/PublicationsCatalogue/Fieldwork/Pages/GeologicalFieldwork2007.aspx>> [October 2012].
- Simpson, K. (2013): Update on Geoscience BC's 2012 geophysical programs; *in* Geoscience BC Summary of Activities 2012, Geoscience BC, Report 2013-1, p. 1–4.
- Ward, B.C., Leybourne, M.I. and Sacco, D.A. (2012): Heavy mineral analysis of till samples within the QUEST Project area, central British Columbia (NTS 093J); *in* Geoscience BC Summary of Activities 2011, Geoscience BC, Report 2012-1, p. 59–68, URL <http://www.geosciencebc.com/i/pdf/SummaryofActivities2011/SoA2011_Ward.pdf> [November 2012].

Dease Lake Geoscience Project: Geochemical Characteristics of Tsaybahe, Stuhini and Hazelton Volcanic Rocks, Northwestern British Columbia (NTS 104I, J)

J.M. Logan, British Columbia Ministry of Energy, Mines and Natural Gas, Victoria, BC, Jim.Logan@gov.bc.ca

O. Iverson, University of Wisconsin, Eau Claire, WI

Logan, J.M. and Iverson, O. (2013): Dease Lake Geoscience Project: geochemical characteristics of Tsaybahe, Stuhini and Hazelton volcanic rocks, northwestern British Columbia (NTS 104I, J); in Geoscience BC Summary of Activities 2012, Geoscience BC, Report 2013-1, p. 11–32.

Introduction

The BC Geological Survey's Dease Lake Geoscience Project was part of Geoscience BC's QUEST-Northwest initiative, a program launched in 2011 to stimulate exploration in the northwestern part of the province along Highway 37 (Figure 1). In 2011, the BC Geological Survey completed four field-based studies located within a 70 km radius of the Dease Lake community (Logan et al., 2012a, Figure 1b). These studies investigated regional aspects of stratigraphy, magmatic evolution and metallogeny along part of the Stikine arch, within the broader footprint of the QUEST-Northwest airborne geophysical survey (Simpson, 2012). They included regional bedrock mapping of the Dease Lake and Little Tuya River map areas (Logan et al., 2012b, c); detailed studies of the ages, emplacement history and mineralization of the Hotailuh batholith (van Straaten et al., 2012a, b) and Snow Peak pluton (Moynihan and Logan, 2012); and a lithological and geochemical characterization of the Middle Triassic Tsaybahe Group (Iverson et al., 2012a).

The Dease Lake study area is situated within the Stikine terrane, an extensive subduction-generated island arc magmatic complex that includes Late Triassic and Early Jurassic calcalkaline and alkaline plutons that are associated with significant Cu-Au mineralization. Calcalkaline and alkaline Cu-Au porphyry deposits in Stikinia are hosted in thick successions of Late Triassic to Early Jurassic(?) volcanic rocks and comagmatic calcalkaline (Scott et al., 2008) and alkaline plutons (Barr et al., 1976; Lueck and Russell, 1994). The deposits are localized along parallel linear belts within high(?) level magmatic centres characterized by zones of brecciation and alkali-rich hydrothermal alteration. The volcanic stratigraphy adjacent to magmatic centres often records the evolution of magmatism

Keywords: *QUEST-Northwest mapping, regional bedrock mapping, integrated multidisciplinary studies, geochemistry, Stikine terrane, Triassic–Jurassic magmatism, Tsaybahe, Stuhini, Hazelton, Hotailuh*

This publication is also available, free of charge, as colour digital files in Adobe Acrobat® PDF format from the Geoscience BC website: <http://www.geosciencebc.com/s/DataReleases.asp>.

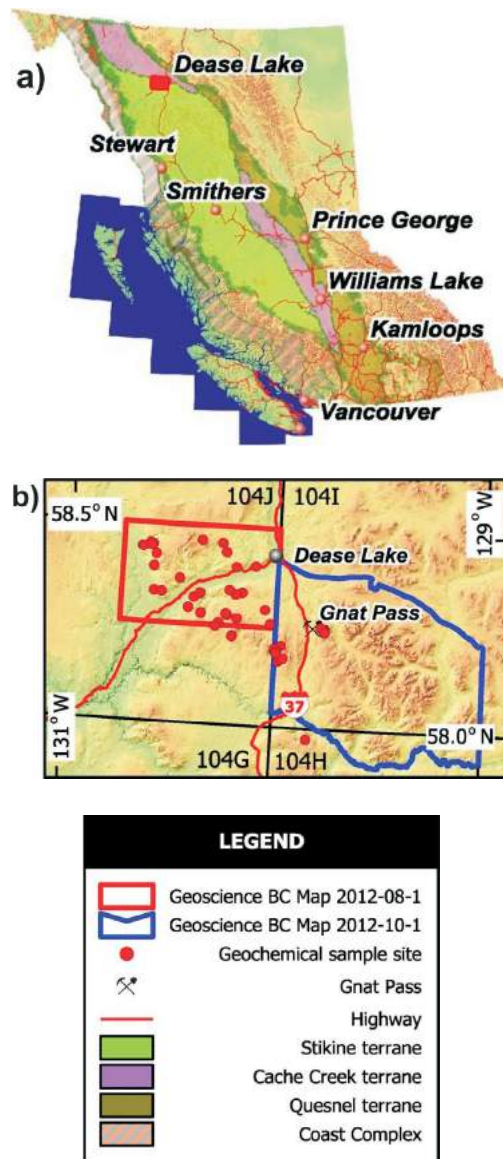


Figure 1. Location of the QUEST-Northwest Mapping–BC Geological Survey Dease Lake Geoscience Project on the **a)** British Columbia terrane map (after Massey et al., 2005); detailed view **b)** straddles the area covered by the Dease Lake (NTS 104J) and Cry Lake (NTS 104I) 1:250 000 map sheets at Dease Lake, and shows the locations of Geoscience BC Map 2012-08-1, Geoscience BC Map 2012-10-1 and the sample locations for the geochemistry study discussed in this paper.

through changes in mineralogy (pyroxene, hornblende or plagioclase porphyry flows) and chemistry (i.e., alkali-rich stratigraphy), or through the presence of mineralized subvolcanic clasts—all of which can provide vectors to guide exploration for Cu-Au mineralization (Fox, 1975; Allen et al., 1976; Panteleyev et al., 1996; Logan and Bath, 2006).

In this paper major, trace and rare earth element chemical characteristics of volcanic rocks collected during the 2011 programs, carried out by the BC Geological Survey in the area of the Dease Lake (104J) and Cry Lake (104I) map sheets (Figure 1), are presented. Volcanic rocks were collected from the Middle Triassic Tsaybahe Group to characterize the initiation of Triassic arc magmatism and from the Late Triassic Stuhini Group to characterize its ongoing evolution, which periodically culminated in porphyry Cu–Au±Mo mineralization (i.e., Schaft Creek, Galore Creek and Red Chris deposits). A third suite comprises samples collected from a Early to Middle Jurassic volcanic and sedimentary succession, assigned to the Hazelton Group, that is the same age as the host rocks at the Eskay Creek gold mine (Alldrick et al., 2004).

Regional Stratigraphy

The area covered by the Dease Lake and Cry Lake map sheets (NTS 104J and I, Figure 1) straddles the boundary between the Cache Creek and Stikine terranes, marked by the early Middle Jurassic south-directed King Salmon thrust fault (Gabrielse, 1998). At this latitude the Stikine terrane is composed of three overlapping island arc successions, spanning 200 m.y. from Devonian to Middle Jurassic, and is represented by volcanic and sedimentary rocks of the Paleozoic Stikine assemblage, the Triassic Tsaybahe/Stuhini Group and the Jurassic Hazelton Group. Arc-related plutonic rocks include the Devonian-Carboniferous Forrest Kerr suite, the Late Triassic Stikine and Copper Mountain suites, the Early Jurassic Texas Creek suite and the Middle Jurassic Three Sisters suite (Anderson, 1983, 1993; Woodsworth et al., 1991; Brown et al., 1996; Logan et al., 2000). These plutonic suites are best exposed along the Stikine arch, an east-trending area of uplifted Jurassic and older rocks that bound the northern margin of the Bowser Basin. Long-lived arc magmatism in the Stikine arch has produced diverse styles of magmatism (calcalkaline and alkaline) and large Cu–Au–Ag±Mo mineral deposits associated with some intrusive centres (i.e., Snip, Galore Creek, Schaft Creek and Kemess).

The oldest Stikine rocks in the study area are Early Permian limestone, phyllite, chert and metavolcanic rocks exposed in north to northeasterly trending structural culminations. Volcaniclastic beds and coarse pyroxene-phyric basalt breccias unconformably overlie these foliated late Paleozoic rocks (Figure 2) and correlate with Early and Middle

Triassic cherty sedimentary rocks and pyroxene-phyric breccias of the Tsaybahe Group to the south (Read, 1983, 1984). The green augite porphyry volcanic rocks that characterize the type section at Tsaybahe Mountain (Read and Psutka, 1990) are not easily distinguished from the younger Stuhini Group rocks and, as a result, Gabrielse (1998) included the Tsaybahe rocks as a unit within the Stuhini Group, and considered this group to encompass all Triassic volcanic and related sedimentary rocks in Stikinia. For litho-geochemical comparison in this study, the term Tsaybahe Group has been retained for all the pre-Late Triassic crowded-augite-phyric basalt overlying Paleozoic rocks (Logan et al., 2012c).

The Tsaybahe Group basalt breccias in the Dease Lake area (Gabrielse, 1998; Logan et al., 2012c) dip north below a pile of Late Triassic Stuhini Group arc rocks ~2050 m thick, comprised of pyroxene-rich volcaniclastic rocks and rare pyroxene-phyric, plagioclase-phyric and aphyric basalt flows that generally fine upward into a stratigraphic section that is dominated by unstratified coarse volcaniclastic deposits. The Stuhini volcaniclastic strata are pyroxene- and plagioclase-crystal-rich matrix-supported boulder to granule conglomerates dominated by pyroxene±plagioclase porphyry clasts with lithic arenites and rare well-bedded siltstone. The uppermost unit of the Stuhini Group comprises volcaniclastic rocks and basalt flows, and is unconformably(?) overlain by Early Jurassic Takwahoni Formation quartz-bearing conglomerate and sandstone (Figure 2) of the Whitehorse Trough.

Marsden and Thorkelson (1992) include all Early and Middle Jurassic volcanic and related sedimentary rocks of Stikinia in the Hazelton Group. As a result, the Hazelton Group includes a wide variety of rock types that formed in diverse volcanic environments over a large region. The Hazelton Group in northern Stikinia overlies Late Triassic calcalkaline and alkaline volcanic and sedimentary rocks of the Stuhini Group and associated arc plutonic rocks, and is overlain by Middle Jurassic sedimentary rocks of the Bowser Lake Group.

Southeast of the study area, in the area covered by the Spatsizi River map sheet (104H), Late Triassic Griffith Creek volcanic rocks, Early Jurassic Cold Fish and Mount Brock volcanic rocks, and Middle Jurassic Spatsizi sedimentary rocks comprise the Hazelton Group (Evenchick and Thorkelson, 2005). Brown et al. (1992) describe a Toarcian to Aalenian calcalkaline volcanic and sedimentary succession of Hazelton Group rocks at Cone Mountain, 125 km southwest of Dease Lake within the area covered by the Telegraph Creek map sheet (104G). Like the section east of Gnat Pass (this study), the lower unit contains an abundant fauna that suggest a Toarcian age, but rather than unconformably overlying intrusive rocks of the Late Triassic Cake Hill Pluton (Henderson and Perry,

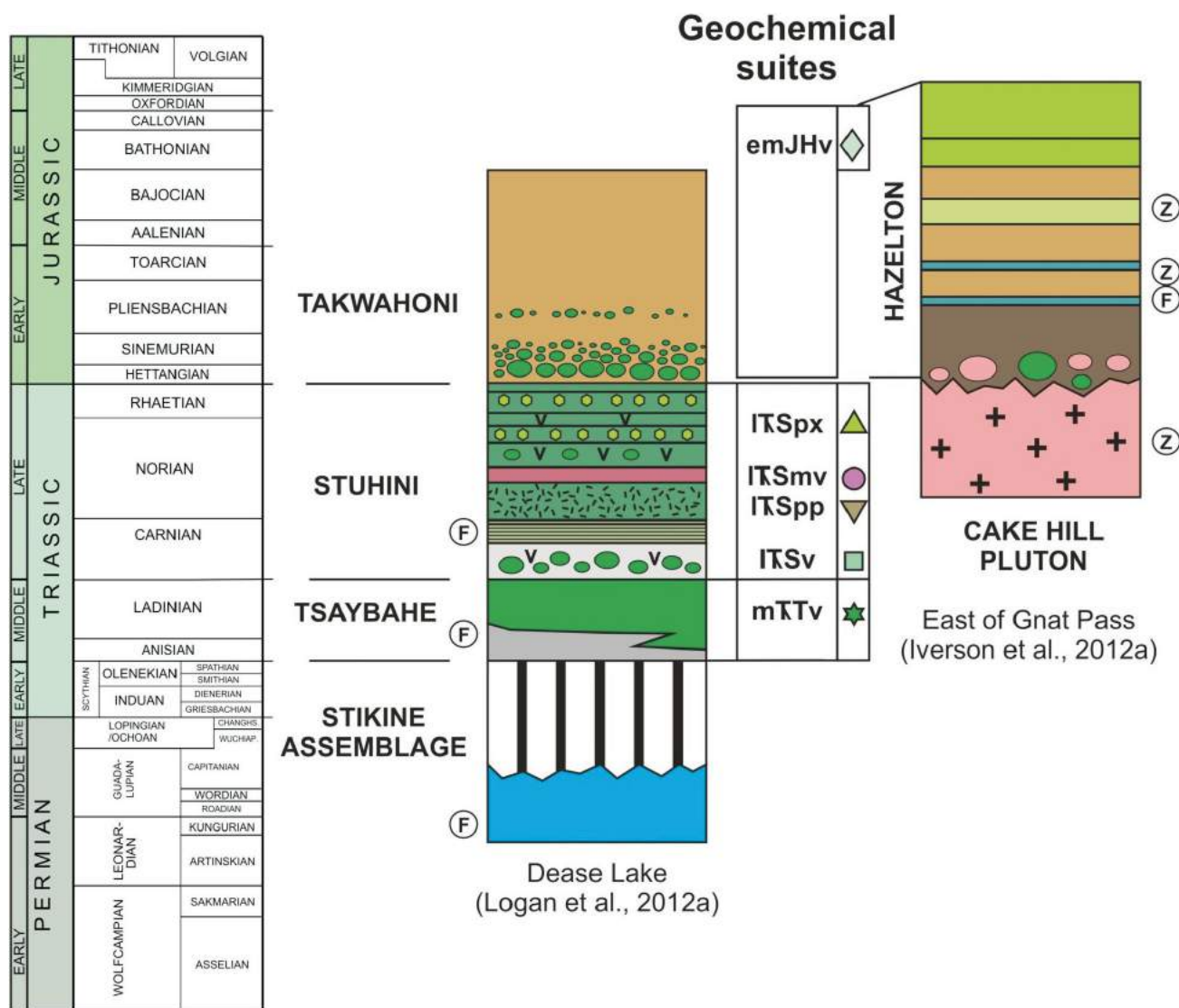


Figure 2. Two schematic sections illustrating the stratigraphic and plutonic relationships for Stikine terrane rocks in the study area. Abbreviations: F, fossils; Z, U/Pb zircon ages described and referenced in text. Symbols for the six geochemical suites discussed in text: mTTv, Middle Triassic Tsaybahe pyroxene-phyric basalt; ITSv, Late Triassic Stuhini aphyric basalts; ITSpp, Late Triassic Stuhini plagioclase-phyric basalt and andesite; ITSmv, Late Triassic Stuhini latite porphyry; ITSpx, Late Triassic Stuhini pyroxene-phyric basalt; emJHv, Early to Middle Jurassic Hazelton pyroxene porphyry.

1980), it overlies folded and faulted late Norian Stuhini Group strata (Brown et al., 1992).

Southeast of Dease Lake and 5 km east of Gnat Pass, is a well exposed, upright section of Early to Middle Jurassic sedimentary and volcanic rocks (Iverson, et al., 2012a) that nonconformably overly Late Triassic quartz monzonite of the Cake Hill pluton (Anderson, 1983; Gabrielse, 1998; Figure 2). Coarse pyroxene-phyric basalt breccia and volcanic conglomerate comprise the upper part of the section, which has been dated as Toarcian using fossils (Henderson and Perry, 1981), but is possibly as young as Bajocian, as dated with detrital zircons (Iverson et al., 2012a, b). The volcanic rocks are included in the Hazelton Group because of their age, but are lithologically similar to pyroxene-phyric basalt

breccias of the Middle Triassic Tsaybahe and Late Triassic Stuhini groups.

Lithochemochemistry

Analytical Techniques

A total of 55 least-altered lithochemochemical samples were collected: 42 volcanic rocks from 5 different units and 13 intrusive rocks from 5 plutonic suites (Table 1). This paper focuses on the geochemical results of the Tsaybahe, Stuhini and Hazelton groups (n=39). The samples were jaw crushed at the BC Geological Survey sample preparation facilities in Victoria. The crushed samples were sent to Activation Laboratories in Ancaster (Ontario), where they

Table 1. Part I: Major oxide analytical results for volcanic and intrusive rocks collected from the area covered by the Dease Lake (104J) and Cry Lake (104I) map sheets, northern British Columbia.

Geochemical	Sample numbers	Original	Easting	Northing	Unit ⁵	Sample description ¹	Analyte Symbol:											Total	
							SiO ₂	Al ₂ O ₃	Fe ₂ O ₃ ^(T)	MnO	MgO	CaO	Na ₂ O	K ₂ O	TiO ₂	P ₂ O ₅	LOI		
							Unit:												
							Detection limit:												
							F-ICP-AES												
62245	JLO-30-303-2	430165	6459334	MPTV	Alkali olivine basalt		48.15	15.22	10.26	0.161	6.37	7.97	3.42	1.91	1.726	0.87	1.61	97.65	
62266	LDI-9-73	406431	6473405	MPTV	Alkali olivine basalt		45.42	14.95	9.87	0.167	5.75	9.45	3.53	2.97	2.095	0.82	5.43	100.5	
62256	JLO-12-117	419804	6481015	PaSPgd	Hb-bt qtz granodiorite		63.93	15.68	4.8	0.092	1.54	3.9	3.72	3.35	0.502	0.29	0.62	98.42	
62256 Dup	JLO-12-117	419804	6481015	PaSPgd	Hb-bt qtz granodiorite		-	-	-	-	-	-	-	-	-	-	-	-	
622456 Orig	JLO-12-117	419804	6481015	PaSPgd	Hb-bt qtz granodiorite		-	-	-	-	-	-	-	-	-	-	-	-	
Difference ³	JLO-12-117	419804	6481015	PaSPgd	Hb-bt qtz granodiorite		-	-	-	-	-	-	-	-	-	-	-	-	
62262	TMC-2-15	427037	6460554	MJPM	Hb-bt qtz monzodiorite		53.55	17.78	8.89	0.155	3.77	7.68	3.74	2.77	0.987	0.31	0.28	99.9	
62252	TMC-2-16	427372	6460293	MJPM	Hb-bt qtz monzodiorite		65.9	16.39	3.94	0.067	1.27	3.34	3.88	4.07	0.402	0.15	0.83	100.2	
62241	OIV-3-41	428976	6454429	MJPM	Bt-hb monzonite dike		56.54	17.44	7.91	0.068	3.06	5.78	4.02	3.4	0.763	0.28	1.57	100.8	
62244	JLO-21-208	441811	6450829	MJPM	Hb-bt quartz monzonite		72.47	14.59	1.9	0.113	0.32	1.24	4.34	4.46	0.219	0.06	0.36	100.1	
62271	LDI-19-165	425101	6458048	MJPM	Hb-bt qtz monzonite		64.04	16.77	4.54	0.103	1.5	3.99	3.89	3.63	0.467	0.18	0.82	99.92	
62272	LDI-19-165dup	425101	6458048	MJPM	Hb-bt qtz monzonite		62.61	16.66	4.36	0.1	1.45	3.93	3.87	3.56	0.449	0.19	0.8	97.98	
Difference ³	LDI-19-165dif	425101	6458048	MJPM	Hb-bt qtz monzonite		0.56	0.16	1.01	0.74	0.85	0.38	0.13	0.49	0.98	1.35	0.62	0.49	
62249	DMO-33-288	438158	6461969	MJPM	Hb monzodiorite		55.19	16.29	8.83	0.117	3.1	5.68	3.59	4.01	0.824	0.41	1.17	99.2	
62257	DMO-23-182	439708	6458108	MJPM?	Hb porphyry		50.66	16.84	9.75	0.2	4.09	6.54	4.25	2.16	0.782	0.34	2.95	98.56	
62251	TMC-7-51	427980	6467206	MJHsy	Syenite		53.08	17.47	7.71	0.184	2.22	5.4	4.31	5.57	0.667	0.35	3.39	100.4	
62242	JLO-9-77	426788	6477834	LJqfp	Plag porphyry dike		66.57	16.42	2.87	0.052	1.27	3.6	4.56	1.48	0.359	0.12	2.95	100.2	
62242 Dup	JLO-9-77	426788	6477834	LJqfp	Plag porphyry dike		-	-	-	-	-	-	-	-	-	-	-	-	
62242 Orig	JLO-9-77	426788	6477834	LJqfp	Plag porphyry dike		-	-	-	-	-	-	-	-	-	-	-	-	
Difference ³	JLO-9-77	426788	6477834	LJqfp	Plag porphyry dike		-	-	-	-	-	-	-	-	-	-	-	-	
-	11OIV4-51A	455201	6457065	emJHv	augite porphyry		49.65	16.13	10.84	0.184	5.79	8.14	3.32	1.44	0.85	0.30	2.72	99.36	
-	11OIV4-51B	455201	6457065	emJHv	augite porphyry		48.99	16.53	10.53	0.184	5.25	8.89	2.19	2.47	0.86	0.31	2.51	98.71	
-	11OIV4-51C	455201	6457065	emJHv	augite porphyry		48.72	15.94	9.92	0.175	5.18	10.65	2.24	1.98	0.8	0.29	3.19	99.09	
-	11OIV4-54	454810	6457137	emJHv	augite porphyry		49.16	15.78	11.31	0.214	6.4	8.61	3.02	1.38	0.86	0.29	3.09	100.11	
-	11OIV4-55	454734	6457158	emJHv	augite porphyry		47.98	16.17	11.51	0.207	5.74	9.91	1.84	1.98	0.9	0.33	3.10	99.67	
-	11OIV4-59	454470	6457278	emJHv	augite porphyry		49.68	13.34	10.11	0.187	8.93	10.63	1.83	1.26	0.76	0.15	2.46	99.34	
-	11OIV4-60	454247	6457302	emJHv	augite porphyry		46.67	14.16	10.96	0.195	7.32	11.88	1.49	1.78	0.79	0.26	3.81	99.31	
-	11OIV4-61	454066	6457422	emJHv	augite porphyry		47.19	14.82	11.31	0.209	7.03	11.43	2.07	1.4	0.81	0.27	3.46	99.99	
62258	DMO-19-154	408808	6466301	TJgb	Hb diorite		47.84	19.3	10.44	0.22	3.94	11.03	3.59	1.2	0.902	0.56	1.82	100.8	
62248	JLO-22-215	419963	6460563	TJgb	Hb gabbro, diorite		45.81	15.21	11.88	0.193	8.38	12.01	2.22	1.35	1.069	0.25	1.94	100.3	
62248 Dup	JLO-22-215	419963	6460563	TJgb	Hb gabbro, diorite		45.96	15.33	11.91	0.193	8.33	12	2.23	1.36	1.068	0.25	1.94	100.6	
622482 Orig	JLO-22-215	419963	6460563	TJgb	Hb gabbro, diorite		45.67	15.1	11.85	0.193	8.43	12.02	2.22	1.35	1.071	0.25	1.94	100.1	
Difference ³	JLO-22-215	419963	6460563	TJgb	Hb gabbro, diorite		0.16	0.38	0.13	0	0.30	0.04	0.11	0.18	0.07	0	0	0.12	
62263	JLO-20-190	455198	6456114	LITCH	Bt-hb qtz monzodiorite		66.71	16.53	3.45	0.075	1.26	2.91	5.12	3.68	0.388	0.15	0.62	100.9	
62237	JLO-14-141-2	406973	6476844	ITSpx	Augite-phyric basalt		45.65	11.52	11.51	0.212	8.97	11.59	1.96	2.66	0.699	0.74	4.72	100.2	

Table 1. Part I (continued)

Geochemical	Sample location ¹		Analyte Symbol: %											F-ICP-AES		LOI	Total	
	Original	Eastings	Northings	Unit ⁵	Sample description	Detection limit:	SiO ₂	Al ₂ O ₃	Fe ₂ O ₃ ^(T)	MnO	MgO	CaO	Na ₂ O	K ₂ O	TiO ₂			P ₂ O ₅
62243	JLO-16-161-2	403267	6478913	ITSpX	Augite-phyric basalt	0.01	50.34	16.8	10.41	0.16	4.7	7.8	4.21	1.74	0.946	0.31	2.95	100.4
62259	JLO-16-153	405565	6479260	ITSpX	Augite-phyric basalt	0.01	49.03	14.98	11.58	0.181	5.9	7.84	2.49	3.53	0.847	0.34	2.25	98.97
62260	JLO-16-153dup	405565	6479260	ITSpX	Augite-phyric basalt	0.01	48.51	14.64	11.45	0.182	5.96	7.94	2.47	3.44	0.838	0.34	2.3	98.08
Difference ³	JLO-16-153diff	405565	6479260	ITSpX	Augite-phyric basalt	0.01	0.27	0.57	0.28	0.14	0.25	0.32	0.20	0.65	0.27	0	0.55	0.23
62250	DMSO-505blank			Blank			99.89	0.06	0.4	0.004	0.01	0.02	0.02	< 0.01	0.002	< 0.01	0.08	100.5
62247	DMSO-20-158	431568	6466583	ITSmv	Trachyte porphyry	0.01	50.04	16.49	8.21	0.236	2.02	5.27	2.86	6.59	0.642	0.31	7.04	99.71
62255	DMSO-33-286	429718	6466035	ITSmv	Latite	0.01	48.78	14.43	9.27	0.2	2.98	5.09	4.64	4.63	0.722	0.33	8.32	99.39
-	11JLO21-203	442981	6452092	ITSmv	Plag-phyric basalt	0.01	51.75	17.59	9.06	0.063	2.17	6.4	3.46	4.98	0.844	0.56	1.73	98.61
62253	DMSO-29-246	417886	6464947	ITSpP	Plag-phyric basalt	0.01	54.1	17.85	9.96	0.178	2.62	7.74	3.61	1.21	0.947	0.3	2.29	100.8
62254	DMSO-30-255	406627	6466547	ITSpP	Plag-phyric basalt	0.01	48.36	18.13	11.16	0.2	3.66	9.98	3.14	1.34	1.062	0.26	1.95	99.23
62239	DMSO-18-138	406068	6479589	ITSpP	Plag-phyric basalt	0.01	52.09	17.78	9.77	0.271	3.16	3.87	2.79	6.74	0.778	0.74	2.97	101
62261	JLO-17-172	413803	6470151	ITSpP	Plag-phyric basalt	0.01	60.53	17.7	5.2	0.188	1.33	3.42	6.7	3.11	0.81	0.39	1.61	101
62268	LDI-12-96	405326	6479731	ITSpP	Plag-phyric basalt	0.01	53.55	18.45	7.02	0.274	2.39	1.67	0.9	11.15	0.822	0.35	2.19	98.77
62269	LDI-12-97	405246	6479876	ITSpP	Plag-phyric basalt	0.01	62.07	16.68	5.01	0.206	0.76	1.5	6.92	4.29	0.804	0.3	0.72	99.25
62269 Orig	LDI-12-97	405246	6479876	ITSpP	Plag-phyric basalt	0.01	-	-	-	-	-	-	-	-	-	-	-	-
62269 Dup	LDI-12-97	405246	6479876	ITSpP	Plag-phyric basalt	0.01	-	-	-	-	-	-	-	-	-	-	-	-
Difference ³	LDI-12-97	405246	6479876	ITSpP	Plag-phyric basalt	0.01	-	-	-	-	-	-	-	-	-	-	-	-
62273	DMSO-38-337	419651	6466174	ITSpP	Plag-phyric basalt	0.01	50.13	16.81	11.88	0.159	4.05	8.62	2.46	1.75	0.879	0.25	2.2	99.19
62240	JLO-5-42	435063	6474098	ITSpV	Aphanitic basalt	0.01	46.99	16.92	10.8	0.144	5.23	12.55	3.05	0.02	0.826	0.19	4.16	100.9
62246	DMSO-3-23	429719	6473685	ITSpV	Aphyric basalt	0.01	45.54	13.46	12.1	0.248	6.41	10.31	3.24	1.72	0.821	0.11	5.54	99.5
62264	JLO-16-162	403037	6478945	ITSpV	Plag crystal tuff	0.01	52.19	17.76	8.51	0.173	3.73	7.19	2.78	1.84	0.843	0.32	2.77	98.12
62267	LDI-12-95	405578	6479353	ITSpV	Aphanitic basalt	0.01	50.96	15.34	10.4	0.164	5.42	7.92	4.61	1.16	0.83	0.31	2.26	99.36
62270	LDI-16-137	424170	6457044	mTTv	Augite phyric basalt	0.01	47.68	14.2	11.36	0.188	7.46	10.84	2	3.12	1.045	0.54	1.09	99.53
62238	JLO-23-227	416358	6462047	mTTv	Plag-augite porphyry	0.01	42.34	13.36	10.51	0.32	5.26	16.53	3.2	0.56	0.847	0.23	7.81	101
-	11OIV1-2	450904	6425990	mTTv	augite porphyry	0.01	48.41	13.01	10.99	0.208	9.52	10.88	1.1	1.58	0.82	0.44	1.94	98.90
-	11LDI18-145B	442227	6447684	mTTv	augite porphyry	0.01	49.91	12.01	10.34	0.17	8.92	9.55	0.56	3.72	0.54	0.54	0.00	96.26
-	11LDI18-147	442601	6447993	mTTv	augite porphyry	0.01	50.95	16.73	10.14	0.187	6.08	6.46	3.86	2.03	0.7	0.24	0.77	98.15
-	11LDI18-151	443194	6448373	mTTv	augite porphyry	0.01	48.97	13.22	9.79	0.164	8.99	10.62	1.46	3.19	0.69	0.64	1.10	98.83
-	11LDI18-152	443642	6448548	mTTv	augite porphyry	0.01	49.04	13.47	9.79	0.15	8.34	11.59	1.73	2.93	0.64	0.52	0.98	99.18
-	11OIV3-39	428941	6454305	mTTv	augite porphyry	0.01	45.91	14.81	12.36	0.178	5.45	13.9	1.73	1.4	0.82	0.27	1.56	98.39
-	11OIV5-72	441164	6450773	mTTv	augite porphyry	0.01	45.84	14.25	11.84	0.306	7.37	15.14	0.74	1.67	0.54	0.39	0.42	98.50
-	11OIV5-73	441106	6450910	mTTv	augite porphyry	0.01	47.91	13.33	11.55	0.195	8.16	10.12	1.79	3.07	0.69	0.57	0.83	98.21
-	11OIV5-74	441143	6451142	mTTv	augite porphyry	0.01	48.3	13.36	10.73	0.236	8.24	11.25	1.64	2.56	0.75	0.61	0.78	98.45
-	11OIV5-75	441154	6451175	mTTv	augite porphyry	0.01	50.23	13.86	9.09	0.212	7.82	10.68	2.63	2.11	0.74	0.63	0.85	98.84
-	11JLO21-211-2	441542	6450144	mTTv	augite porphyry	0.01	48.79	14.19	9.7	0.172	7.26	12.42	1.54	2.84	0.63	0.44	0.51	98.49

Table 1. Part I (continued)

Geochemical	Original	Easting	Northing	Unit ⁵	Sample description	Analyte Symbol: SiO ₂ Al ₂ O ₃ Fe ₂ O ₃ (^T) MnO MgO CaO Na ₂ O K ₂ O TiO ₂ P ₂ O ₅ LOI Total											
						%	%	%	%	%	%	%	%	%	%	%	%
-	11JLO21-212	441537	6450031	mTTv	augite porphyry	49.04	14.46	9.7	0.16	8.04	11.85	1.9	2	0.64	0.43	0.64	98.86
62265	LDI-4-29	425618	6480362	PzTCCv	metabasalt	49.45	14.55	13.71	0.191	6.04	7.06	4.35	0.27	2.015	0.24	2.43	100.3
62265 Orig	LDI-4-29	425618	6480362	PzTCCv	metabasalt	49.44	14.48	13.7	0.19	6.05	7.02	4.39	0.27	2.012	0.24	2.43	100.2
62265 Dup	LDI-4-29	425618	6480362	PzTCCv	metabasalt	49.47	14.63	13.71	0.191	6.04	7.1	4.31	0.27	2.018	0.24	2.43	100.4
Difference ³	LDI-4-29	425618	6480362	PzTCCv	metabasalt	0.02	0.26	0.02	0.13	0.04	0.28	0.46	0	0.07	0	0	0.05
62274	MRG1standard	-	-	Standard	-	39.63	8.4	17.32	0.167	13.7	14.77	0.71	0.18	3.794	0.06	1.38	100.1
Expected ²	MRG1standard	-	-	Standard	-	39.12	8.47	17.94	0.17	13.6	14.7	0.74	0.18	3.77	0.08	2.23	100.95
Difference ³	MRG1standard	-	-	Standard	-	0.3	-0.2	-0.9	-0.4	0.2	0.1	-1.0	0.0	0.2	-7.1	-11.8	-0.2
62275 ⁴	SY3standard	-	-	Standard	-	59.54	11.57	6.5	0.321	2.61	8.09	4.03	4.33	0.147	0.55	1.19	98.87
62275 Orig	SY3standard	-	-	Standard	-	59.24	11.47	6.53	0.323	2.61	8.14	3.98	4.27	0.146	0.55	1.19	98.45
62275 Dup	SY3standard	-	-	Standard	-	59.85	11.67	6.46	0.32	2.61	8.03	4.07	4.39	0.149	0.55	1.19	99.28
Expected ²	SY3standard	-	-	Standard	-	59.68	11.76	6.49	0.32	2.67	8.25	4.12	4.23	0.15	0.54	1.31	99.52
Difference ³	SY3standard	-	-	Standard	-	-0.2	-0.6	0.2	0.2	-0.6	-0.3	-0.9	0.2	-0.7	0.5	-2.4	-0.3
Difference ³	SY3standard	-	-	Standard	-	0.1	-0.2	-0.1	0.0	-0.6	-0.7	-0.3	0.9	-0.2	0.5	-2.4	-0.1

¹ Sample location in UTM NAD83, Zone 9 V

² Recommended values for CANMET standards shaded green, difference between original and duplicate or expected values shaded blue, informational values unshaded (Govindaraju, 1994).

³ Difference calculated as follows: $0.5 \cdot 100 \cdot \frac{(x1-x2)}{(x1+x2)}$

⁴ Average value of Activation Labs' duplicate analysis of powdered material

⁵ Units: MPTv, Miocene-Pliocene Tuya basalt; PaSPgd, Paleocene Snow Peak granodiorite; MJPm, Middle Jurassic Pailen monzonite; MJHsy, Middle Jurassic Hluey syenite; LjJqfp, Late Jurassic quartz feldspar porphyry; emJHv, early to middle Jurassic Hazelton basalt; T.Jgb, Triassic-Jurassic hornblende gabbro; LTCH, Late Triassic-Coke Hill pluton; ITSpX, Late Triassic Stuhini pyroxene porphyry; ITSmv, Late Triassic Stuhini latite porphyry; ITSpp, Late Triassic Stuhini plagioclase porphyry; ITSV, Middle Triassic Stuhini aphyric basalt; mTTv, Middle Triassic Tsaybath pyroxene porphyry; PzTCCv, Paleozoic-Triassic Cache Creek basalt

Abbreviations: F-ICP-AES, fusion-inductively coupled plasma-atomic emission spectrometry; Hb, hornblende; Bt, biotite; Plag, plagioclase; Qtz, quartz; T, total iron

Table 1, Part II: Trace and rare earth element analytical results for volcanic and intrusive rocks collected from the area covered by the Dease Lake (104J) and Cry Lake (104I) map sheets, northern British Columbia.

Original sample no.	F-ICP-MS										F-ICP-MS												
	Be	Sc	V	Cr	Cr	Co	Ni	Ni	Cu	Zn	Ga	Ge	As	Rb	Y	Zr	Nb	Mo	Ag	In	Sn	Sb	Cs
Analyte symbol:	ppm	ppm	ppm	ppm	ppm	ppm	ppm	ppm	ppm	ppm	ppm	ppm	ppm	ppm	ppm	ppm	ppm	ppm	ppm	ppm	ppm	ppm	ppm
Unit:	ppm	ppm	ppm	ppm	ppm	ppm	ppm	ppm	ppm	ppm	ppm	ppm	ppm	ppm	ppm	ppm	ppm	ppm	ppm	ppm	ppm	ppm	ppm
Detection limit:	1	1	5	20	5	1	20	1	10	30	1	0.5	5	1	0.5	1	0.2	2	0.5	0.1	1	0.2	0.1
JLO-30-303-2	2	22	219	160	162	28	90	88	30	110	18	1.2	<5	26	29.5	191	23.1	<2	1.6	<0.1	1	<0.2	0.7
LDI-9-73	2	18	198	130	136	31	100	102	40	100	19	1.3	<5	63	22.6	248	91.7	3	1.7	<0.1	2	<0.2	6.5
JLO-12-117	2	7	78	<20	<5	6	<20	4	<10	<30	18	1.3	<5	101	16.2	97	18.5	13	0.8	<0.1	<1	<0.2	4.6
JLO-12-117dup	-	-	-	-	-	-	-	4	-	-	-	-	-	-	-	-	-	-	-	-	-	-	-
JLO-12-117orig	-	-	-	-	-	-	-	4	-	-	-	-	-	-	-	-	-	-	-	-	-	-	-
JLO-12-117dif	-	-	-	-	-	-	-	0	-	-	-	-	-	-	-	-	-	-	-	-	-	-	-
TMC-2-15	2	23	301	<20	15	22	<20	13	90	80	19	1.3	<5	56	21.7	106	4.4	<2	1	<0.1	<1	<0.2	1.5
TMC-2-16	2	7	71	<20	10	7	<20	6	130	<30	16	1.5	<5	108	21.1	179	8	2	1.2	<0.1	1	<0.2	1.6
OIV-3-41	1	17	203	<20	<5	17	<20	10	100	<30	17	1.3	<5	65	20.6	114	4.6	<2	0.8	<0.1	1	0.3	0.3
JLO-21-208	3	2	17	<20	7	1	<20	2	<10	50	16	1.8	<5	100	20.9	195	9.8	<2	1.4	<0.1	1	0.3	1
LDI-19-165	2	8	87	<20	<5	7	<20	7	<10	40	17	0.9	<5	84	24.2	204	9.5	<2	1.5	<0.1	1	<0.2	1.4
LDI-19-165dup	2	8	80	<20	12	7	<20	7	<10	40	17	1.4	<5	86	24.4	216	9.3	<2	1.2	<0.1	2	<0.2	1.5
LDI-19-165dif	0	0	2.10	0	0	0	0	0	0	0	0	10.87	0	0.59	0.21	1.43	0.53	0	5.56	0	16.67	0	1.72
DMO-33-288	3	19	188	<20	17	20	<20	12	80	40	18	1.3	<5	122	28.4	297	13.7	<2	2	<0.1	2	1.1	1.2
DMO-23-182	<1	22	252	30	38	21	<20	16	60	60	18	1.6	<5	36	15.8	52	1.9	<2	0.5	<0.1	<1	0.8	0.2
TMC-7-51	4	13	198	<20	9	16	<20	8	20	70	18	1.3	<5	162	24.9	261	13.3	3	2.2	<0.1	1	1.9	2.1
JLO-9-77	<1	6	57	<20	14	6	<20	10	30	40	19	0.7	<5	25	6.4	67	1.3	<2	0.6	<0.1	<1	1	0.6
JLO-9-77dup	-	-	-	-	-	-	-	10	-	-	-	-	-	-	-	-	-	-	-	-	-	-	-
JLO-9-77orig	-	-	-	-	-	-	-	10	-	-	-	-	-	-	-	-	-	-	-	-	-	-	-
JLO-9-77dif	-	-	-	-	-	-	-	0	-	-	-	-	-	-	-	-	-	-	-	-	-	-	-
11OIV4-51A	-	29	283	212	44	29	-	-	169	75	17	1.9	<5	25	15.4	60	1.5	<2	<0.5	<0.1	<1	<0.2	0.9
11OIV4-51B	-	26	275	149	38	21	-	-	166	79	18	1.8	<5	34	16.7	62	1.5	<2	<0.5	<0.1	<1	<0.2	0.8
11OIV4-51C	-	27	257	175	37	28	-	-	189	69	19	2.4	<5	25	16.3	64	1.7	<2	<0.5	<0.1	<1	<0.2	<0.1
11OIV4-54	-	31	290	215	40	37	-	-	147	63	17	1.9	<5	20	15.2	57	1.3	<2	<0.5	<0.1	<1	<0.2	0.2
11OIV4-55	-	28	303	154	41	25	-	-	173	79	19	2.2	<5	24	16.4	50	1.1	<2	<0.5	<0.1	<1	<0.2	2.1
11OIV4-59	-	37	240	264	42	58	-	-	105	72	15	2.2	<5	20	17.2	63	1.1	<2	<0.5	<0.1	<1	<0.2	1
11OIV4-60	-	41	277	201	44	36	-	-	126	72	17	2.5	<5	24	14.6	41	0.4	<2	<0.5	<0.1	<1	<0.2	<0.1
11OIV4-61	-	39	295	209	46	37	-	-	128	65	17	2.1	<5	19	14.6	41	0.5	<2	<0.5	<0.1	<1	<0.2	0.3
DMO-19-154	<1	19	289	<20	14	21	<20	8	190	110	22	1.5	<5	21	23.2	20	1.7	<2	<0.5	<0.1	<1	<0.2	0.6
JLO-22-215	<1	50	428	180	169	37	70	67	60	70	17	1.6	<5	22	16	28	1.2	<2	<0.5	<0.1	<1	<0.2	0.4
JLO-22-215dup	<1	50	429	170	37	70	70	70	60	70	17	1.8	<5	22	16.2	28	1.2	<2	<0.5	<0.1	<1	<0.2	0.4
JLO-22-215orig	<1	50	427	180	37	70	70	70	60	70	17	1.4	<5	21	15.8	27	1.2	<2	<0.5	<0.1	<1	<0.2	0.4
JLO-22-215dif	0	0	0.12	1.43	0	0	0	0	0	0	0	6.25	0	1.16	0.62	0.91	0	0	0	0	0	0	0
JLO-20-190	2	5	69	<20	18	5	<20	7	<10	40	20	1.5	<5	84	11.9	134	5.3	<2	1.3	<0.1	<1	0.3	1.1
JLO-14-141-2	2	38	322	290	297	36	70	69	160	90	13	2.5	<5	47	14	43	3.2	<2	<0.5	<0.1	<1	0.4	0.5

Table 1. Part II (continued)

Original sample no.	F-ICP-MS		Cr ppm	Cr ppm	Co ppm	Ni ppm	Ni ppm	Cu ppm	Zn ppm	Ga ppm	Ge ppm	As ppm	Rb ppm	Y ppm	Zr ppm	Nb ppm	Mo ppm	Ag ppm	In ppm	Sn ppm	Sb ppm	Cs ppm	
	Be ppm	Sc ppm																					V ppm
JLO-16-161-2	<1	29	294	40	44	26	20	26	60	100	18	1.8	<5	37	19.9	72	1.9	<2	<0.5	<0.1	<1	0.4	0.7
JLO-16-153	<1	32	312	70	79	29	30	21	120	80	17	1.3	<5	73	18.9	56	1.3	<2	<0.5	<0.1	<1	<0.2	1.2
JLO-16-153dup	<1	33	313	70	76	30	30	24	120	90	18	1.7	<5	76	19.6	57	1.3	<2	<0.5	<0.1	<1	<0.2	1.3
JLO-16-153dif	0	0.77	0.08	0	0.97	0.85	0	3.33	0	2.94	1.43	6.67	0	1.01	0.91	0.44	0	0	0	0	0	0	2
DMO50-505blank	<1	<1	<5	<20	11	<1	<20	<1	<10	<30	<1	1.5	<5	<1	<0.5	<1	<0.2	<2	<0.5	<0.1	<1	<0.2	<0.1
DMO-20-158	3	13	191	<20	<5	17	<20	8	10	130	18	1.1	7	165	24.1	233	11.8	<2	1.8	<0.1	2	2.9	8.1
DMO-33-286	1	19	113	<20	24	16	<20	10	150	160	13	0.9	33	86	21.2	182	8.8	<2	1.3	<0.1	<1	1.8	0.3
11JLO21-203	2	17	248	40		23	<20	-	70	40	20	2.2	25	92	24.9	177	11.4	<2	1.8	<0.1	<1	3.3	2
DMO-29-246	<1	28	285	<20	12	18	<20	5	180	100	19	1.3	<5	24	21.4	51	1.3	<2	<0.5	<0.1	<1	0.4	1.8
DMO-30-255	<1	31	380	30	40	23	20	18	200	90	18	1.8	<5	20	19.4	50	1.3	<2	<0.5	<0.1	<1	0.4	0.2
DMO-18-138	2	8	157	<20	8	18	<20	7	230	160	17	1	<5	101	24.8	85	4.2	<2	0.7	<0.1	<1	0.3	1
JLO-17-172	2	6	140	<20	8	7	<20	3	40	150	22	1.7	<5	32	26.8	123	6.7	<2	1	<0.1	1	1.1	0.6
LDI-12-96	2	6	160	<20	<5	8	<20	4	200	130	18	1.4	<5	235	24.1	111	4.4	<2	0.8	<0.1	1	1	10.6
LDI-12-97	2	5	139	<20	<5	4	<20	3	20	160	17	1.1	<5	49	21.5	85	3.5	<2	0.5	<0.1	1	0.5	2.7
LDI-12-97orig	-	-	-	-	-	-	-	3	-	-	-	-	-	-	-	-	-	-	-	-	-	-	-
LDI-12-97dup	-	-	-	-	-	-	-	3	-	-	-	-	-	-	-	-	-	-	-	-	-	-	-
LDI-12-97dif	-	-	-	-	-	-	-	0	-	-	-	-	-	-	-	-	-	-	-	-	-	-	-
DMO-38-337	<1	30	346	40	43	29	20	25	180	90	18	1.3	<5	36	18.2	51	1.6	<2	<0.5	<0.1	<1	0.4	1
JLO-5-42	<1	32	344	60	61	31	30	25	120	70	21	2.1	<5	<1	15.6	48	1.5	<2	<0.5	<0.1	<1	<0.2	0.5
DMO-3-23	<1	55	382	220	234	42	50	59	100	80	13	0.7	<5	32	14.7	33	1	3	<0.5	<0.1	<1	<0.2	0.7
JLO-16-162	1	20	207	<20	12	16	<20	8	50	90	19	1.2	<5	58	22.2	100	2.7	<2	0.7	<0.1	<1	0.3	0.8
LDI-12-95	<1	29	287	50	56	27	20	19	110	90	15	1.6	<5	18	19	60	2	<2	<0.5	<0.1	<1	<0.2	0.8
LDI-16-137	2	42	349	150	155	33	60	64	120	100	16	2	<5	51	19.7	72	2.3	<2	0.6	<0.1	<1	<0.2	0.5
JLO-23-227	<1	38	373	30	22	26	20	16	130	70	14	1.5	<5	7	15.7	33	0.7	<2	<0.5	<0.1	<1	0.3	0.1
11OIV1-2	-	46	278	376		47	88	-	127	66	14	2	<5	30	15.5	47	0.4	<2	<0.5	<0.1	<1	<0.2	0.3
11LDI18-145B	-	31	243	506		48	94	-	193	67	12	2	<5	43	11	28	<0.2	<2	<0.5	<0.1	<1	<0.2	0.9
11LDI18-147	-	27	280	279		39	82	-	210	76	15	1.9	<5	38	13.1	36	0.4	<2	<0.5	<0.1	<1	0.4	2.4
11LDI18-151	-	35	253	362		40	79	-	151	73	13	2.3	<5	51	13.2	43	0.7	<2	<0.5	<0.1	<1	<0.2	1.6
11LDI18-152	-	37	259	266		35	45	-	81	63	14	2.1	<5	52	12.2	33	0.6	<2	<0.5	<0.1	<1	0.3	0.8
11OIV3-39	-	36	288	178		40	30	-	40	42	16	2	<5	19	16.4	47	0.4	<2	<0.5	<0.1	<1	0.5	0.8
11OIV5-72	-	36	223	393		44	83	-	5	147	14	2.3	<5	24	10.8	28	<0.2	<2	<0.5	<0.1	1	1.4	0.6
11OIV5-73	-	29	274	283		38	75	-	12	99	14	2.1	<5	46	14.5	43	0.3	<2	<0.5	<0.1	<1	0.5	1.1
11OIV5-74	-	38	283	265		42	68	-	156	93	14	2.7	<5	43	14.4	44	0.2	<2	<0.5	<0.1	<1	<0.2	1.2
11OIV5-75	-	31	257	266		38	101	-	46	124	13	2.1	<5	46	14	45	0.3	<2	<0.5	<0.1	<1	<0.2	1.8
11JLO21-211-2	-	33	250	262		36	44	-	123	49	13	2.1	<5	45	12.3	30	0.7	<2	<0.5	<0.1	<1	0.7	0.9

Table 1. Part II (continued)

Analyte symbol: Unit: Detection limit:	Be	Sc	V	Cr	Cr	Co	Ni	Ni	Cu	Zn	Ga	Ge	As	Rb	Y	Zr	Nb	Mo	Ag	In	Sn	Sb	Cs	
	ppm	ppm	ppm	ppm	ppm	ppm	ppm	ppm	ppm	ppm	ppm	ppm	ppm	ppm	ppm	ppm	ppm	ppm	ppm	ppm	ppm	ppm	ppm	
Original sample no.	F-ICP-MS											F-ICP-MS												
	INAA	F-ICP-MS	TD-ICP	INAA	F-ICP-MS	TD-ICP	INAA	F-ICP-MS	TD-ICP	INAA	F-ICP-MS	TD-ICP	INAA	F-ICP-MS	TD-ICP	INAA	F-ICP-MS	TD-ICP	INAA	F-ICP-MS	TD-ICP	INAA	F-ICP-MS	TD-ICP
11JLO21-212	-	40	263	294	39	55	-	168	49	15	2.4	<5	38	13.2	36	0.8	<2	<0.5	<0.1	<1	0.3	0.7		
LDI-4-29	<1	45	422	30	37	40	41	500	140	18	1.8	<5	4	31.6	134	8.6	<2	0.9	<0.1	<1	<0.2	0.7		
LDI-4-29orig	<1	45	422	30	39	40	40	500	140	18	1.8	<5	4	31.4	133	8.5	<2	0.9	<0.1	<1	0.5	0.7		
LDI-4-29dup	<1	45	423	30	40	40	40	500	140	18	1.9	<5	4	31.7	135	8.8	<2	1	<0.1	<1	<0.2	0.8		
LDI-4-29dif	0	0	0.06	0	0.63	0	0	0	0	0	1.35	0	0	0.24	0.37	0.87	0	2.63	0	0	0	3.33		
MRG1standard	<1	54	541	430	440	79	170	179	130	220	19	1.4	<5	7	12.1	99	18.1	<2	1.2	<0.1	6	0.7	0.6	
MRG1expected	0.61	55	526	430	430	87	193	193	134	191	17	0.73	8.5	14	108	20	0.87	0.11			3.6	0.86	0.57	
MRG1dif	-0.5	0.7	0.0	0.6	-2.4	-3.2	-1.9	-0.8	3.5	2.8			-4.8	-3.6	-2.2	-2.5		41.6			12.5	-5.1	1.3	
SY3standard	24	8	55	<20	54	7	<20	7	20	250	33	2.4	18	197	675	351	182	<2	2.4	<0.1	7	3.3	2.6	
SY3orig	24	8	55	<20	7	<20	<20	20	250	33	2.2	18	195	675	357	183	<2	2.3	<0.1	8	0.2	2.6		
SY3dup	24	8	55	<20	8	<20	<20	10	250	32	2.6	19	198	674	345	180	<2	2.4	<0.1	7	6.4	2.7		
SY3expected	20	6.8	50	11	11	8.8	11	17	244	27	1.4	18.8	206	718	320	148	1	1.5			6.5	0.31	2.5	
SY3dif	4.5	4.1	2.4		-5.7			4.1	0.6	5.0	11.1	-1.1	-1.4	-1.5	2.7	5.3		10.5			5.2	-10.8	1.0	
SY3dif	4.5	4.1	2.4		-2.4			-13.0	0.6	4.2	15.0	0.3	-1.0	-1.6	1.9	4.9		11.5			1.9	45.4	1.9	

Abbreviations: F-ICP-MS, fusion-inductively coupled plasma-mass spectrometry; INAA, instrumental neutron activation analysis; TD-ICP, total digestion-inductively coupled plasma-mass spectrometry. Recommended values for CANMET standards shaded green, difference between original and duplicate or expected values shaded blue, informational values unshaded (Govindaraju, 1994).

Table 1. Part III: Trace and rare earth element analytical results for volcanic and intrusive rocks collected from the area covered by the Dease Lake (104J) and Cry Lake (104I) map sheets, northern British Columbia.

Original sample no.	F-ICP-MS														Ba ppm										
	Analyte:	La	Ce	Pr	Nd	Sm	Eu	Gd	Tb	Dy	Ho	Er	Tm	Yb		Lu	Hf	Ta	W	Ti	Pb	Bi	Th	U	Sr
Detection limit:	0.05	0.05	0.01	0.05	0.01	0.005	0.01	0.01	0.01	0.01	0.01	0.01	0.005	0.01	0.002	0.1	0.01	0.5	0.05	5	0.1	0.05	0.01	2	3
JLO-30-303-2	38.1	82.5	10.1	41.4	8.02	2.44	7.02	0.94	5.27	0.99	2.81	0.392	2.59	0.42	4	1.27	<0.5	0.17	9	<0.1	3.06	1.53	1486	1250	
LDI-9-73	53.7	102	11.2	41.4	7.55	2.39	5.47	0.86	4.4	0.82	2.14	0.303	1.94	0.31	4.8	6.74	<0.5	0.15	<5	<0.1	8.65	2.59	908	1042	
JLO-12-117	26.4	51.5	6.01	23.6	4.51	1.18	3.29	0.54	2.72	0.52	1.48	0.222	1.61	0.29	2.5	1.66	65	0.84	<5	<0.1	10.6	3.09	575	953	
JLO-12-117dup	-	-	-	-	-	-	-	-	-	-	-	-	-	-	-	-	-	-	-	-	-	-	-	-	
JLO-12-117orig	-	-	-	-	-	-	-	-	-	-	-	-	-	-	-	-	-	-	-	-	-	-	-	-	
JLO-12-117dif	-	-	-	-	-	-	-	-	-	-	-	-	-	-	-	-	-	-	-	-	-	-	-	-	
TMC-2-15	19.5	40.9	5.02	21.2	4.69	1.33	4.59	0.7	3.91	0.8	2.31	0.319	1.97	0.33	2.8	0.28	<0.5	0.21	11	0.1	3.94	1.49	714	974	
TMC-2-16	27.7	50.5	5.53	21.3	4.17	0.957	3.6	0.57	3.25	0.71	2.03	0.31	2.42	0.44	4.2	0.68	<0.5	0.41	8	<0.1	14	3.15	451	1091	
OIV-3-41	20.4	39.6	4.68	18.6	4.61	1.23	3.9	0.6	3.33	0.68	1.98	0.314	2.13	0.38	2.8	0.29	<0.5	0.15	<5	<0.1	5.26	2.26	537	1220	
JLO-21-208	35.2	63.6	6.64	24.6	4.17	0.931	3.37	0.51	3.02	0.69	2.15	0.324	2.53	0.45	4.7	0.77	<0.5	0.37	14	0.1	10.2	3.16	183	1489	
LDI-19-165	28.6	55.8	6.35	23.9	5.12	1.21	3.99	0.66	3.75	0.77	2.53	0.392	2.49	0.47	5	0.82	<0.5	0.32	9	<0.1	11.4	2.89	469	1077	
LDI-19-165dup	29.3	55.2	6.24	23.9	4.72	1.07	3.8	0.65	3.87	0.83	2.46	0.388	2.65	0.43	5.3	0.79	<0.5	0.37	10	<0.1	10.4	2.82	469	1071	
LDI-19-165dif	0.60	0.27	0.44	0	2.03	3.07	1.22	0.38	0.79	1.88	0.70	0.26	1.56	2.34	1.46	0.93	0	3.62	2.63	0	2.29	2.45	0	0.14	
DMO-33-288	40.1	79.4	9.14	34.9	7.25	1.35	6.15	0.85	4.74	0.94	2.73	0.443	3.1	0.51	6.8	0.98	<0.5	0.12	5	<0.1	17.2	5.64	657	971	
DMO-23-182	12.5	26.9	3.42	16.1	3.58	1.23	3.3	0.49	2.71	0.55	1.55	0.221	1.56	0.26	1.3	0.12	<0.5	0.33	<5	<0.1	2.67	1.63	554	726	
TMC-7-51	46.8	91.4	10.8	41	7.59	1.71	5.69	0.83	4.27	0.83	2.36	0.367	2.47	0.43	5.7	0.94	<0.5	0.23	8	<0.1	22.7	9.65	1244	1450	
JLO-9-77	5.3	12.2	1.71	7.01	1.45	0.525	1.66	0.22	1.14	0.22	0.63	0.092	0.57	0.09	1.8	0.09	<0.5	0.16	<5	<0.1	0.64	0.44	586	411	
JLO-9-77dup	-	-	-	-	-	-	-	-	-	-	-	-	-	-	-	-	-	-	-	-	-	-	-	-	
JLO-9-77orig	-	-	-	-	-	-	-	-	-	-	-	-	-	-	-	-	-	-	-	-	-	-	-	-	
JLO-9-77dif	-	-	-	-	-	-	-	-	-	-	-	-	-	-	-	-	-	-	-	-	-	-	-	-	
11OIV4-51A	15.1	31.1	3.9	17.5	4.19	1.2	3.68	0.57	3.23	0.64	1.73	0.258	1.67	0.26	1.6	0.1	25.3	<0.05	<5	<0.1	1.98	0.82	857	593	
11OIV4-51B	16.5	33.9	4.3	19	4.35	1.38	3.8	0.61	3.38	0.65	1.81	0.275	1.86	0.3	1.7	0.05	20.5	0.05	6	<0.1	1.99	0.81	823	984	
11OIV4-51C	16.3	33	4.12	17.6	3.97	1.2	3.7	0.58	3.23	0.61	1.74	0.269	1.79	0.28	1.7	0.05	18.1	<0.05	5	<0.1	2.01	0.9	399	630	
11OIV4-54	15.2	31.2	4.01	17.6	4.08	1.18	3.62	0.58	3.3	0.65	1.81	0.278	1.83	0.29	1.6	0.03	13.8	0.16	6	<0.1	1.92	0.77	660	550	
11OIV4-55	15.6	31.8	4.02	18.8	4.28	1.29	3.86	0.59	3.42	0.66	1.76	0.258	1.69	0.28	1.4	0.05	12.8	0.15	6	<0.1	1.67	0.65	634	915	
11OIV4-59	8.88	19.5	2.6	12.2	3.18	0.94	3.15	0.55	3.4	0.68	1.94	0.294	1.96	0.32	1.6	0.03	14	<0.05	<5	<0.1	1.08	0.45	414	395	
11OIV4-60	12.7	26.6	3.52	16	4.05	1.23	3.67	0.57	3.21	0.61	1.7	0.25	1.64	0.26	1.3	<0.01	9.9	<0.05	<5	<0.1	1.32	0.51	523	747	
11OIV4-61	13.2	27.2	3.54	16.2	3.87	1.31	3.58	0.53	3.14	0.6	1.72	0.244	1.58	0.25	1.2	<0.01	10.3	<0.05	<5	<0.1	1.4	0.56	574	662	
DMO-19-154	10.9	26.8	3.8	18.9	4.77	1.53	4.97	0.68	4.1	0.82	2.37	0.315	1.95	0.32	0.8	0.04	<0.5	0.08	<5	<0.1	0.6	0.25	750	370	
JLO-22-215	6.3	15.7	2.31	11.3	3.22	1.06	3.38	0.55	2.95	0.55	1.51	0.23	1.55	0.24	1	0.06	<0.5	0.08	<5	<0.1	1.06	0.6	351	244	
JLO-22-215dup	6.32	15.9	2.33	11	3.38	1.09	3.21	0.56	3.04	0.56	1.52	0.232	1.58	0.24	1	0.06	<0.5	0.08	<5	<0.1	1.08	0.65	351	245	
JLO-22-215orig	6.28	15.6	2.29	11.7	3.07	1.03	3.55	0.54	2.86	0.54	1.49	0.229	1.53	0.25	1	0.05	<0.5	0.07	<5	<0.1	1.03	0.55	351	244	
JLO-22-215dif	0.16	0.48	0.43	1.54	2.40	1.42	2.51	0.91	1.53	0.91	0.50	0.33	0.80	1.14	0	4.55	0	3.33	0	0	1.18	4.17	0	0.10	
JLO-20-190	18	34.8	4.16	16.1	2.96	0.888	2.33	0.36	1.97	0.39	1.2	0.179	1.1	0.18	3.7	0.45	<0.5	0.3	11	<0.1	5.57	1.6	921	1649	
JLO-14-141-2	10.7	22.6	2.88	12.1	3.05	0.91	2.76	0.46	2.56	0.51	1.41	0.193	1.29	0.22	1.3	0.14	<0.5	0.16	8	<0.1	2.69	1.02	356	616	
JLO-16-161-2	10.8	23.8	3.13	14.2	3.72	1.18	4.11	0.62	3.33	0.69	2.05	0.309	2.08	0.35	2	0.14	<0.5	0.1	<5	<0.1	1.8	0.92	414	461	
JLO-16-161-3	7.88	18.2	2.58	11.3	3.48	1.08	3.67	0.6	3.49	0.7	2.01	0.307	2.15	0.35	1.7	0.06	<0.5	0.15	<5	<0.1	1.3	0.62	529	1094	

Table 1. Part III (continued)

Analyte:	La	Ce	Pr	Nd	Sm	Eu	Gd	Tb	Dy	Ho	Er	Tm	Yb	Lu	Hf	Ta	W	Tl	Pb	Bi	Th	U	Sr	Ba
Unit:	ppm	ppm	ppm	ppm	ppm	ppm	ppm	ppm	ppm	ppm	ppm	ppm	ppm	ppm	ppm	ppm	ppm	ppm	ppm	ppm	ppm	ppm	ppm	ppm
Detection limit:	0.05	0.05	0.01	0.05	0.01	0.005	0.01	0.01	0.01	0.01	0.01	0.01	0.005	0.01	0.002	0.1	0.01	0.5	0.05	5	0.1	0.05	0.01	2
Original sample no.	F-ICP-MS																							
JLO-16-153 dup	8.24	18.5	2.53	13.3	3.51	1.15	3.58	0.55	3.35	0.68	1.96	0.308	2.17	0.36	1.6	0.05	<0.5	0.2	<5	<0.1	1.19	0.63	524	1075
JLO-16-153dif	1.12	0.41	0.49	4.07	0.21	1.57	0.62	2.17	1.02	0.72	0.63	0.08	0.23	0.85	1.52	4.55	0	7.14	0	0	2.21	0.4	0.24	0.44
DMO50-505blank	0.34	0.76	0.08	0.32	0.08	0.011	0.06	<0.01	0.02	<0.01	<0.01	<0.005	0.01	0	<0.1	<0.01	<0.5	<0.05	<5	<0.1	0.09	0.01	<2	3
DMO-20-158	41	79.9	9.36	35.2	7.27	1.76	5.27	0.78	3.89	0.76	2.41	0.35	2.44	0.38	5.1	0.85	<0.5	0.48	8	<0.1	19.7	7.67	359	1219
DMO-33-286	29	57.8	6.69	26.8	5.46	1.27	4.81	0.63	3.64	0.75	2.24	0.346	2.41	0.39	4.2	0.65	<0.5	0.23	9	<0.1	12.8	2.65	379	924
11JLO21-203	43.1	81.6	9.68	35.9	7.3	1.63	5.61	0.85	4.83	0.89	2.52	0.37	2.58	0.43	3.8	0.85	35.6	0.11	6	<0.1	11.6	4.14	1199	1652
DMO-29-246	8.36	19.4	2.67	13.3	3.54	1.21	3.9	0.61	3.8	0.8	2.34	0.349	2.37	0.38	1.5	0.1	<0.5	0.06	<5	<0.1	1.34	0.76	514	572
DMO-30-255	7.58	16.9	2.34	11.3	3.18	1.1	3.85	0.58	3.42	0.71	2.07	0.299	2.05	0.33	1.5	0.09	<0.5	0.08	<5	<0.1	1.3	0.73	279	1189
DMO-18-138	17.1	37.3	4.98	21.9	5.48	1.48	4.92	0.78	4.33	0.87	2.55	0.381	2.51	0.42	2.3	0.21	<0.5	0.22	10	<0.1	3.09	1.73	718	2365
JLO-17-172	19.9	41.8	5.3	24.8	5.71	1.55	4.71	0.83	4.32	0.93	2.78	0.423	2.8	0.45	3.3	0.49	<0.5	0.18	8	<0.1	3.21	2.03	341	835
LDI-12-96	19.1	37.9	4.74	20.2	4.69	1.51	4.56	0.7	3.98	0.82	2.45	0.392	2.56	0.4	2.9	0.26	<0.5	0.45	15	<0.1	3.34	2.17	564	3770
LDI-12-97	15	32.2	4.16	18.5	4.29	1.32	3.98	0.71	3.75	0.73	1.96	0.285	1.9	0.3	2.6	0.23	<0.5	0.1	<5	<0.1	2.87	0.52	151	465
LDI-12-97orig	-	-	-	-	-	-	-	-	-	-	-	-	-	-	-	-	-	-	-	-	-	-	-	-
LDI-12-97dup	-	-	-	-	-	-	-	-	-	-	-	-	-	-	-	-	-	-	-	-	-	-	-	-
LDI-12-97dif	-	-	-	-	-	-	-	-	-	-	-	-	-	-	-	-	-	-	-	-	-	-	-	-
DMO-38-337	7.68	17.5	2.39	11.5	2.87	0.997	3.14	0.52	3.19	0.68	1.97	0.293	1.9	0.3	1.5	0.09	<0.5	0.07	<5	<0.1	1.48	0.73	358	650
JLO-5-42	10.5	22.1	2.86	13	3.1	0.916	2.93	0.5	2.77	0.56	1.58	0.229	1.44	0.23	1.5	0.11	<0.5	<0.05	<5	0.1	1.98	0.84	98	20
DMO-3-23	6.84	15.1	2.01	9.69	2.88	0.856	2.89	0.47	2.7	0.54	1.5	0.223	1.59	0.24	1.1	0.05	<0.5	0.33	<5	<0.1	1.24	0.48	341	834
JLO-16-162	11.6	26.3	3.47	15.9	3.79	1.24	3.98	0.65	3.75	0.82	2.43	0.368	2.37	0.38	2.8	0.2	<0.5	0.14	<5	<0.1	2.53	1.53	529	592
LDI-12-95	7.72	17	2.39	11.3	3.18	1.01	3.31	0.57	3.38	0.67	2	0.293	1.87	0.3	1.8	0.06	<0.5	0.06	<5	<0.1	1.2	0.58	411	236
LDI-16-137	8.86	21.2	2.81	13.4	3.58	1.04	3.6	0.63	3.39	0.7	1.94	0.296	1.89	0.3	2	0.14	<0.5	0.11	<5	<0.1	1.42	0.73	925	1378
JLO-23-227	3.98	9.58	1.49	7.7	2.16	0.833	2.64	0.47	2.9	0.61	1.73	0.261	1.66	0.25	1.1	0.04	<0.5	<0.05	<5	<0.1	0.48	0.34	423	243
11OIV1-2	6.13	14.8	2.22	10.2	2.98	0.953	3.3	0.53	3.2	0.65	1.86	0.276	1.73	0.26	1.4	0.03	18.6	<0.05	<5	<0.1	1.05	0.41	258	369
11LDI18-145B	4.65	10.4	1.48	7.22	2.05	0.699	2.42	0.4	2.34	0.47	1.34	0.204	1.37	0.22	0.9	<0.01	23.3	<0.05	<5	<0.1	0.79	0.4	453	572
11LDI18-147	4.5	9.74	1.45	6.94	2.01	0.76	2.54	0.43	2.67	0.56	1.59	0.243	1.57	0.25	1.0	0.06	25.4	0.05	<5	<0.1	0.67	0.33	588	716
11LDI18-151	8.41	19.6	2.59	11.4	2.8	0.868	2.74	0.46	2.75	0.52	1.44	0.219	1.45	0.23	1.2	0.01	22.2	0.05	<5	<0.1	1.61	0.62	506	1013
11LDI18-152	7.89	17.6	2.33	9.78	2.4	0.762	2.55	0.43	2.54	0.52	1.5	0.213	1.37	0.22	1.0	0.05	18.1	<0.05	23	0.2	1.64	0.67	349	487
11OIV3-39	8.53	17.5	2.42	11.4	3.19	0.974	3.48	0.55	3.34	0.68	1.93	0.281	1.8	0.28	1.4	0.07	33.3	<0.05	<5	<0.1	0.84	0.88	352	214
11OIV5-72	4.4	9.72	1.36	6.43	1.77	0.76	2.06	0.34	2.08	0.41	1.2	0.184	1.24	0.19	0.9	<0.01	22.7	<0.05	14	<0.1	0.77	1.81	365	430
11OIV5-73	7.28	15.9	2.16	10.2	2.83	0.785	2.84	0.48	2.88	0.6	1.62	0.241	1.67	0.27	1.3	<0.01	10.1	0.07	7	<0.1	1.28	0.89	416	539
11OIV5-74	7.62	17.6	2.49	12	3.12	0.992	3.33	0.56	3.22	0.61	1.76	0.271	1.74	0.27	1.4	<0.01	21.8	<0.05	9	<0.1	1.67	0.71	504	699
11OIV5-75	8.18	19	2.58	12.1	3.07	0.933	3.1	0.51	2.93	0.58	1.67	0.233	1.49	0.23	1.4	0.14	20.8	0.13	7	<0.1	1.72	0.84	563	544
11JLO21-211-2	4.25	9.75	1.4	6.98	2.06	0.729	2.4	0.41	2.48	0.5	1.39	0.212	1.38	0.22	0.9	<0.01	18.9	<0.05	<5	<0.1	0.84	0.42	488	597
11JLO21-212	4.56	10.8	1.58	7.59	2.11	0.777	2.44	0.43	2.73	0.55	1.56	0.228	1.44	0.23	1.1	0.02	22.5	<0.05	<5	<0.1	0.94	0.4	404	447
LDI-4-29	8.22	22.6	3.34	16.5	4.84	1.62	5.52	0.96	5.53	1.13	3.2	0.451	3.02	0.51	3.3	0.6	<0.5	<0.05	<5	<0.1	0.83	0.34	196	49
LDI-4-29orig	8.41	22.7	3.29	16.1	4.8	1.67	5.42	0.95	5.53	1.13	3.16	0.446	2.97	0.52	3.1	0.59	<0.5	<0.05	<5	<0.1	0.86	0.35	196	50
LDI-4-29dup	8.02	22.5	3.39	16.9	4.89	1.58	5.61	0.97	5.53	1.13	3.25	0.455	3.06	0.51	3.5	0.61	<0.5	<0.05	<5	<0.1	0.8	0.33	196	49

Table 1. Part III (continued)

Analyte:	La	Ce	Pr	Nd	Sm	Eu	Gd	Tb	Dy	Ho	Er	Tm	Yb	Lu	Hf	Ta	W	Tl	Pb	Bi	Th	U	Sr	Ba	
Unit:	ppm	ppm	ppm	ppm	ppm	ppm	ppm	ppm	ppm	ppm	ppm	ppm	ppm	ppm	ppm	ppm	ppm	ppm	ppm	ppm	ppm	ppm	ppm	ppm	
Detection limit:	0.05	0.05	0.01	0.05	0.01	0.005	0.01	0.01	0.01	0.01	0.01	0.005	0.01	0.002	0.1	0.01	0.5	0.05	5	0.1	0.05	0.01	2	3	
F-ICP-MS																									
Original sample no.																									
LDI-4-29dif	1.19	0.22	0.75	1.21	0.46	1.38	0.86	0.52	0	0	0.70	0.50	0.75	0.54	3.03	0.83	0	0	0	0	1.81	1.47	0	0.51	
MRG1standard	9.21	25.7	3.63	17.2	4.28	1.5	4.13	0.55	2.8	0.51	1.2	0.133	0.77	0.12	3.8	0.87	<0.5	<0.05	9	0.2	0.83	0.3	270	52	
MRG1expected	9.8	26	3.4	19.2	4.5	1.39	4	0.51	2.9	0.49	1.12	0.11	0.6	0.12	3.76	0.8	0.3	0.055	10	0.13	0.93	0.24	266	61	
MRG1dif	-1.6	-0.3	1.6	-2.7	-1.3	1.9	0.8	1.9	-0.9	1.0	1.7	4.7	6.2	0.0	0.3	2.1			-2.6	10.6	-2.8	5.6	0.4	-4.0	
SY3standard	1210	2150	208	690	119	17	104	19.2	117	25.5	77.7	11.3	63.9	8.51	10.2	24.7	<0.5	1.31	394	0.4	991	667	302	450	
SY3orig	1210	2150	208	688	118	17	106	19.2	118	24.8	77.1	11.3	63.6	8.54	9.8	24.9	<0.5	1.27	372	0.3	984	670	301	448	
SY3dup	1220	2150	209	691	119	17	102	19.3	117	26.1	78.3	11.3	64.3	8.47	10.6	24.4	<0.5	1.34	415	0.4	999	663	303	452	
SY3expected	1340	2230	223	670	109	17	105	18	118	29.5	68	11.6	62	7.9	9.7	30	1.1	1.5	133	0.8	1003	650	302	450	
SY3dif	-2.5	-0.9	-1.7	0.7	2.0	0.0	0.2	1.6	0.0	-4.3	3.1	-0.7	0.6	1.9	0.3	-4.6		-4.2	23.7	-22.7	-0.5	0.8	-0.1	-0.1	
SY3dif	-2.3	-0.9	-1.6	0.8	2.2	0.0	-0.7	1.7	-0.2	-3.1	3.5	-0.7	0.9	1.7	2.2	-5.1		-2.8	25.7	-16.7	-0.1	0.5	0.1	0.1	

Abbreviation: F-ICP-MS, fusion-inductively coupled plasma-mass spectrometry

Recommended values for CANMET standards shaded green, difference between original and duplicate or expected values shaded blue, informational values unshaded (Govindaraju, 1994).

were pulverized in a mild steel mill to prevent Cr and Ni contamination and analyzed for major and trace elements using a lithium metaborate plus lithium tetraborate fusion technique. The milled samples were mixed with a flux of lithium metaborate and lithium tetraborate and fused in an induction furnace at 1150°C. The melt was immediately poured into a solution of 5% nitric acid and mixed continuously until completely dissolved. This aggressive fusion technique ensures that the entire sample, including resistate phases, dissolves. The samples were analyzed for major oxides using an inductively coupled plasma–atomic emission spectrometry (ICP-AES) technique and trace elements, including rare earth elements, using an inductively coupled plasma–mass spectrometry (ICP-MS) technique. Nickel was analyzed by an ICP-MS technique following a four acid digestion; beginning with hydrofluoric acid, followed by a mixture of nitric and perchloric acid, and finally hydrochloric acid dissolution. With this near total digestion technique, certain resistate phases (e.g., zircon, monazite, sphene, gahnite, chromite, cassiterite, rutile and barite) may be only partly solubilized. Chromium was analyzed using instrumental neutron activation analysis (INAA), whereby samples were irradiated in a nuclear reactor and, following a 7-day decay, gamma rays measured on germanium detectors. Analytical techniques and detection limits for all major oxides and trace elements are listed in Table 1. Two blind CANMET standards (see Govindaraju, 1994 for reference values) and two blind duplicates of the jaw-crushed material were included in the sample batch. Additional internal quality control duplicate analyses from Activation Labs on powdered samples are also listed in Table 1.

During sample collection every effort was taken to avoid altered material. We removed any obvious surface weathering, veins and amygdules. However, petrography shows that many of the samples are significantly altered, making the use of major elements for classification or discrimination of petrochemical environments suspect. Geochemical results presented in Table 1 show acceptable total weight percent values (between 96.3 and 101 wt. %) and loss on ignition values (between 0.28 and 7.8 wt. %).

Geochemical Suites Description and Results

Tsaybahe Group

The Tsaybahe Group comprises mafic volcanic rocks interlayered with Middle Triassic limestone, chert and siliceous thin-bedded sedimentary rocks. It is exposed in the canyon of the Stikine River (Read, 1984) and extends north into the Dease Lake area (Gabrielse, 1998; Logan et al., 2012b, c). The unit is characterized by thick accumulations (200–270 m) of crowded augite-phyric basalt, basalt breccia and volcanic-derived clastic rocks. The basalt contains 1–3 mm, dark green euhedral pyroxene phenocrysts (20–30%) and 0.5–1 mm, stubby white plagioclase laths (5–20%) within an aphanitic, often vesicular or amygdaloidal

green- or orange-weathering groundmass (Figure 3a, b, plane-polarized light and crossed nicols). The basalt is deformed and hornfelsed to a biotite-bearing metavolcanic rock adjacent to the Middle Jurassic Pallen Creek pluton (Logan et al., 2012c), but elsewhere it is only weakly altered to lower greenschist mineral assemblages that do not define a penetrative foliation.

Eight samples of flow breccia, two samples of tuff breccia and one sample from a massive flow plot in subalkalic basalt and andesite fields on the Zr/Ti versus Nb/Y classification diagram of Pearce (1996) (Figure 4a). All the samples plot as shoshonite or high-K calcalkaline series on the SiO₂ versus K₂O diagram of Peccerillo and Taylor (1976) and in the arc field (Shervais, 1982) and calcalkaline-arc basalt field (Wood, 1980) on tectonic discrimination diagrams (Figure 4b, c, d). Typical of basalts formed in arc settings, all Tsaybahe samples are characterized on a primitive mantle-normalized spider diagram by light rare earth element (LREE) and Th enrichment, and Nb and Ti depletion, (Figure 5a). However, the Tsaybahe volcanic rocks show distinctly less LREE enrichment than Late Triassic Stuhini basalts from the Iskut River (Zagorevski et al., 2012) and Dease Lake areas (Figure 5a–f).

Stuhini Group

Souther (1971) included all Late Triassic volcanic and sedimentary rocks that lie above a Middle Triassic unconformity and below the Late Triassic Sinwa limestone in the Stuhini Group. In the Dease Lake area the Stuhini Group has been subdivided into six Late Triassic map units (Gabrielse, 1998; Logan et al., 2012b; Figure 2). From oldest to youngest these are as follows: unit 1, a basal volcanoclastic unit of mixed, massive to thickly bedded reworked volcanic rocks and rare aphyric basalt flows that generally fine upward into unit 2, a well-bedded section of sandstone-siltstone with Late Triassic bivalves. Units 1 and 2 are overlain by unit 3, a thick package of coarse plagioclase-phyric basalt and andesite flows, and subordinate clastic rocks, and unit 4, isolated, thin units of alkalic, sparse K-feldspar-phyric latite and maroon basalt. Unit 5 is composed of pyroxene±plagioclase-phyric monomict flow breccia and rare pillowed basalt that are interlayered within unit 6, an upper unit of massive volcanoclastic rocks containing plagioclase- and pyroxene-phyric basalt clasts. Four petrologically distinct suites of volcanic rocks are recognized within the Late Triassic Stuhini Group: aphyric basalt (TKSv), plagioclase porphyry (TKSpp), latite porphyry (TKSmv) and pyroxene porphyry (TKSpx, Figure 2). The plagioclase and latite porphyries of units 3 and 4 respectively are mainly restricted to the medial stratigraphic position between reworked volcanoclastic rocks of units 2 and 5. The aphyric and pyroxene-phyric basalt suites are concentrated in the area south of Ross Creek (Logan et al., 2012c), within the upper volcanoclastic unit 6.

Aphyric Basalt

Aphyric basalt and basaltic andesite flows occur throughout the massive, cliff-forming units of chaotic, nongraded, matrix-supported cobble to pebble volcanic conglomerate and associated volcanic sandstone that dominate the lower and uppermost parts of the Stuhini Group. The volcanic

rocks include aphyric to sparsely plagioclase-phyric coherent flows, tuff breccia and lapilli tuff.

Four samples of aphyric flow and one sample of sparse plagioclase-phyric crystal tuff were collected for analyses. Two are from the area south of Ross Creek and two are from the upper volcaniclastic unit north of the Tanzilla River at

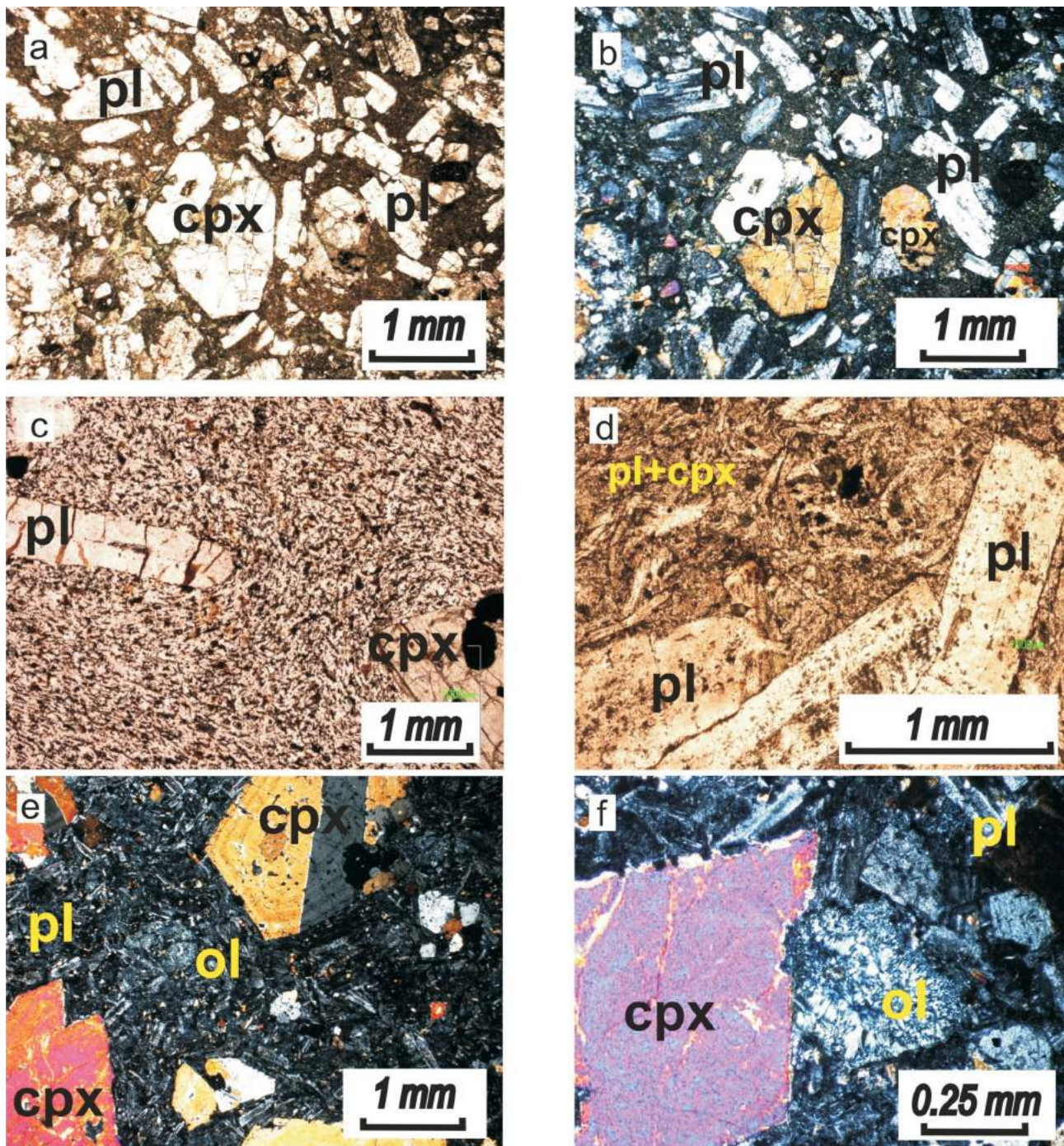


Figure 3. Photomicrographs of Middle Triassic, Late Triassic and Early to Middle Jurassic volcanic units: **a)** Tsaybahe crowded augite-plagioclase-phyric basalt breccia, plane-polarized light; **b)** crossed nicols; **c)** Stuhini sparse plagioclase-phyric andesite; **d)** Stuhini crowded plagioclase-phyric basalt; **e)** Hazelton pyroxene-phyric basalt with twinned and oscillatory zoned inclusion-rich augite phenocrysts in plagioclase-pyroxene-olivine matrix (crossed nicols); **f)** detail of intergrown augite and olivine crystal in Hazelton pyroxene-phyric basalt (crossed nicols). Abbreviations: cpx, clinopyroxene; ol, olivine; pl, plagioclase.

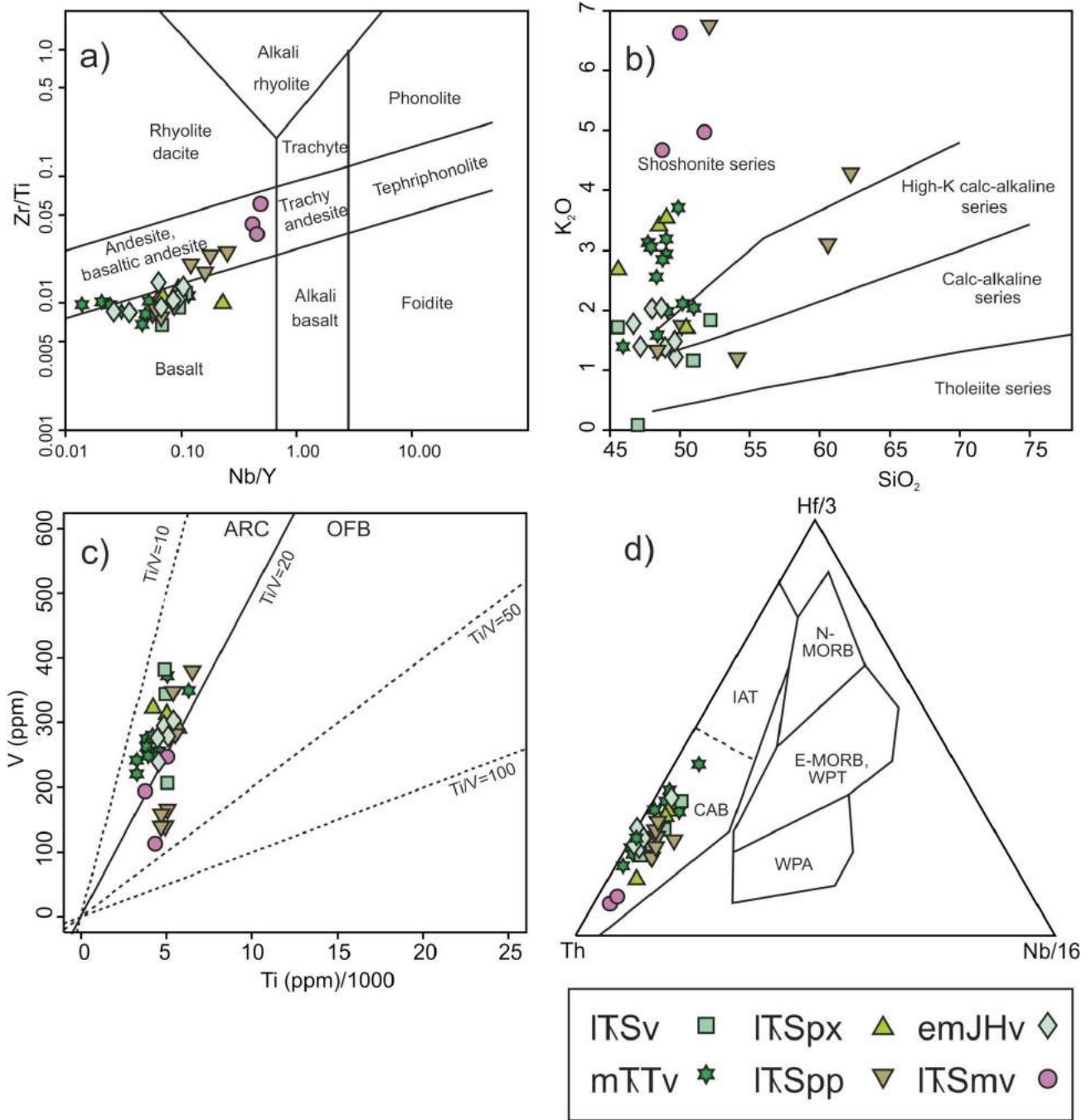


Figure 4. a) A Nb/Y vs. Zr/Ti classification diagram (Pearce, 1996) showing compositional range and classification for the Middle and Late Triassic and Early to Middle Jurassic basalt in the study area. **b)** Classification diagram based on SiO₂ vs. K₂O (after Peccerillo and Taylor, 1976), used to distinguish shoshonitic, high-K calcalkaline, calcalkaline and tholeiitic series rocks. **c)** Tectonic discrimination diagram based on Ti vs. V (after Shervais, 1982), used to distinguish between arc and non-arc basalt. **d)** Tectonic discrimination diagram based on Th-Hf-Ta (after Wood, 1980), used to identify arc basalt (high Th/Ta) and theoretically distinguish between calcalkaline basalt, tholeiitic-arc basalt and non-arc basalts. Symbols: mTTv, Middle Triassic Tsaybahe pyroxene-phyric basalt; ITKsv, Late Triassic Stuhini aphyric basalts; ITKspp, Late Triassic Stuhini plagioclase-phyric basalt and andesite; ITKsmv, Late Triassic Stuhini latite porphyry; ITKspx, Late Triassic Stuhini pyroxene-phyric basalt; emJHv, Early to Middle Jurassic Hazelton pyroxene-phyric basalt. Abbreviations: CAB, calcalkaline basalt; IAT, island arc tholeiite; E- and N-MORB, enriched and normal mid-ocean-ridge basalt; OFB, ocean floor basalt; WPA, within-plate alkaline basalts; WPT, within-plate tholeiites.

Tatsho Creek (Logan et al., 2012c). All plot in the subalkalic basalt field on the Zr/Ti versus Nb/Y classification diagram (Figure 4a) of Pearce (1996) and occupy either the shoshonite, high-K, calcalkaline or the tholeiite series fields on the SiO₂ versus K₂O diagram (Figure 4b) of Peccerillo and Taylor (1976). All samples occupy the arc field (Shervais, 1982) and calcalkaline-arc basalt field

(Wood, 1980) on tectonic discrimination diagrams (Figure 4c, d).

The aphyric volcanic samples are characterized by LREE and Th enrichment, and Nb and Ti depletion, characteristic of basalts formed in arc settings (Figure 5b). The primitive mantle-normalized trace-element profiles of the basalts

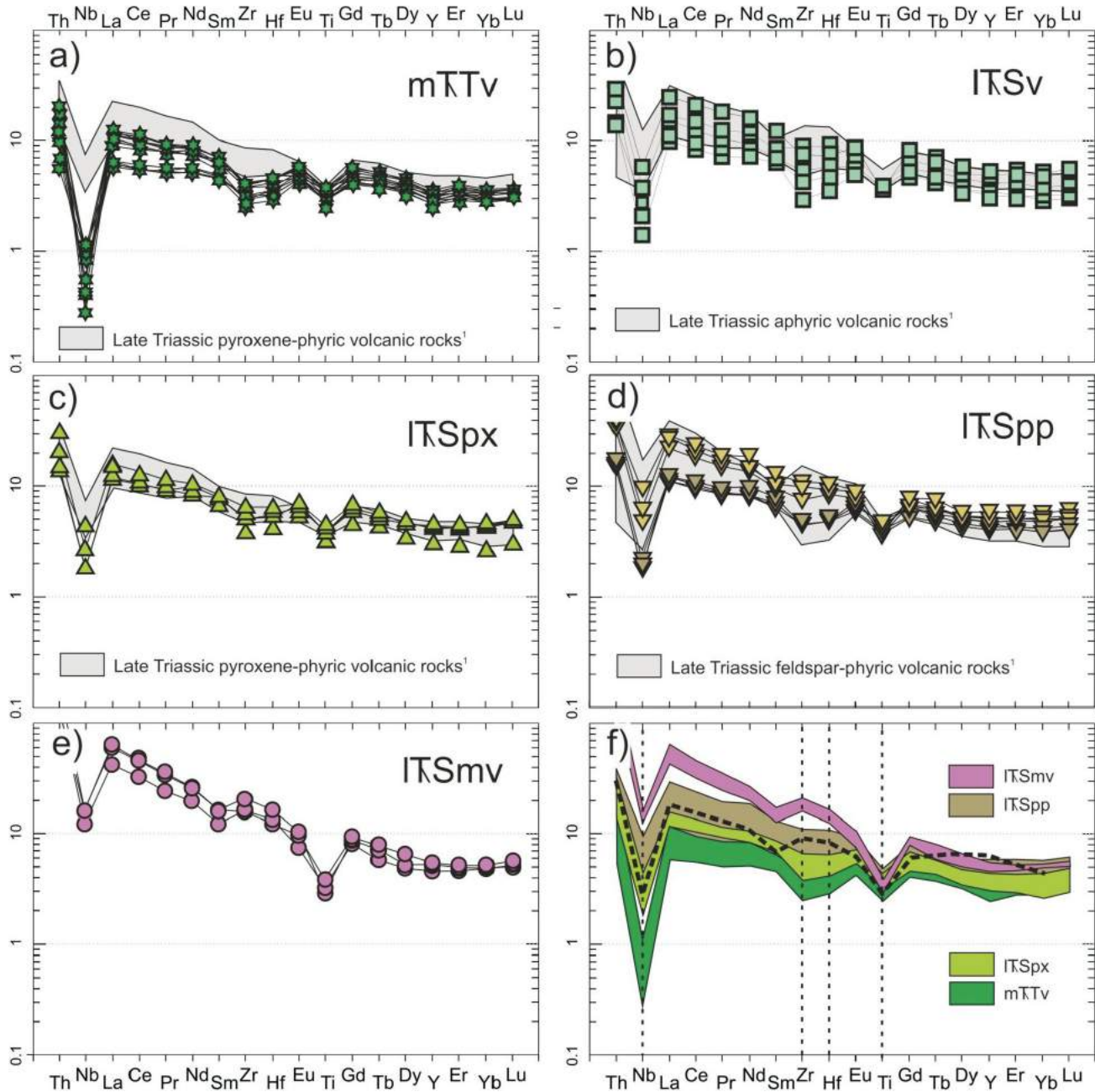


Figure 5. Primitive mantle-normalized (Sun and McDonough, 1989) extended trace-element profiles of Middle Triassic Tsaybahe and Late Triassic Stuhini Group volcanic rocks: **a)** Middle Triassic Tsaybahe pyroxene-phyric basalt; **b)–e)** Late Triassic Stuhini aphyric basalt, pyroxene-phyric basalt, plagioclase-phyric andesite (light green) and basalt (dark olive), and maroon latite; **f)** compares Tsaybahe pyroxene-phyric basalt, Stuhini pyroxene-phyric basalt, plagioclase-phyric basalt and maroon basalts with a typical calcalkaline island-arc basalt from the Sunda Arc (Jenner, 1996). Data source for comparison: ¹ Zagorevski et al., 2012. Symbols: mTTv, Middle Triassic Tsaybahe pyroxene-phyric basalt; ITSv, Late Triassic Stuhini aphyric basalts; ITSpp, Late Triassic Stuhini plagioclase-phyric basalt and andesite; ITSmv, Late Triassic Stuhini latite porphyry; ITSpx, Late Triassic Stuhini pyroxene-phyric basalt.

overlap aphyric basalts assigned to the Stuhini Group in adjacent areas (Figure 5b, f; Zagorevski et al., 2012) and also overlap pyroxene- and plagioclase-phyric volcanic rocks from this study.

Pyroxene Porphyry

Pyroxene-rich basalt flows, breccias and volcanoclastic rocks are the hallmark of the Stuhini Group in northwestern Stikinia (Souther, 1971, 1972; Anderson, 1993; Gabrielse, 1998; Logan et al., 2000), and these rock types are widely developed in the study area. Coherent pyroxene-phyric flow units are often complexly interlayered with coarse breccias dominated by pyroxene-phyric fragments and finer epiclastic units rich in pyroxene crystals; generally these units could not be mapped separately. Where distinguished, single flow units are commonly from 5 to 12 m thick, with massive interiors and flow-top breccias. Some flows contain subequal amounts of pyroxene and plagioclase phenocrysts, and others contain a much greater quantity of pyroxene than plagioclase phenocrysts. The former are characterized by typically quite small (~1–2 mm), subequal proportions of green or black pyroxene and white plagioclase laths in a fine-grained green groundmass. The pyroxene-phyric flows consist of typically 2–8 mm euhedral augite phenocrysts in a fine-grained green groundmass.

Three samples from massive flows (plus one duplicate) were collected from the area south of Ross Creek and northeast of the headwaters of Auguschidle Creek. They plot in the subalkalic basalt field on the Zr/Ti versus Nb/Y classification diagram (Figure 4a) of Pearce (1996). All plot as shoshonite or high-K calcalkaline series on the SiO₂ versus K₂O diagram (Figure 4b; Peccerillo and Taylor, 1976) and in the arc field (Shervais, 1982) and calcalkaline-arc basalt field (Wood, 1980) on tectonic discrimination diagrams (Figure 4c, d). The Stuhini pyroxene±plagioclase porphyry samples are characterized by LREE and Th enrichment, and Nb and Ti depletion, characteristic of basalts formed in arc settings (Figure 5c). The primitive mantle-normalized trace-element profiles of the basalts overlap pyroxene-phyric basalts assigned to the Stuhini Group in adjacent areas (Figure 5c, f; Zagorevski et al., 2012).

Plagioclase Porphyry

The plagioclase-phyric volcanic rocks of unit 3 comprise two suites: basaltic plagioclase-phyric flows occur south of the Tanzilla River and andesitic plagioclase-phyric flow rocks occupy isolated areas north of the Tanzilla River (Logan et al., 2012b, c). Both suites contain white- to cream-coloured, 2–8 mm euhedral plagioclase phenocrysts, sometimes glomeroporphyritic, in a fine-grained green groundmass. Intergrown fine plagioclase microlites and clinopyroxene form a pilotaxitic matrix, with sparse pyroxene phenocrysts present locally in the basaltic unit (Figure 3c, d). The plagioclase porphyry flows are generally coherent, unlike fragment-rich breccia deposits of the

monolithic pyroxene porphyries. Immediately south of Ross Creek (Logan et al., 2012b, c) is a distinctive trachytic plagioclase-phyric andesite characterized by glassy 4–7 mm euhedral plagioclase crystals (5–7%) within a very fine grained dark groundmass that locally is glassy green and characterized by spherulitic devitrification textures.

Four of the eight samples plot in subalkalic basalt field and four in the andesite field on the Zr/Ti versus Nb/Y classification diagram (Figure 4a) of Pearce (1996). On an AFM diagram (not shown) the basalt samples are transitional tholeiitic to calcalkaline and the andesite calcalkaline. The andesite samples plot as shoshonite or high-K calcalkaline series, the basalts plot as high-K calcalkaline or calcalkaline series on the SiO₂ versus K₂O diagram (Figure 4b; Peccerillo and Taylor, 1976). The plagioclase-phyric andesite has low vanadium abundances and Ti/V ratios and plot as non-arc basalts on Ti versus V diagram (Figure 4c; Shervais, 1982). These samples illustrate the problem of using this classification with calcalkaline lavas which commonly crystallize magnetite (strong affinity for V) leading to erroneous arc/non-arc designations. However, in the Zr versus Ti (Pearce and Cann, 1973, not shown) and Th-Hf-Nb (Wood, 1980) diagrams, which are unaffected by vanadium compatibility during calcalkaline basalt evolution, all plagioclase porphyry samples occupy calcalkaline arc basalt fields (Figure 4d).

The plagioclase porphyries are characterized by LREE and Th enrichment, and Nb and Ti depletion, characteristic of arc volcanism (Figure 5d). The primitive mantle-normalized trace-element profiles of the basalt are distinctly less enriched in LREE compared to the andesite and both overlap plagioclase-phyric basalts assigned to the Stuhini Group in adjacent areas (Figure 5d; Zagorevski et al., 2012).

Latite Porphyry

Unit 4 of the Stuhini Group includes a distinctive package of salmon pink-weathering porphyritic latite, trachyte, maroon-weathering basalt and epiclastic rocks that crop out northwest of Hluey Lakes along the Hluey Lake service road adjacent to a pink-weathering syenite porphyry (Logan et al., 2012a, c). Samples were collected from a maroon-coloured basalt/latite with abundant calcite-filled vesicles, and phenocrysts of plagioclase, K-feldspar and biotite in an aphanitic groundmass that locally displays trachytic flow textures. It is uncertain whether the potassic character of these rocks is primary or can be attributed entirely to alteration from the adjacent syenite.

Chemical data for the maroon volcanic unit is under-represented (n=3) and suspect due to the substantial amounts of secondary alteration minerals visible in thin section (K-feldspar, hematite, carbonate, chlorite and quartz) and reflected in the high loss-on-ignition (LOI) values (Table 1).

The samples plot as subalkalic andesite to alkali basalt/trachyte on the Zr/Ti versus Nb/Y classification diagram (Figure 4a) of Pearce (1996). All three samples plot as shoshonite on the SiO₂ versus K₂O diagram (Peccerillo and Taylor, 1976) and in the calcalkaline arc basalt fields (Shervais, 1982; Wood, 1980) on tectonic discrimination diagrams (Figure 4b, c, d).

The primitive mantle-normalized extended trace-element plots for the maroon volcanic unit are characterized by LREE and Th enrichment, and Nb and Ti depletion, characteristic of arc volcanic rocks (Figure 5e). This unit has distinctly higher LREE abundances than any of the other mafic volcanic units studied, and also has elevated Zr and Hf values, implying either an evolved source or extensive liquid evolution (Münker et al., 2004).

Hazelton Group

The Early to Middle Jurassic rocks exposed east of Gnat Pass are subdivided into five units (Anderson, 1983; Gabrielse, 1998; Iverson et al., 2012a, Figures 2, 3). Units 1–3 include 625 m of thin- or medium-bedded volcanic lithic arenite with pebble conglomerate, siltstone and siliceous ash tuff layers. Units 4 and 5 are monomict pyroxene-phyric basalt conglomerate and flow breccias. Five samples of basalt from the uppermost flow unit (unit 5 of Iverson et al., 2012a) and two samples of basaltic dikes cutting unit 3 sedimentary rocks (Iverson et al., 2012a, Figure 2) were analyzed. The basalt is a coarse pyroxene±plagioclase±olivine-phyric rock (Figure 3e, f) typically unaltered, but containing a lower greenschist-facies metamorphic assemblages of epidote, calcite, quartz and pyrite. It is dominated by euhedral, twinned and oscillatory-zoned inclusion-rich clinopyroxene phenocrysts within a finer grained groundmass of plagioclase laths, subhedral to anhedral olivine phenocrysts pseudomorphed by serpentine and chlorite, pyroxene and opaque minerals.

All Hazelton Group samples plot in the subalkalic basalt field on the Zr/Ti versus Nb/Y classification diagram (Figure 4a) of Pearce (1996) and cluster around the overlapping fields of shoshonite and high-K calcalkaline series at SiO₂ concentrations between 47–50 wt. % on the SiO₂ versus K₂O diagram (Figure 4b) of Peccerillo and Taylor (1976). They plot in the arc field (Shervais, 1982) and calcalkaline-arc basalt field (Wood, 1980) on tectonic discrimination diagrams (Figure 4c, d) and are tholeiitic to transitional calcalkaline on the AFM diagram (Irvine and Baragar, 1971, not shown).

The Hazelton pyroxene porphyry samples are characterized by Th and LREE enrichment, and Nb and Ti depletion, characteristic of basalts formed in arc settings (Figure 6a). The trace-element profiles overlap pyroxene-phyric basalts assigned to the Stuhini Group in the study area and adjacent areas (Figure 6a).

Discussion

The primitive mantle-normalized extended trace-element plots for the Middle Triassic, Late Triassic and Early to Middle Jurassic basalt samples all display LREE and Th enrichment, and Nb and Ti depletion, characteristic of calcalkaline basalts generated in an arc setting or derived from the subarc lithospheric mantle (Jenner, 1996; Figures 5, 6).

The normalized trace-element profiles for the LREEs (La, Ce, Pr, Nd) and middle rare earth elements (MREEs; Sm, Eu, Gd, Tb, Dy, Ho) for the Middle and Late Triassic basalts show progressive enrichment with progressively higher stratigraphic position and relatively younger ages (increasing La/Sm_{NC}; Table 2). The heavy rare earth element (HREE; Er, Tm, Yb, Lu) abundances overlap but conform to this same pattern. The normalized trace-element profiles for the Late Triassic basalts overlap Late Triassic aphyric, pyroxene-phyric and plagioclase-phyric basalts of the Stuhini Group in adjacent areas (Figure 5; Zagorevski et al., 2012). The relatively high concentration of P₂O₅ in the Tsaybahe pyroxene porphyries (approximately twice the average wt. % P₂O₅ of the other basalt units) is hard to reconcile with these being the most primitive type of basalt (i.e., highest MgO, Cr and Ni and lowest Y and Nb/Zr; Table 2).

The normalized trace-element profiles for the Hazelton basalts east of Gnat Pass overlap the profiles from Early Jurassic Cold Fish and Mount Brock basalts of the Hazelton Group (Figure 6b) in the adjacent Spatsizi map area (104H; Evenchick and Thorkelson, 2005) but not the profiles from rift basalts of the Early to Middle Jurassic Willow Ridge Complex (Figure 6c) in the Telegraph Creek map area (104G; Barresi and Dostal, 2005). The Willow Ridge Complex comprises a bimodal suite of basalt, basaltic andesite and rhyolite, which spans the Toarcian-Aalenian boundary (Early Jurassic to Middle Jurassic) and is age-equivalent to the host rocks at Eskay Creek (Alldrick et al., 2004). Primitive mantle-normalized trace-element abundance patterns for the mafic rocks from the Willow Ridge Complex show a slight enrichment of LREEs sloping from Th to Sm and a slight negative Nb anomaly (Barresi and Dostal, 2005).

The primitive mantle-normalized extended trace-element plots for the Hazelton basalt also overlap the plots for intrusive rocks of the age-equivalent Middle Jurassic Three Sisters pluton (van Straaten et al., 2012b), but more precisely match the trace-element pattern for hornblende-augite gabbro of the Late Triassic Beggerlay Creek pluton (van Straaten et al., 2012b; Figure 6d). The relative abundances and trace-element patterns of the Hazelton basalt also overlap those of Late Triassic pyroxene-phyric basalt from the study area and the Iskut River area (Figure 6a; Zagorevski et al., 2012), suggesting that successive Mesozoic arc mag-

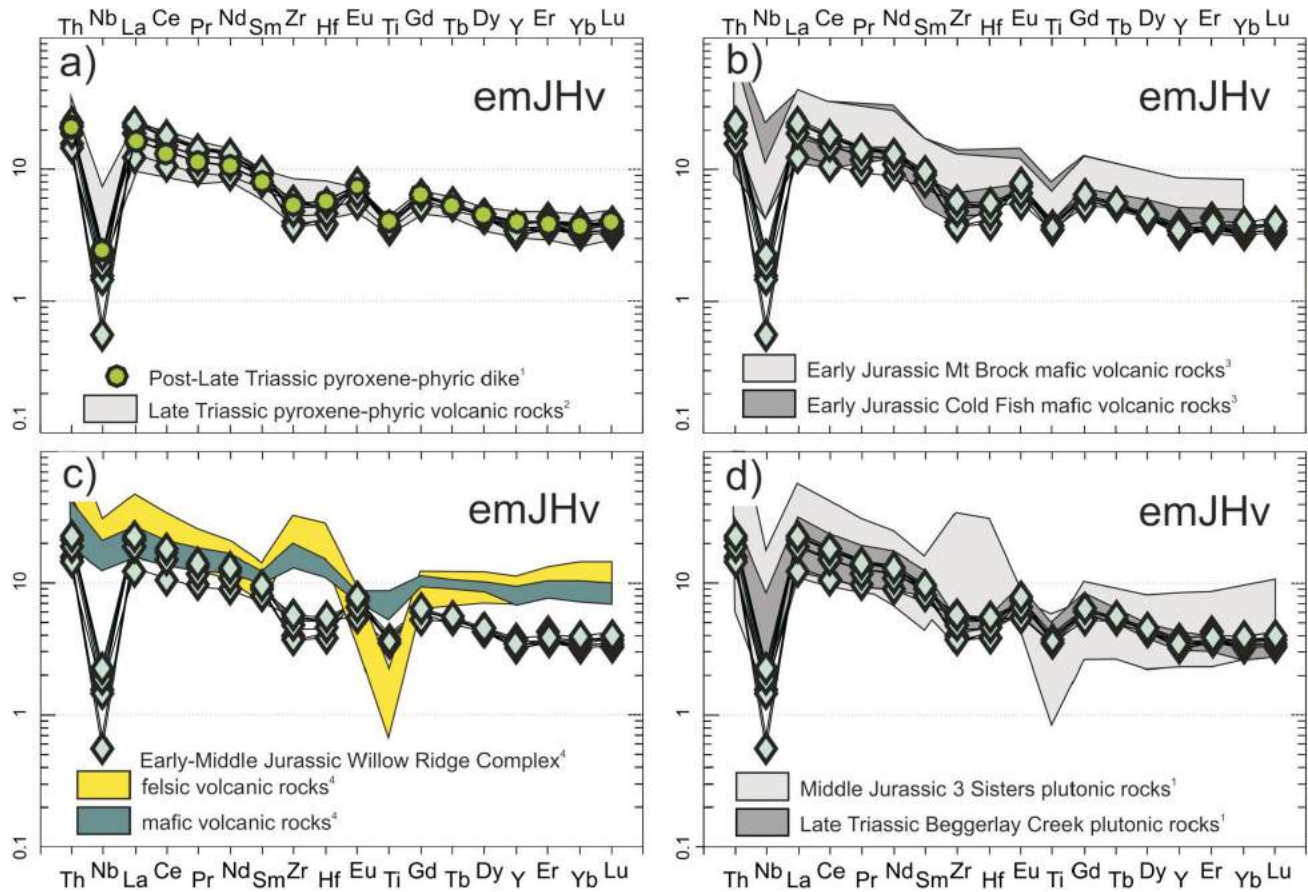


Figure 6. Primitive mantle-normalized (Sun and McDonough, 1989) extended trace-element profiles of Early to Middle Jurassic Hazelton Group pyroxene-phyric basalt. Data sources for comparison: ¹ van Straaten et al. (2012b); ² Zagorevski et al. (2012), plus analyses from this study; ³ Evenchick and Thorkelson (2005); ⁴ Barresi and Dostal (2005). Symbol: emJHv, Early to Middle Jurassic Hazelton pyroxene porphyry.

mas were likely generated from similar subduction-modified mantle and erupted rapidly with relatively short residence time in the upper crust to prevent substantial fractionation or assimilation of more felsic material. In addition, a post-Late Triassic pyroxene-phyric dike that cuts the ca. 221 Ma Cake Hill pluton (Anderson and Bevier, 1992; van Straaten et al., 2012a) has an identical primitive mantle-normalized trace-element pattern as the Hazelton basalt, suggesting it may represent a feeder dike to the overlying Hazelton Group volcanic rocks (Figure 6a).

Alteration Guides for Exploration

Major element mobility of K₂O, Na₂O and CaO during even low-grade alteration is well established (Davies et al., 1979) and, in areas peripheral to magmatic centres, understanding element mobility can provide exploration vectors within hydrothermal alteration zones (Barrett and MacLean, 1993). The latite porphyry and plagioclase-phyric andesite suites of the Stuhini Group are characterized by elevated K₂O and/or Na₂O related to secondary alteration. The latite porphyry samples have high LOI values, mobile low field strength elements (LFSEs) including Th, and are

located adjacent to a potassic intrusive centre and Cu-Au prospect (MINFILE 104J 013; BC Geological Survey, 2012). However, alteration in the plagioclase-phyric andesite samples is more subtle, with only slightly elevated LOI values and no nearby intrusion or geophysical expression

Table 2. Selected element concentrations and ratios for the Middle Triassic, Late Triassic and Early to Middle Jurassic basalts collected from the area covered by the Dease Lake (104J) and Cry Lake (104I) map sheets, northwestern British Columbia.

Unit ¹	La/Sm _{NC}	La/Sm _{NC} ²	P ₂ O ₅ ² (wt %)	Ni/Cr ²	Y ² (ppm)	Nb/Zr ²
emJHv	1.80–2.65	2.32	0.29	0.172	15.4	0.02
ITSmv	3.42–3.81	3.42	0.33	0.375	22.2	0.04
ITSpp	1.52–2.62	2.04	0.3	0.417	21.5	0.04
ITSv	1.53–2.18	1.77	0.25	0.376	17.3	0.03
ITSpx	1.46–2.26	1.69	0.34	0.387	19.2	0.02
mTTv	1.33–2.12	1.59	0.52	0.269	13.2	0.01

¹ Unit: mTTv, Middle Triassic Tsaybahe pyroxene-phyric basalt; ITSv, Late Triassic Stuhini aphyric basalts; ITSpp, Late Triassic Stuhini plagioclase-phyric basalt and andesite; ITSmv, Late Triassic Stuhini latite porphyry; ITSpx, Late Triassic Stuhini pyroxene-phyric basalt; emJHv, Early to Middle Jurassic Hazelton pyroxene porphyry

² Average values

Abbreviation: NC, chondrite normalized

(Aeroquest Airborne, 2012) indicative of a buried intrusion in the area. Regional geochemical data (Jackaman, 2012) for the area south of Ross Creek, where three of the four plagioclase-phyric andesite samples originate, indicate two streams draining the area with anomalous copper values (within the 95th percentile) that warrant follow-up.

Conclusions

Middle Triassic, Late Triassic and Early to Middle Jurassic pyroxene-phyric volcanic rocks occur in northern Stikinia (Brown et al., 1992; Gabrielse, 1998; Iverson et al., 2012a). In this study, they have similar physical characteristics, mineralogy and chemistry, which make them difficult to distinguish from one another without independent age constraints. They have primitive mantle-normalized extended trace-element patterns that display LREE and Th enrichment, and Nb and Ti depletion, characteristic of calcalkaline basalts generated in an arc setting. These geochemical patterns overlap those from correlative units in adjacent areas (Evenchick and Thorkelson, 2005; Zagorevski et al., 2012) and are also similar to those from Late Triassic and Middle Jurassic calcalkaline plutonic suites in the region (van Straaten et al., 2012b).

The Early to Middle Jurassic pyroxene-phyric rocks of the Hazelton Group east of Gnat Pass are the same age as the Willow Ridge Complex (Alldrick et al., 2004) and the basalts of the Salmon River Formation (Anderson and Thorkelson, 1990) at Eskay Creek. However, the basalts at Eskay Creek have a tholeiitic, N-MORB signature (Barrett and Sherlock, 1996), which is different from the calcalkaline, arc signature of the volcanic rocks east of Gnat Pass.

Acknowledgements

Geoscience BC provided financial and logistical support for the field collection of samples in 2011 and follow-up analyses in 2012. Many thanks to C. Sluggett for cheerfully and efficiently managing the project. This paper was substantially improved through review by P. Scharizza.

References

Aeroquest Airborne (2012): Report on a helicopter-borne magnetic survey (Aeroquest Job #11-046) for Geoscience BC; Geoscience BC, Report 2012-2, 11 p.

Allen, D.G., Panteleyev, A. and Armstrong, A.T. (1976): Galore Creek; *in* Porphyry Deposits of the Canadian Cordillera, A. Sutherland Brown, (ed.), Canadian Institute of Mining and Metallurgy, Special Volume 15, p. 402–414.

Alldrick, D.J., Stewart, M.L., Nelson, J.L. and Simpson, K.A. (2004): Tracking the Eskay Rift through northern British Columbia—geology and mineral occurrences of the upper Iskut River area; BC Ministry of Energy, Mines and Natural Gas, Geological Fieldwork 2003, Paper 2004-01, p. 1–18.

Anderson, R.G. (1983): Geology of the Hotailuh batholith and surrounding volcanic and sedimentary rocks, north-central

British Columbia; Carleton University, Ottawa, Ph.D. thesis, 669 p.

Anderson, R.G. (1984): Late Triassic and Jurassic magmatism along the Stikine Arch and the geology of the Stikine batholith, north-central British Columbia; *in* Current Research, Part A, Geological Survey of Canada, Paper 84-1A, p. 67–73.

Anderson, R.G. (1993): A Mesozoic stratigraphic and plutonic framework for northwestern Stikinia (Iskut River area), northwestern British Columbia; *in* Mesozoic Paleogeography of the Western United States, II: Los Angeles, CA, G. Dunne and K. McDougall (ed.), Society of Economic Paleontologists and Mineralogists, Pacific Section, p. 477–494.

Anderson, R.G. and Bevier, M.L. (1992): New Late Triassic and Early Jurassic U-Pb zircon ages from the Hotailuh batholith, Cry Lake map area, north-central British Columbia; *in* Radiogenic Age and Isotope Studies, Report 6, Geological Survey of Canada, Paper 92-2, p. 145–152.

Anderson, R.G. and Thorkelson, D.J. (1990): Mesozoic stratigraphy and setting for some mineral deposits in Iskut River map area, northwestern British Columbia; *in* Current Research, Part E, Geological Survey of Canada, Paper 90-1E, p. 131–139.

Barr, D.A., Fox, P.E., Northcote, K.E. and Preto, V.A. (1976): The alkaline suite porphyry deposits: a summary; *in* Porphyry Deposits of the Canadian Cordillera, A. Sutherland Brown (ed.), Canadian Institute of Mining and Metallurgy, Special Volume 15, p. 359–367.

Barresi, T. and Dostal, J. (2005): Geochemistry and petrography of Upper Hazelton Group volcanics: VHMS-favourable stratigraphy in the Iskut River and Telegraph Creek map areas, northwestern British Columbia; *in* Geological Fieldwork 2004, BC Ministry of Energy, Mines and Natural Gas, Paper 2005-01, p. 39–47.

Barrett, T.J. and MacLean, W.H. (1994): Chemostratigraphy and hydrothermal alteration in exploration for VHMS deposits in greenstones and younger volcanic rocks; *in* Alteration and Alteration Processes associated with Ore-forming Systems, D.R. Lentz (ed.), Geological Association of Canada, Short Course Notes, v. 11, p. 433–467.

Barrett, T.J. and Sherlock, R.L. (1996): Geology, lithochemistry and volcanic setting of the Eskay Creek Au-Ag-Cu-Zn deposit, northwestern British Columbia; *Exploration and Mining Geology*, v. 5, p. 339–368.

BC Geological Survey, (2012): MINFILE BC mineral deposits database; BC Ministry of Energy, Mines and Natural Gas <<http://minfile.ca/>> [November 2012].

Brown, D.A., Greig, C.J., Bevier, M.L. and McClelland, W.C. (1992): U-Pb zircon ages for the Hazelton Group and Cone Mountain and Limpoke plutons, Telegraph Creek map area, northwestern British Columbia: age constraints on volcanism and deformation; *in* Radiogenic Age and Isotopic Studies, Report 6; Geological Survey of Canada, Paper 92-2, p. 153–162.

Brown, D.A., Gunning, M.H. and Greig, C.J. (1996): The Stikine Project: geology of Western Telegraph Creek map area, northwestern British Columbia; BC Ministry of Energy, Mines and Natural Gas, Bulletin 95, 175 p.

Davies, J.F., Grant, R.W.E. and Whitehead, R.E.S. (1979): Immobile trace elements and Archean volcanic stratigraphy in the Timmins mining area, Ontario; *Canadian Journal of Earth Sciences*, v. 16, p. 305–311.

- Evenchick, C.A. and Thorkelson, D.J. (2005): Geology of the Spatsizi River map area, north-central British Columbia; Geological Survey of Canada, Bulletin 577, 189 p.
- Fox, P.E. (1975): Alkaline rocks and related mineral deposits of the Quesnel Trough, British Columbia, Cordilleran Section; Geological Association of Canada, Symposium on Intrusive Rocks and Related Mineralization of the Canadian Cordillera, Program and Abstracts, p. 12.
- Gabrielse, H. (1998): Geology of Cry Lake and Dease Lake map areas, north-central British Columbia; Geological Survey of Canada, Bulletin 4, 118 p.
- Govindaraju, (1994): 1994 compilation of working values and sample description for 383 geostandards; Geostandards Newsletter, v. 18, issue S1, p. 1–158.
- Henderson, C.M. and Perry, D.G. (1981): A Lower Jurassic heteropod bryozoan and associated biota, Turnagain Lake, British Columbia; Canadian Journal of Earth Sciences, v. 18, p. 457–468.
- Irvine, T.N. and Baragar, W.R. (1971): A guide to the chemical classification of the common volcanic rocks; Canadian Journal of Earth Sciences, v. 8, p. 523–548.
- Iverson, O., Mahoney, J.B. and Logan, J.M. (2012a): Dease Lake Geoscience Project, Part IV: Tsaybahe group: lithological and geochemical characterization of Middle Triassic volcanism in the Stikine Arch, north-central British Columbia; *in* BC Ministry of Energy, Mines and Natural Gas, Geological Fieldwork 2011, Report 2012-1, p. 17–22, URL <http://www.empr.gov.bc.ca/Mining/Geoscience/PublicationsCatalogue/Fieldwork/Documents/2011/03_Iverson_2011.pdf> [November 2012].
- Iverson, O., Mahoney, J.B. and Logan, J.M. (2012b): Reassessment of Triassic and Jurassic volcanic strata in the Dease Lake region, northern British Columbia; Geological Association of Canada, Pacific Section, Cordilleran Tectonics Workshop 2012, Victoria British Columbia, poster.
- Jackaman, W. (2012): QUEST-Northwest Project: new regional geochemical survey and sample reanalysis data (NTS 104F, G, H, I, J), northern British Columbia; *in* Geoscience BC Summary of Activities 2011, Report 2012-1, p. 15–18, URL <http://www.geosciencebc.com/i/pdf/SummaryofActivities2011/SoA2011_Jackaman.pdf> [October 2012].
- Jenner, G.A. (1996): Trace element geochemistry of igneous rocks: geochemical nomenclature and analytical geochemistry; *in* Trace Element Geochemistry of Volcanic Rocks: Applications for Massive Sulfide Exploration, D.A. Wyman (ed.), Geological Association of Canada, Short Course Notes, v. 12, p. 51–77.
- Logan, J.M. and Bath, A.B. (2006): Geochemistry of Nicola Group basalt from the central Quesnel Trough at the Latitude of Mount Polley (NTS 093A/5, 6, 11, 12), central British Columbia; *in* BC Ministry of Energy, Mines and Natural Gas, Geological Fieldwork 2005, Report 2006-1, p. 83–98, URL <<http://www.empr.gov.bc.ca/Mining/Geoscience/PublicationsCatalogue/Fieldwork/Documents/2005/Paper09.pdf>> [November 2012].
- Logan, J.M., Drobe, J.R. and McClelland, W.C. (2000): Geology of the Forrest Kerr-Mess Creek area, northwestern British Columbia (NTS 104B/10, 15 & 104G/2 & 7W); BC Ministry of Energy, Mines and Natural Gas, Bulletin 104, 132 p.
- Logan, J.M., Diakow, L.J., van Straaten, B.I., Moynihan, D.P. and Iverson, O. (2012a): QUEST-Northwest Mapping, BC Geological Survey Dease Lake Geoscience Project, northern British Columbia; *in* Geoscience BC, Summary of Activities 2011, Report 2012-1 p. 5–14, URL <http://www.geosciencebc.com/i/pdf/SummaryofActivities2011/SoA2011_Logan.pdf> [November 2012].
- Logan, J.M., Moynihan, D.P. and Diakow, L.J. (2012b): Dease Lake Geoscience Project, Part I: Geology and mineralization of the Dease Lake (104J/8) and east-half of the Little Tuya River (104J/7E) map sheets, northern British Columbia; *in* Geological Fieldwork 2011, BC Ministry of Energy, Mines and Natural Gas, Geological Fieldwork 2011, Report 2012-1, p. 23–44, URL <http://www.empr.gov.bc.ca/Mining/Geoscience/PublicationsCatalogue/Fieldwork/Documents/2011/04_Logan_2011.pdf> [November 2012].
- Logan, J.M., Moynihan, D.P., Diakow, L.J. and Van Straaten, B.I. (2012c): Dease Lake - Little Tuya River Geology, NTS 104J/ 08 & 07E; Geoscience BC Map 2012-08-1 and BC Ministry of Energy, Mines and Natural Gas, Open File Map 2012-04, 1:50 000 scale.
- Lueck, B.A. and Russell, J.K. (1994): Silica-undersaturated, zoned alkaline intrusions within the British Columbia cordillera; *in* Geological Fieldwork 1993, BC Ministry of Energy, Mines and Natural Gas, Paper 1994-1, p. 311–315.
- Marsden, H. and Thorkelson, D.J. (1992): Geology of the Hazelton volcanic belt in British Columbia: implications for the Early to Middle Jurassic evolution of Stikinia; Tectonics, v. 11 (6), p. 1266–1287.
- Massey, N.W.D., MacIntyre, D.G., Desjardins, P.J. and Cooney, R.T. (2005): Digital geology map of British Columbia: whole province; BC Ministry of Energy, Mines and Natural Gas, GeoFile 2005-1.
- Moynihan, D.P. and Logan, J.M. (2012): Age, emplacement and mineralization of the Cretaceous Snow Peak pluton; *in* Geological Fieldwork 2011, BC Ministry of Energy, Mines and Natural Gas, Paper 2012-1, p. 69–74.
- Münker, C., Wömer, G., Yogodzinski, G. and Churikova, T. (2004): Behaviour of high field strength elements in subduction zones: constraints from Kamchatka-Aleutian arc lavas; Earth and Planetary Science Letters, v. 224, p. 275–293.
- Panteleyev, A., Bailey, D.G., Bloodgood, M.A. and Hancock, K.D. (1996): Geology and mineral deposits of the Quesnel River-Horse fly map area, central Quesnel Trough, British Columbia (NTS 93A/5, 6, 7, 11, 12, 13; 93B/9, 16; 93G/1; 93H/4); BC Ministry of Energy, Mines and Natural Gas, Bulletin 97, p. 156.
- Pearce, J.A. and Cann, J.R. (1973): Tectonic setting of basic volcanic rocks determined using trace element analyses; Earth and Planetary Science Letters, v. 19, p. 290–300.
- Peccerillo, A. and Taylor, S.R. (1976): Geochemistry of Eocene calc-alkaline volcanic rocks from the Kastamonu area, northern Turkey; Contribution to Mineralogy and Petrology, v. 58, p. 63–81.
- Read, P.B. (1983): Geology, Classy Creek (104J/2E) and Stikine Canyon (104J/1W), British Columbia; Geological Survey of Canada, Open File Map 940, 1:50 000 scale.
- Read, P.B. (1984): Geology, Klastine River (104G/16E), Ealue Lake (104H/13W), Cake Hill (104I/4W) and Stikine Canyon (104J/1E), British Columbia; Geological Survey of Canada, Open File Map 1080, 1:50 000 scale.
- Read, P.B. and Psutka, J.F. (1990): Geology, Ealue Lake east-half (104H/13E) and Cullivan Creek (104H/14) map areas, Brit-

- ish Columbia; Geological Survey of Canada, Open File Map 2241, 1:50 000 scale.
- Scott, J.E., Richards, J.P., Heaman, L.M., Creaser, R.A. and Salazar, G.S. (2008): The Schaft Creek porphyry Cu-Mo-(Au) deposit, northwestern British Columbia; *Exploration and Mining Geology*, v. 17, p. 163–196.
- Shervais, J.W. (1982): Ti-V plots and the petrogenesis of modern and ophiolitic lavas; *Earth and Planetary Science Letters*, v. 59, p. 101–118.
- Simpson, K.A. (2012): QUEST-Northwest: Geoscience BC's new minerals project in northwest British Columbia (104G, 104J, parts of NTS 104A, B, F, H, I, K, 103O, P); *in* Geoscience BC, Summary of Activities 2011, Report 2012-1, p. 1–4. URL <http://www.geosciencebc.com/i/pdf/SummaryofActivities2011/SoA2011_Simpson.pdf> [November 2012].
- Souther, J.G. (1971): Geology and mineral deposits of Tulsequah map-area, British Columbia; Geological Survey of Canada, Memoir 362, p. 76.
- Souther, J.G. (1972): Telegraph Creek map area, British Columbia; Geological Survey of Canada, Paper 71-44, p. 38.
- Sun, S.-s. and McDonough, W.F. (1989): Chemical and isotopic systematics of oceanic basalts: implications for mantle composition and processes; *in* Magmatism in the Ocean Basins, A.D. Saunders and M.J. Norry (ed.), Geological Society Special Publication 42, p. 313–345.
- van Straaten, B.I., Logan, J.M. and Diakow, L.J. (2012a): Dease Lake Geoscience Project, Part II: preliminary report on the Mesozoic magmatic history and metallogeny of the Hotailuh batholith and surrounding volcanic and sedimentary rocks; *in* Geological Fieldwork 2011, BC Ministry of Energy, Mines and Natural Gas, Report 2012-1, p. 99–120. URL <http://www.empr.gov.bc.ca/Mining/Geoscience/PublicationsCatalogue/Fieldwork/Documents/2011/08_van_Straaten_2011.pdf> [November 2012].
- van Straaten, B.I., Logan, J.M. and Diakow, L.J. (2012b): Mesozoic magmatic history and metallogeny of the Hotailuh batholith (NWBC); BC Ministry of Energy, Mines and Natural Gas, GeoFile 2012-08 and Geoscience BC Map 2012-10-1, 1:50 000 scale.
- Wood, D.A. (1980): The application of the Th-Hf-Ta diagram to problems of tectonomagmatic classification and to establishing the nature of crustal contamination of basaltic lavas of the British Tertiary volcanic province; *Earth and Planetary Science Letters*, v. 50, p. 11–30.
- Woodsworth, G.J., Anderson, R.G. and Armstrong, R.L. (1991): Plutonic regimes; *in* Geology of the Cordilleran Orogen in Canada, H. Gabrielse and C.J. Yorath (ed.), Geological Survey of Canada, Geology of Canada, no. 4, p. 491–531.
- Zagorevski, A., Mihalynuk, M.G. and Logan, J.M. (2012): Geochemical characteristics of Mississippian to Pliensbachian volcanic and hypabyssal rocks in the Hoodoo Mountain area (NTS104B/14E); *in* Geological Fieldwork 2012, BC Ministry of Energy, Mines and Natural Gas, Paper 2012-1, p. 121–134. URL <http://www.empr.gov.bc.ca/Mining/Geoscience/PublicationsCatalogue/Fieldwork/Documents/2011/09_Zagorevski_2011.pdf> [November 2012].

Re-Release of the Mineral Deposit Research Unit's Iskut River Area Maps (1989–1993), Northwestern British Columbia (NTS 104B/08, /09, /10, Parts of 104B/01, /07, /11)

P.D. Lewis, Eldorado Gold Corporation, Vancouver, BC, peterl@eldoradogold.com

C.J.R. Hart, Mineral Deposit Research Unit, University of British Columbia, Vancouver, BC

K.A. Simpson, Geoscience BC, Vancouver, BC

Lewis, P.D., Hart, C.J.R. and Simpson, K.A. (2013): Re-release of the Mineral Deposit Research Unit's Iskut River area maps (1989–1993), northwestern British Columbia (NTS 104B/08, /09, /10, parts of 104B/01, /07, /11); in Geoscience BC Summary of Activities 2012, Geoscience BC, Report 2013-1, p. 33–36.

Introduction

Between 1989 and 1993, the Mineral Deposit Research Unit (MDRU) at the University of British Columbia conducted the study *Metallogenesis of the Iskut River Area, Northwestern British Columbia* (the Iskut River Area Project). This project was undertaken in response to intense interest by the mineral exploration and mining industry and the need for an integrated approach to metallogenesis and discovery in the region. The original maps associated with this project were released in Lewis et al. (2001) as Adobe Acrobat® PDF files of AutoCAD® line drawings. Geoscience BC and MDRU are re-releasing these highly detailed maps to the public in a modern GIS format, which will be a valuable contribution to the BC exploration industry.

Iskut River Area Project

The MDRU's Iskut River Area Project was sponsored by 17 companies, and received additional financial support from the Natural Sciences and Engineering Research Council of Canada (NSERC) and the Science Council of British Columbia. The study included collaboration with the Geological Survey of Canada and the British Columbia Geological Survey, and involved one research associate, three postdoctoral fellows and five M.Sc. students at the University of British Columbia. Supporting companies included at the time BP Canada, Inc., International Corona Corp., Homestake Canada Ltd., Kenrich Mining Corp., Noranda Inc., Teck Corporation, Cominco Ltd., Granges Inc., Kennecott Canada Inc., Lac Minerals Ltd., Placer Dome Inc., and partial support from Ecstall Mining Corp., Newhawk Gold Mines Ltd., Skyline Gold Corp., Gulf In-

ternational Minerals Ltd., Prime Resources Group Inc. and Solomon Resources Ltd.

The Iskut River area (Figure 1) is a relatively small (approximately 100 by 60 km) but metallogenically well-endowed segment of the Canadian Cordillera. It is host to a range of economically significant ore deposits and styles of mineralization including porphyry Cu and Cu-Au, skarn Cu-Au, shear-hosted Au-Ag, epithermal Au-Ag and volcanic-hosted massive sulphide-sulphosalt systems. The past-producing Eskay Creek, Snip and Johnny Mountain gold mines are within the project area. To the south are the past-producing Granduc volcanogenic massive sulphide deposit and the active Stewart mining camp. Recent exploration in the region continues to demonstrate the significant discovery potential of the region and in particular the substantial Au and Cu-Au endowment. Discovery successes are evident at projects such as Brucejack, Snowfield and Kerr-Sulphurets-Mitchell (KSM).

The MDRU's Iskut River Area Project was established to develop a better understanding of the variety of mineral occurrences, their settings and controls within the Iskut River area. The project integrated numerous deposit-specific studies and metallogenic research with regional structural and stratigraphic mapping. Details of the project are principally contained within a 26 chapter volume published by MDRU in June 2001 (Lewis et al., 2001). Other project details were published as theses and as provincial and federal geological survey papers.

The major deliverable of the project, 1:50 000 maps of NTS 104B/08, /09, /10 and parts of 104B/01, /07, /11, resulted from four years of intense field mapping led by the senior author. These maps were based on a lithofacies mapping approach and integrated lithochemical sampling, radiometric dating and biostratigraphic studies to unravel the complex volcano-sedimentary succession in the Iskut River area. Also incorporated were data from industry supporters of the project. Detailed geological information sup-

Keywords: *Iskut River, northwestern British Columbia, volcanic facies mapping, structural mapping*

This publication is also available, free of charge, as colour digital files in Adobe Acrobat® PDF format from the Geoscience BC website: <http://www.geosciencebc.com/s/DataReleases.asp>.

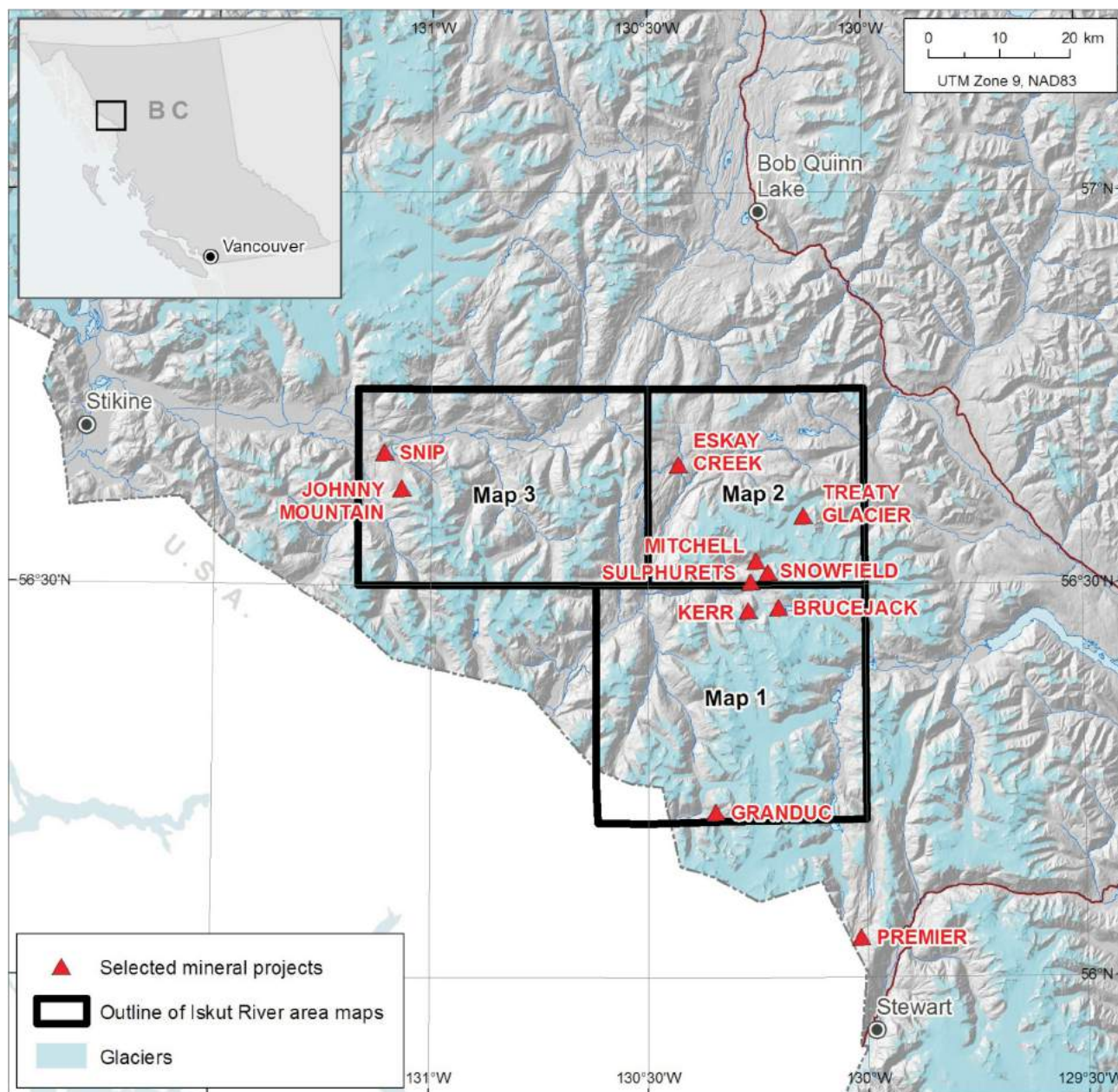


Figure 1. Location of the Iskut River area showing the outlines of the three revised 1:50 000 scale maps (Maps 1, 2, 3), which include NTS map sheets 104B/08, /09, /10 and parts of 104B/01, /07, /11, northwestern British Columbia. Select mineral projects are shown. Kerr, Sulphurets and Mitchell are collectively referred to as the KSM project. Data from GeoBase® (2004), Massey et al. (2005), Natural Resources Canada (2007), GeoBC (2008) and BC Geological Survey (2012).

porting the maps can be found in Chapter 6 of Lewis et al. (2001).

Revised Maps

The MDRU’s Iskut River area maps were originally produced and released as AutoCAD line drawings in Lewis et al. (2001). Geoscience BC converted the original AutoCAD linework to topologically correct features in ArcGIS format and the revised maps will be released as ArcGIS shapefiles and PDF digital maps. The three 1:50 000 scale maps (Figure 1; Maps 1, 2, 3) cover an area

of approximately 1512 km² and include NTS map sheets 104B/08, /09, /10 and parts of 104B/01, /07, /11. They illustrate the complex volcano-sedimentary stratigraphy, structural architecture and intrusive complexity of this highly prospective region of the province and provide some of the most detailed and comprehensive mapping data available to the public for this region (Figure 2).

Summary

As an ArcGIS product, Geoscience BC and the Mineral Deposit Research Unit’s newly revised maps of the Iskut River

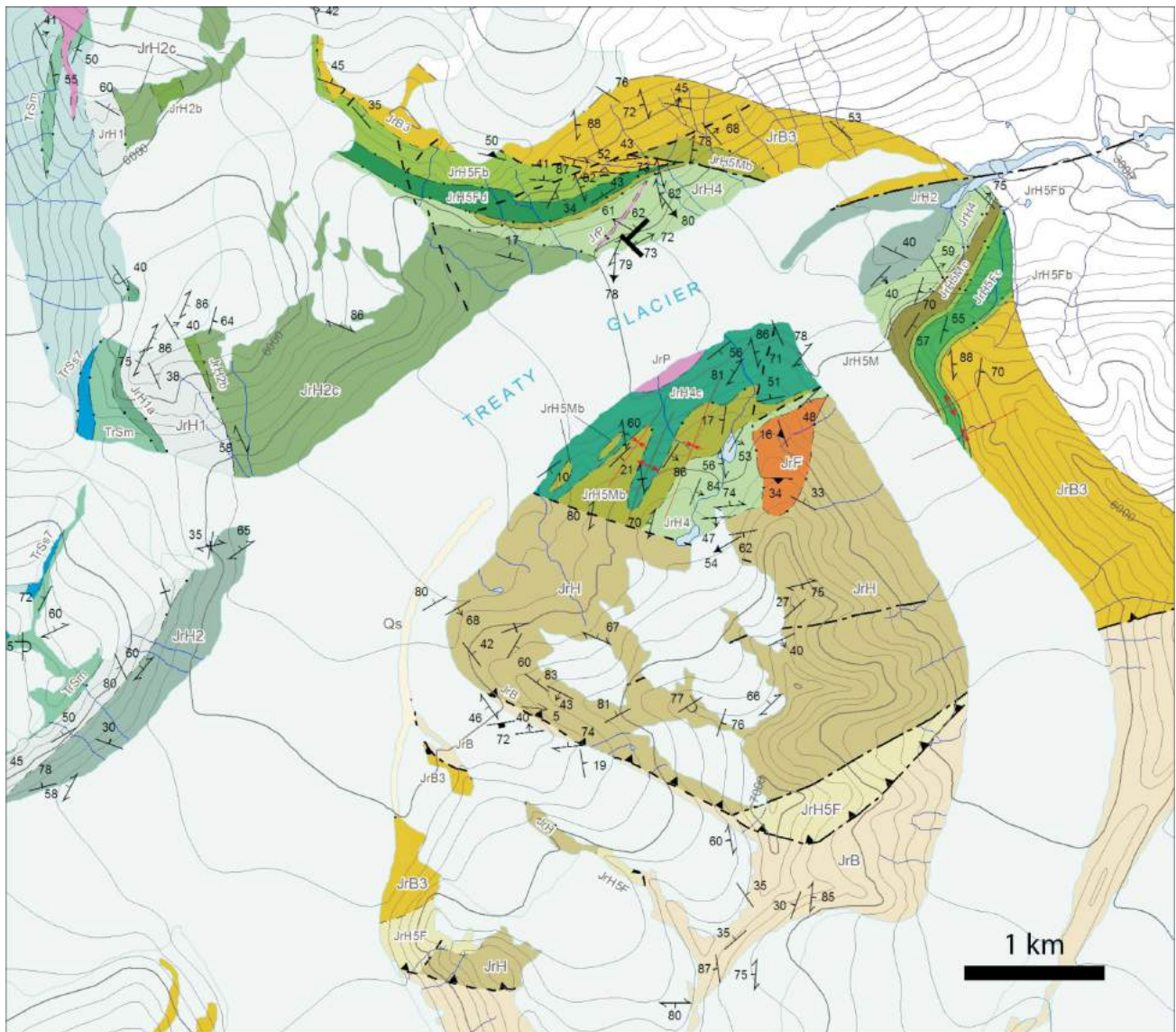


Figure 2. Portion of Map 2 from the Treaty glacier area, northwestern British Columbia, illustrating the level of detail of the mapping and the quality of the newly released maps.

area will provide the mining and exploration industry with some of the most detailed volcano-sedimentary facies and structural information available for this highly prospective part of the province. The new maps will be available for download free of charge from both Geoscience BC's website (www.geosciencebc.com) and the Mineral Deposit Research Unit's website (www.mdru.ubc.ca) in early 2013.

Acknowledgments

The digital elevation model in Figure 1 was prepared by K. Shimamura and F. Ma created the final figure. F. Ma is thanked for providing Figure 2. The manuscript benefited from reviews by C. Sluggett.

References

BC Geological Survey (2012): MINFILE BC mineral deposits database; BC Ministry of Energy, Mines and Natural Gas, URL <<http://minfile.ca/>> [November 2012].

GeoBase® (2004): Canadian digital elevation data; Natural Resources Canada, URL <<http://www.geobase.ca/geobase/en/data/cded/description.html>> [November 2012].

Lewis, P., Toma, A. and Tosdal, R.M. (2001): Metallogeneses of the Iskut River area, northwestern British Columbia; Mineral Deposit Research Unit, Special Publication Number 1, 337 p.

Massey, N.W.D., MacIntyre, D.G., Desjardins, P.J. and Cooney, R.T. (2005): Digital geology map of British Columbia: whole province; BC Ministry of Energy, Mines and Natural Gas, GeoFile 2005-1, URL <<http://www.empr.gov.bc.ca/Mining/Geoscience/PublicationsCatalogue/GeoFiles/Pages/2005-1.aspx>> [November 2012].

Natural Resources Canada (2007): Atlas of Canada base maps; Natural Resources Canada, Earth Sciences Sector, URL <<http://geogratis.gc.ca/geogratis/en/option/select.do?id=0BCF289A-0131-247B-FDBD-4CC70989CBCB>> [November 2012].

GeoBC (2008): TANTALIS - parks, ecological reserves, and protected areas; BC Ministry of Forests, Lands and Natural Resource Operations, database, URL <<https://apps.gov.bc.ca/pub/geometadata/metadataDetail.do?recordUID=54259&recordSet=ISO19115>> [November 2012].

Porphyry Indicator Minerals (PIMs) from Alkalic Porphyry Copper-Gold Deposits in South-Central British Columbia (NTS 092, 093)

M.A. Celis, Mineral Deposit Research Unit, University of British Columbia, Vancouver, BC, mcelis@eos.ubc.ca

C.J.R. Hart, Mineral Deposit Research Unit, University of British Columbia, Vancouver, BC

F. Bouzari, Mineral Deposit Research Unit, University of British Columbia, Vancouver, BC

T. Bissig, Mineral Deposit Research Unit, University of British Columbia, Vancouver, BC

T. Ferbey, British Columbia Geological Survey, Victoria, BC

Celis, M.A., Hart, C.J.R., Bouzari, F., Bissig, T. and Ferbey, T. (2013): Porphyry Indicator Minerals (PIMs) from alkalic porphyry copper-gold deposits in south-central British Columbia (NTS 092, 093); in Geoscience BC Summary of Activities 2012, Geoscience BC, Report 2013-1, p.37–46.

Introduction

The common occurrence of resistate minerals in mineralized and altered portions of British Columbia's alkalic porphyry copper deposits suggests that these minerals can be utilized as indicators of mineralization and used for exploration in terrains covered by glacial till. Porphyry indicator minerals (PIMs) have been shown to have unique physical and chemical characteristics, which emphasize their potential application to the exploration of concealed deposits in BC (Bouzari et al., 2011).

Porphyry indicator minerals are chemically stable in weathered environments, have a high specific gravity, are sufficiently coarse-grained and display characteristic features, all of which can directly link them to a porphyry-related alteration assemblage. These minerals typically display unique physical properties, such as colour, size and shape, which allow their presence to be used as a prospecting tool in a manner similar to that in which kimberlite indicator minerals (KIMs) are used. Moreover, the chemical compositions of PIMs can further identify and confirm mineralizing environments that relate directly to specific alteration zones in porphyry systems. Although easy to collect in heavy-mineral concentrates, these PIMs have rarely been used in porphyry exploration. Therefore, by evaluating the presence, abundance, relative proportions and compositions of PIMs from surficial materials, it is possible to follow-up geophysical and stream-sediment geochemical anomalies, which can act as vectors toward concealed alkalic porphyry copper deposits in highly prospective terranes, such as Quesnellia and Stikinia, in central BC. The purpose of this project is to identify the occurrence, types,

relative amounts and compositions of selected PIMs in several alkalic porphyry deposits in order to elucidate important PIM signatures.

The main objectives of this research are to

- determine assemblages and occurrence of indicator minerals within different alteration and mineralization types of selected BC alkalic porphyry Cu-Au deposits;
- determine the diagnostic physical parameters and chemical compositions of indicator minerals, particularly apatite, garnet, magnetite and diopside; and
- establish criteria for use of resistate minerals as an exploration tool for alkalic porphyry deposits in south-central BC

This report summarizes results of fieldwork and sampling from the Mount Polley, Mount Milligan and Copper Mountain deposits in BC during August and October 2012; sampling at the Lorraine deposit is planned for 2013. Preliminary observations on the alteration assemblages and resistate minerals from each site are presented.

Alkalic Porphyry Deposits in BC

Cordilleran porphyry deposits have a diverse anatomy, as well as mineralization and alteration styles. These deposits formed during two separate time intervals: Late Triassic to Middle Jurassic and Late Cretaceous to Eocene. The Early Mesozoic deposits formed either during or after Late Triassic arc formation in the Quesnel and Stikine terranes, and prior to terrane accretion onto the North American continent (McMillan et al., 1995); they include associations with both calcalkalic and alkalic igneous rocks. Calcalkalic varieties include the Island Copper Cu-Mo-Au deposit, and the Highland Valley, Kemess and Gibraltar Cu-Mo deposits (McMillan et al., 1995). The alkalic Cu-Au deposits include Galore Creek, Mount Polley, Mount Milligan and Copper Mountain. Younger Late Cretaceous to Eocene por-

Keywords: PIMs, resistate minerals, alkalic porphyry deposits

This publication is also available, free of charge, as colour digital files in Adobe Acrobat® PDF format from the Geoscience BC website: <http://www.geosciencebc.com/s/DataReleases.asp>.

phyry deposits formed in an intracontinental arc setting after the accretion and assembly of the Cordilleran terranes; they are mostly related to calcalkaline magmatism and examples include the Granisle porphyry Cu-Au(\pm Mo) deposit and Endako porphyry Mo deposits. Only Early Mesozoic alkalic porphyry deposits were selected for this study; these are the Mount Polley, Mount Milligan, Copper Mountain and Lorraine deposits (Figure 1).

Alteration Assemblages and Resistate Minerals

Alkalic porphyry deposits are generally characterized by small-volume pipe-like intrusions, a medium to relatively small areal extent and a lack of advanced argillic alteration. Phyllic alteration is restricted to fault zones and evidence of

connection to high-sulphidation epithermal deposits is not commonly observed (Chamberlain et al., 2007). A Late Triassic to Early Jurassic magmatic arc defines two suites of alkalic intrusions, silica-saturated and silica-undersaturated, both hosting Cu-Au porphyry deposits in BC. Silica-undersaturated-intrusion suites are locally zoned and their composition varies from pyroxenite to syenite. Their mineralogy is characterized by variable amounts of aegirine-augite, K-feldspar, biotite, titanite, apatite, melanitic garnet, hornblende, plagioclase and magnetite (Lueck and Russell, 1994). The silica-saturated-intrusion suites vary from diorite to monzonite and their mineralogy is characterized by variable amounts of augite, biotite, magnetite, plagioclase, K-feldspar and apatite; hornblende and titanite are less common, and quartz is rare (Table 1; Lueck and Russell, 1994).

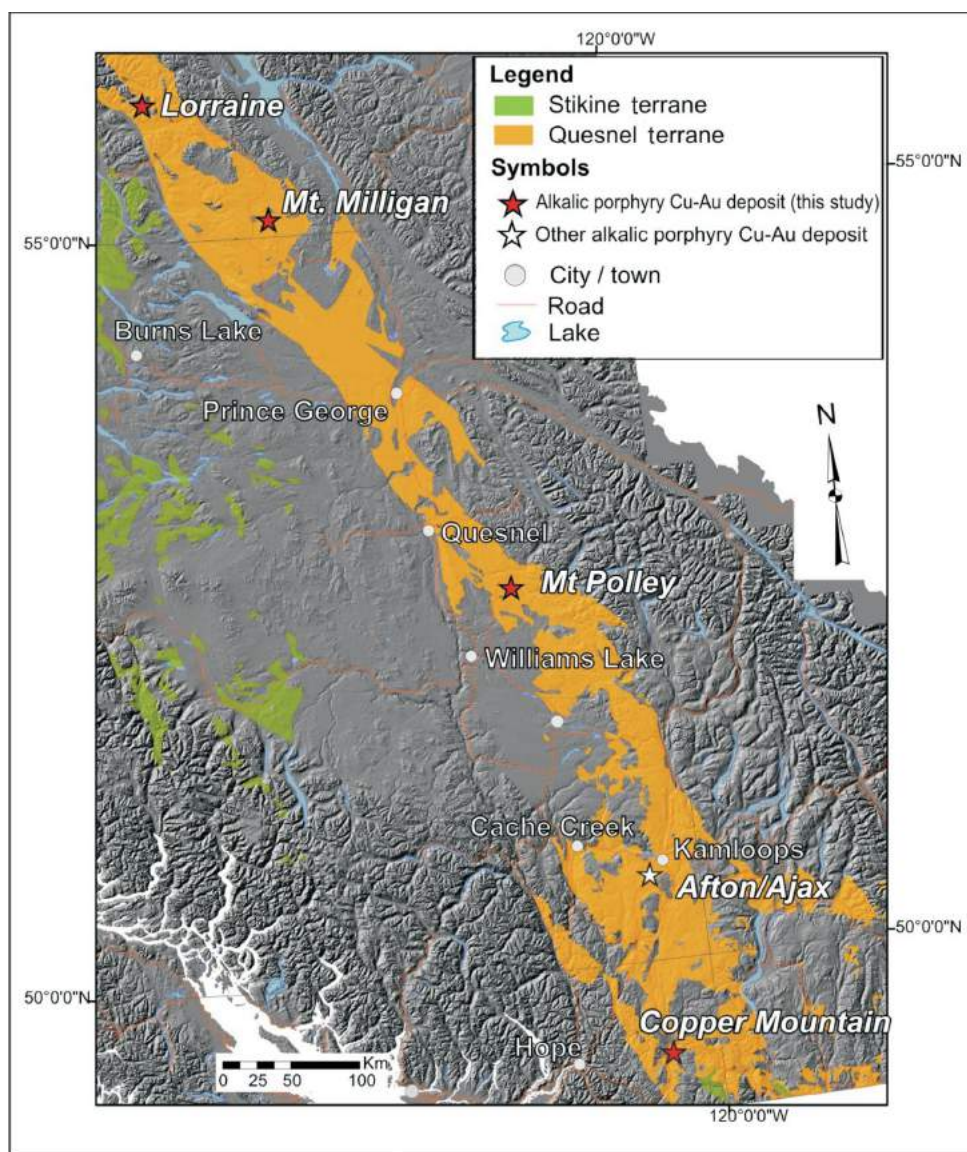


Figure 1. Digital elevation map showing Triassic and Early Jurassic Quesnel and Stikine terranes of central-south British Columbia and location of selected deposits (modified from Bissig et al., 2010).

Field and Analytical Methods

Sampling

Fieldwork and sampling were carried out at the Mount Polley, Mount Milligan and Copper Mountain porphyry copper deposits during August and October 2012. These deposits represent both silica-saturated and silica-undersaturated classes of alkalic porphyry deposits. A total of 49 rock samples were collected from the three sites. The main purpose of the initial sampling survey was to characterize the resistate minerals that occur with each alteration assemblage. Core samples (~30 cm long) were collected from both altered and unaltered rock units at each site in order to determine which resistate-mineral phases are indicators for copper mineralization. Larger (2–4 kg) hand specimens were also collected from outcrops, as well as open-pit benches, for heavy-mineral separation. Glacial-till samples (10–15 kg) were collected from Mount Polley (n=5) and Mount Milligan (n=7). These samples were taken from glacial sediments at or near the mine sites. The objective of till sampling was to identify the fraction and occurrences of PIMs in glacial till, which partly covers the deposit. Results will be compared with the bedrock heavy-mineral separates in a future publication.

Methods

A wide range of analytical techniques are being utilized to characterize the physical and chemical properties of resistate minerals, with emphasis on physical properties such as shape, size, dimensions, color, luminescence and infrared and ultraviolet spectroscopic properties. Selected mineral species will be analyzed for their trace-element composition to characterize and differentiate barren from mineralized systems. Representative till sediments will be analyzed to study the effects of transport and distribution of PIMs. Initial activity consists of petrographic work on core samples, hand specimens and thin polished sections of bedrock materials in order to characterize the in situ abundance and physical properties of indicator minerals.

Preliminary Observations

Mount Polley

Mount Polley is centred within and surrounds several diorite to monzonite (Figure 2a, b) intrusions with associated igneous breccia bodies. Alteration at Mount Polley consists of three concentrically-zoned alteration assem-

blages (Fraser et al., 1995): a potassic core (Figure 2c) surrounded by a garnet-epidote zone with minor magnetite (Figure 2d) and an outer propylitic rim. The potassic core has been further divided into three distinct zones: an actinolite (250 m wide), a biotite (100 m wide) and a K-feldspar-albite (1 km wide) zone (Hodgson et al., 1976; Bailey and Hodgson, 1979). Apatite (Figure 3a) and titanite (Figure 3b) occur in small amounts as accessory minerals, whereas magnetite is massive (Figure 3c) and widely distributed within the potassic core. An outer ‘green alteration’ rim is observed in peripheral parts of the deposit and includes a mineral assemblage of epidote, chlorite with calcite veins and variable amounts of disseminated pyrite (Figure 2e).

Mount Milligan

Mount Milligan consists of three main monzonite stocks (Figure 4a, b) of Middle Jurassic age (MBX, South Star and Rainbow dike) hosted within the Late Triassic Takla Group volcanic sequence (Sketchley et al., 1995; Jago and Tosdal, 2009). Two alteration patterns are recognized: a zone of intense potassic alteration (Figure 4c), which consists of K-feldspar±biotite±magnetite, lies between the MBX stock and the Rainbow dike; lower temperature ‘green alteration’ (Figure 4d), consisting of epidote+chlorite+illite±pyrite, typically occurs below the footwall of the monzonitic Rainbow dike, where it overprints potassic alteration in volcanic hostrocks (Jago and Tosdal, 2009).

A fluid-flow alteration pattern affects the Takla volcanic sequence. These rocks have high permeability, allowing lateral migration of high-temperature magmatic fluids generating pervasive K-feldspar alteration of the volcanic rocks close to the stocks and ‘green alteration’ of epidote-chlorite-calcite veins and disseminated pyrite on the distal zones (Chamberlain et al., 2007).

Copper Mountain

The Copper Mountain deposit is centred on two principal Late Triassic intrusions, predominately of pyroxene diorite to monzonite and syenite (Figure 5a), hosted within the Triassic Nicola volcanic sequence (Stanley et al., 1992). Alteration patterns and assemblages at Copper Mountain consist of an early-stage pre-mineralization hornfels alteration, which is overprinted by sodic and potassic alteration. Hornfels alteration consists of the recrystallization of mafic and intermediate volcanic hostrocks, which is reflected by the presence of a dark purple, dark grey or black, fine-

Table 1. Characteristics of alkalic intrusions associated with porphyry deposits in south-central British Columbia (from Lang et al., 1995).

Alkalic porphyry types	Hostrock	Mineralogy	Resistate mineral	BC examples
Silica undersaturated	Pyroxenite to syenite	Aegirine-augite, biotite, plagioclase, K-feldspar, hornblende	Magnetite, garnet, apatite, titanite	Mount Polley, Lorraine, Galore Creek
Silica saturated	Diorite to monzonite	Augite, biotite, plagioclase, K-feldspar, hornblende	Magnetite, garnet, apatite, titanite	Mount Milligan, Copper Mountain

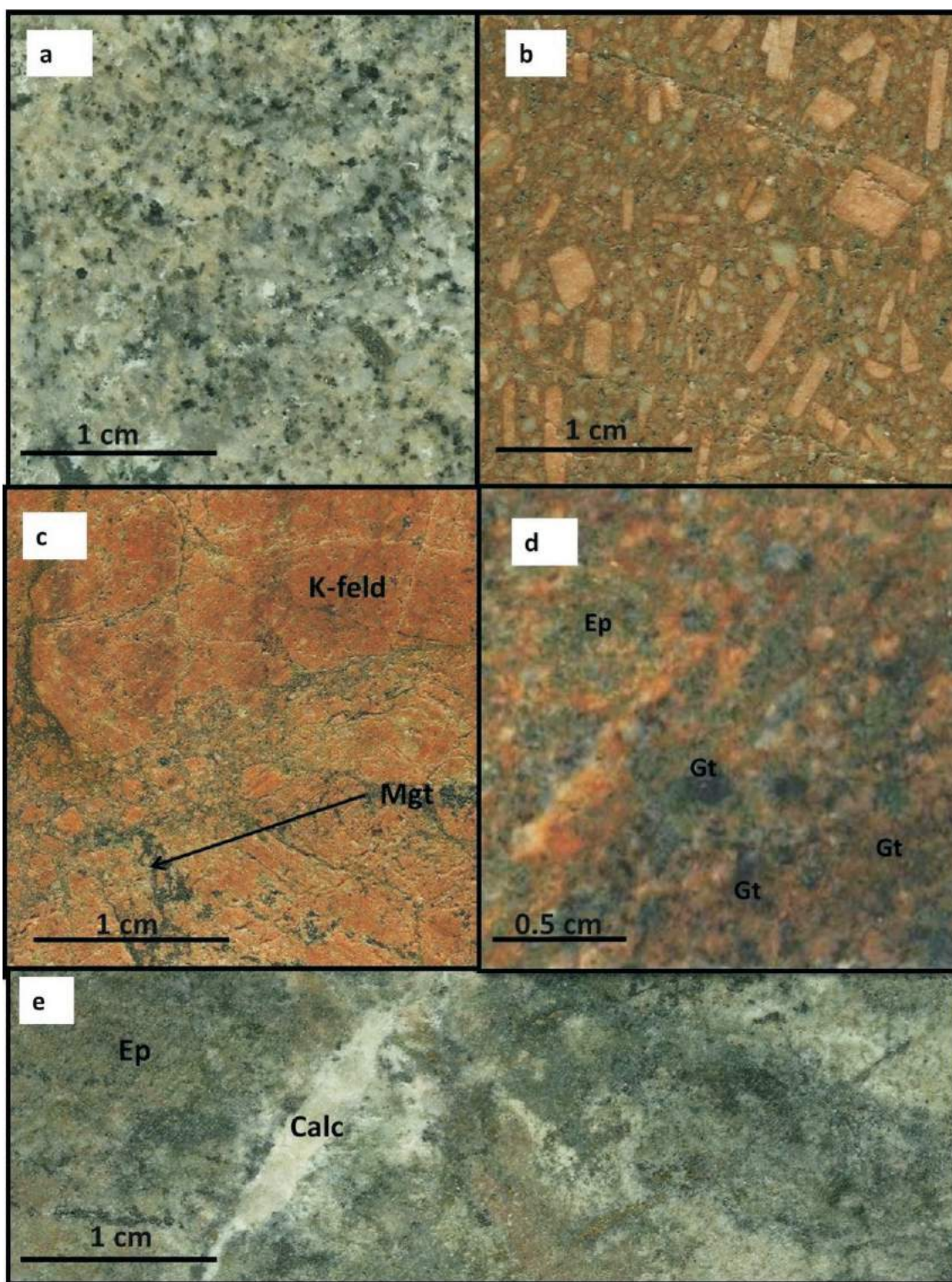


Figure 2. Photomicrographs of mineral assemblages of the Mount Polley deposit, south-central British Columbia, showing **a)** equigranular, medium-grained, light grey monzonite, with 30% K-feldspar, 60% plagioclase and 10% mafic minerals, taken from the road leading to the tailings (Polley_10, UTM Zone 10, 5822071N, 592687E; elevation 890 m); **b)** megacrystic porphyry from Wight pit (Polley_6, 5825240N, 592860E; elevation 921 m); **c)** pervasive K-feldspar alteration with narrow magnetite veinlets overprinting the original texture of the rock, sampled from Springer pit (SD12132-43m); **d)** garnet-epidote alteration assemblage overprinting potassic alteration, from Springer pit (SD12132-309m); **e)** 'green alteration' assemblage of epidote+chlorite±calcite±pyrite with characteristic green color, also from Springer pit, (SD12132-91m). Sample number followed by UTM co-ordinates are given for samples collected from outcrops; ore sample ID consists of hole number followed by depth. Abbreviations: Calc, calcite; Ep, epidote; Gt, garnet; K-feld, K-feldspar; Mgt, magnetite.

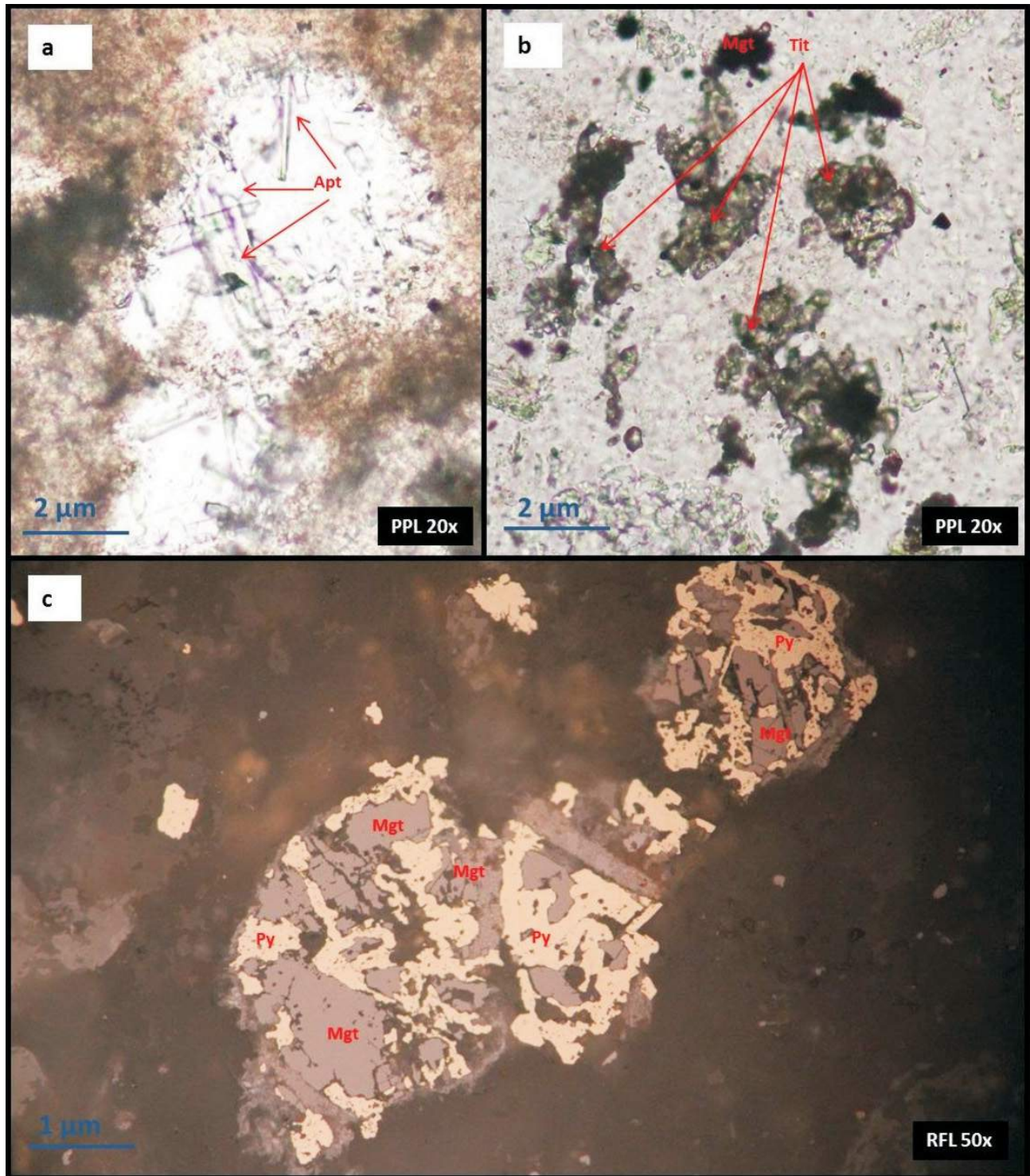


Figure 3. Photomicrographs of resistate minerals of the Mount Polley deposit, south-central British Columbia, showing **a)** apatite phenocrysts with long euhedral shapes, transparent in plan polarized light (PPL) as inclusions in a large altered-plagioclase phenocryst, from Springer pit (SD0981_92.3m); **b)** pale brownish titanite phenocrysts and very high relief in PPL intergrowth with magnetite phenocryst (Polley_12, UTM Zone 10 5825173N, 590993E; elevation 1052 m); **c)** abundant magnetite intergrowth with pyrite, from Wight pit (WB04102_237m). Sample number followed by UTM co-ordinates are given for samples collected from outcrops; core sample ID consists of hole number followed by depth. Abbreviations: Apt, apatite; Mgt, magnetite; Py, pyrite; Tit, titanite.

grained conchoidally fractured diopside+primary biotite+plagioclase+magnetite (Preto, 1972). Sodic alteration (Figure 5b) is restricted to the central portions of the deposit and is expressed as a bleached, typically pale greyish-green or mottled white and grey alteration of the host rock. It is characterized by albite after feldspar, by chlorite, epidote and diopside after mafic minerals, and by the partial destruction of magnetite (Stanley et al., 1992). Potassic alteration (Figure 5c) locally crosscuts zones of earlier sodic-calcic alteration and is widely distributed in the deposit; it is characterized by a pink K-feldspar-replacing plagioclase. Mafic mineral replacements by secondary biotite, epidote, calcite and minor chlorite are also characteristic of potassic alteration. In general, potassic alteration affects a larger total

volume of rock than sodic-calcic alteration; both alterations are characterized by high amounts of K-feldspar and mafic mineral replacement (Stanley et al., 1992).

A 'green alteration' assemblage (Figure 5d) of epidote+chlorite+calcite±pyrite typically occurs at the periphery of the deposit, replacing mafic minerals, but it may occur in the central parts along with the potassic alteration; it is generally dark to light or pale green and not texturally destructive. Plagioclase and K-feldspar replacement by albite+epidote+calcite is also common. Pyrite, hematite (specular) and subordinate magnetite locally occur (Stanley et al., 1992). However, it is possible that this alteration, which is mapped as pyrolytic at the mine, consists of several over-

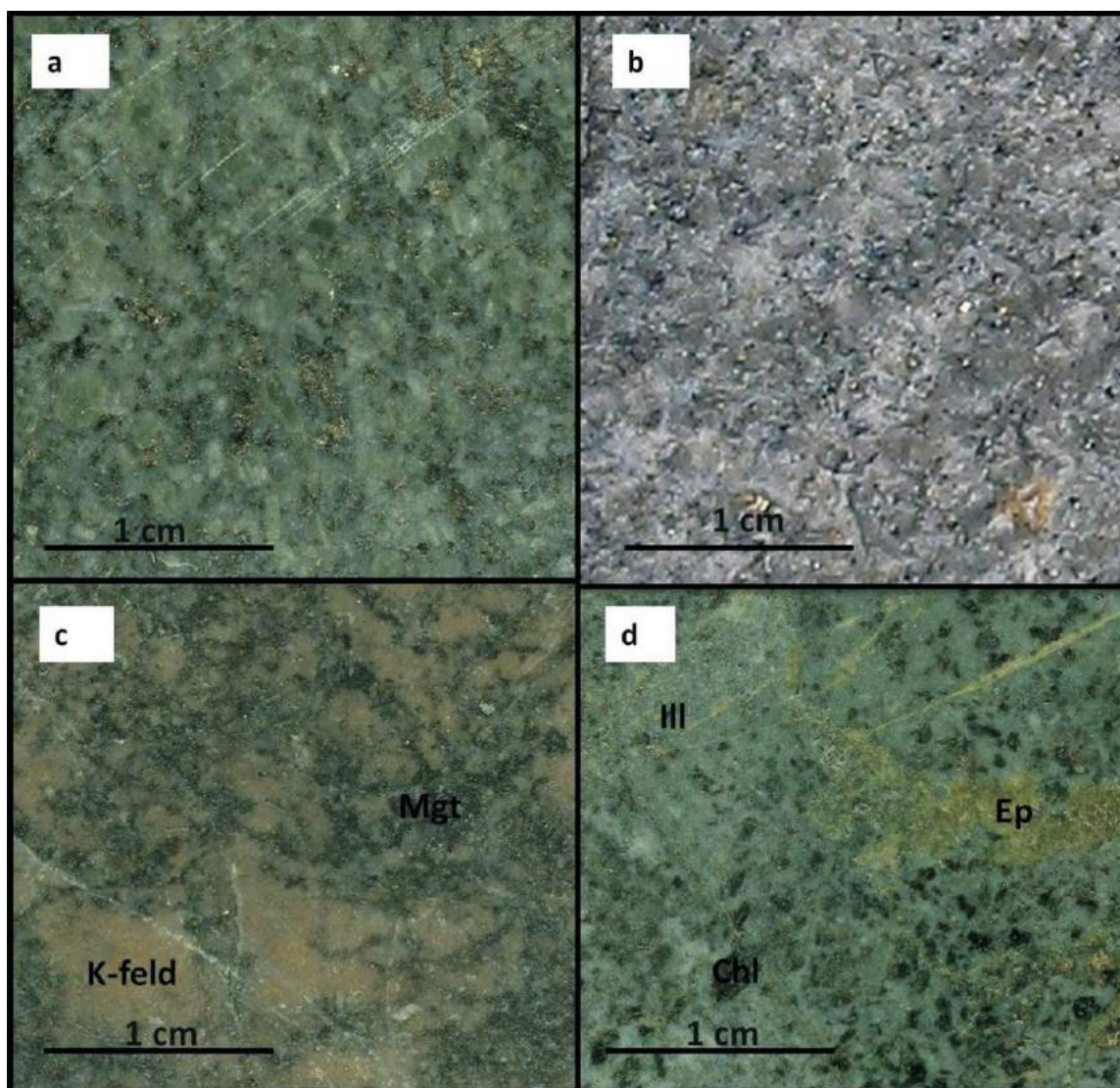


Figure 4. Photomicrographs of mineral assemblages of the Mount Milligan deposit, south-central British Columbia, showing **a**), equigranular, medium- to fine-grained, grey monzonite from the MBX stock (111015_286.1m); **b**) equigranular, medium-grained, pinkish-grey monzonite from the South Star stock (06_957_180m); **c**) potassic alteration assemblage of K-feldspar matrix with disseminated magnetite from the 66 Zone (07992-47m); **d**) 'green alteration' assemblage of epidote+chlorite+illite from the Southern Star stock (06957-212.7m). Core sample ID consists of hole number followed by depth. Abbreviations: Chl, chlorite; Ep, epidote; Ill, illite; K-feld, K-feldspar; Mgt, magnetite.

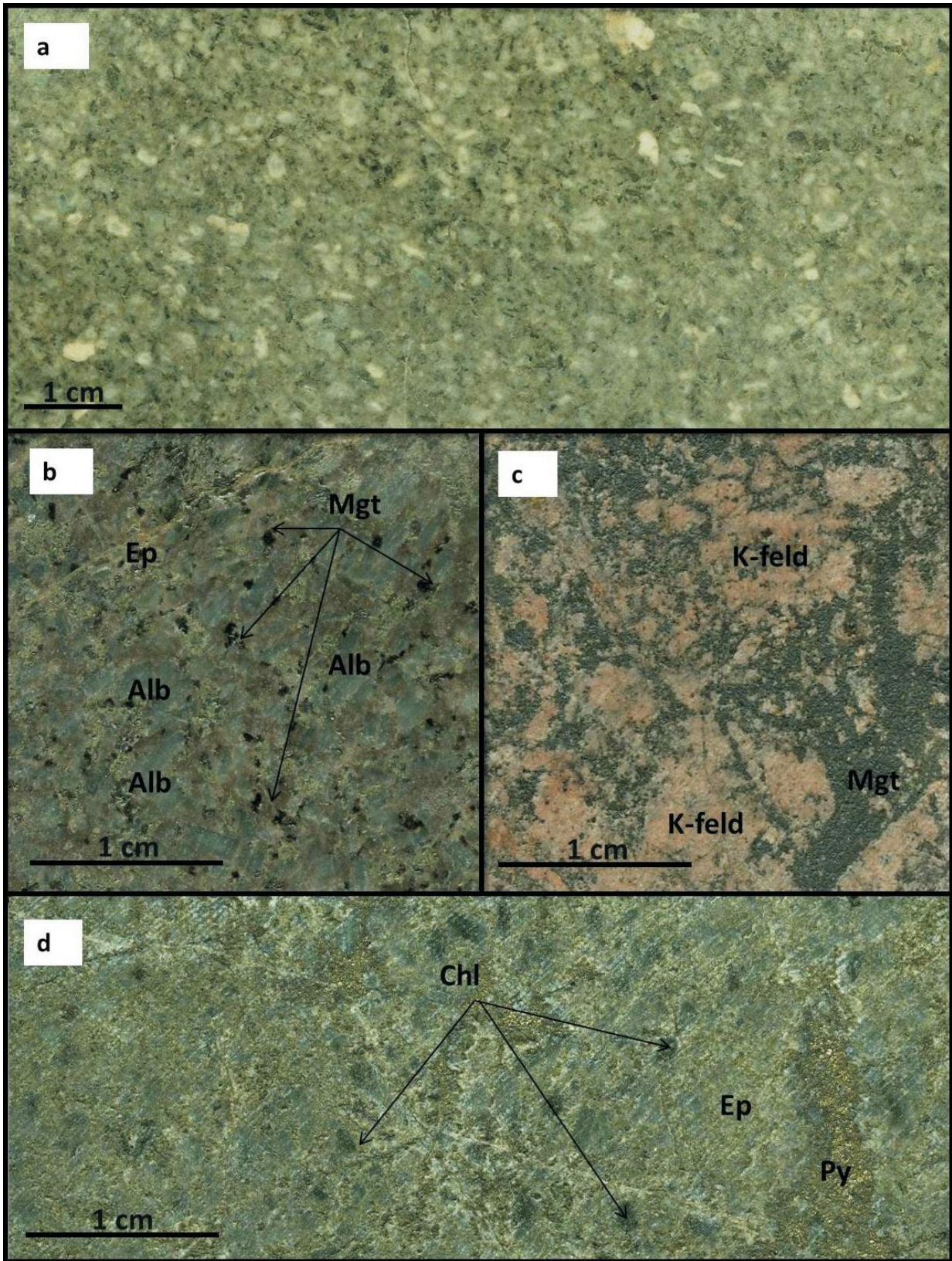


Figure 5. Photomicrographs of mineral assemblages of the Copper Mountain deposit, south-central British Columbia, showing **a)** diorite porphyry from Pit 2 (CM12P219_607m); **b)** sodic-calcic alteration assemblage of epidote+albite+magnetite from Alabama pit (CM12AB_19m); **c)** intense potassic alteration of K-feldspar matrix with disseminated magnetite from Pit 2 (CM12P221_413m); **d)** 'green alteration' assemblage of epidote+chlorite+calcite+pyrite from Pit 2 (CM12P223_352m). Core sample ID consists of hole number followed by depth. Abbreviations: Alb, albite; Chl, chlorite; Ep, epidote; K-feld, K-feldspar; Mgt, magnetite; Py, pyrite.

printing assemblages given its wide range of minerals and occurrence. Late-stage (post-mineralization) kaolinite alteration and sericite-chlorite-clay (SCC) alteration are structurally controlled and occur only locally. Texturally destructive kaolinite alteration consists of kaolinite+sericite+calcite+pyrite±epidote±chlorite±minor quartz; SCC alteration does not obliterate original textures and is typically pale green due to the presence of green clays (Stanley et al., 1992).

The main resistate minerals of interest at Copper Mountain, consisting of apatite, titanite, zircon, magnetite and possibly diopside, occur with the hostrock and associated alteration assemblages (Table 2).

Discussion

Alteration styles at Mount Polley, Mount Milligan and Copper Mountain, are similar, largely dominated by potassic assemblages. However, the size of the potassic zone, its mineralogy and the extent of the sodic-calcic and overprinting chlorite-epidote alterations vary from one deposit to the next, which in turn is expected to influence the occurrence and abundance of resistate minerals. At Mount Polley, the potassic alteration is more extensive than sodic-calcic alteration, with very strong orange, pervasive K-feldspar, biotite, actinolite and abundant disseminated magnetite overprinting the hostrock. A garnet-epidote+magnetite assemblage surrounds the potassic core. At Mount Milligan, potassic alteration is characterized by abundant K-feldspar±biotite±magnetite, which is surrounded by a epidote+chlorite+illite±pyrite assemblage. Garnet wasn't recognized but apatite and titanite occur with potassic alteration. Copper Mountain has widespread sodic (albite+diopside+epidote) and potassic (K-feldspar+biotite+magnetite) alterations. Some particular features of this deposit are pegmatitic K-feldspar+biotite veins and a

patchy 'green alteration' assemblage of epidote+chlorite+calcite±pyrite as well as an early-stage hornfels alteration. Apatite and titanite of the potassic alteration and diopside of the hornfels and sodic alterations are known resistate accessory minerals.

Therefore, it is evident that accessory minerals, such as apatite, titanite and magnetite, occurring with the potassic alteration and typically intergrown with Ti-bearing and sulphide phases, are the main candidates for PIMs studies in these deposits. Silicate minerals, such as diopside with sodic-calcic alteration and garnet with calcsilicate alteration, provide further PIMs potential. The occurrence and abundance of sodic-calcic alteration vary from one deposit to the next but this alteration commonly forms a larger zone outside the main mineralized zone, thus expanding the target volume of favourable PIMs hostrock. Additionally, alteration assemblages, such as chlorite-epidote-calcite, overprinting earlier potassic alteration, are common in the studied deposits. These lower-temperature assemblages can modify the texture and composition of the previously formed resistate minerals.

Future Work

Future work will include petrographic descriptions of the resistate minerals occurring in each alteration assemblage and hostrock type. This will be followed by more detailed analysis of selected resistate minerals in order to determine those diagnostic physical parameters and chemical compositions that will characterize indicator minerals in alkalic porphyry systems. A Mineral Liberation Analyzer (MLA), which is an automated scanning electron microscope, will be used for this purpose; the MLA provides information on mineral-species abundance, grain-size distribution, grain shape and composition. In addition to this, selected mineral separates will be characterized by cathodoluminescence

Table 2. Hostrocks, alteration assemblages, ore mineral assemblages and resistate minerals of the Mount Polley, Mount Milligan and Copper Mountain deposits, south-central British Columbia.

Deposit	Host rock	Alteration assemblages	Ore assemblages	Resistate minerals
Mount Polley	Diorite-monzonite	Actinolite, biotite, K-feldspar	Chalcopyrite, bornite, galena	Magnetite, apatite, titanite
		K-feldspar, magnetite		Magnetite, apatite, garnet
	Igneous breccia	Epidote, chlorite, calcite, pyrite		
Mount Milligan	Porphyritic monzonite	K-feldspar, biotite, magnetite	Chalcopyrite, bornite	Magnetite, apatite, titanite
		Epidote, chlorite, illite, pyrite		Magnetite, apatite, titanite
Copper Mountain	Diorite to monzonite	Biotite, K-feldspar	Chalcopyrite, bornite	Magnetite, apatite, titanite
		Albite, diopside, epidote, calcite		Apatite, titanite, zircon, diopside
	Syenite	Epidote, chlorite, calcite, pyrite		

and X-ray diffractometry, and subsequently will be analyzed for trace elements by laser-ablation inductively coupled plasma–mass spectrometry. Finally, whole-rock geochemistry of till samples may provide correlations between the abundance of indicator minerals and till composition and could be used as a proxy to reduce the number of heavy-mineral–concentrate samples required. By integrating these techniques, the most valid and cost-effective mechanism for characterizing PIMs can be established.

Acknowledgments

The authors would like to thank Copper Mountain Mining Corporation, Imperial Metals Corporation and Thompson Creek Metals Company Inc. for allowing access and sampling at their Copper Mountain, Mount Polley and Mount Milligan deposits, respectively. Geoscience BC is thanked for its generous financial contribution in support of this project. The authors also thank M. Allan of the Mineral Deposit Research Unit, for his review of and comments on this report.

References

- Bouzari, F., Hart, C.J.R., Barker, S. and Bissig, T. (2011): Porphyry Indicator Minerals (PIMs) A new exploration tool for concealed deposits in south-central British Columbia; Geoscience BC Report 2011-17, 31 p., URL <http://www.geosciencebc.com/i/project_data/GBC_Report2011-7/GBC_Report2011-07_BCMEM%20OF2011-1.pdf> [November 23, 2012].
- Bailey, D.G. and Hodgson, C.J. (1979): Transported altered wallrock in lahatic breccias at Cariboo-Bell Cu-Au porphyry deposit, British Columbia; *Economic Geology*, v.74, p.125–128.
- Bissig, T., Vaca, S., Schiarizza, P. and Hart, C. (2010): Geochemical and physical variations in the Late Triassic Nicola Arc and metallogenic implications, central British Columbia (NTS 092P, 093A, N): preliminary results; *in* Geoscience BC Summary of Activities 2009, Geoscience BC, Report 2010-1, p. 49–52, URL <http://www.geosciencebc.com/i/pdf/SummaryofActivities2009/SoA2009_Bissig_red.pdf> [November 23, 2012].
- Chamberlain, C.M., Jackson, M., Jago, C.P., Pass, H.E., Simpson, K.A., Cooke, D.R. and Tosdal, R.M. (2007): Toward an integrated model for alkaline porphyry copper deposits in British Columbia (NTS 093A, N; 104G); *in* Geological Fieldwork 2006, BC Ministry of Energy, Mines and Natural Gas, Report 2007-1, p. 259–273, URL <<http://www.empr.gov.bc.ca/Mining/Geoscience/PublicationsCatalogue/Fieldwork/Documents/26-Chamberlain.pdf>> [November 23, 2012].
- Fraser, T.M., Stanley, C.R., Nikic, Z.T., Pesalj, R. and Gorc, D. (1995): The Mount Polley copper-gold alkaline porphyry deposit, south-central British Columbia; *in* Porphyry Deposits of the Northern Cordillera, T.G. Schroeter (ed.), Canadian Institute of Mining and Metallurgy, Special Volume 46, p.609–622.
- Hodgson, C.J., Bailes, R.J. and Verzosa, R.S. (1976): Cariboo-Bell; *in* Porphyry Deposits of the Canadian Cordillera, A. Sutherland Brown (ed.), Canadian Institute of Mining and Metallurgy, Special Volume 15, p.388–396.
- Jago, C.J. and Tosdal, R.M. (2009): Distribution of alteration in an alkaline porphyry copper-gold deposit at Mount Milligan, central British Columbia (NTS 094N/01); *in* Geoscience BC Summary of Activities 2008, Geoscience BC, Report 2009-1, p.33–48, URL <http://www.geosciencebc.com/i/pdf/SummaryofActivities2008/SoA2008-Jago_reduced.pdf> [November 23, 2012].
- Lang, J.R., Lueck, B., Mortensen, J.K., Russell, J.K., Stanley, C.R. and Thompson, J.F.H. (1995): Triassic–Jurassic silica-undersaturated and silica-saturated alkalic intrusions in the Cordillera of British Columbia: implications for arc magmatism; *Geology*, v.23, p.451–454.
- Lueck, B.A. and Russell, J.K. (1994): Silica-undersaturated, zoned alkaline intrusions within the British Columbia Cordillera; *in* Geological Fieldwork 1993, B. Grant and J. Newell (ed.), BC Ministry of Energy, Mines and Natural Gas, Paper 1994-1, p.311–315, URL <<http://www.empr.gov.bc.ca/Mining/Geoscience/PublicationsCatalogue/Fieldwork/Documents/1993/311-318-lueck.pdf>> [November 23, 2012].
- McMillan, W.J., Thompson, J.F.H., Hart, C.J.R. and Johnston, S.T. (1995): Regional geological and tectonic setting of porphyry deposits in British Columbia and Yukon Territory; *in* Porphyry Deposits of the Northwestern Cordillera of North America, T.G. Schroeter (ed.), Canadian Institute of Mining and Metallurgy, Special Volume 46, p.40–57.
- Preto, V.A.G. (1972): Geology of Copper Mountain, British Columbia; BC Ministry of Energy, Mines and Natural Gas, Bulletin 59, 87 p., URL <<http://www.empr.gov.bc.ca/Mining/Geoscience/PublicationsCatalogue/BulletinInformation/BulletinsAfter1940/Pages/Bulletin59.aspx>> [November 23, 2012].
- Sketchley, D.A., Rebagliati, C.M. and DeLong, C. (1995): Geology, alteration and zoning patterns of the Mt. Milligan copper-gold deposits; *in* Porphyry Deposits of the Northwestern Cordillera of North America, T.G. Schroeter (ed.), Canadian Institute of Mining and Metallurgy, Special Volume 46, p.650–665.
- Stanley, C.R., Holbek, P.M., Huyck, H.L.O., Lang, J.R., Preto, V.A.G., Blower, S.J. and Bottaro, J.C. (1992): Geology of the Copper Mountain alkaline Cu-Au porphyry deposit, Princeton, British Columbia; Canadian Institute of Mining, Metallurgy and petroleum, Special Volume 46, p.552–562.

Use of Organic Media in the Geochemical Detection of Blind Porphyry Copper-Gold Mineralization in the Woodjam Property Area, South-Central British Columbia (NTS 093A/03, /06)

D.R. Heberlein, Heberlein Geoconsulting, North Vancouver, BC, dave@hebgeoconsulting.com

C.E. Dunn, Colin Dunn Consulting Inc., North Saanich, BC

W. Macfarlane, Acme Analytical Laboratories, East Vancouver, BC

Heberlein, D.R., Dunn, C.E. and Macfarlane, W. (2013): Use of organic media in the geochemical detection of blind porphyry copper-gold mineralization in the Woodjam property area, south-central British Columbia (NTS 093A/03, /06); in Geoscience BC Summary of Activities 2012, Geoscience BC, Report 2013-1, p. 47–62.

Introduction

This paper covers activities conducted under a Geoscience BC project entitled “Evaluation of plant exudates to assist in mineral exploration and the development of simple and cost effective field procedures and analytical methods”. Large areas prospective for porphyry and epithermal-style mineralization in central British Columbia are covered by either glaciofluvial sediments or young basalt units. In areas where the cover is unconsolidated material of glacial origin, recently completed Geoscience BC-funded projects significantly advanced the understanding of the underlying bedrock geology and have demonstrated means of seeing through this type of cover using geochemistry (e.g., Cook and Dunn, 2007; Dunn et al., 2007; Barnett and Williams, 2009; Heberlein, 2010; Heberlein and Samson, 2010; Heberlein and Dunn, 2011). However, geochemistry is not commonly used to investigate the underlying geology in those areas covered by young basalt flows. The present study is aimed at establishing a geochemical strategy to see through basalt cover, using a variety of analytical techniques on a variety of organic or organically-derived sample media to test what works best.

Plant Exudates

It has long been established that plant exudates can contain metals translocated from underlying mineralization, through the plant and into the sap. The most dramatic of these discoveries is that of the Sève Bleue tree (*Sebertia acuminata*) from New Caledonia. Its name comes from the bright blue sap that derives the colour from the extraordinarily high concentrations of Ni that it contains (Jaffré et al., 1976); the sap was found to contain a phenomenal

25.74% Ni on a dry-weight basis. Plant exudates (saps, fluids transpired through leaf pores, salts and particulates on leaf surfaces, which have crystallized from the plant fluids) may provide a simple and cost-effective sample medium. The authors are not aware of any published records of these media being used for geochemical exploration purposes in BC.

Application to Exploration

Kyuregyan and Burnutyan (1972) demonstrated that plant saps could be used in exploration for Au, because the sap Au content was significantly higher than that of other aqueous extracts of the plant material or of the underlying soil. Saps from birch are the most studied, both because of the ubiquity of birch in the boreal forests (especially Siberia and Finland) and of their strong sap flow in the spring. Krendelev and Pogrebnyak (1979) conducted a sampling program in an area of permafrost over an intensively fractured and hydrothermally-altered Au-mineralized stockwork in Transbaikal, where most of the Au is associated with pyrite and there is a 0.5–4 m cover of unconsolidated sediments. The mean Au content from analysis of 73 samples was reported as 0.011–0.33 ppb; Zn concentrations in fresh sap from trees growing over Zn-rich ore reached 17.2 ppm. The authors observed that, in the vascular system of the birch species studied (*Betula platyphylla*), there is no biological barrier against the absorption of Zn and concluded that the best anomaly to background contrast was obtained by calculating the $Zn/(K+Ca+Mg)$ ratio. Harju and Huldén (1990) conducted an exhaustive survey in southern Finland, where they collected sap samples from many species of birch (mostly *Betula verrucosa*) over a 10-year period. Sap samples collected along transects over a zone of base-metal mineralization revealed clear anomalies of Ag, Cd, Zn and Pb above the orebody (Figure 1). More details of the use of saps in exploration are summarized in Dunn (2007).

In addition, consideration was given to the collection of cuticle and salt particulates on leaf tissues. This collection

Keywords: deep-penetrating geochemistry, Woodjam, copper-gold porphyry, biogeochemistry, exudates, bark, spruce, Ah soils, charcoal, soil pH, soil conductivity

This publication is also available, free of charge, as colour digital files in Adobe Acrobat® PDF format from the Geoscience BC website: <http://www.geosciencebc.com/s/DataReleases.asp>.

technique was tested by Barringer (1975), who compared the geochemical expression in soil, conifer vegetation and vegetation particulates sampled over Zn mineralization in Ontario. Later, some interesting positive results were recorded over Cu/Pb/Zn sulphides in the United Kingdom by Horler et al. (1980).

Benefits to the Mining Industry

This study is designed to provide the mineral-exploration community with a better understanding of different organic sampling media that can be used for biogeochemical exploration in regions with thick glacial sediment or Tertiary basalt cover. It provides comparisons of metal concentrations in vegetation, the Ah-soil horizon and charcoal debris, and assesses the relative capabilities of each medium for preserving the secondary geochemical dispersion patterns related to a blind mineral deposit. The study also examines metal concentrations in saps, leaf coatings and transpired fluids to determine whether direct sampling of these 'exudates' is an effective way of detecting blind mineralization. If successful, exudate geochemistry could provide the exploration community with an alternative sampling medium for local- and regional-scale geochemical sampling programs in areas where conventional soil-sampling methods are found to be ineffective.

Project Area

Test sites selected for this study lie within Gold Fields Canada Exploration (Vancouver) and Consolidated Woodjam Copper Corp.'s (Vancouver) Woodjam property, which is located in the Cariboo Mining District of central BC (NTS map areas 093A/03, /06; Figure 2). The property, which consists of 178 mineral claims totalling 58 470 ha, is located about 65 km to the northeast of Williams Lake. Horsefly, the nearest settlement and logistical base for the fieldwork, lies within the property boundary and is accessible by a paved road from Williams Lake. The two test sites, known as Deerhorn and Three Firs (also formally known as Megalloy; Figure 2), lie 8 and 12 km respectively to the southeast and south of Horsefly; both are readily accessible via a network of well-maintained logging roads.

Surficial Environment

The project area lies at the boundary between the Fraser Plateau and Quesnel Highland physiographic regions of central BC (Holland, 1964). The terrain in the study areas has characteristics of both regions. The Deerhorn test site lies at a fairly sharp transition between relatively flat rolling topography typical of the Fraser Plateau on the western side of the mineralized zone, to low hills of the Quesnel Highland to the east (Figure 2). Elevations across the Deerhorn sample traverse, which crosses the transition, vary from 900 m at the western end to 1030 m at the highest point, close to the eastern end. A number of small lakes and ponds

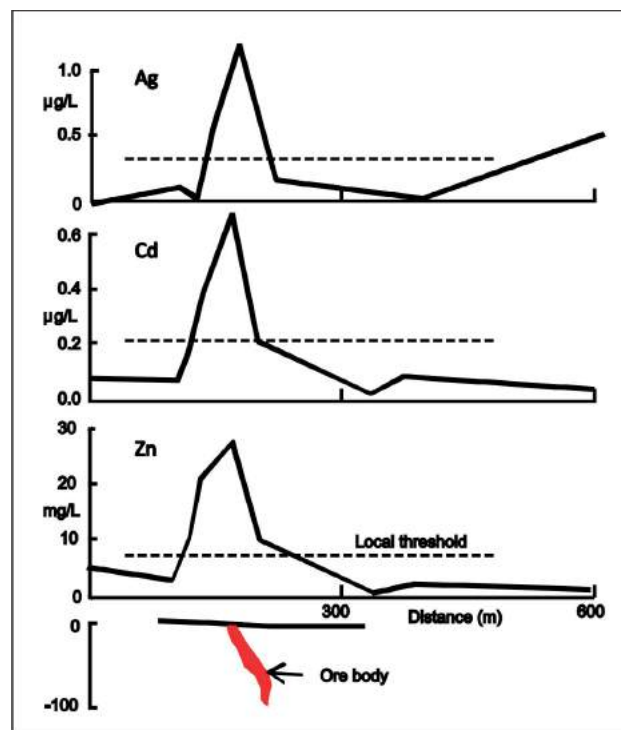


Figure 1. Transect across a skarn-type polymetallic sulphide deposit in Finland. Concentrations of Ag, Cd and Zn in birch sap (*Betula verrucosa*) are given in $\mu\text{g/L}$ (ppb), whereas that of Zn is given in mg/L (after Harju and Huldén, 1990).

are scattered throughout the area and are linked by small streams and boggy depressions, which form part of a dendritic drainage pattern connecting with the Horsefly River, some 5 km to the northeast of Deerhorn. The Three Firs test site lies in a similar physiographic setting to Deerhorn (Figure 2). More than half of the Three Firs sample traverse crosses relatively flat terrain typical of the Fraser Plateau, where elevations range from 975 to 1000 m asl. At these lower elevations, a number of swamps and small creeks define a northwest-flowing dendritic drainage pattern, which merges with Woodjam Creek, some 8 km to the northwest. The terrain gradually rises eastward into the rounded hills of the Quesnel Highland, where the maximum elevation at the eastern end of the line is 1140 m.

Quaternary glacial deposits cover extents of mineralization at both study areas (Levson, 2010). To the east of Deerhorn, surficial deposits consist of an intermittent till veneer, which mantles the hillsides and becomes thicker in topographic depressions. The maximum thickness of the till is unknown but the presence of outcrops on the northern flank of the hillside east of Deerhorn suggests that it is likely to be no more than a few metres thick. Glacial landforms, such as drumlinoid features, are present in this area and east of the sample traverse. Their long axes indicate a west-northwesterly ice-flow direction. Cover thickens rapidly westward onto the lowlands and drilling at Deerhorn has shown that the bedrock surface is buried beneath up to 60 m of till and

glaciofluvial sediments (Skinner, 2010; del Real et al., 2013). Surficial deposits on the eastern shore of Mica lake and southern limit of the projected mineralized zone consist of well-sorted sand and gravel of probable glaciofluvial origin; the distribution of these deposits is unknown.

At Three Firs, the cover environment is complicated by the presence of a Tertiary basalt unit (Chilcotin Group?) beneath the glacial deposits. Drilling has shown that the basalt probably obscures a part of the mineralized zone. It consists of fresh, black, highly vesicular lava ranging from 2 to 20 m thick (A. Rainbow, pers. comm., 2012). Nicola Group rocks at its lower contact are intensely weathered over sev-

eral metres in what is likely to be a paleoregolith. This clay- and oxide-rich zone is alternatively interpreted as a fault-gouge zone by Gold Fields Canada Exploration geologists (A. Rainbow, pers. comm., 2012). The extent of volcanic cover is unknown, although its distribution is most likely restricted to paleovalleys rather than forming a continuous cap over the mineralized area. This would be typical of other occurrences of Chilcotin Group flows in the region (Dohaney, 2009). Surficial deposits at Three Firs consist predominantly of till, which forms a blanket 40 to 100 m thick over the Nicola Group and basalt unit (A. Rainbow, pers. comm., 2012). There is no outcrop in the vicinity of the mineralization. Till cover appears to thin gradually east-

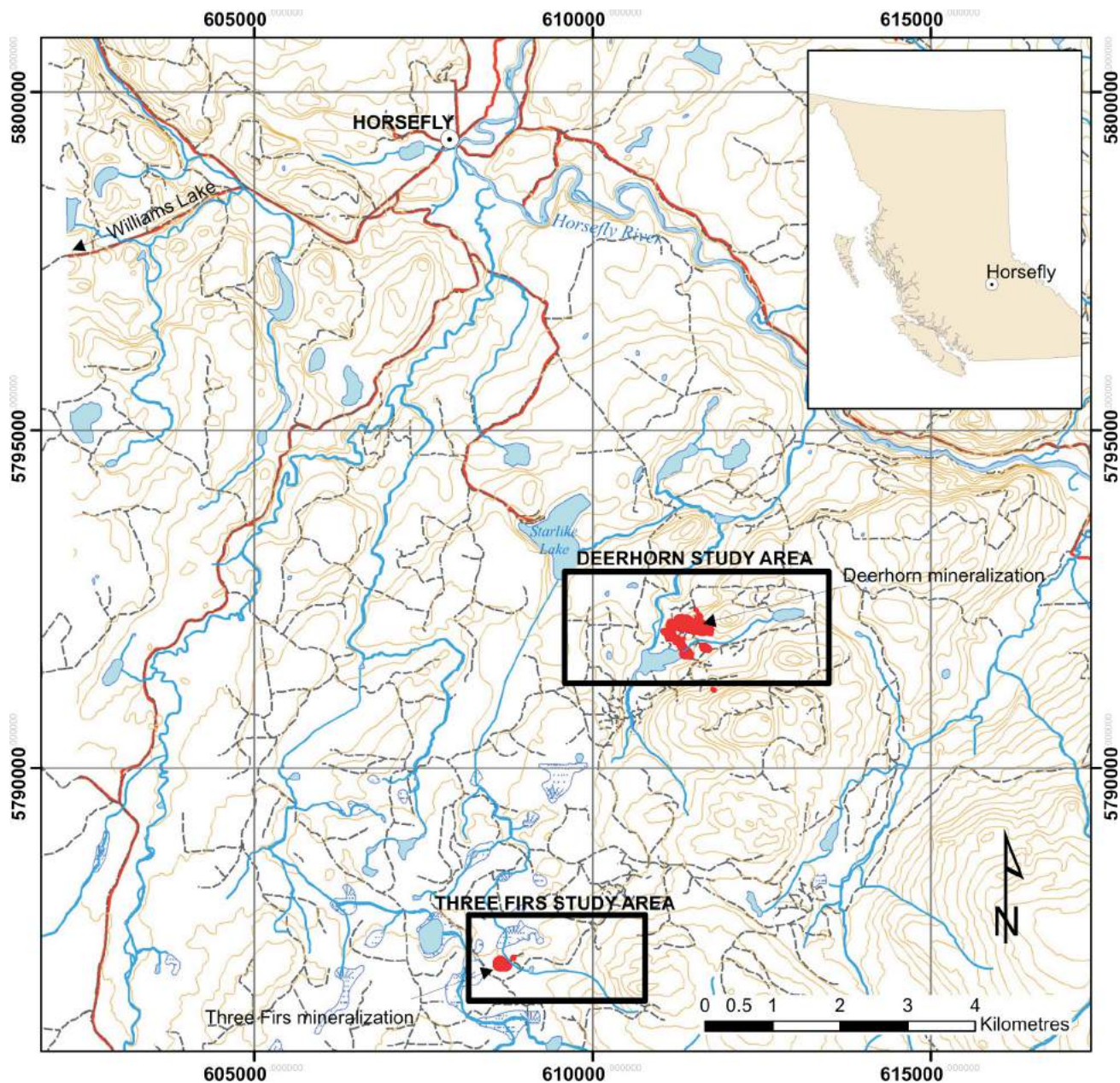


Figure 2. Location of study areas at the Woodjam property, south-central British Columbia. Red shapes represent the surface projection of mineralization defined by the +0.20 g/t Au equivalent cutoff (J. Blackwell, pers. comm., 2012).

ward and outcrops of a distinctive ‘turkey-track’ feldspar porphyry become widespread in the east-central part of the sample traverse. On the hillside, at the eastern end of the traverse, till cover is present as a thin veneer no more than a metre or two thick.

Regional Geological Setting

The Woodjam property area lies in the southern part of the highly prospective Quesnel terrane: a Late Triassic to Early Jurassic magmatic arc complex, which extends for most of the length of the Canadian Cordillera. It is flanked to the east by assemblages of Proterozoic and Paleozoic carbonate and siliciclastic rocks of ancestral North American affinity, but is separated from them by a sliver of oceanic basalt and chert of the Slide Mountain terrane (Schiarizza et al., 2009). Oceanic rocks of the Late Paleozoic to Early Mesozoic Cache Creek terrane bound the Quesnel terrane to the west (Figure 3). The southern part of the Quesnel terrane hosts a number of important Cu-Au porphyry deposits; nearby examples include Gibraltar and Mount Polley.

In the Woodjam property area, the Quesnel terrane is represented by Middle to Upper Triassic volcano-sedimentary rocks of the Nicola Group (Figure 3). Locally this consists of a shallow northwest-dipping sequence of volcanic and volcanic-derived sedimentary rocks, which include augite-phyric basalt flows and polymictic breccias containing latite, trachyte and equivalent volcanic clasts (Skinner, 2010). Sandstones and conglomerates are intercalated with the volcanic units. A suite of more or less coeval intrusions of alkaline to calcalkaline affinity intrudes the volcanic and sedimentary sequence. These intrusions include the Early Jurassic Takomkane batholith, located to the south and east of the project area, and a number of smaller syenite, monzonite, quartz monzonite and monzodiorite stocks and dikes within the Woodjam property itself; many of these are associated with Cu-Au mineralization (J. Blackwell, pers. comm., 2012).

The Woodjam South property contains several centres of Early Jurassic porphyry-style Cu-Mo-Au mineralization (Schiarizza et al., 2009). Style of mineralization, hostrocks and metal association vary from one mineralized centre to

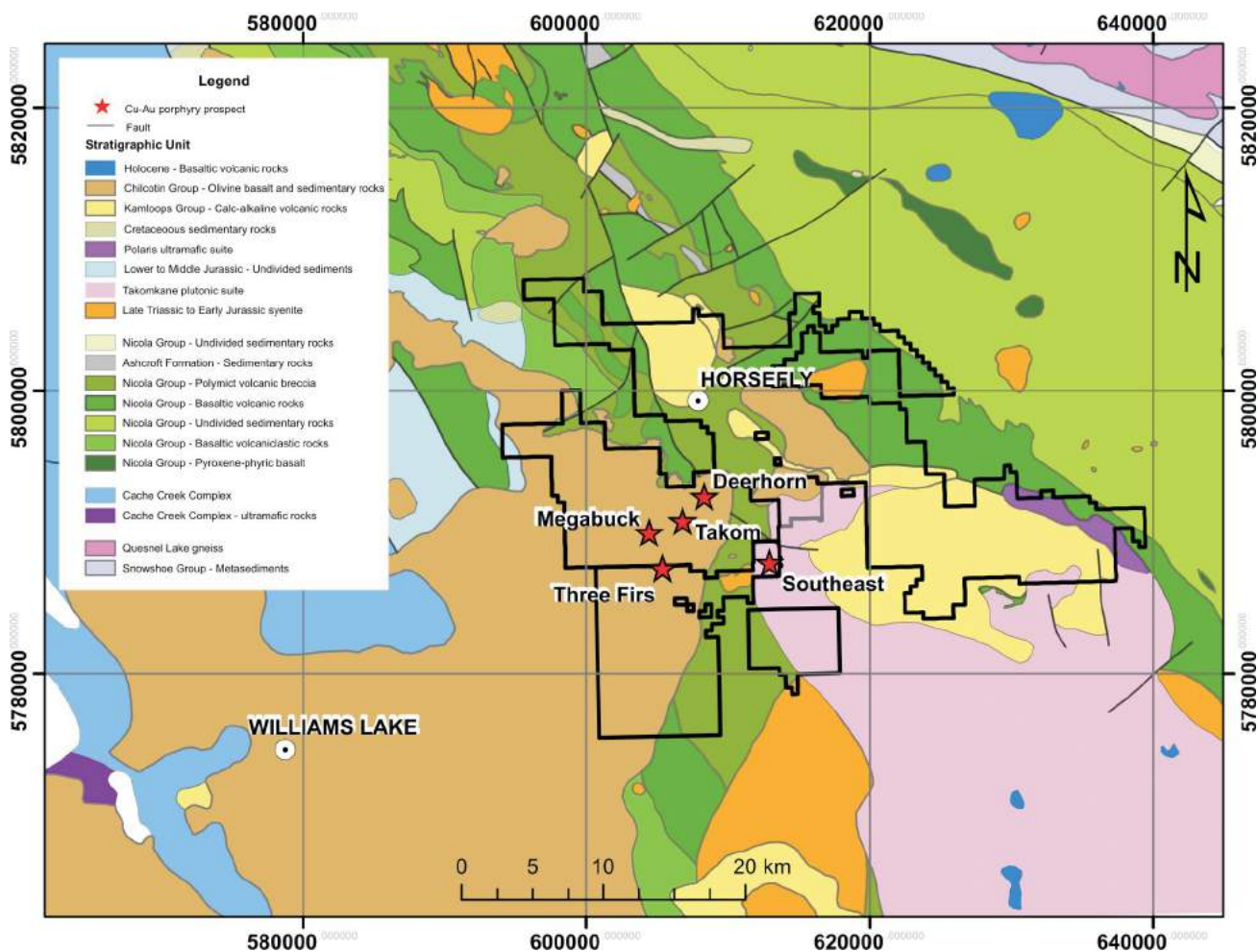


Figure 3. Regional geology of the Woodjam property area, south-central British Columbia.

another; these include the Southeast, Takom, Megabuck, Deerhorn and Three Firs (Megalloy) prospects (Figures 3 and 4). The Southeast zone is currently at the most advanced stage of exploration and has an inferred, pit-constrained resource of 146.5 Mt grading 0.33% Cu (Sherlock et al., 2012). Copper-molybdenum mineralization is hosted

in intrusive rocks, which form part of the Takomkane batholith. Deerhorn is the next most advanced prospect and is currently undergoing exploration drilling. It is characterized by Cu-Au mineralization hosted in Nicola Group volcanic rocks and a series of small porphyry stocks and dikes (see below). The remaining prospects are all at the explor-

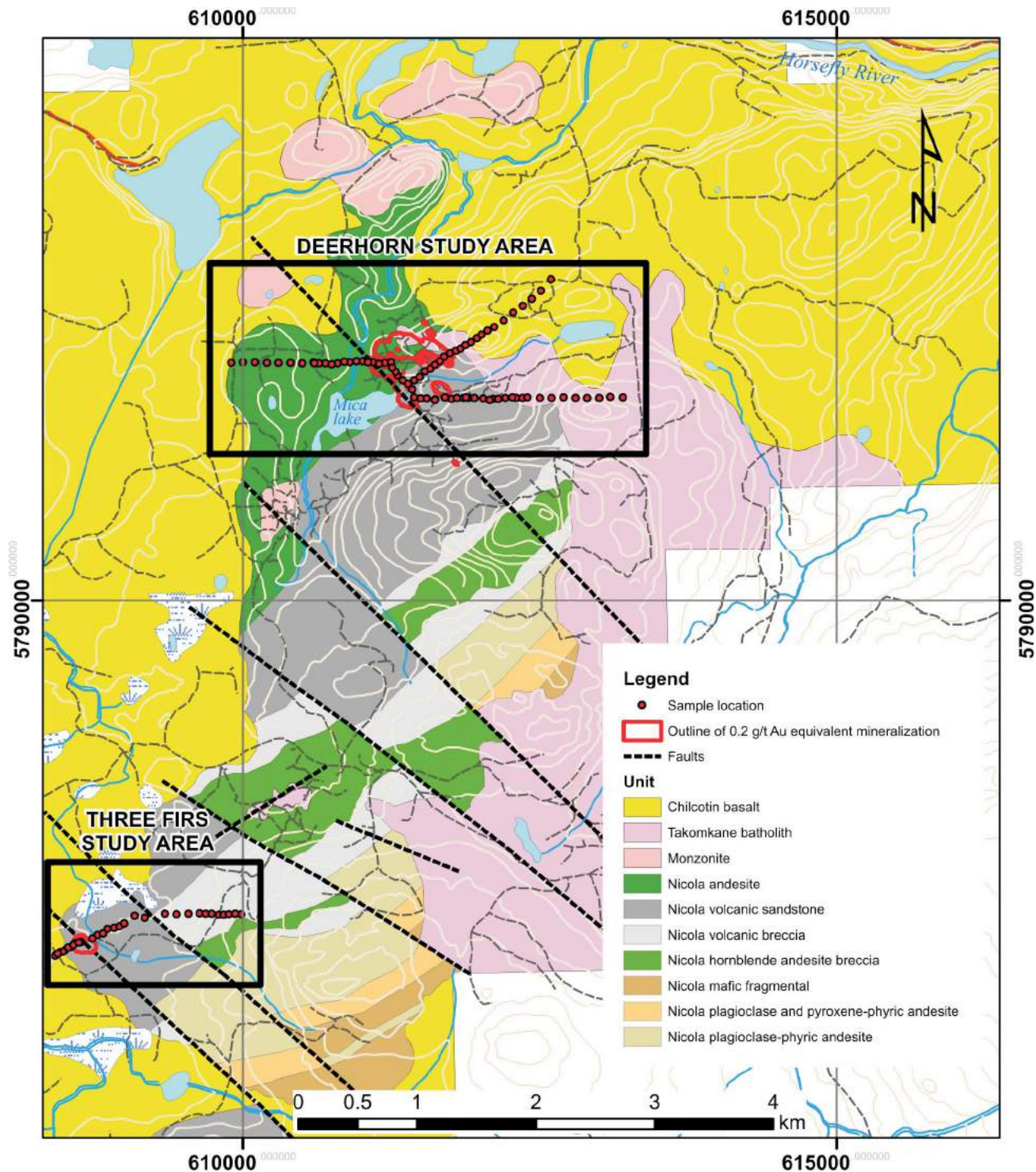


Figure 4. Bedrock geology of the Woodjam South property area, south-central British Columbia (after Del Real et al., 2013; J. Blackwell, pers. comm., 2012). Place name with the generic in lower case is unofficial.

atory drilling stage. Three Firs represents a new discovery that was made early in 2012 (Consolidated Woodjam Copper Corp., 2012a); it is currently in the initial drill-testing stage. Nicola Group rocks in much of the western part of the Woodjam South property area and an area to the east of Deerhorn are covered by younger Cenozoic rocks belonging to the Chilcotin Group (Bevier, 1983; Dohaney, 2009). These consist of olivine basalt lavas, tuffs and sedimentary units, including sandstone, siltstone, shale and conglomerate. This younger volcanic and sedimentary rock cover masks prospective areas of the underlying Nicola Group.

Geology of Test Areas

Deerhorn

Deerhorn is a blind zone of porphyry Cu-Au-style mineralization, which was discovered by drilling a large chargeability anomaly in 2007 (Skinner, 2010). The mineralization, shown by the red +0.20 g/t Au equivalent outline in Figures 2 and 4, is the surface projection of a pipe-like body containing a higher-grade shoot, which plunges at a moderate angle to the southeast (J. Blackwell, pers. comm., 2012). Its dimensions are approximately 350 m in strike, 100 m in width and 200 m in depth (Consolidated Woodjam Copper Corp., 2012b). Higher grade mineralization is enclosed within a much more extensive lower-grade envelope defined by a quartz and magnetite stockwork, veinlets and disseminated chalcopyrite mineralization. Low-grade mineralization is locally associated with a chargeability anomaly that extends northwest of the Deerhorn drilling and continues south and west to the Megabuck East and Megabuck prospects, which suggests that the three prospects are likely part of a single larger mineralized system.

Geological mapping and reconstruction of the bedrock geology from drilling by Gold Fields Canada Exploration (Figure 4; J. Blackwell, pers. comm., 2012) indicates that the mineralization is hosted in a northeast-striking, northwest-dipping package of Nicola Group andesite and volcanic sandstone. Higher-grade mineralization is associated with a number of northwest-striking dike-like monzonite bodies 30–75 m wide, which cross the contact between volcanic-derived sandstone units in the southeast and andesitic rocks in the northwest of the mineralized zone. The intrusion and volcano-sedimentary units are offset by sets of west-northwest- and northeast-striking faults (J. Blackwell, pers. comm., 2012). Copper-Au mineralization subcrops beneath a variable cover of Quaternary glacial and glaciofluvial deposits. The deposits consist of a till blanket up to 40 m thick over the mineralization and a sequence of overlying glaciofluvial sand and gravel exposed in roadcuts near the southeastern shore of Mica lake. The distribution of these deposits is unknown but they are not likely to be extensive.

Three Firs (Megalloy)

Bedrock geology of the Three Firs study area is not exposed. Mineralization was discovered at this prospect during the early spring of 2012. At the time of sampling for this study, only three holes had encountered significant Cu and Au mineralization. What makes this study area appealing from a deep-penetrating-geochemistry standpoint is the presence of a basalt unit, inferred to be part of the Chilcotin Group, which overlies at least part of the mineralized zone. The extent of the basalt is unknown and it is difficult to determine from the interpretation of ground and airborne magnetic data. A basalt cap at least 30 m thick covering the underlying altered and mineralized Nicola Group rocks has been intersected by drilling. Figure 4 illustrates the known distribution of basalt and the surface projections of the mineralized drill intersections.

Quaternary glacial sediments overlie the basalt; where observed in drill road exposures, the sediments appear to consist of a boulder till containing abundant large rounded clasts (up to 1 m in diameter) of a distinctive ‘turkey-track’ andesite porphyry that is known to outcrop near the eastern end of the sample traverse and immediately to the southeast. The size and composition of the boulders indicate that the till is locally derived and possibly forms only a thin veneer across the survey area.

Field Procedures

The Woodjam area is in the sub-boreal spruce biogeoclimatic zone, dominated by white spruce and/or Engelmann spruce hybrids, to the west and the interior cedar-western hemlock biogeoclimatic zone to the east. Douglas fir occurs in the drier areas, with some large trees, and some lodgepole pine and western red cedar. Birch and poplar, scattered throughout, are the most common deciduous species. The understory has shrub alder. Samples were collected along traverses across the surface projections of the known Cu-Au mineralization (Figure 5). The Deerhorn traverse (Figure 5a) is 3500 m long with sample sites spaced at 100 m intervals in background areas and at 50 m intervals over the projected Cu-Au mineralization. The eastern and western thirds of the traverse have east-west orientations, while the central part over the mineralized zone is oriented northwest-southeast in order to avoid Mica lake. At Three Firs (Figure 5b), the traverse line is 1650 m long. The western half over the Cu-Au mineralization has a northeasterly orientation and the eastern half is aligned east-west. Again sample sites were spaced at 50 m intervals over the known mineralization and at 100 m intervals in inferred background areas; background could only be achieved at the eastern end of the line. Sampling was not possible to the west of the mineralization due to the proximity of the property boundary.

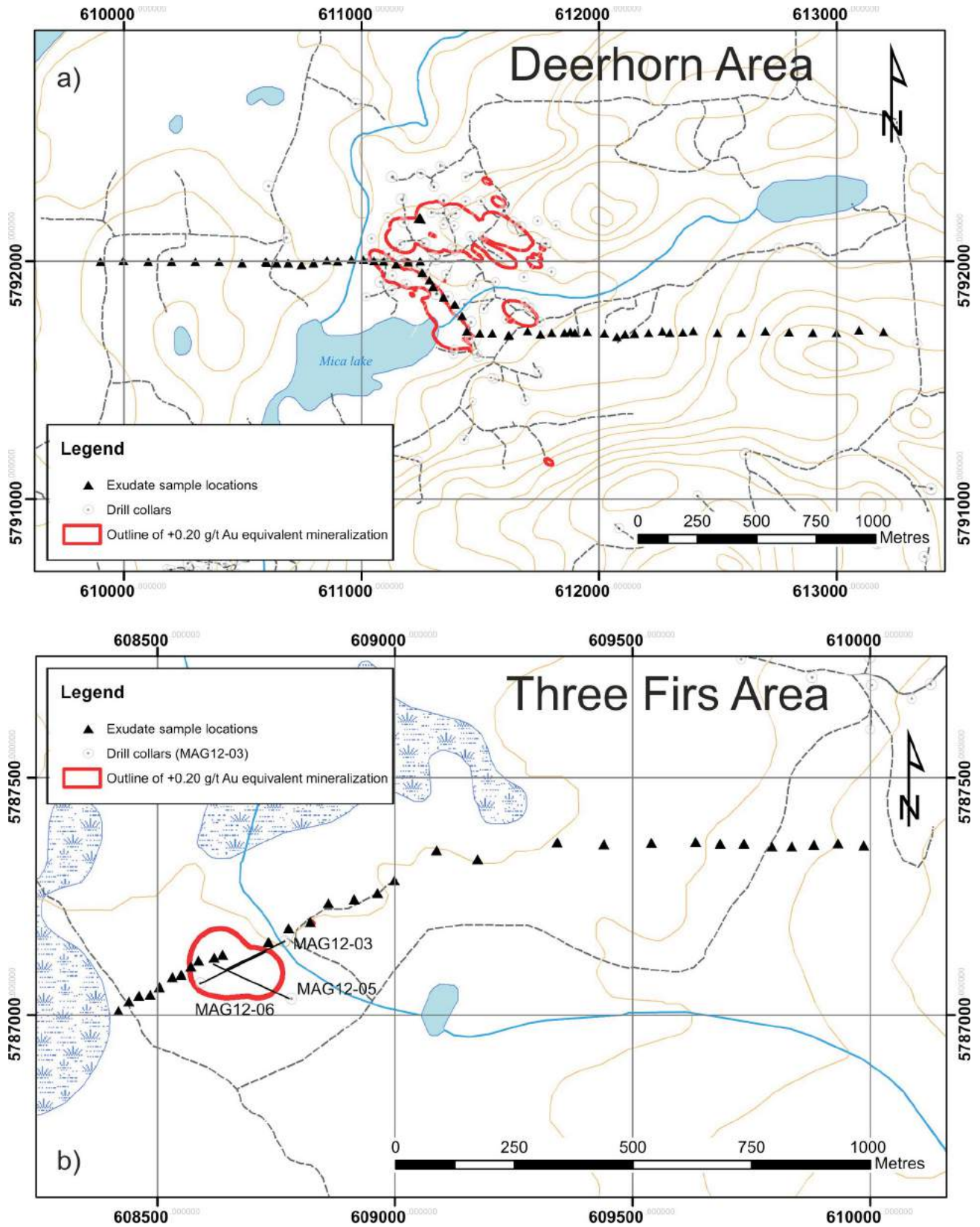


Figure 5. Location of sample sites at the Woodjam property, south-central British Columbia: **a)** Deerhorn traverse; **b)** Three Firs traverse. The red outline denotes the surface projection of the +0.20 g/t Au equivalent mineralization. Place name with the generic in lower case is unofficial.

Samples were collected on two occasions. The bulk of the sampling was completed in early July. Initial results indicated that the lines sampled should be extended in order to reach well into ‘background’ areas. Furthermore, the quality of some of the foliar samples from the exudate component might have been compromised; therefore, some additional sampling was warranted, as well as some repeat sampling to determine if significant seasonal differences in chemistry had taken place. This follow-up phase was undertaken during a two-day period at the beginning of September.

Vegetation and Exudates

For the vegetation sampling, the dominant tree species proved to be white spruce, which were therefore the focus for the biogeochemical sampling. Both twigs and outer bark were sampled, and the spruce trunks proved to be good sources for the collection of congealed sap. Alder were sufficiently abundant that leaves could be readily collected for some of the surface-wax tests.

Vegetation

The outer bark from white spruce (*Picea glauca*) was obtained by scraping the scales from around the circumfer-

ence of a single large tree using a hardened-steel paint scraper, and pouring the scales into a standard kraft paper soil bag (a fairly full bag contained approximately 50 g; Figure 6a).

Samples of twigs and needles of white spruce comprising the most recent 5–7 years of growth were snipped from around the circumference of a single tree. In central BC, this amount of growth is typically about a hand-span in length, at which point, the twig diameter is 4–5 mm (Figure 6b). This diameter is quite critical because many trace elements concentrate in the bark part of the twig, whereas the woody tissue (the cortex) has lower concentrations of most elements. Consequently, unless there is a consistency in the diameters of the twigs that are collected, any analysis of twig tissue can result in variability among samples simply because of the differing ratios of woody tissue to twig bark. The twig with needles samples were placed into porous polypropylene bags (‘Hubco’ Inc.’s Sentry II). The use of plastic bags is to be avoided because samples soon release their moisture and become very soggy; if there is any delay in processing they develop moulds and lose their integrity.

In the laboratory, all vegetation samples were thoroughly dried at 80°C in an oven with a forced-air fan for 24 hours to



Figure 6. Sampling procedure for white-spruce bark and twigs at the Woodjam property, south-central British Columbia.

remove moisture. The needles could then be separated from the twigs. In preparation for chemical analysis, each bark sample was then milled to a powder using a Wiley mill. The spruce twigs, less the needles, were weighed in aluminum trays, which were placed in a kiln dedicated to plant tissues, and reduced to ash by controlled ignition at 475°C for 24 hours.

Plant Exudates

Several different types of plant exudates were collected (Figures 7–9):

- White-spruce sap, the congealed material that had accumulated on the surface of the tree trunks, tended to exude from the sites of dead branches or damaged surfaces (e.g., grazed by falling trees). A pocket knife, or the paint scraper used also for removing outer-bark scales (Figure 7a), was used to delicately pick/scrape off a sufficient amount of the congealed sap (about 1 g; Figure 7b) to fill a small polyethylene vial. Two or three minutes were usually sufficient to collect the required amount.
- Leaves of alder were collected in order to strip off the surface waxes using chloroform. During the first phase of the survey (July, 2012), they were stuffed into 250 mL polyethylene bottles and the lids screwed on tightly. This proved not to be the optimal procedure, since the leaves soon turned brown and started to decompose unless they were refrigerated the day of collection. During the second phase (early September), they were put into kraft paper sample bags.
- The current year's growth of spruce twigs and needles was snipped from several branches following the same procedures as those used for the alder leaves. Though these did not deteriorate like the alder, they were nevertheless put into kraft paper sample bags during the second phase of sampling.

- During a hot summer's day, plants transpire fluids through the stomata on their foliage. Gold has been reported in these fluids from studies in Siberia (Kyuregyan and Burnutyán, 1972). In order to collect this material (referred to here as 'transpired fluids'), plastic bags were tied over the twigs of several spruce trees and left in the hot sunshine for a day (Figure 8a). At the end of the day, the sites were revisited and the accumulated liquid was poured from the plastic bags into plastic vials and sealed (Figure 8b). On a cool day no 'sweats' accumulated, whereas on a hot day more than 50 mL was obtained from each tree. During the first phase of sample collection, more than 50 mL of fluid was collected in a single sunny day. During the second phase, when it was cool and cloudy, no fluids accumulated. The bags were left for a week (including some sunny days), after which Gold Fields Canada Exploration personnel were able to return to the sample sites and retrieve the fluids that had transpired during that period.

Horler et al. (1980) experimented with the collection of plant-surface particles from gorse bushes in southwestern England and concluded that the analysis of these particulates provided a useful geochemical indicator. Attempts were made to collect these particulates using the same type of cyclone (with a similar vacuum attachment) as that described in the paper by Horler et al. (1980; Figures. 8c and d). Unfortunately, because there had been substantial rain just prior to both field visits, no particulates could be collected; all plant surfaces (mostly alder and spruce in the field area) failed to produce any particulate material.

Ah and Charcoal Samples

Ah-soil-horizon sampling involved rolling back the surface moss-mat and leaf-litter layer (LF and LFH horizon) and scraping the black humic material accumulated at the



Figure 7. Collection of white-spruce sap at the Woodjam property, south-central British Columbia: **a)** congealed sap on trunks; **b)** sample size of approximately 1g.



Figure 8. Collection of exudate samples at the Woodjam property, south-central British Columbia: **a)** and **b)** transpired fluids; **c)** and **d)** surface particulates, using a vacuum and cyclone system.

top surface of the mineral soil profile. In order to obtain enough material (50–75 g) and to create a composite sample to reduce within-site variability, several areas were sampled at each sample station. Samples were placed in kraft paper sample bags. An Ah-horizon sample and a charcoal sample (where present) were collected at each site. Charcoal fragments were hand-picked from the Ah horizon and placed in Ziploc® plastic bags. The amount and size of fragments present was found to be quite variable from station to station. At some locations, only minute chips (<1 mm) were obtained and it was necessary to collect charcoal from several spots within a 10 m radius of the sample location in order to collect sufficient material for a sample (approximately 50 g). At other sample sites, carbonized twigs, bark or wood could be sampled relatively easily.

Quality Control

Quality control measures employed for this study included the collection of field duplicate samples for each sample type as well as the insertion of ‘blind’ control samples (milled or ashed vegetation of similar matrix and known

composition) for the vegetation analysis. A total of seven field duplicates were collected for each sample type at randomly selected sample sites. At each site, material was col-



Figure 9. Photograph shows all media collected for the exudate study (except charcoal) at the Woodjam property in south-central British Columbia.

lected using exactly the same procedures as the original sample and from within 5 m of the original sample. Control samples for the vegetation were inserted at a frequency of 1 per 10 field samples.

Analytical Methods

Table 1 provides a summary of the types of materials collected for the exudate study and the analytical protocols used. Analysis of the milled dry bark samples was carried out at Acme Analytical Laboratories Ltd. (Vancouver) using their 1VE2-MS method. This involves dissolution of a 1 g aliquot of milled material in nitric acid followed by aqua-regia digestion, heating on a hot plate, then diluting to a constant weight with de-ionized water; the analytical finish is by inductively coupled plasma–mass spectrometry (ICP-MS).

Ashed spruce-twig samples were sent to Acme Analytical Laboratories Ltd., where 0.25 g aliquots were dissolved in modified aqua regia (method code Group 1F) and analyzed by ICP-MS and inductively coupled plasma–emission spectrometry (ICP-ES) for 53 elements and selected REE. Saps were analyzed at Queen’s University Facility for Isotope Research (QFIR) by digesting 0.5 g of sample in 6 ml of concentrated nitric acid using a microwave digestion system manufactured by Anton Paar. Microwave power was set at 1400W and the total cycle time was 40 minutes, including power ramp up and cool down. Clear solutions with no solid residues were obtained and analyzed for 55 elements on an Element sector field ICP-MS manufactured by Thermo Fisher Scientific Inc. Transpired fluids were analyzed directly on the sector field ICP-MS at QFIR for the same suite of elements as the saps. Minimum dilutions were achieved by spiking 4 mL of sample with 80 µL of ultrapure concentrated nitric acid to provide a matrix with maximum instrumental sensitivity: the combination of minimum dilution and maximum sensitivity was necessary to effectively assess this very low-concentration medium. Alder leaves

were placed in ultrapure chloroform and processed for 5 minutes in an ultrasonic bath to remove surface waxes and crystallized exudates. The leachate was then transferred into clean Teflon[®] beakers and allowed to evaporate to dryness in a Class 1000 cleanroom. The residue was then taken up in 2% nitric acid and analyzed on the sector field ICP-MS at QFIR.

Field Measurements

Soil pH and Electrical Conductivity Measurements

Samples for soil pH and electrical conductivity (EC) measurements were collected from both study areas (Figure 5). Where possible, material was collected from the top centimetre of the leached Ae horizon (in podzol profiles) and from the top of the B horizon, where the Ae horizon was either absent or poorly developed (e.g., in brunisol profiles). At sample sites with poor drainage, where organic material comprises the upper part of the profile, no sample was collected. Samples were placed in heavy-duty double-seal Ziploc[®] plastic bags.

Conductivity measurements were made on a 1:1 slurry of soil in demineralized water using a VWR[®] conductivity meter. Soil pH readings were taken on the same slurry using a double-junction pHTestr[®] 30 handheld pH meter manufactured by Oakton[®] Instruments. The instrument was calibrated daily using standard pH buffer solutions at pH 4.00, 7.00 and 10.00. Two pH measurements were taken on each sample: the first one 20 seconds after immersion of the electrode into the slurry and a second, 20 seconds after adding one drop of 10% hydrochloric acid and stirring. Readings were recorded into an Excel[®] spreadsheet and converted to H⁺ concentrations for interpretation.

Table 1. Sample media and analytical methods employed on plant tissues and exudates, south-central British Columbia.

Medium	No. of samples	Process	Analysis	Survey area
White spruce twigs	69	Needles separated and twigs reduced to ash	Acme method 1F04 ¹	Deerhorn and Three Firs
White spruce outer bark	68	Milled to powder - analysis of dry tissue	Acme method 1VE2	Deerhorn and Three Firs
Alder leaves	41	Leached in chloroform to remove surface waxes	QFIR - HR-ICP-MS ²	Deerhorn
First year white spruce twigs with needles	41	Leached in chloroform to remove surface waxes	QFIR - HR-ICP-MS	Deerhorn
Spruce sap (congealed)	43	Microwave digestion in concentrated nitric acid	QFIR - HR-ICP-MS	Deerhorn
Transpired fluids	10	Analysis by direct aspiration after spiking with 4 mL of sample with 80 µL of ultrapure nitric acid	QFIR - HR-ICP-MS	Deerhorn
Leaf surface particulates	0	Unsuccessful - no samples	None	Deerhorn
Ah	72	Dried, sieved and digested in modified aqua regia	Acme method 1F04	Deerhorn and Three Firs
Charcoal	72	Dried, milled and digested in modified aqua regia	Acme method 1F04	Deerhorn

¹ Acme Analytical Laboratories Ltd., Vancouver, BC; all analyses by inductively coupled plasma-mass spectrometry (ICP-MS), supplemented by inductively coupled plasma-emission spectrometry, except those at QFIR done using high resolution (HR) ICP-MS

² Queen's University Facility for Isotope Research (QFIR), Kingston, Ontario, in collaboration with W. Macfarlane

Preliminary Results

Many of the analytical results, particularly those related to the plant exudate samples, were pending at the time this report was prepared. Nevertheless preliminary analytical results for some of the other sample media, namely charcoal, spruce bark and twigs are available for discussion. Patterns for selected elements for each of these media are described below.

Charcoal

Results for four elements from the Deerhorn area are illustrated in Figure 10. The profile plots show the approximate position of the surface projection of the mineralization (defined by the +0.20 g/t Au equivalent cutoff) as a red bar. This part of the traverse also corresponds to the segment with a northwestern orientation, as shown in Figure 5a. The plots show the raw values for Rb, Ca, As and Cu.

Rubidium results (Figure 10a) show two distinct features. Over the mineralization it defines a moderate contrast, multiple peak response. The strongest peak (6.1 ppm) coincides with the southeastern half of the projected mineralized zone. A second, slightly lower, contrast peak (2.5 ppm) occurs about 100 m to the west of the projected mineralization. Together these features appear to define an asymmetrical rabbit-ear-like pattern. The source of Rb is likely to be the potassic alteration associated with the Cu-Au mineralization at depth. A second high-contrast response occurs further east, in an area that is interpreted as being underlain by unmineralized rock. This feature has almost as much contrast as the response over the mineralization (to 5.3 ppm). The cause of this feature is not known but there are two possible explanations. One is the presence of subcropping syenite near the eastern edge of the feature; these K-rich rocks are a probable source of Rb. The second possible explanation is hydromorphic enrichment in a swampy drainage, the position of which is indicated by the blue bar in Figure 10a.

Calcium results (Figure 10b) highlight the position of the mineralization with a rabbit-ear-like pattern. A sharp single-sample response (2.6%) coincides with the southeastern edge of the zone. Over the central and northwestern part of the zone, Ca values are moderately elevated above background and increase to a maximum over the northwestern limit of the projected mineralization (1.8%). Rabbit-ear patterns in Ca and other pH-sensitive elements are well documented over the edges of blind sulphide bodies (e.g., Smee, 1997; Heberlein and Samson, 2010) and are thought to be caused by redistribution of these elements in response to variations in near-surface pH caused by oxidation of sulphides at depth (Smee, 1998). Calcium does not show a corresponding enrichment to the second Rb response on the eastern part of the line; this suggests that the rubidium feature is not likely to be related to sulphide mineralization.

Two elements related to the mineralization are illustrated in Figures 10c and d. Arsenic (Figure 10c) defines a sharp single-sample feature (13.3 ppm) located near the southeastern margin of the mineralized zone. There is no corresponding peak over the opposite margin. Values are at background levels for the rest of the line, with no significant enrichment in the swampy drainage to the east. Antimony shows a similar pattern (see Figure 11). Copper, on the other hand, has a relatively noisy profile (Figure 10d). Background concentrations average about 5 ppm but there is considerable variation above and below this level. Nevertheless, there does appear to be a low-contrast response to the mineralized zone, which has the form of a rabbit-ear anomaly. The two peaks (13.3 and 16.2 ppm) coincide closely with the projected edges of the underlying mineralization. Like Rb, Cu shows significant enrichment over the swampy area east of the mineralized zone, where two adjacent samples define a moderate-contrast feature with a maximum value of 17.1 ppm coinciding with the western edge of the swamp (charcoal could not be collected from the middle of the swampy area). This response is interpreted as a hydromorphic anomaly.

Vegetation

It should be noted that, in the case of the spruce bark, the dry matter was used for analysis, whereas the spruce twigs were reduced to ash prior to analysis. The ashing process results in approximately a 50-fold increase in element concentrations because the ash yield is only about 2% of the dry tissue. This process serves to bring concentration levels of some elements to well above the detection levels, resulting in more precise data. Elements illustrated for the spruce bark (Figure 11) are Cs (a surrogate for Rb and K), Cu and Sb (with a geochemical affinity for As).

Cesium is an element that can occur in association with Au deposits. It occurs with Au deposits at Hemlo and Getchell, occurring primarily in the mineral galkhaite $[(Cs,Tl)(Hg,Cu,Zn)_6(As,Sb)_4Si_2]$. It has also been noted in vegetation peripheral to the Au-As-Sb mineralization at the top of Mount Washington, Vancouver Island, and in plants surrounding the hydrothermal pools on the North Island of New Zealand (Dunn, 2007). Whereas Cs, Rb and K are all alkali elements, which tend to show similar patterns in rocks and soils, they sometimes adopt different paths in vegetation. This is primarily because K is an essential structural element in plant tissues and Rb is required in trace amounts, whereas Cs has no known function. Consequently, Cs in plants is a better indicator of potassic alteration than K itself (Figure 11a). Copper is another essential element for plant metabolism, which is why increased concentrations in plants growing over Cu-rich mineralization are generally quite subtle; this situation is illustrated in the Cu pattern of dry spruce bark (Figure 11b). Antimony tends to follow As and, in the spruce bark (Figure 11c), the high-

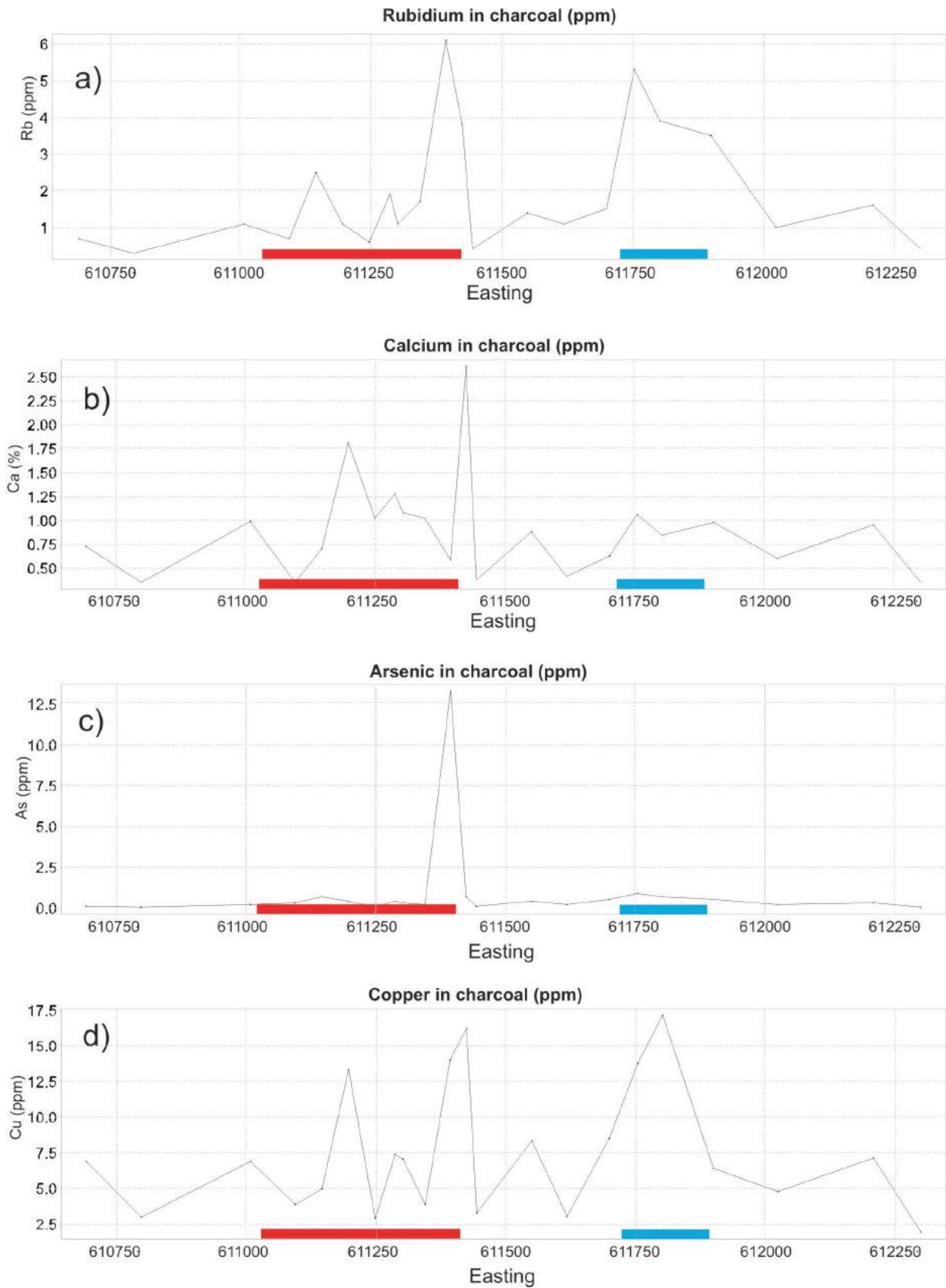


Figure 10. Results for selected elements in charcoal at the Woodjam property, south-central British Columbia: **a)** rubidium; **b)** calcium; **c)** arsenic and **d)** copper. The surface projection of the mineralization, defined by the +0.20 g/t Au equivalent cutoff, is shown by the red bar. The blue bar indicates the approximate location of a swampy drainage.

est concentration (although at low levels) coincides with the highest As in the charcoal (see Figure 10a).

In the spruce-twig ash, Cs (Figure 12a) presents a similar picture to that of Cs in the dry spruce bark. Similarly, Sb has by far the highest concentration directly over the surface projection of the mineralization (Figure 12b; see also As in Figure 10c). The highest Au concentration occurs over the southeastern part of the mineralized zone, and the lowest Au values are adjacent to the northwestern (Figure 12b) area of the zone.

Discussion and Conclusions

Preliminary results demonstrate that several of the organic media (charcoal, spruce bark and spruce twigs) all exhibit elevated levels of several elements, which indicate both alteration (Cs, Rb) and mineralization (Cu, As, Sb and Au). A second phase of sampling has extended the Deerhorn transect both to the east and west to help better define the significance of the anomalous signatures that were observed. It appears that the elevated concentrations of alkali metals may be reflecting a zone of potassic alteration,

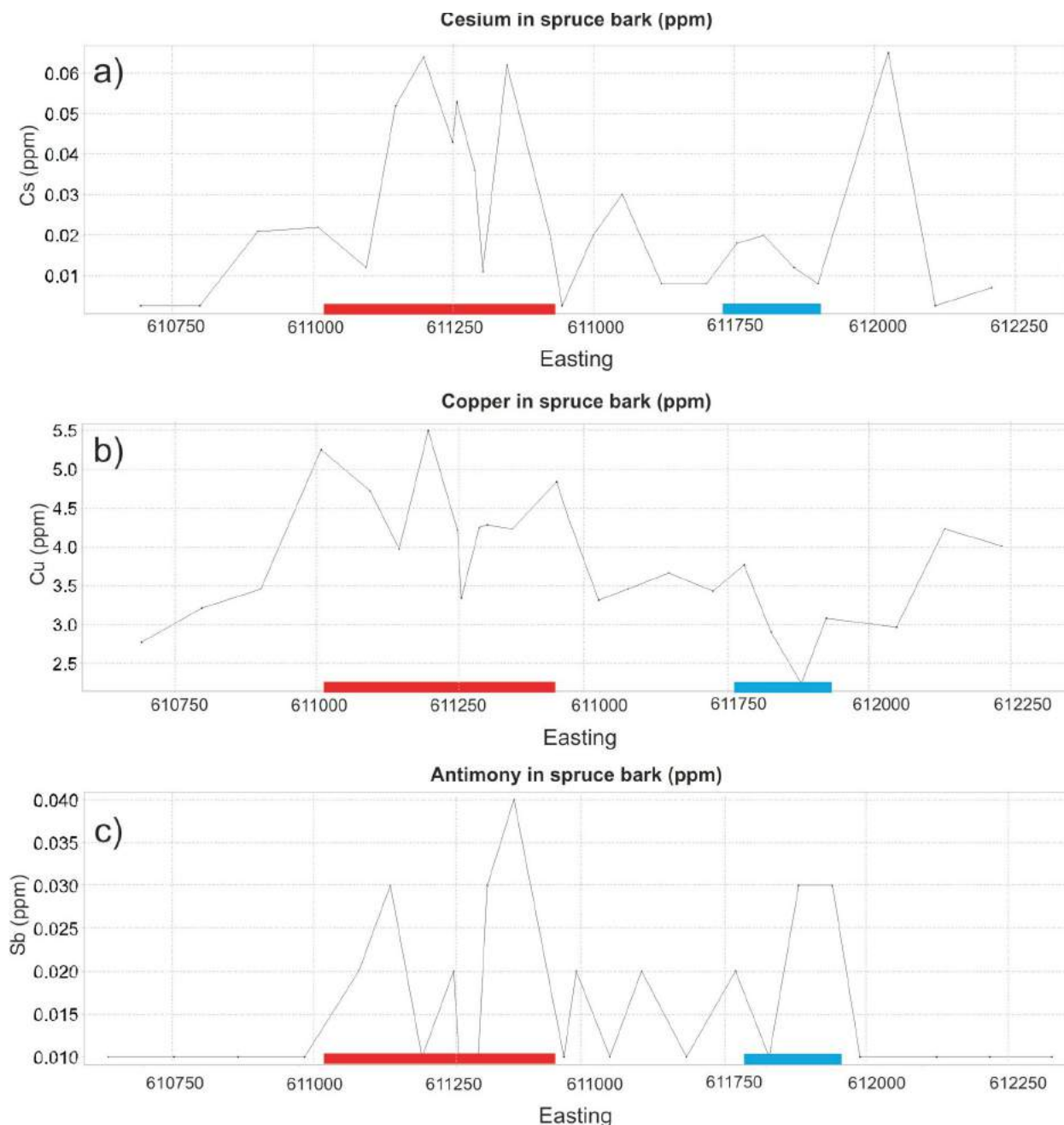


Figure 11. Results for selected elements in spruce bark at the Woodjam property, south-central British Columbia: **a)** cesium; **b)** copper and **c)** antimony. The surface projection of the mineralization, defined by the +0.20 g/t Au equivalent cutoff, is shown by the red bar. The blue bar indicates the approximate location of a swampy drainage.

within which commodity (Cu and Au) and pathfinder (As and Sb) elements are relatively concentrated. At the time of writing, no analytical data had been received for the saps and other exudate liquids. Attempts to obtain plant particulates from leaf surfaces have proven to be unsuccessful, which suggests that this is not a practical approach to exploration in the central BC environment.

Acknowledgments

The authors would like to thank Gold Fields Canada Exploration and Consolidated Woodjam Copper Corp. for allow-

ing them access to the Woodjam property, and for providing them with much of the base-map data included in this report; they also appreciate their generous logistical support during the sampling campaigns. A special thank you to R. Sherlock, T. Skinner, J. Blackwell and A. Rainbow of Gold Fields Canada Exploration for their advice during the planning stages of the project and for their helpful suggestions and corrections to this manuscript. The authors also thank G. Heberlein, M. Eckfeldt and S. Lehman for their assistance with the sampling. They also acknowledge Acme Analytical Laboratories Ltd. and Queens University Facility for Isotope Research for their contributions to the ana-

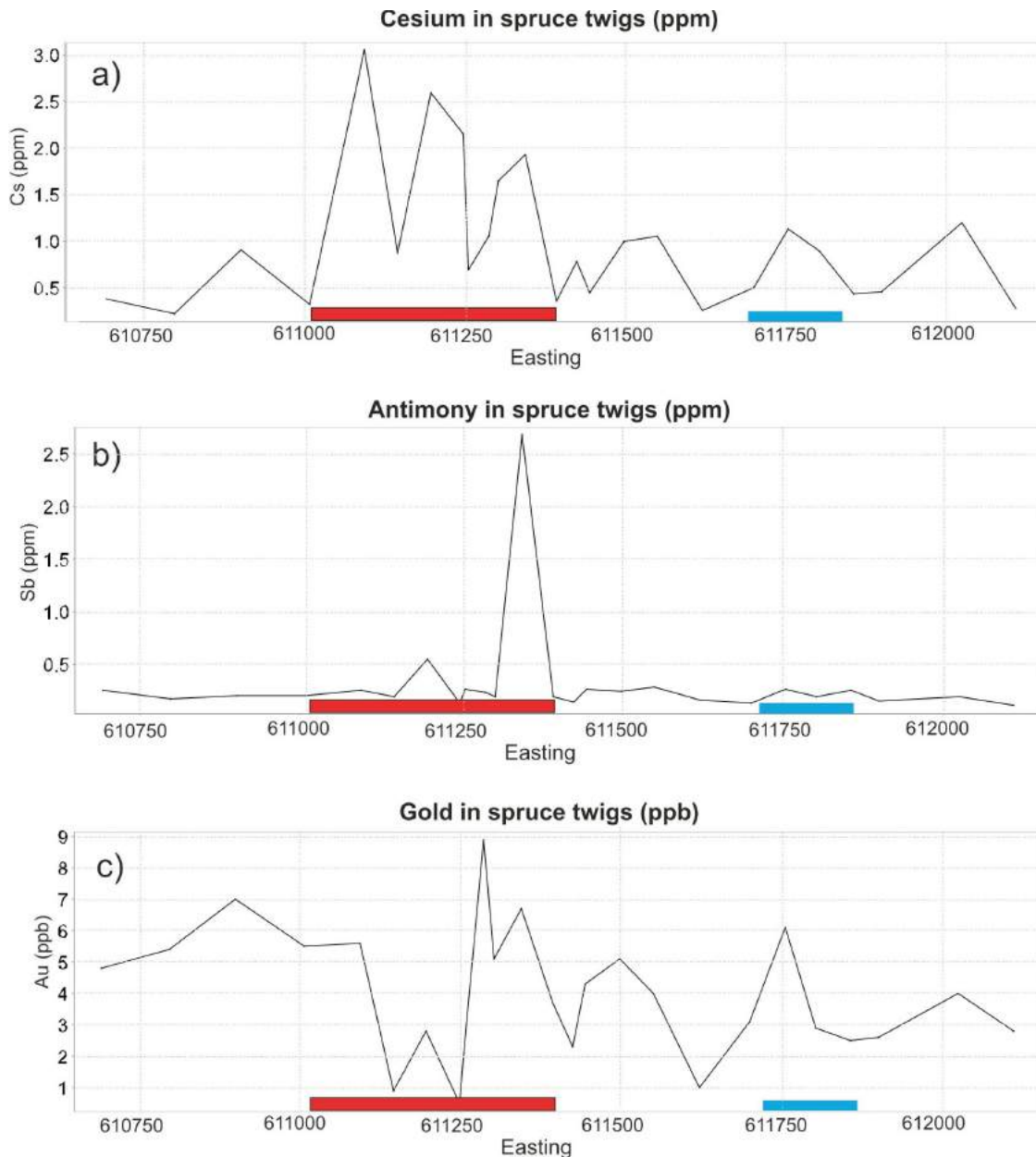


Figure 12. Results for selected elements in spruce-twig ash at the Woodjam property, south-central British Columbia: **a)** cesium, **b)** gold and **c)** antimony. The surface projection of the mineralization, defined by the +0.20 g/t Au equivalent cut-off, is shown by the red bar. The blue bar indicates the approximate location of a swampy drainage.

lytical work, and R. Lett and B. Smee for their reviews and helpful suggestions for improvements to the manuscript. Finally, the authors thank Geoscience BC for its financial support, without which this project would not have been possible.

References

- Barnett, C. T and Williams, P.M. (2009): Using geochemistry and neural networks to map geology under glacial cover (NTS 93 [all sheets], 94A, 94B, 94C, 94D); Geoscience BC, Report 2009-3, URL <<http://www.geosciencebc.com/s/2009-03.asp>> [August 2011].
- Barringer, A.R. (1977): AIRTRACE—An airborne geochemical exploration technique; in Proceedings of the first annual William T. Pecora memorial symposium, P.W. Woll and W.A. Fischer (ed.), Sioux Fall, South Dakota, October 1975, p. 211–251.
- Bevier, M. L. (1983) Regional stratigraphy and age of Chilcotin Group basalts, south-central British Columbia; Canadian Journal of Earth Sciences, v. 20, no. 4, p. 515–524.
- Consolidated Woodjam Copper Corp. (2012a): New gold-copper zone discovered at the Woodjam North property; Consolidated Woodjam Copper Corp., press release, August 7, 2012, URL <<http://www.woodjamcopper.com/2012/08/07/gold-copper-zone-discovered-woodjam-north-property/>> [October, 2012].
- Consolidated Woodjam Copper Corp. (2012b): Woodjam North; Consolidated Woodjam Copper Corp., URL <<http://www.woodjamcopper.com/projects/woodjam-north/>> [October 2012].
- Cook, S.J. and Dunn, C.E. (2007): Final report on results of the Cordilleran Geochemistry Project: a comparative assessment of soil geochemical methods for detecting buried mineral deposits—3Ts Au-Ag prospect, central British Columbia; Geoscience BC, Paper 2007-7, 225 p., URL <<http://www.geosciencebc.com/s/2007-07.asp>> [September, 2012].
- Del Real, I., Hart, C.J.R., Bouzari, F., Blackwell, J.L., Rainbow, A., Sherlock, R. and Skinner, T. (2013): Paragenesis and alteration of the Southeast and Deerhorn porphyry deposits, Woodjam property, central British Columbia (parts of NTS 093A); in Geoscience BC Summary of Activities 2012, Geoscience BC, Report 2013-1, p. 77–86.
- Dohaney, J.A.M. (2009): Distribution of the Chilcotin Group basalts, British Columbia; M.Sc. thesis, University of British Columbia, 124 p., 2 maps, URL <<https://circle.ubc.ca/handle/2429/24161>> [October, 2012].
- Dunn, C.E. (2007): Biogeochemistry in mineral exploration; in Handbook of Exploration and Environmental Geochemistry, Volume 9, M. Hale (ed.), Elsevier, Amsterdam, 464 p.
- Dunn, C.E., Cook, S.J. and Hall, G.E.M. (2007): Halogens in surface exploration geochemistry: Evaluation and development of methods for detecting buried mineral deposits; Geoscience BC, Report 2007-10, URL <<http://www.geosciencebc.com/s/2007-10.asp>> [September, 2012].
- Harju, L. and Huldén, S.G. (1990): Birch sap as a tool for biogeochemical prospecting; Journal of Geochemical Exploration, v. 37, p. 351–365.
- Heberlein, D.R. (2010): Comparative study of partial and selective extractions of soils over blind porphyry copper-gold mineralization at Kwanika and Mount Milligan, central British Columbia (NTS 093N/01, /19): fieldwork, soil conductivity and pH results; in Geoscience BC Summary of Activities 2009, Geoscience BC Report 2010-1, p. 11–24, URL <<http://www.geosciencebc.com/s/SummaryofActivities.asp?ReportID=379075>> [October, 2012].
- Heberlein, D. R. and Samson, H. (2010): An assessment of soil geochemical methods for detecting copper-gold porphyry mineralization through Quaternary glaciofluvial sediments at the Kwanika Central Zone, north-central British Columbia; Geoscience BC, Report, 2010-3, p. 1–89, URL <<http://www.geosciencebc.com/s/2010-03.asp>> [October, 2012].
- Heberlein, D.R. and Dunn, C.E. (2011): The application of surface organic materials as sample media over deeply buried mineralization at the Kwanika Central Zone, north-central British Columbia (NTS 93N); Geoscience BC, Report 2011-3, p. 1–75, URL <<http://www.geosciencebc.com/s/2011-03.asp>> [October, 2012].
- Holland, S.S. (1964): Landforms of British Columbia, a physiographic outline; BC Ministry of Energy, Mines and Natural Gas, Bulletin 48, 138 p.
- Horler, D.N.H., Barber, J. and Barringer, A.R., (1980): A multi-elemental study of plant surface particles in relation to geochemistry and biogeochemistry; Journal of Geochemical Exploration, v. 13, p. 41–50.
- Jaffré, T., Brooks, R.R., Lee, J. and Reeves, R.D. (1976): *Sebertia acuminata*: a nickel-accumulating plant from New Caledonia; Science, v. 193, p. 579–580.
- Krendelov, F.P. and Pogrebnyak, Yu.F. (1979): Gold and zinc concentrations in birch sap as prospecting indicators for these metals; Doklady Akademii nauk SSSR 234, p. 250–252.
- Kyuregyan, E. A. and Burnutyan, R.A. (1972): Gold in the juice of plants as a method for its detection (in Russian); Izd-vo Akademii nauk Ar. SSSR 25, p. 83–85.
- Levson, V. (2010): Surficial geology of the Woodjam project area; Gold Fields Canada Exploration, unpublished internal report.
- Schiarizza, P., Bell, K. and Bayliss, S. (2009): Geology and mineral occurrences of the Murphy Lake area, south-central British Columbia (NTS 093A/03); in Geological Fieldwork 2008, BC Ministry of Energy, Mines and Natural Gas, Paper 2009-1, p. 169–187.
- Sherlock, R., Poos, P.E. and Trueman, A. (2012): NI 43-101 Technical Report for 2011 Activities on the Woodjam South Property; Gold Fields Canada Exploration, 184 p., URL <<http://woodjamcopper.com/data/NI%2043-101%20Woodjam%20Technical%20Report.pdf>> [October 2012].
- Skinner, T. (2010): Report on the 2010 Activities on the Woodjam North Property; BC Ministry of Energy, Mines and Natural Gas, Assessment Report 32 302, 81 p., URL <http://aris.empr.gov.bc.ca/search.asp?mode=repsum&rep_no=32302> [October, 2012].
- Smee, B.W. (1997): The formation of surficial geochemical pattern over buried epithermal gold deposits in desert environments. Results of a test of partial extraction techniques; in Exploration '97, Symposium Volume, Toronto, p. 301–314.
- Smee, B.W. (1998): A new theory to explain the formation of soil geochemical responses over deeply covered gold mineralization in arid environments; Journal of Geochemical Exploration, v. 61, p. 149–172.

Geochemical Techniques for Detection of Blind Porphyry Copper-Gold Mineralization under Basalt Cover, Woodjam Prospect, South-Central British Columbia (NTS 093A/03, /06)

T. Bissig, Mineral Deposit Research Unit, University of British Columbia, Vancouver, BC, tbissig@eos.ubc.ca

D.R. Heberlein, Heberlein Geoconsulting, North Vancouver, BC

C.E. Dunn, Colin Dunn Consulting Inc., North Saanich, BC

Bissig, T., Heberlein, D.R., Dunn, C.E. (2013): Geochemical techniques for detection of blind porphyry copper-gold mineralization under basalt cover, Woodjam prospect, south-central British Columbia (NTS 093A/03, /06); *in* Geoscience BC Summary of Activities 2012, Geoscience BC, Report 2013-1, p. 63–78.

Introduction

This paper outlines activities conducted under the Geoscience BC project entitled: “Seeing through Chilcotin basalts: the geochemical signal of what is hidden underneath (092P, 093A, C)”. Field components of the study were undertaken in conjunction with another Geoscience BC project in the same area entitled: “Evaluation of plant exudates to assist in mineral exploration and the development of simple and cost effective field procedures and analytical methods” (see Heberlein et al., 2013).

Large areas prospective for porphyry and epithermal-style mineralization in central British Columbia are covered by either glaciofluvial sediments or young basalt units, most importantly of the Miocene to Pleistocene Chilcotin Group (Figure 1). Other recently completed Geoscience BC-funded projects have demonstrated that geochemical methods can assist in seeing through exotic cover (e.g., Cook and Dunn, 2007; Dunn et al., 2007; Barnett and Williams, 2009; Heberlein, 2010; Heberlein and Samson, 2010; Heberlein and Dunn, 2011). In areas where basaltic lavas cover the bedrock, application of exploration-geochemistry techniques has received relatively little attention in investigating the underlying bedrock, in part due to a lack in BC of basalt-covered sites with well-known mineralization, where deep-penetrating geochemical methods could be tested. The present study is aimed at establishing a geochemical strategy to see through the basalt cover, using a variety of analytical techniques on different sample media. Porphyry mineralization at the Woodjam prospect (Figure 1), the study site chosen for this project, occurs in close

proximity to basalt cover and may also be present underneath.

Chilcotin Basalt

The Chilcotin Group comprises mostly olivine-phyric basalt as coherent lavas, lesser tuffs and sedimentary units including sandstone, siltstone, shale and conglomerate (Bevier, 1983; Dohaney, 2009). Basalt units, considered to be part of the Chilcotin Group, include Late Oligocene and Miocene, and locally as young as Pleistocene, lavas (Bevier, 1983). These units are not hydrothermally altered and weather to brown and dark grey colours. They typically

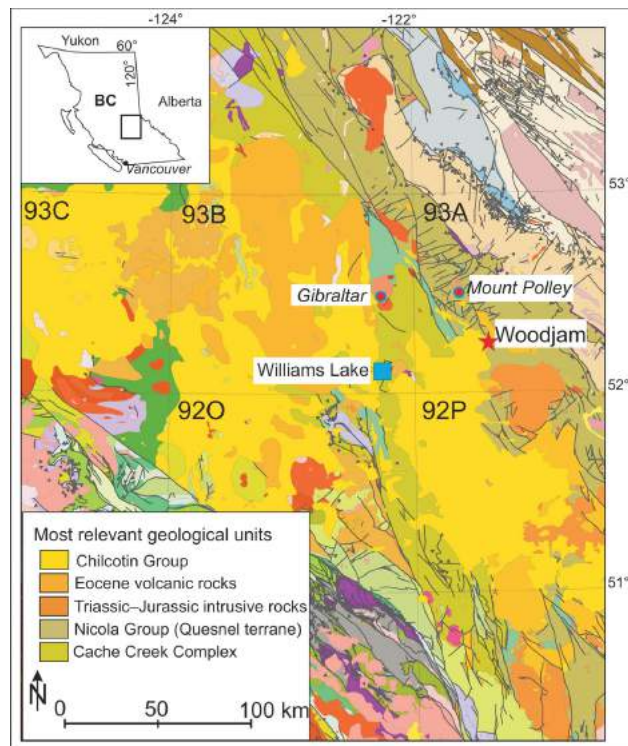


Figure 1. Regional geology of central British Columbia and location of the Woodjam study area as well as the nearby major porphyry deposits of Gibraltar and Mount Polley (after Massey et al., 2005); see inset for location within British Columbia.

Keywords: deep-penetrating geochemistry, Woodjam, copper-gold porphyry, basalt cover, selective leach, soil pH and conductivity

This publication is also available, free of charge, as colour digital files in Adobe Acrobat® PDF format from the Geoscience BC website: <http://www.geosciencebc.com/s/DataReleases.asp>.

consist of highly vesiculated coherent lavas, featuring variable degrees of columnar jointing. Chemically, they cover a broad range of compositions, from alkali olivine-basalt and basaltic andesite to less common hawaiite, mugearite and trachyandesite (Dohaney, 2009). Traditionally, Chilcotin basalt units have been mapped as extensive plateaus (e.g., Massey et al., 2005; Figure 1) and are best exposed in the incised valleys of present-day rivers. Recent work (Andrews and Russell, 2008; Dohaney, 2009) has established that most of the basalt lavas actually followed low-lying topography and, in many places where the Chilcotin Group is mapped, the basalt cover may be thin or absent, making exploration in those areas potentially viable. Their presence in the subsurface is commonly indicated by angular boulders and colluvial debris. Chilcotin Group rocks are also widely covered by Quaternary glacial sediments.

Geochemically the Chilcotin Group basalt units are distinctive from the underlying Triassic Nicola Group basalt flows and basalt-derived volcanoclastic sediments. In contrast to the Nicola Group (Vaca, 2012), these units have higher Ti, Ta, Nb, Th, U and light rare earth element contents, do not have a clear-cut arc signature, and plot in the tholeiitic and within-plate fields (Figure 2; Dohaney, 2009). The Nicola Group and along-strike equivalent Takla Group commonly host porphyry Cu-Au mineralization, including the Woodjam prospect (Figures 1, 3) where the field sampling for this study was carried out, whereas the Chilcotin Group basalt units are not known to be mineralized.

Benefits to the Mining Industry

This study is designed to test whether a geochemical signal of mineralization under basalt cover can be detected in the near-surface environment. It also aims to provide the mineral-exploration community with a better understanding of different sampling media that can be used for geochemical exploration in regions with basalt cover. The study provides comparisons of element concentrations in soils and plants (spruce) subjected to various total-analysis and selective-leach methods, and assesses the relative capabilities of each medium for recording the secondary geochemical-dispersion patterns of the geology, including blind mineral deposits under cover. It also examines the trace-element composition of coatings and materials within vesicles in the basalt units; a selection of results is reported herein.

Project Area

Test sites selected for this study lie within Gold Fields Canada Exploration and Consolidated Woodjam Copper Corp.'s Woodjam property, which is located in the Cariboo Mining District of central BC. (NTS map areas 093A/03, /06; Figure 3). The property, which consists of 178 mineral claims totalling 58 470 ha, lies about 50 km to the northeast of Williams Lake. Horsefly, the nearest settlement and lo-

gistical base for the fieldwork, is within the property boundary and is accessible by a paved road from Williams Lake.

The two test sites, known as Deerhorn and Three Firs (formerly known as Megalloy; Figure 3), lie 8 and 12 km respectively to the southeast and south of Horsefly; both are readily accessible via a network of well-maintained logging roads. Within those areas, one east-oriented and one east-northeast-oriented sample traverse pass from glaciofluvial sediment-covered areas into glaciofluvial sediment-and/or basalt-covered areas. In both transects, mineralization is known to underlie the unconsolidated sediments near the transition to basalt-covered areas. At the time of writing, no mineralized zone directly underlying basalt cover had been defined by drilling, although one (MAG-12-04) of three angled drillholes (Figure 3; Consolidated Woodjam Copper Corp., 2012a) at Three Firs passes through about 60 m of glaciofluvial material and about 30 m of basalt into mineralized bedrock. The top of the bedrock, which is fragmental and clay rich, contains Fe and Mn oxides just below the basalt; this can be interpreted as a paleoregolith but it may also be interpreted as fault gouge.

Surficial Environment

The project area lies at the boundary between the Fraser Plateau and Quesnel Highland physiographic regions of central BC (Holland, 1964). The terrain in the study areas has characteristics of both regions. The Deerhorn test site lies at a fairly sharp transition between relatively flat, rolling topography typical of the Fraser Plateau on the western side of the mineralized zone, and low hills of the Quesnel Highland to the east (Figure 3). Elevations across the Deerhorn sample traverses, which cross the transition, vary from 900 m at the west to 1030 m at the highest point, close to the eastern end. A number of small lakes and ponds are dotted throughout the area; the largest of these is Mica lake, which lies on the southwestern side of the mineralized zone. Lakes are linked by small streams and boggy depressions, which form part of a dendritic drainage pattern connecting with the Horsefly River about 5 km to the northeast of Deerhorn. Three Firs lies in a similar physiographic setting to Deerhorn (Figure 3). More than half of the Three Firs sample traverse crosses relatively flat terrain typical of the Fraser Plateau, where elevations range from 975 to 1000 m asl. At these lower elevations, a number of swamps and small creeks define a northwest-flowing dendritic drainage pattern, which merges with Woodjam Creek some 8 km to the northwest. The terrain gradually rises eastward into the rounded hills of the Quesnel Highland, where the maximum elevation at the eastern end of the line is 1140 m.

Quaternary glacial deposits cover the mineralization at both study areas. To the east of Deerhorn, surficial deposits consist of an intermittent till veneer, which mantles the hill-

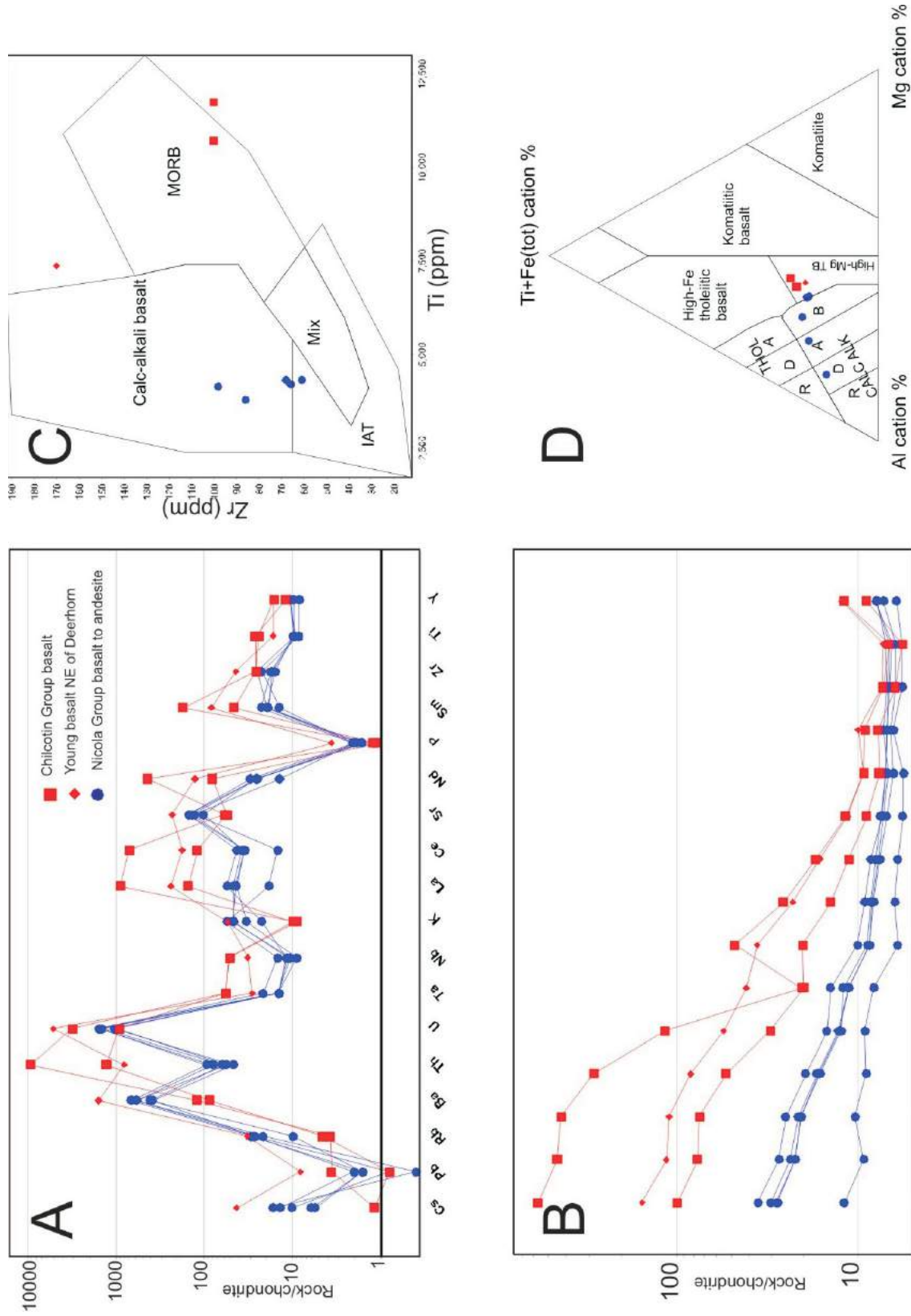


Figure 2. Whole-rock geochemistry of basalt to basaltic andesite in the Woodjam area, south-central British Columbia. Blue symbols indicate Triassic Nicola Group and red squares, Late Oligocene to Pliocene Chilcotin Group basalt sampled in the western part of the Woodjam property. Red diamonds indicate one sample taken northeast of the Deerhorn study area. The Nicola Group samples have an arc signature, whereas the Chilcotin and Deerhorn basalt units have a within-plate to tholeiitic signature: **a)** and **b)** chondrite-normalized spider diagrams (chondrite values from Sun and McDonough, 1989); **c)** basalt classification diagram; **d)** Jensen cation plot (Pearce et al., 1973; Jensen 1976) for basalt classification (diagrams modified from Rollinson, 1993; data for Nicola Group basalt units from Vaca, 2012).

sides and becomes thicker in topographic depressions. The maximum thickness of the till is unknown but the presence of outcrops on the northern flank of the hillside east of Deerhorn suggests that it is likely to be no more than a few metres thick at that location. Glacial landforms, such as drumlinoid features, are present in this area and east of the sample traverse. Their long axes indicate a west-northwesterly ice-flow direction. Cover thickens rapidly westward

onto the lowlands and drilling at Deerhorn has shown that the bedrock surface is buried beneath up to 60 m of till and glaciofluvial sediments (Skinner, 2010; Del Real et al., 2013). Surficial deposits on the eastern shore of Mica lake and southern limit of the projected mineralized zone (Figure 3) consist of well-sorted sand and gravel of probable glaciofluvial origin; the distribution of these deposits is unknown. A hill consisting of basaltic rocks assigned to the

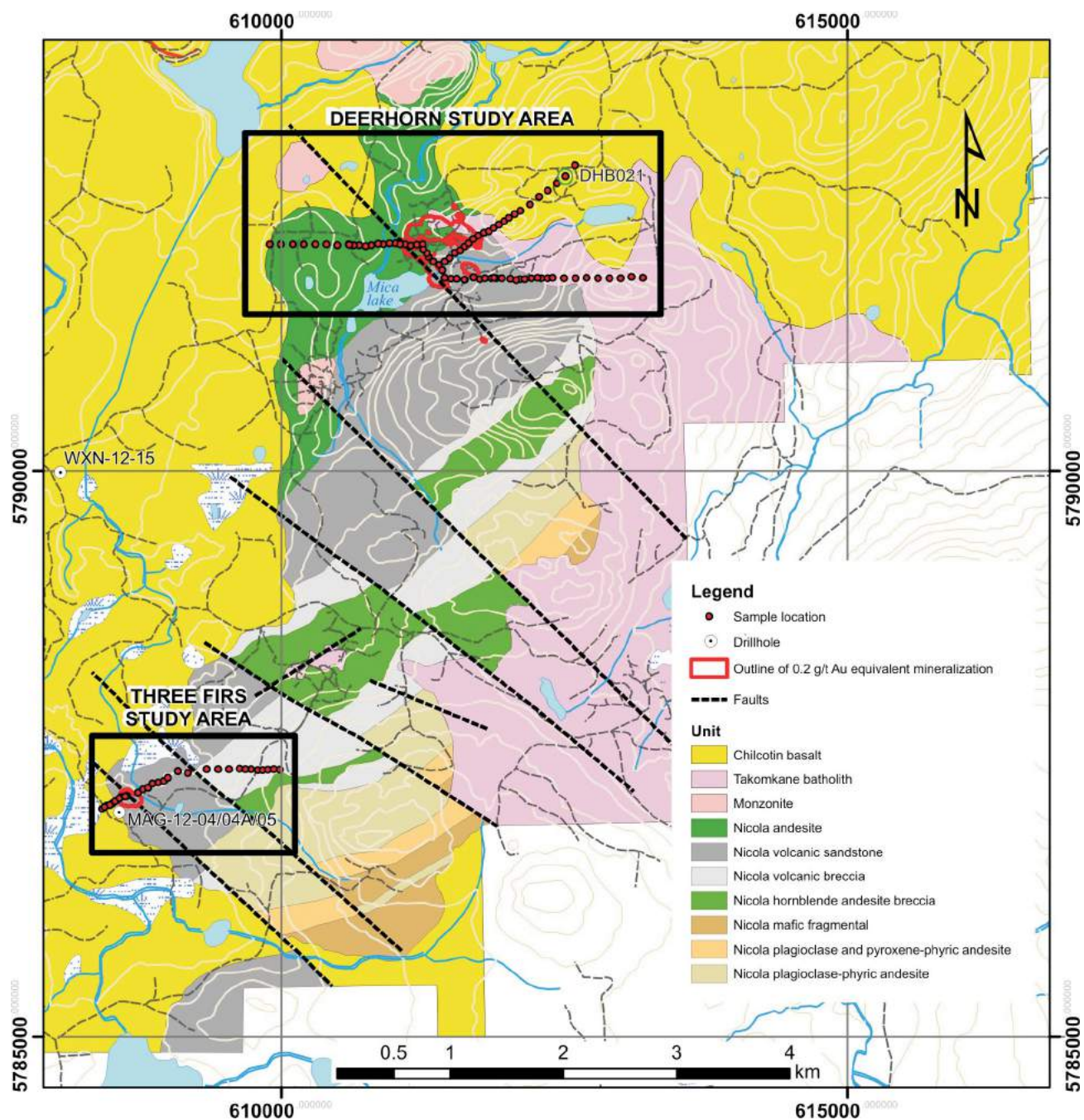


Figure 3. Bedrock geology of the Woodjam South prospect, south-central British Columbia. (modified from Del Real et al., 2013; J. Blackwell, pers. comm., 2012). Map is in UTM NAD 83 projection, Zone 10. Red outlines denote surface projection of the +0.2 g/t Au equivalent mineralization; black dots show soil-sample locations. Specific drillhole and sample locations mentioned in the text are indicated. Abbreviations: IAT, island-arc tholeiite; MORB, mid-ocean ridge basalt. Place name with the generic in lower case is unofficial.

Chilcotin Group lies to the east-northeast of the mineralized zone (Figure 3). Samples collected along the east-, northeast-oriented traverse largely come from this basalt-covered area. The depth to bedrock below the basalt flows and potential presence of mineralization below this basalt is unknown.

At Three Firs, the cover environment contains a Tertiary basalt unit beneath the glacial deposits in the western part of the sample traverse. Drilling has indicated that the basalt may cover a part of the mineralized zone. The basalt consists of a fresh, black, highly vesicular flow unit up to 20 m thick. Nicola Group rocks at its lower contact are fragmented and intensely clay-altered over several metres in what is either a gouge-filled fault zone or a paleoregolith. The extent of basalt cover is unknown, although its distribution is most likely restricted to paleovalleys rather than forming a continuous cap over the mineralized area. This would be typical of other occurrences of Chilcotin Group flows in the region (Dohaney, 2009). Surficial deposits at Three Firs consist predominantly of glacial till, which forms a blanket 40–100 m thick. There is no outcrop in the vicinity of the mineralization. Till cover appears to thin gradually eastward and outcrops of a distinctive ‘turkey-track’ feldspar porphyritic andesite become widespread in the east-central part of the sample traverse. On the hillside, at the eastern end of the traverse, till cover is present as a thin veneer of no more than a metre or two thick.

Regional Geological Setting

The Woodjam prospect lies in the southern part of the highly prospective Quesnel terrane: a Late Triassic to Early Jurassic magmatic arc complex, which extends for most of the length of the Canadian Cordillera. It is flanked to the east by assemblages of Proterozoic and Paleozoic carbonate and siliciclastic rocks of ancestral North American affinity, but is separated from them by a sliver of oceanic basalt and chert of the Slide Mountain terrane (Schiarizza et al., 2009). Oceanic rocks of the Late Paleozoic to Early Mesozoic Cache Creek terrane bound the Quesnel terrane to the west. The southern part of the Quesnel terrane hosts a number of important Cu-Au porphyry deposits; nearby examples include Gibraltar and Mount Polley.

In the Woodjam area, the Quesnel terrane is represented by Middle to Upper Triassic volcano-sedimentary rocks of the Nicola Group (Figures 1, 3). Locally, this consists of a shallow northwest-dipping sequence of volcanic and volcanic-derived sedimentary rocks, which include augite-phyric basalt flows and polymictic breccias containing latite, trachyte and equivalent volcanic clasts (Gold Fields Canada Exploration, unpublished data, 2012). Sandstone and conglomerate are intercalated with the volcanic units. A suite of more or less coeval intrusions of alkaline to calcalkaline affinity intrudes the volcanic and sedimentary se-

quence. These intrusions include the Early Jurassic Takomkane batholith, located to the south and east of the project area, and a number of smaller syenite, monzonite, quartz monzonite and monzodiorite stocks and dikes within the Woodjam property itself, many of which are associated with Cu-Au mineralization.

The Woodjam South property contains several centres of Early Jurassic porphyry-style Cu-Mo-Au mineralization (Schiarizza, 2009; Sherlock et al., 2012; Mineral Deposit Research Unit, unpublished data, 2011). Style of mineralization, host rocks and metal association vary from one mineralized centre to another; these include the Southeast, Takom, Megabuck, Deerhorn and Three Firs zones (Figure 3; Del Real et al., 2013). The Southeast zone is at the most advanced stage of exploration and is currently undergoing advanced exploration drilling. Copper-molybdenum mineralization is hosted in intrusive rocks, which form part of the Takomkane batholith. Deerhorn is the next most advanced prospect and is currently at the advanced exploration drilling stage. It is characterized by Cu-Au mineralization hosted in Nicola Group volcanic rocks and a series of small porphyry stocks and dikes (see below). The remaining prospects are all at the exploratory drilling stage. Three Firs represents a new discovery that was made early in 2012 (Consolidated Woodjam Copper Corp., 2012a); it is currently in the initial drill-testing stage. Nicola Group rocks in much of the western part of the Woodjam South property area and an area to the east of Deerhorn are covered by younger Cenozoic basalt flows belonging to the Chilcotin Group. This younger volcanic- and sedimentary-rock cover masks prospective areas of the underlying Nicola Group.

Geology of Test Areas

Deerhorn

Deerhorn is a blind zone of porphyry Cu-Au-style mineralization, which was discovered by drilling a large chargeability anomaly in 2007 (Skinner, 2010). The mineralization, defined by the red +0.2 g/t Au equivalent outline in Figure 3, is the surface projection of a pipe-like body containing a higher-grade shoot, which plunges at a moderate angle to the southeast (Gold Fields Canada Exploration, unpublished data, 2012). Its dimensions are approximately 350 m in strike, 100 m in width and 200 m in depth (Consolidated Woodjam Copper Corp., 2012b). Higher-grade mineralization is enclosed within a much more extensive lower-grade envelope defined by quartz and magnetite stockwork and veinlets, and disseminated chalcopyrite mineralization. Low-grade mineralization is coincident with an arcuate chargeability anomaly, which extends northwest of the Deerhorn drill site and continues south and west to the Megabuck East and Megabuck prospects.

Geological mapping and reconstruction of the bedrock geology from drilling by Gold Fields Canada Exploration

(Figure 3; J. Blackwell, pers. comm., 2012) indicate that the mineralization is hosted in a southwest-striking, northwest-dipping package of Nicola Group andesite and volcanic-derived sandstone. Higher-grade mineralization is associated with a number of northwest-striking dike-like monzonite bodies, which cross the contact between volcanic-derived sandstone in the southeast and andesite in the northwest of the mineralized zone. The intrusion and volcano-sedimentary units are offset by sets of west-northwest- and northeast-striking faults (Gold Fields Canada Exploration, unpublished data, 2012). Mineralization subcrops beneath a variable cover of Quaternary glacial and glaciofluvial deposits, which consist of a till blanket up to 40 m thick over the mineralization and a sequence of overlying glaciofluvial sand and gravel exposed in roadcuts near the southeastern shore of Mica lake; the extent of these deposits is unknown. To the northeast of the mineralized area, coherent basalt flows, presumably of the Chilcotin Group, are present. The thickness of these basalts is unknown but they appear to be directly underlying the soil profile in at least part of the area.

Three Firs (Megalloy)

Bedrock geology of the Three Firs study area is not well understood. Mineralization was only discovered at this prospect during the spring of 2012 and, at the time of sampling for this study, only three holes had encountered significant Cu-Au mineralization (Consolidated Woodjam Copper Corporation, 2012a). What makes this study area appealing from a deep-penetrating-geochemistry standpoint is the presence of a basalt unit, inferred to be part of the Chilcotin Group, which overlies at least part of the mineralized zone. The extent of the basalt is unknown and difficult to resolve from the interpretation of ground and airborne magnetic data (Gold Fields Canada Exploration, unpublished data, 2012). Drilling shows that it consists of one or several coherent flows and forms a cap at least 30 m thick overlying the altered and mineralized Nicola Group rocks. The known distribution of basalt and the surface projections of the mineralized drill intersections are illustrated in Figure 3 (Gold Fields Canada Exploration, unpublished data, 2012) and indicated for reference in the geochemical plots below. Overlying the basalt are Quaternary glacial sediments; where observed in drill road exposures, these appear to consist of a boulder till containing abundant large rounded clasts (up to 1 m in diameter) of distinctive ‘turkey-track’ andesite porphyry that is known to outcrop near the eastern end of the sample traverse and immediately to the southeast. The size and composition of the boulders indicate that the till is locally derived and possibly forms only a thin veneer across the survey area.

Field Procedures

Soils

At each sample station, at least one hole was dug to a depth of about 50 cm to collect a few grams of the upper Ae horizon (eluviated greyish zone immediately below the organic-rich Ah horizon) for pH and conductivity measurements, the upper B horizon (Bf or Bm horizon) and the interval of 10–25 cm beneath the base of organic matter for Mobile Metal Ion™ (MMI) analysis. The locations of the sample stations are shown on Figure 3 and the sample types on Figure 4.

Basalt

In addition to whole-rock analyses for three Chilcotin Group basalt samples, eight samples of vesicle infill have been separated (Figure 5). These are both from Chilcotin basalt-proximal and apparently overlying sulphide mineralization at the Three Firs zone, and from drillcore (WNX12-15) from an inferred background area located some 2 km to the north of known mineralization (Figure 3).

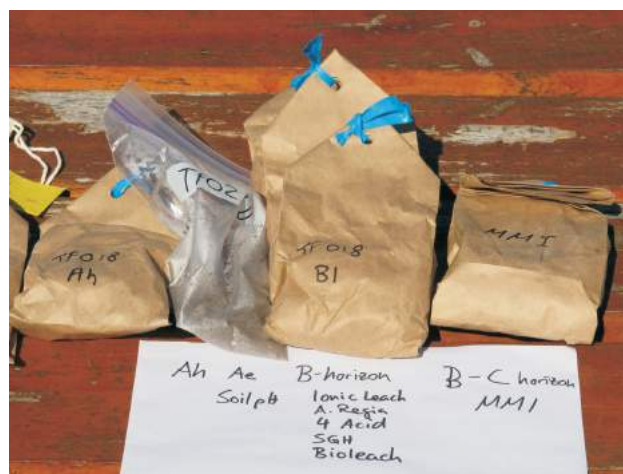


Figure 4. Suite of samples collected at each sample station for this study (not shown are spruce twigs and bark), Woodjam prospect, south-central British Columbia. The samples were collected together with those reported in Heberlein et al. (2013).



Figure 5. Example of vesicular Chilcotin basalt, with beige-brown clay (vermiculite) infill and white calcite infill, from drillhole MAG-12-04 (at 70.9 m) in the Three Firs zone, Woodjam prospect, south-central British Columbia. These two types of infill have been separated and analyzed by inductively coupled plasma-mass spectrometry (ICP-MS) following an aqua-regia digestion to test for a geochemical signature from underlying mineralization.

The vesicle infill consists of clay (poorly crystalline vermiculite) and carbonate (magnesian calcite). Infill was extracted from the crushed rock using hardened-steel tools or, in the case of carbonate infill, hand-picked from the crushed rock. More than 0.5 g of material was collected and analyzed at ALS Limited (Vancouver) using their MEMS41L package, which consists of inductively coupled plasma–mass spectrometry (ICP-MS) following aqua-regia digestion. The intention of this analytical work is to test the potential for clay- and carbonate-vesicle infill to record a geochemical signal from underlying mineralization; the results are shown in Figure 6.

Analytical Methods

Samples from a range of soil horizons crossing the two zones of mineralization at Woodjam (Deerhorn and Three Firs) were submitted for comparative analysis by several commercially-available total, partial and selective extraction analytical methods. Table 1 provides a summary of the various analytical methods employed, which include:

- **Four-acid near-total digestion/ICP-MS (4 acid):** the sample is digested with perchloric, nitric, hydrofluoric and hydrochloric acids, which dissolve the silicate portion, including most of the resistate minerals.
- **Aqua-regia digestion/ICP-MS (AR):** partial leach (acid-leachable component, especially sulphides, amorphous oxides, carbonates and organic matter).
- **Ionic Leach (IL):** a proprietary sodium-cyanide leach buffered to pH 8.5 using the chelating agents ammonium chloride, citric acid and ethylenediaminetetraacetic acid (EDTA). These dissolve weakly-bound ions attached to particle surfaces.
- **Mobile Metal Ion™ (MMI):** a proprietary method requiring no sample preparation or drying. Elements in a 50 g sample are extracted in weak solutions of organic and inorganic compounds (details not specified). MMI solutions contain strong ligands, which detach and hold in solution the metal ions that are loosely bound to soil particles.
- **Enzyme Leach (EL):** a proprietary method to selectively remove amorphous manganese-oxide coatings on soil particles, and thereby release trace elements into solution that are associated with these coatings.
- **Biobleach (BL):** a proprietary technology designed to digest remnant bacteria, which help to identify the metals associated with soil gas hydrocarbon anomalies.
- **Soil Gas Hydrocarbons (SGH)SM:** a proprietary organic-based geochemical method, which detects 162 organic compounds in the C5 to C17 carbon-number range. These compounds provide a signature directly related to bacteriological interaction with a mineral deposit at depth. Interpretation is undertaken by Activation Laboratories Ltd. (Ancaster, Ontario).

- **Organo-Sulphur Geochemistry (OSG):** a proprietary method similar to SGH in its rationale, in that it involves the selective extraction of 105 organo-sulphur-based compounds in the C7–C17 carbon series. It involves a very weak leach, almost aqueous, which isolates the compounds by high-resolution capillary-column gas chromatography.
- **pH and electrical conductivity (EC):** measured on Ae-horizon or top of B-horizon soil samples collected from immediately beneath the organic-rich Ah layer. This zone is optimal for stable H-ion signatures and assists in delineating carbonate remobilization caused by changes in pH at the edges of electrochemical cells over buried sulphide mineralization.

Field Measurements

Soil pH and Electrical Conductivity Measurements

Samples for soil pH and electrical conductivity (EC) measurements were collected from both study areas. Where possible, material was collected from the top centimetre of the leached Ae horizon (in podzol profiles) and from the top of the B horizon, where the Ae horizon was either absent or poorly developed (e.g., in brunisol profiles). At sample sites with poor drainage, where organic material comprises the upper part of the profile, no sample was collected. Samples were placed in heavy-duty double-seal Ziploc[®] plastic bags.

Conductivity measurements were made on a 1:1 slurry of soil in demineralized water using a VWR[®] conductivity meter. Soil pH readings were taken on the same slurry using a double-junction pHTestr[®] 30 handheld pH meter manufactured by Oakton[®] Instruments. The instrument was calibrated daily using standard pH-buffer solutions at pH 4.00, 7.00 and 10.00. Two pH measurements were taken on each sample: the first one 20 seconds after immersion of the electrode into the slurry and the second, 20 seconds after adding one drop of 10% hydrochloric acid and stirring. The acidified pH (pHa) is an indication of the buffer capacity of the soils and the closer the pHa values are to the original pH, the greater the buffering capacity. Readings were recorded into an Excel[®] spreadsheet and converted to H⁺ concentrations and inverse-difference hydrogen (IDH) measurements for interpretation. The IDH measurement is the inverse of the difference between acidified and non-acidified H⁺ concentrations in the soil and is a measure of the buffering capacity of carbonate remobilized around reduced chimneys (Hamilton, 1998). The results are presented in Figures 7–9.

Quality Control

Quality control measures employed for this study included the collection of field duplicate samples for each sample

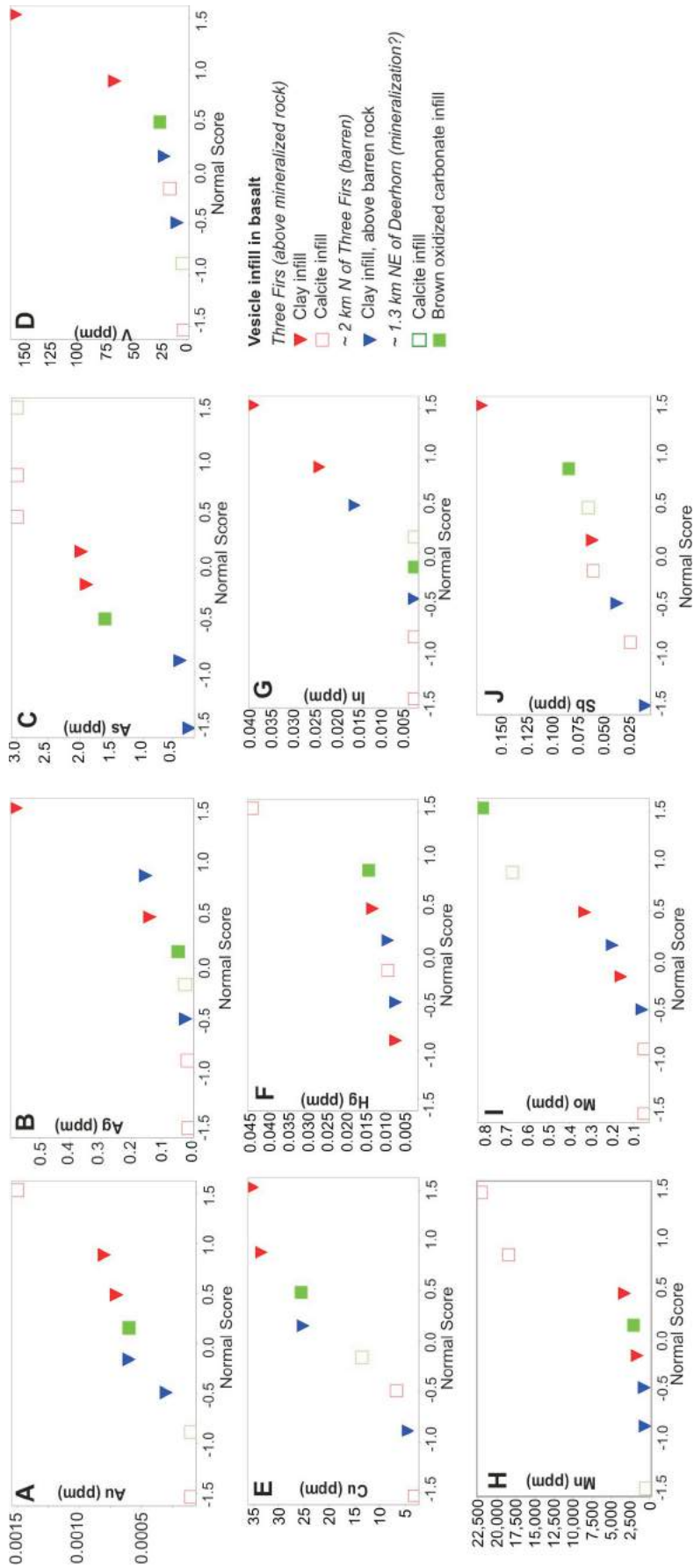


Figure 6 Chemistry (aqua regia) of vesicle infill in Chilcotin basalt, Woodjam prospect, south-central British Columbia. The x-axis on the probability plots shows the normal score in units of standard deviation for: **a**) Au; **b**) Ag; **c**) Cu; **d**) V; **e**) Cu; **f**) Hg; **g**) In; **h**) Mn; **i**) Mo; **j**) Sb. Analytical values are given in parts per million (ppm).

Table 1. Sample media and analytical methods employed. In addition to those listed, Ah horizon and spruce bark and twigs were collected (see Heberlein et al., 2013) at the Woodjam prospect, south-central British Columbia.

Sample medium	Analytical package	Laboratory	No. of samples	Description
B horizon (upper)	ME-MS41	ALS ¹	70	Standard aqua-regia leach (AR)
B horizon (upper)	ME-MS41L	ALS	70	Ultratrace aqua-regia digestion (high sensitivity)
B horizon (upper)	ME-MS61	ALS	70	4 acid strong leach (near-total digestion)
B horizon (upper)	Au-ST43L/aqua regia	ALS	70	Supertrace level gold (0.01 ppb)
B horizon (upper)	Ionic Leach	ALS	70	Sodium-cyanide leach buffered to pH 8.5
B horizon (upper)	Enzyme Leach	Actlabs ²	70	Proprietary weak leach (amorphous oxide coatings)
B horizon (upper)	SGH-GC-MS	Actlabs	50	Proprietary weak leach-organic compounds
B horizon (upper)	OSG-HR-GC	Actlabs	50	Proprietary weak leach-sulphur compounds
B horizon (upper)	Bioleach	Actlabs	70	Proprietary weak leach-remnant from bacteria
B horizon (10-25 cm depth)	MMI	SGS ³	27	Proprietary weak leach (loosely bound surface coatings)
Vesicle infill	ME-MS41L	ALS	8	Ultratrace AR digestion (high sensitivity)
Basalt whole rock	CCP-PKG01	ALS	3	Lithium-borate fusion and complete characterization

¹ ALS Chemex (Vancouver)

² Activation Laboratories Ltd. (Ancaster, Ontario)

³ SGS Minerals Services (Lakefield, Ontario)

type; a total of 9 field duplicates were collected for each sample at randomly selected sample sites. At each site, material was collected using exactly the same procedures as that used for the original sample and from within 5 m of the original sample's location. In this report, analytical values for field duplicates are plotted for B-horizon soil samples and IDH measurements (Figure 9). Although some local-scale variability in soil pH and conductivity as well as As in B-horizon soil is apparent, the difference between original and duplicate sites is less than the overall variability in the apparent background of the sampled profile. The exception is one sample location (DHB021) in the Deerhorn north-east-oriented sample line, where As values in the original B-horizon sample are double to triple those of the duplicate sample, irrespective of the digestion method used. Conductivity and pH values are similar between the original and duplicate sites. Because the elevated As values were obtained on two different aliquots sent to two different laboratories (ALS Limited, Vancouver, and Activation Laboratories Ltd., Ancaster, Ontario), the discrepancy between the original and duplicate samples is interpreted as the result of local-scale variability in the soil rather than sampling or analytical error.

Results

A selection of preliminary analytical results is presented below. A complete description of the results will be presented in a final report to Geoscience BC in early 2013.

Vesicle Infill in Basalt

Some pathfinder elements, including As, Sb, In and V are present in concentrations 5–8 times higher in clay-filled amygdulites (vermiculite) near mineralization compared to similar amygdulites in basalt over unmineralized Nicola Group (Figure 6). Gold, Ag, Mn and Cu values are also elevated in vesicular clay over mineralization. Based on two

samples from Three Firs, the calcite amygdulites appear to have higher As, Mn and Hg values than the clay amygdulites over the mineralization. Unfortunately, carbonate-filled amygdulites were not present at the background basalt location to the north of the mineralized zone. Carbonate amygdulites sampled from basalt found near the eastern end of the northeastern transect at Deerhorn (DHB021, Figure 3) contain elevated Cu and Mo and As values (Figure 6). Soil samples at this locality are also anomalous for As (see below).

Soil pH and Conductivity

Soil H⁺ and conductivity results are shown in Figures 7 and 8. Although there is considerable scatter in the data, some general patterns are apparent. Hydrogen-ion concentrations are highest over mineralization at Deerhorn and at the western margin of projected mineralization at Three Firs. The acidified H⁺ (H⁺a) values are higher near the margins than directly above the mineralized zones at both localities, although high H⁺a values do also occur distal to mineralization (Figures 7, 8). At Deerhorn, H⁺ and H⁺a concentrations are generally lower over basalt than in areas where only glacial sediments cover the bedrock (Figure 7). Electrical conductivity at Three Firs is highest at the margins of the mineralized zone but relatively low directly above it. At Deerhorn this pattern is less obvious and elevated EC values occur at the margins of mineralized zones as well as distally. In general, the IDH data mimic the conductivity data quite well. At Three Firs, the highest IDH values occur at the western end of the line, where the presence of carbonate reacting with HCl acid was recorded in the B-horizon soil sample. It is noteworthy that at site DHB021 (Figure 3) at Deerhorn, there are coincident high EC and IDH values over basalt. This sample site also coincides with apparently elevated Cu, Mo and As in carbonate vesicle infill (Figure 6).

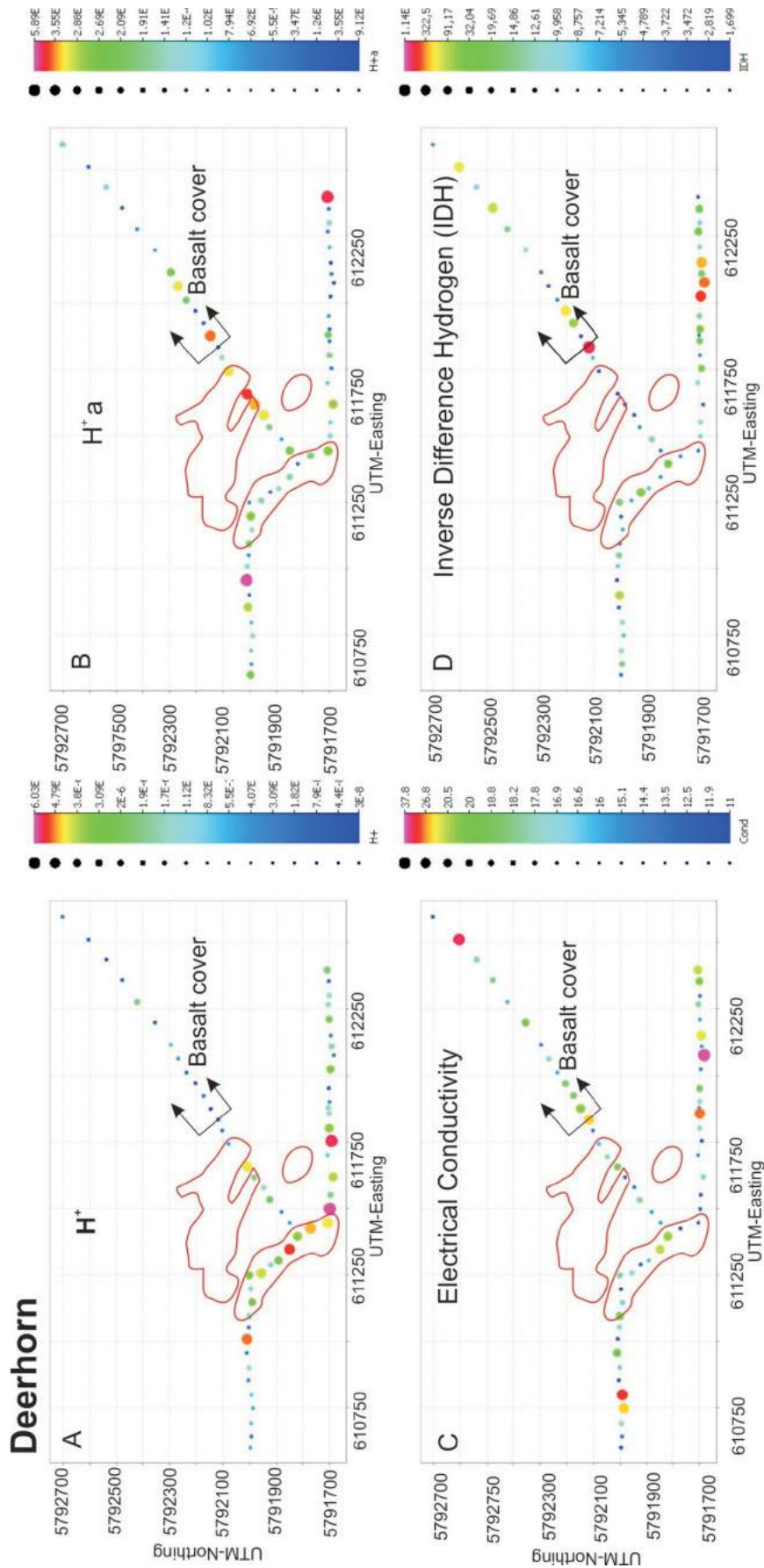


Figure 7. Soil pH and conductivity data for the Deerhorn survey area, Woodjam prospect, south-central British Columbia. Areas under basalt cover and surface projection of the mineralization, defined by the 0.2 g/t Au equivalent contours, are represented by graphs showing **a)** H^+ , concentration of hydrogen ions ($-\text{inverse of pH}$); **b)** $H^+ a$, concentration of hydrogen ions after addition of 1 drop of 10% HCl acid; **c)** electrical conductivity; **d)** inverse hydrogen difference, $1/(H^+ a - H^+)$.

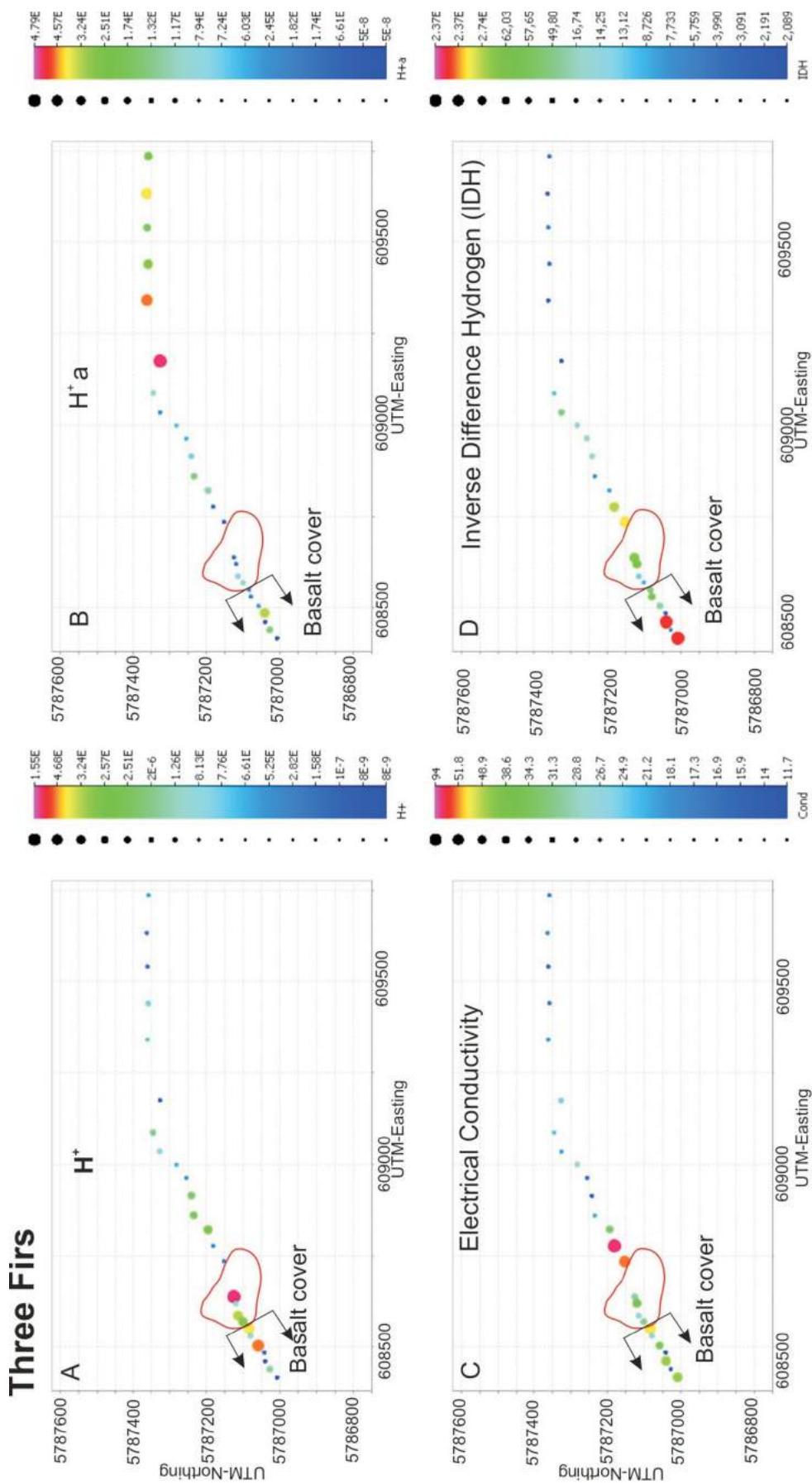
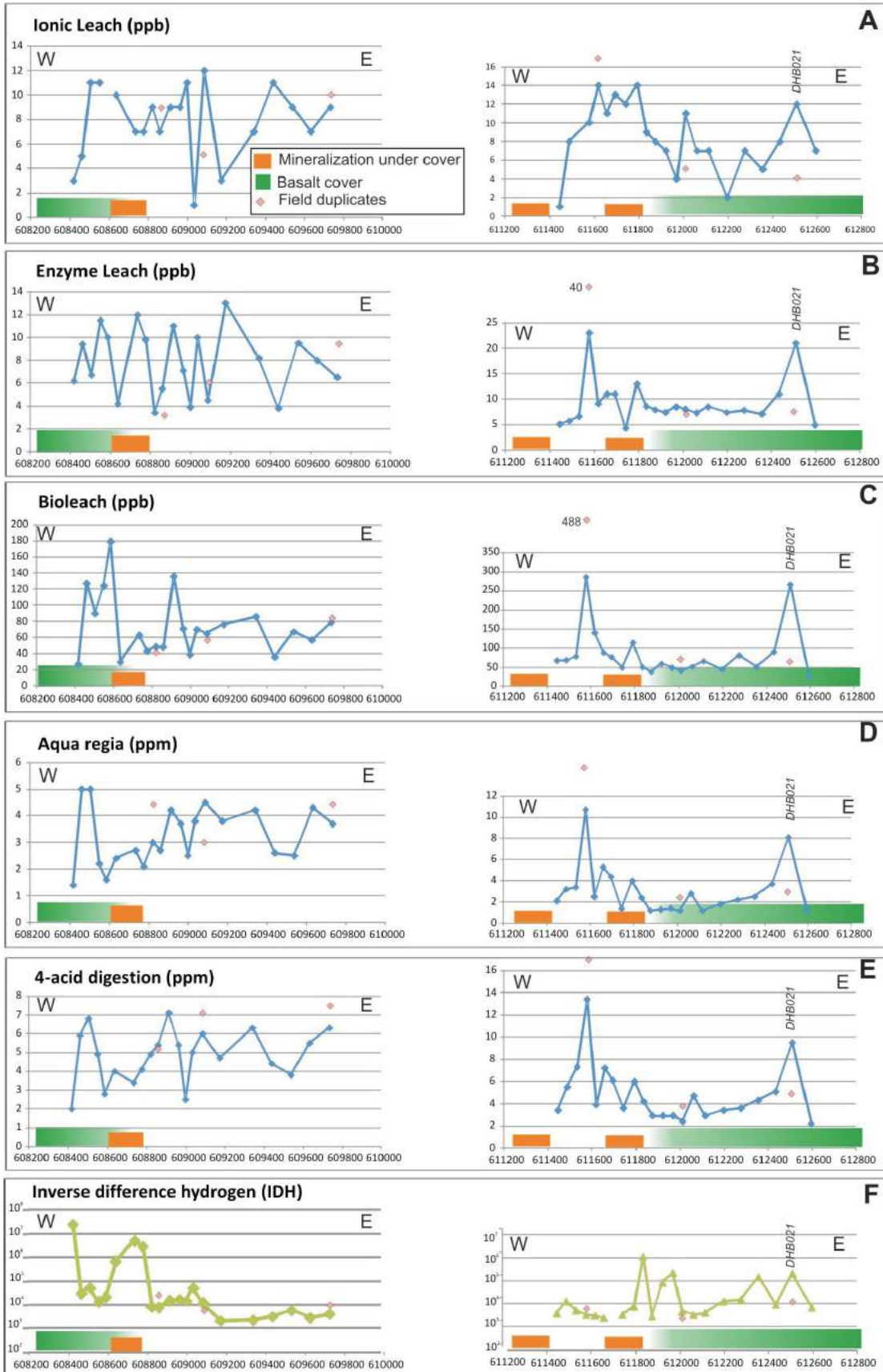


Figure 8. Soil pH and conductivity data for the Three Firs survey area, Woodjam prospect, south-central British Columbia. Areas under basalt cover and surface projection of the mineralization, defined by the 0.2 g/t Au equivalent contours, are represented by graphs showing **a)** H^+ , concentration of hydrogen ions ($-inverse\ of\ pH$); **b)** H^+a , concentration of hydrogen ions after addition of 1 drop of 10% HCl acid; **c)** electrical conductivity; **d)** inverse hydrogen difference, $1/(H^+a - H^+)$.

Three Firs As in B-horizon soils

Deerhorn As in B-horizon soils (NE line)



B-Horizon Soil Geochemistry

For the purposes of this paper, As results were chosen to illustrate the variations in response between the different analytical techniques over the partly basalt-covered areas at Three Firs and the northeast-oriented sample traverse at Deerhorn (Figure 9). Arsenic is a common pathfinder element used in porphyry exploration and accumulates at redox gradients, such as above the edge of mineralization (Hamilton, 1998; Pfeifer et al., 2004). It was chosen because elevated concentrations of it were also observed in amygdules in basalt (Figure 6). At Three Firs, elevated As values occurring in the vicinity of the mineralized zone are most clearly observed in the results obtained from the Bioleach and aqua-regia digestions. Arsenic values at the edges of the mineralized zone are double to triple the values of soils directly above the mineralization. Enzyme Leach and Ionic Leach results are noisy and do not show any recognizable pattern. The response from the 4-acid digestion does seem to mimic the aqua-regia results but the data are of lower contrast near the mineralization. It is noteworthy that the westernmost 4 to 5 samples at Three Firs were collected where basalt is inferred to underlie the glaciofluvial sediments. The results of the Bioleach and aqua-regia digestions reveal that several of these samples contain elevated As (Figure 9). The IDH results are also shown on Figure 9 for comparison. The samples directly above mineralization are about three orders of magnitude lower than on either margin, although the highest value at the western extreme of the sampled line does not coincide with elevated As values in the aqua-regia and Bioleach data.

On the Deerhorn northeastern sample traverse, As concentrations are highest between the two mineralized areas (orange bars on Figure 9). Slightly elevated As values are also evident in the eastern part of the mineralized area, near the location at which the basalt cover is inferred to start. As seen at Three Firs, the aqua-regia and Bioleach results show 2–4 fold increases in As concentrations between the mineralized zones compared to soils directly above mineralization. However, in contrast to Three Firs, Enzyme Leach and 4-acid digestions also show similar patterns; Ionic Leach lacks a recognizable signal for this element. The second sample from the eastern end of the Deerhorn traverse (site DHB021) also exhibits consistently high As concentrations in all extractions, which coincides with a

←
Figure 9. Comparison of As geochemistry using different methods on B-horizon soils taken in partly basalt-covered east-northeast-oriented transects (see Figure 3 for locations), Woodjam prospect, south-central British Columbia. The left column is for the Three Firs area, the right column for the Deerhorn area. The results for different methods are presented, from weak digestion at the top to strong digestion at the bottom: **a)** Ionic Leach; **b)** Enzyme Leach; **c)** Bioleach; **d)** aqua regia; **e)** 4 acid; **f)** inverse-difference–hydrogen (IDH) data are shown for comparison. Pink diamonds depict the analytical values for the field duplicates.

relatively high IDH value (approximately 2×10^5) and high As concentrations in carbonate-vesicle infill (Figures 6, 7).

Implications for Exploration Geochemistry in Basalt-Covered Areas

Preliminary data analysis suggests that soils directly over basalt-covered areas (i.e., northeast of Deerhorn) have some inherent geochemical characteristics, such as lower H^+ (or elevated pH), that distinguish them from areas only covered by glaciofluvial sediments. This may be explained by the more reactive nature of the relatively mafic Chilcotin Group basalt units compared to the underlying Nicola Group. The high IDH and conductivity values at Three Firs, and less clearly at Deerhorn, may be related to remobilized carbonate at the margins of a possible reduced chimney above mineralization. The IDH response does not appear to be distinct between basalt-covered areas and those that are only covered by glaciofluvial sediment. The analytical results also suggest that the geochemical signal of As can be seen through both types of cover. This is exemplified at Three Firs, where elevated As was detected in soils above basalt cover adjacent to known mineralization.

Both at Deerhorn and Three Firs, the Bioleach and aqua-regia techniques provide good contrast results. Preliminary comparison with SGH and OSG data, and interpretations provided by Activation Laboratories Ltd. (Sutherland, 2012), suggest a positive anomaly of low molecular-weight SGH and sulphur allotrope coincident with high As values.

At Deerhorn, near the eastern limit of the sample traverse, there are coincident IDH, conductivity and soil As responses. All methods, except Ionic Leach, define an interpretable pattern. It is unknown to what extent these responses indicate the presence of underlying mineralization because of the poor precision provided by the field duplicate samples. However, this response cannot be explained as a result of hydromorphic concentration because the sample location does not coincide with a break in slope or poorly drained ground. One possible explanation is that soil anomalies may be influenced by the fracture permeability in the basalt cover. Further sampling is necessary to delineate the small-scale soil geochemical variability and potential significance of this feature.

Although the dataset is limited, results from clay and carbonate amygdules in the basalt suggest that this sample medium may be capable of recording a signal from mineralization under basalt cover. Mobile ions from the underlying mineralization are perhaps being captured by adsorption onto clay, whereas in carbonate some of the elements present in comparatively high concentrations may form part of the calcite-crystal structure (e.g., Mn, Cu). These may reflect the immediate wallrock composition or elements mobilized from below. In the samples studied here, carbonate amygdules have only been encountered where nearby min-

eralization is known or where soils are anomalous in As. Therefore, it can, be hypothesized that vesicle-filling carbonate could be an indication of pH gradients that occur at the margins of reduced chimneys above oxidizing sulphides (cf. Hamilton, 1998). Clearly, further study and more extensive sampling are necessary to confirm the potential use of vesicle and/or fracture infill as a geochemical-exploration tool.

Acknowledgments

The authors thank Gold Fields Canada Exploration and Consolidated Woodjam Copper Corp. for allowing them access to the Woodjam property and for providing them with much of the base-map data included in this report. They also appreciate their generous logistical support during the sampling campaigns. A special thank you to R. Sherlock and A. Rainbow for their advice during the planning stages of the project and to A. Annejohn and M. Eckfeldt for their assistance with the sampling. They also acknowledge Activation Laboratories Ltd. and ALS Limited for their generous contributions to the analytical work, and C. Hart and J. Blackwell for their reviews and helpful suggestions for improvements to the manuscript. Finally, the authors thank Geoscience BC for its financial support, without which this project would not have been possible.

References

- Andrews, G.D.M. and Russell, J.K. (2008): Cover thickness across the southern Interior Plateau, British Columbia (NTS 092O, P; 093A, B, C, F): constraints from water-well records; Geoscience BC Summary of Activities 2007, Geoscience BC, Report 2008-1, p. 11–20.
- Barnett, C.T. and Williams, P.M. (2009): Using geochemistry and neural networks to map geology under glacial cover; Geoscience BC, Report 2009-3, 27 p., URL <<http://www.geosciencebc.com/s/2009-03.asp>> [November 2012].
- Bevier, M. L. (1983) Regional stratigraphy and age of Chilcotin Group basalts, south-central British Columbia: Canadian Journal of Earth Sciences, v. 20, no. 4, p. 515–524.
- Consolidated Woodjam Copper Corp. (2012a): New gold-copper zone discovered at the Woodjam North property; Consolidated Woodjam Copper Corp., press release, August 7, 2012, URL <<http://www.woodjamcopper.com/2012/08/07/gold-copper-zone-discovered-woodjam-north-property/>> [November 2012].
- Consolidated Woodjam Copper Corp. (2012b): Woodjam North; Consolidated Woodjam Copper Corp., URL <<http://www.woodjamcopper.com/projects/woodjam-north/>> [November 2012].
- Cook, S.J. and Dunn, C.E. (2007): Final report on results of the Cordilleran Geochemistry Project: a comparative assessment of soil geochemical methods for detecting buried mineral deposits—3Ts Au-Ag prospect, central British Columbia; Geoscience BC, Report 2007-7, 225 p., URL <<http://www.geosciencebc.com/s/2007-07.asp>> [November 2012].
- del Real, I., Hart, C.J.R., Bouzari, F., Blackwell, J.L., Rainbow, A., Sherlock, R. and Skinner, T. (2012): Paragenesis and alteration of the Southeast Zone and Deerhorn porphyry deposits, Woodjam property, central British Columbia (parts of 093A); in Geoscience BC Summary of Activities 2012, Geoscience BC, Report 2013-1, p. 79–90.
- Dohaney, J. A.M. (2009): Distribution of the Chilcotin Group basalts, British Columbia; MSc thesis, University of British Columbia, 124 p., 2 maps, URL <<https://circle.ubc.ca/handle/2429/24161>> [November 2012].
- Dunn, C.E., Cook, S.J. and Hall, G.E.M. (2007): Halogens in surface exploration geochemistry: evaluation and development of methods for detecting buried mineral deposits; Geoscience BC, Report 2007-10, URL <<http://www.geosciencebc.com/s/2007-10.asp>> [November 2012].
- Hamilton, S.M. (1998): Electrochemical mass-transport in overburden: a new model to account for the formation of selective leach geochemical anomalies in glacial terrain; Journal of Geochemical Exploration, v 63, p. 155–172.
- Heberlein, D.R. (2010): Comparative study of partial and selective extractions of soils over blind porphyry copper-gold mineralization at Kwanika and Mount Milligan, central British Columbia (NTS 093N/01, /19): fieldwork, soil conductivity and pH results; in Geoscience BC Summary of Activities 2010, Geoscience BC, Report 2010-1, p. 11–24., URL <<http://www.geosciencebc.com/s/SummaryofActivities.asp?ReportID=379075>> [November 2012].
- Heberlein, D.R. and Dunn, C.E. (2011): The application of surface organic materials as sample media over deeply buried mineralization at the Kwanika Central Zone, north-central British Columbia (NTS 93N); Geoscience BC, Report 2011-3, p. 1–74., URL <<http://www.geosciencebc.com/s/2011-03.asp>> [November 2012].
- Heberlein, D. R. and Samson, H. (2010): An assessment of soil geochemical methods for detecting copper-gold porphyry mineralization through Quaternary glaciofluvial sediments at the Kwanika Central Zone, north-central British Columbia; Geoscience BC, Report 2010-3, p. 1–89., URL <<http://www.geosciencebc.com/s/2010-03.asp>> [November 2012].
- Heberlein, D.R., Dunn, C.E. and Macfarlane, W. (2013): Use of organic media in the geochemical detection of blind porphyry copper-gold mineralization in the Woodjam property area, south-central British Columbia (NTS 093A/03, /06); in Geoscience BC Summary of Activities 2012, Geoscience BC, Report 2013-1, p. 47–62.
- Holland, S.S. (1964): Landforms of British Columbia: a physiographic outline; BC Ministry of Energy, Mines and Natural Gas, Bulletin 48, 138 p.
- Jensen, L.S. (1976): A new cation plot for classifying subalkalic volcanic rocks; Ontario Division of Mines, Miscellaneous Paper, no. 66.
- Massey, N.W.D, MacIntyre, D.G., Desjardins, P.J. and Cooney, R.T. (2005): Digital geology map of British Columbia: whole province; BC Ministry of Energy, Mines and Natural Gas, GeoFile 2005-1, URL <<http://www.empr.gov.bc.ca/Mining/Geoscience/PublicationsCatalogue/GeoFiles/Pages/2005-1.aspx>> [November 2012].
- Pearce, J.A. and Cann, J.R. (1973): Tectonic setting of basic volcanic rocks determined using trace element analyses; Earth and Planetary Science Letters, v. 19, p. 290–230.
- Pfeifer, H.-R., Gueye-Girardet, A., Raymond, D., Schlegel, C., Temgoua, E., Hesterberg, D. L. and Chou, J. W. (2004): Dispersion of natural arsenic in the Malcantone watershed,

- southern Switzerland: field evidence for repeated sorption-desorption and oxidation-reduction processes; *Geoderma*, v. 122, p. 205–234.
- Rollinson, H. (1993): Using geochemical data: evaluation, presentation, interpretation; Longman, 177 p.
- Schiarizza, P., Bell, K. and Bayliss, S. (2009): Geology and mineral occurrences of the Murphy Lake area, south-central British Columbia (NTS 093A/03); *in* Geological Fieldwork 2008, BC Ministry of Energy, Mines and Natural Gas, Paper 2009-1, p. 169–187.
- Sherlock, R., Poos, S., Trueman, A. (2012): NI 43-101 Technical report for 2011 activities on the Woodjam South property; Consolidated Woodjam Copper Corp., 185 p., URL <<http://woodjamcopper.com/data/NI%2043-101%20Woodjam%20Technical%20Report.pdf>> [November, 2012]
- Skinner, T. (2010): Report on the 2010 activities on the Woodjam North Property; BC Ministry of Energy, Mines and Natural Gas, Assessment Report 32 302, 81 p., URL <http://aris.empr.gov.bc.ca/search.asp?mode=repsum&rep_no=32302> [November 2012].
- Sun, S.-s. and McDonough, W. F. (1989): Chemical and isotopic systematics of oceanic basalts: implications for mantle compositions and processes; *in* Magmatism in the Ocean Basins, A.D. Saunders and M.J. Norry (ed.), Geological Society of America, Special Publication 42, p. 313–345.
- Sutherland, D. (2012): SGH-soil gas hydrocarbon predictive geochemistry; prepared for the Mineral Deposit Research Unit, Department of Earth and Ocean Sciences, University of British Columbia, unpublished report, 42 p.
- Vaca, S. (2012): Variability in the Nicola/Takla Group basalts and implications for alkalic Cu-Au porphyry prospectivity in the Quesnel terrane, British Columbia, Canada; MSc thesis, University of British Columbia, Vancouver, 148 p., URL <<https://circle.ubc.ca/handle/2429/43192>> [November 2012].

Paragenesis and Alteration of the Southeast Zone and Deerhorn Porphyry Deposits, Woodjam Property, Central British Columbia (Parts of 093A)

I. del Real, Mineral Deposit Research Unit, University of British Columbia, Vancouver, BC, idealreal@gmail.com

C.J.R. Hart, Mineral Deposit Research Unit, University of British Columbia, Vancouver, BC

F. Bouzari, Mineral Deposit Research Unit, University of British Columbia, Vancouver, BC

J.L. Blackwell, Gold Fields Canada Exploration, Vancouver, BC

A. Rainbow, Gold Fields Canada Exploration, Vancouver, BC

R. Sherlock, Gold Fields Canada Exploration, Vancouver, BC

T. Skinner, Gold Fields Canada Exploration, Vancouver, BC

del Real, I., Hart, C.J.R., Bouzari, F., Blackwell, J.L., Rainbow, A., Sherlock, R. and Skinner, T. (2013): Paragenesis and alteration of the Southeast Zone and Deerhorn porphyry deposits, Woodjam property, central British Columbia (parts of 093A); in Geoscience BC Summary of Activities 2012, Geoscience BC, Report 2013-1, p. 79–90.

Introduction

Porphyry deposits of the Late Triassic to Middle Jurassic (216 to 183 Ma) occur in the Quesnel and Stikine terranes in British Columbia. They are subdivided into calcalkalic and alkalic types on the basis of their hostrock chemistry and styles of alteration and mineralization (Lang et al., 1995; McMillan et al., 1995). Alkalic porphyry deposits such as Mount Milligan (MINFILE 093N 194; BC Geological Survey, 2012), Mount Polley (MINFILE 093A 008) and Lorraine (MINFILE 093N 002), and calcalkalic porphyry deposits such as Brenda (MINFILE 092HNE047), Highland Valley (MINFILE 092ISE001) and Gibraltar (MINFILE 093B 006) are examples of these two classes. These porphyry deposits commonly occur as clusters of several porphyry centres. The metal ratios, alteration assemblages and hostrock intrusive textures of each porphyry deposit can vary within each cluster (e.g., Casselman et al., 1995; Fraser et al., 1995). Such differences are commonly attributed to emplacement at different crustal depths of the now spatially related porphyry stocks (e.g., Panteleyev et al., 1996; Chamberlain et al., 2007). Recently, porphyry clusters such as Red Chris (MINFILE 104H 005; Norris, 2011) and Woodjam (MINFILE 093A 078; Figure 1) have been displaying both alkalic and calcalkalic features. However, the genetic and spatial links between the various deposits in each camp, especially with contrasting assemblages (i.e., calcalkalic and alkalic), are not well understood.

The Woodjam property hosts several discrete porphyry deposits, including the Megabuck (Cu-Au; MINFILE 093A 078), Deerhorn (Cu-Au; MINFILE 093E 019), Takom (Cu-Au; MINFILE 093A 206), Southeast Zone (Cu-Mo; MINFILE 093A 124) and the recently discovered Three Firs (Cu-Au; Figure 2). These deposits display various styles and assemblages of alteration and mineralization. The Southeast Zone Cu-Mo deposit is hosted in variable quartz monzonite intrusive units and displays alteration and mineralization comparable to calcalkalic porphyry deposits, whereas the nearby Deerhorn Cu-Au deposit is mainly associated with narrow (<100 m) monzonite intrusive bodies and hosts mineralization similar to alkalic porphyry deposits. These differences have resulted in the separation of the Southeast Zone (SEZ) from the Megabuck and Deerhorn deposits as a different mineralization event (Logan et al., 2011). However, there are attributes of mineralization and alteration that could indicate that at least some deposits within the Woodjam property may be related.

Recent exploration at the Deerhorn Cu-Au deposit has shown two contrasting alteration assemblages of K-feldspar+magnetite, typical of alkalic systems, and illite+tourmaline and Mo mineralization, typical of calcalkalic systems. The SEZ displays some features not typical of calcalkalic deposits, such as sparse quartz veining, and is located less than 4 km from the Deerhorn deposit. These observations suggest that temporal and paragenetic relationships between the two deposits may exist, thus providing a unique opportunity to study the relationship between alkalic and calcalkalic deposits in BC.

Thus, a research project has been jointly initiated by the Mineral Deposit Research Unit at the University of British Columbia, Gold Fields Canada Exploration and Geoscience BC. The focus of this project is to increase the un-

Keywords: *alkalic porphyry, calcalkalic porphyry, Woodjam property*

This publication is also available, free of charge, as colour digital files in Adobe Acrobat® PDF format from the Geoscience BC website: <http://www.geosciencebc.com/s/DataReleases.asp>.

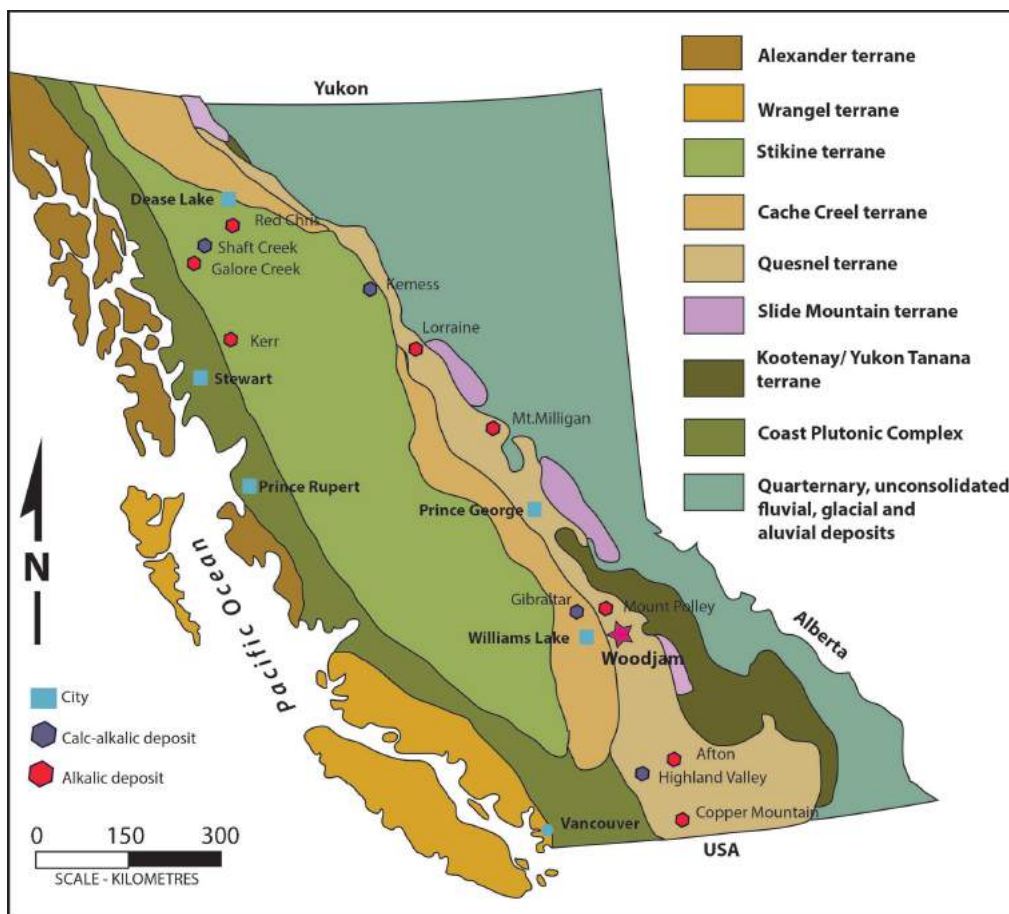


Figure 1. Major tectonic terranes and associated Mesozoic porphyry deposits of the Canadian Cordillera in British Columbia (from McMillan et al., 1995).

Understanding of the paragenesis and alteration of the variable calcalkalic and alkalic deposits and the magmatic evolution in the Woodjam property. Results of this investigation will have important implications in understanding the formation of porphyry clusters and planning the exploration of new targets in known mineralized districts in BC and similar regions worldwide.

Fieldwork was carried out during July and August 2012 and was focused on the Deerhorn and SEZ deposits. Five drillholes along a single cross-section were graphically relogged from each deposit (Figures 2, 3) and sampled. Hostrock texture, alteration assemblages and intensity, vein types, and crosscutting relationships were recorded and form the basis for ongoing detailed petrographic and chemical analyses. Results and discussions presented in this summary are based largely on data and observations collected during this field program.

The Woodjam property is located in the Cariboo Mining Division, central British Columbia, approximately 50 km northeast of Williams Lake (Figure 1). The property is owned by Gold Fields Horsefly Exploration (51%) and Consolidated Woodjam Copper Corporation (49%). The

Southeast Zone is the only deposit with a public pit-constrained resource estimated to be 146.5 Mt at 0.33% Cu (Sherlock et al., 2012).

Tectonic Setting

Much of BC comprises several tectonic blocks that were accreted onto the western margin of ancient North America during the Mesozoic. Three of these accreted terranes, the Quesnel (or Quesnellia), Stikine (or Stikinia) and Cache Creek terranes, form most of the Intermontane Belt that composes much of central BC (Figure 1; Monger and Price, 2002). The Stikine and Quesnel volcanic arc terranes have similar compositions and stratigraphy, and are interpreted to have originally been part of the same arc that was folded in counterclockwise rotation, enclosing the Cache Creek terrane (Mihalynuk et al., 1994). Within the Quesnel and Stikine terranes, the emplacement of pre- to synaccretion of both alkalic and calcalkalic $Cu \pm Mo \pm Au$ deposits occurred between 216 and 187 Ma (McMillan et al., 1995). The Woodjam porphyry cluster is hosted in the Late Triassic to Early Jurassic arc in the central portion of the Quesnel terrane.

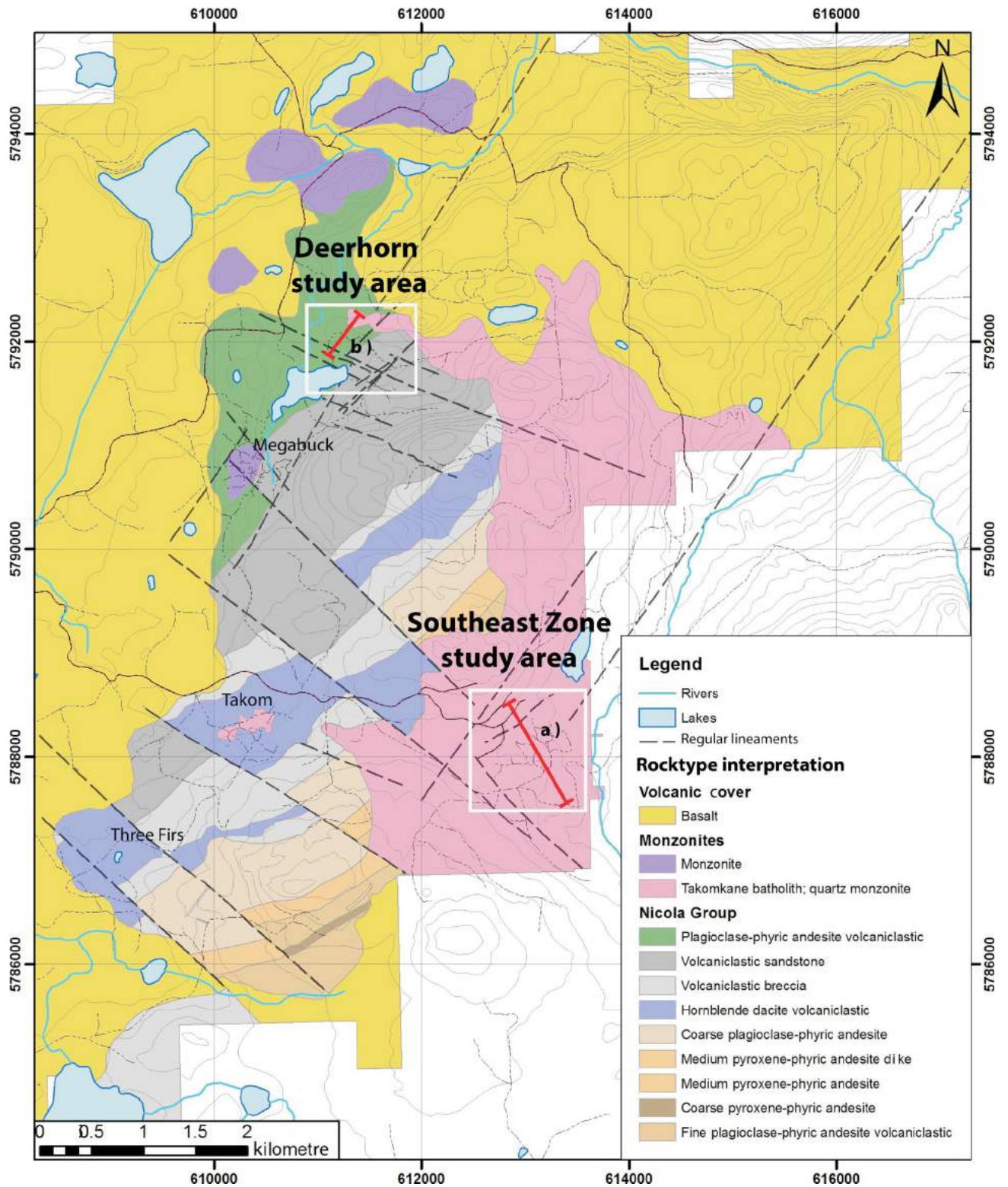


Figure 2. Geology of the Woodjam property. Cross-section lines of drillholes relogged in this study are shown (red line) for the a) Southeast Zone and b) Deerhorn deposits (from Gold Fields Canada Exploration, pers. comm., 2012).

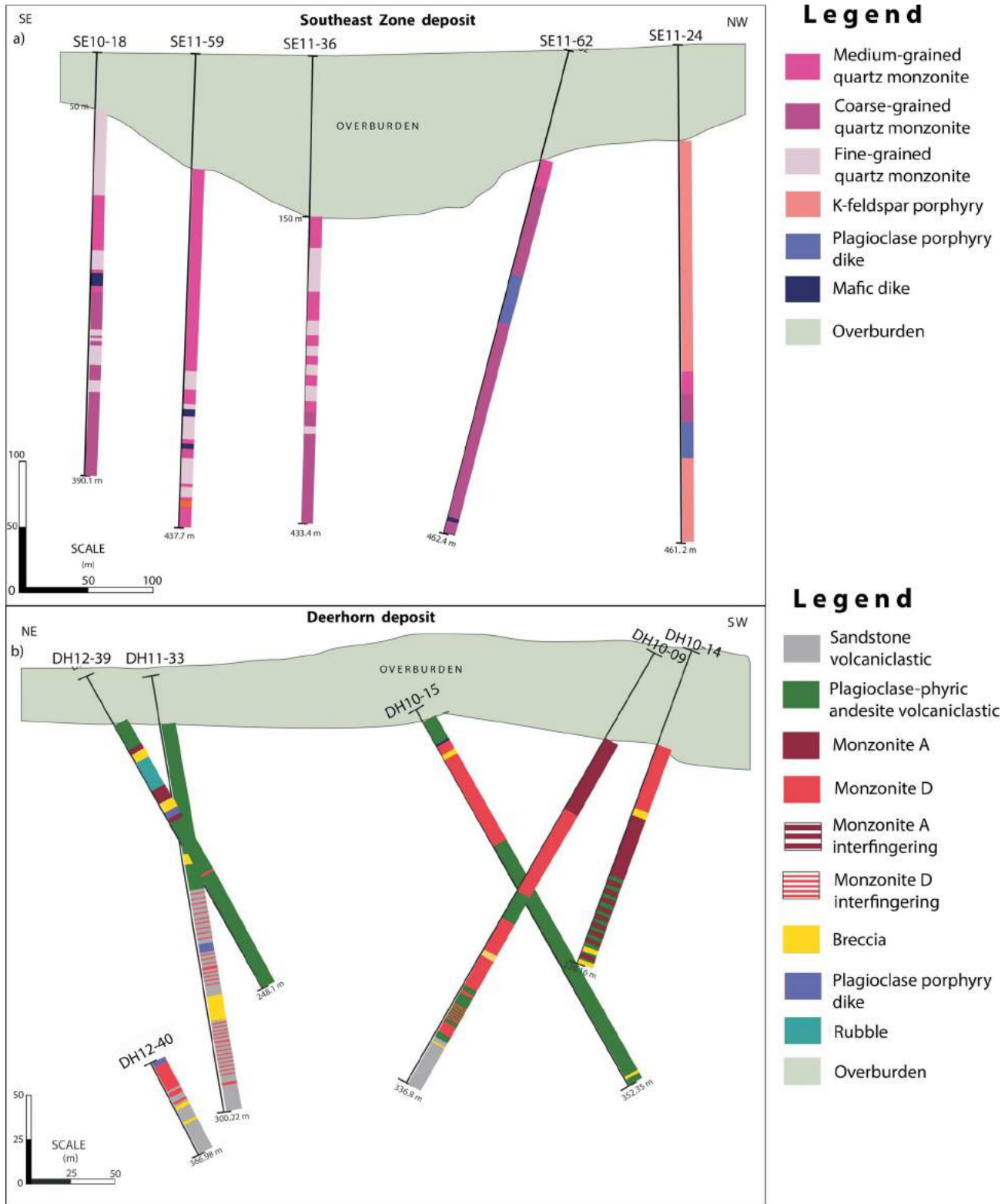


Figure 3. a) Southeast cross-section along the line 613160E, 5788000N, NAD 83, UTM Zone 10 (28.5 m thickness) across the Southeast Zone deposit; **b)** northeast cross section along the line 611230E, 5792020N, NAD 83, UTM Zone 10 (62.5 m thickness) across the Deerhorn deposit.

Regional Geology

The Quesnel terrane consists of upper Paleozoic and lower Mesozoic volcanic, sedimentary and plutonic rocks. The Paleozoic components are unconformably overlain by the Late Triassic and Early Jurassic island arc volcanic and sedimentary strata of the Nicola Group and its northern continuation, the Takla Group (McMillan et al., 1995). The Nicola Group is composed of submarine basaltic to andesitic augite±plagioclase-phyric lava and volcanoclastic and sedimentary units (Mortimer, 1987; Schiarizza et al., 2009; Vaca, 2012). This sequence extends throughout south-central BC.

These rocks were intruded by the Takomkane batholith, a large composite calcalkalic intrusion of largely granitoid composition with a surface expression of approximately 40 by 50 km. The Woodjam Creek unit of the Takomkane batholith occurs on the Woodjam property and comprises granodiorite, monzogranite and quartz monzonite (Schiarizza et al., 2009). The Nicola and Takomkane units are overlain by the Early Miocene to Early Pleistocene basalt of the Chilcotin Group.

Geology of the Woodjam Property

The Woodjam property is hosted by a succession of Triassic–Jurassic Nicola volcanic and volcanosedimentary rocks that are intruded by several Jurassic monzonite to syenite stocks. The Takomkane batholith occurs in the eastern and southern parts of the property (Figure 2) and mainly consists of light-grey to pinkish to white hornblende-biotite granodiorite, monzogranite, quartz monzonite and quartz monzodiorite (Schiarizza et al., 2009). Nicola Group rock units comprise a sequence of plagioclase±pyroxene-phyric andesitic rocks, monomictic and polymictic volcanic breccias, and volcanic mudstones and sandstones, all of which dip moderately to the northwest (Gold Fields, pers. comm., 2012).

Locally, extensive olivine-phyric basalt flows of the Chilcotin Group are characterized by dark grey, aphanitic and vesicular basalt (Schiarizza et al., 2009). The flows have thicknesses of less than 20 m to more than 100 m and they overlie the Nicola stratigraphy.

Several zones of porphyry-type mineralization occur within and around porphyry stocks that intruded the strata of the Nicola Group. The Deerhorn deposit is hosted by multiple monzonite intrusions and volcanic rocks of the Nicola Group, whereas the SEZ deposit is hosted entirely in quartz monzonites of the Takomkane batholith (Gold Fields, pers. comm., 2012; Sherlock et al., 2012).

Hostrock Geology

Southeast Zone Deposit

The SEZ deposit is hosted by a series of texturally variable quartz monzonite intrusive units that strike ~220° and dip ~65–80° to the northwest (Rainbow, 2010). The quartz monzonites are divided texturally into fine-, medium- and coarse-grained units (Figures 3a, 4a; Rainbow, 2010). Fine-grained quartz monzonite cut both medium- and coarse-grained intrusive rocks. Aplite dikes cut all quartz monzonites with sharp contact. All quartz monzonite units are largely equigranular, white-grey to pink and comprise interlocking crystals of plagioclase, potassium feldspar and quartz. Mafic minerals are typically hornblende and less abundant fine-grained biotite. Quartz monzonites are intruded by K-feldspar porphyry (FP) bodies characterized by a phaneritic medium- to coarse-grained groundmass and large euhedral and elongated K-feldspar phenocrysts that occur sporadically throughout the unit. The FP forms a wide (>250 m) intrusion that strikes northeast (Rainbow, 2010; Sherlock et al., 2012). It cuts the quartz monzonite and has a chilled margin in the contact. All quartz monzonites were emplaced pre- to synmineralization and are affected by intense alteration, whereas the FP was probably emplaced during final stages of hydrothermal activity and is typically weakly altered. All of these units were intruded by late postmineralization plagioclase porphyry mafic and andesitic dikes (Rainbow, 2010; Sherlock et al., 2012).

Deerhorn Deposit

The Deerhorn deposit is hosted in both the volcanosedimentary rocks of the Nicola Group and the monzonitic rocks that intrude the Nicola strata (Figure 3b; Gold Fields, pers. comm., 2012; Scott, 2012). The host Nicola Group stratigraphy consists of volcanoclastic sandstone overlain by a plagioclase-phyric andesite with local clast breccia facies (Gold Fields, pers. comm., 2012). These units dip ~25°N in the deposit area and were intruded by at least two monzonite bodies. Monzonite A occurs as pencil-shaped intrusive bodies with irregular margins that intrude the volcanosedimentary rocks of the Nicola Group (Gold Fields, pers. comm., 2012). Intense alteration obliterated much of the primary texture of monzonite A but remnants of plagioclase and biotite phenocrysts are locally preserved. Monzonite D is characterized by plagioclase and hornblende phenocrysts (Gold Fields, pers. comm., 2012) and occurs as dikes with sharp contacts that crosscut monzonite A and Nicola Group stratigraphy (Gold Fields, pers. comm., 2012; Scott, 2012). The highest Cu and Au values occur in monzonite A and in the surrounding volcanic sandstone where grades are locally <1.5 g/t Au and <0.75% Cu (Gold Fields, pers. comm., 2012). Mineralization in monzonite D is mainly pyrite and subordinate chal-

copyrite with Cu grades between 0.1 and 0.3% (Gold Fields, pers. comm., 2012). Postmineralization mafic and andesitic dikes crosscut all the Deerhorn hostrocks and phases of mineralization (Gold Fields, pers. comm., 2012).

Alteration

Hydrothermal alteration in both the Deerhorn and SEZ affected all hostrocks except postmineralization mafic and andesitic dikes. Several alteration assemblages are recognized in each deposit.

Southeast Zone

Potassium feldspar+biotite+magnetite (Table 1) is the earliest alteration assemblage in the SEZ deposit and typically occurs as pervasive alteration of K-feldspar replacing feldspar phenocrysts and biotite with minor magnetite replacing mafic minerals (Figure 4a). Potassium feldspar+biotite+magnetite alteration varies from very intense (i.e., nearly all texture and original minerals are destroyed) in the centre of the deposit to weak (i.e., only secondary biotite and K-feldspar flooding) at the margins of the deposit. Albite alteration is recognized at the northern extent of the deposit where it is juxtaposed against K-feldspar+biotite+magnetite alteration by a large northeast-striking fault. Albite alteration has a distinct bleached appearance and locally obliterates original rock textures (Figure 4b). Both K-feldspar+biotite+magnetite and albite alterations are overprinted by chlorite±epidote±pyrite, illite and hematite alterations (Table 1). At least some of chlorite and epidote occur with albite alteration. The intensity and distribution of chlorite±epidote±pyrite alteration is weakly inversely proportional to the K-feldspar+biotite+magnetite alteration. The former occurs more commonly at the margins of the deposit and is very weak to absent in the core of the deposit. Illite occurs as three visually and possibly paragenetically distinct types: dark green illite that replaces plagioclase phenocrysts, white illite that is fracture controlled and has

locally patchy distribution, and apple green illite that overprints albite and K-feldspar alterations (Figure 4c).

Deerhorn

Alteration assemblages at the Deerhorn deposit are strongly controlled by the distribution of the monzonites (Scott, 2012). Potassium feldspar+biotite+magnetite alteration is very intense in monzonite A and in the volcanic rocks immediately surrounding these intrusions (Table 2, Figure 4d). Monzonite D is only moderately affected by K-feldspar+biotite+magnetite alteration, indicating that it postdated much of main-stage alteration. The K-feldspar+biotite+magnetite alteration is overprinted by chlorite±epidote±pyrite, ankerite, calcite and illite alteration assemblages (Table 2). The chlorite±epidote±pyrite alteration occurs mainly in monzonite D (Figure 4e) and in the surrounding volcanic hostrocks (Figure 3b). Ankerite and calcite veinlets occur throughout all rock types, but are not recognized together. Ankerite occurs in the northeastern extent of the area represented by the cross section, whereas calcite occurs in the centre and southwestern extents. Illite occurs mainly as vein envelope overprinting K-feldspar haloes associated with K-feldspar+biotite+magnetite alteration (Figure 4f).

Tables 1 and 2 summarize the alteration assemblages in both deposits from early to late events, on the basis of field relationships.

Vein Types and Paragenesis

Southeast Zone

The earliest veins in the SEZ deposit are rare magnetite stringers and quartz±chalcopyrite±magnetite veins. These veins occur locally in the core of the porphyry (Figure 5a; i.e., hole SE11-62 in Figure 3a). In the deep central and marginal areas of the SEZ, quartz±chalcopyrite±pyrite±molybdenite±anhydrite (±bornite) veins with K-feld-

Table 1. Description of alteration assemblages at the Southeast Zone deposit, Woodjam property, central British Columbia.

Alteration assemblage	Style	Veinlets	Intensity	Sulphide mineralization	Distribution
K-feldspar+biotite+magnetite	Pervasive replacement. K-feldspar replaces feldspar. biotite and magnetite replace mafic minerals	Magnetite (rare in the SEZ); quartz-chalcopyrite-magnetite; quartz-chalcopyrite-pyrite-molybdenite-(bornite); chalcopyrite±pyrite	Very intense in the core of the porphyry becoming weak in the margins; affects all units except late dikes	Main mineralization occurs with this alteration with py:cpy:mo ratio: core zone: 0.2:3:0; central zone: 1:2:1; marginal zone: 3:1:0.5	Throughout the deposit
Albite	Pervasive, fracture controlled		Very intense to moderate bleach of the rock	Barren	Marginal parts of the deposit
Chlorite±epidote±pyrite	Patchy, selective, vein controlled and vein envelope	Pyrite-epidote±chalcopyrite	Moderate in the margins of the porphyry becoming very weak in the core.	Pyrite and minor chalcopyrite	Throughout the deposit
Illite	Selective and fracture controlled	Illite	Very intense when is fracture controlled bleaching the rock: affects all units except late dikes.	Barren	Shallow and marginal parts
Hematite	Patchy and fracture controlled	Hematite	Very weak to moderate, affects all rocks including plagioclase porphyry dikes	Barren	Marginal parts of the deposit

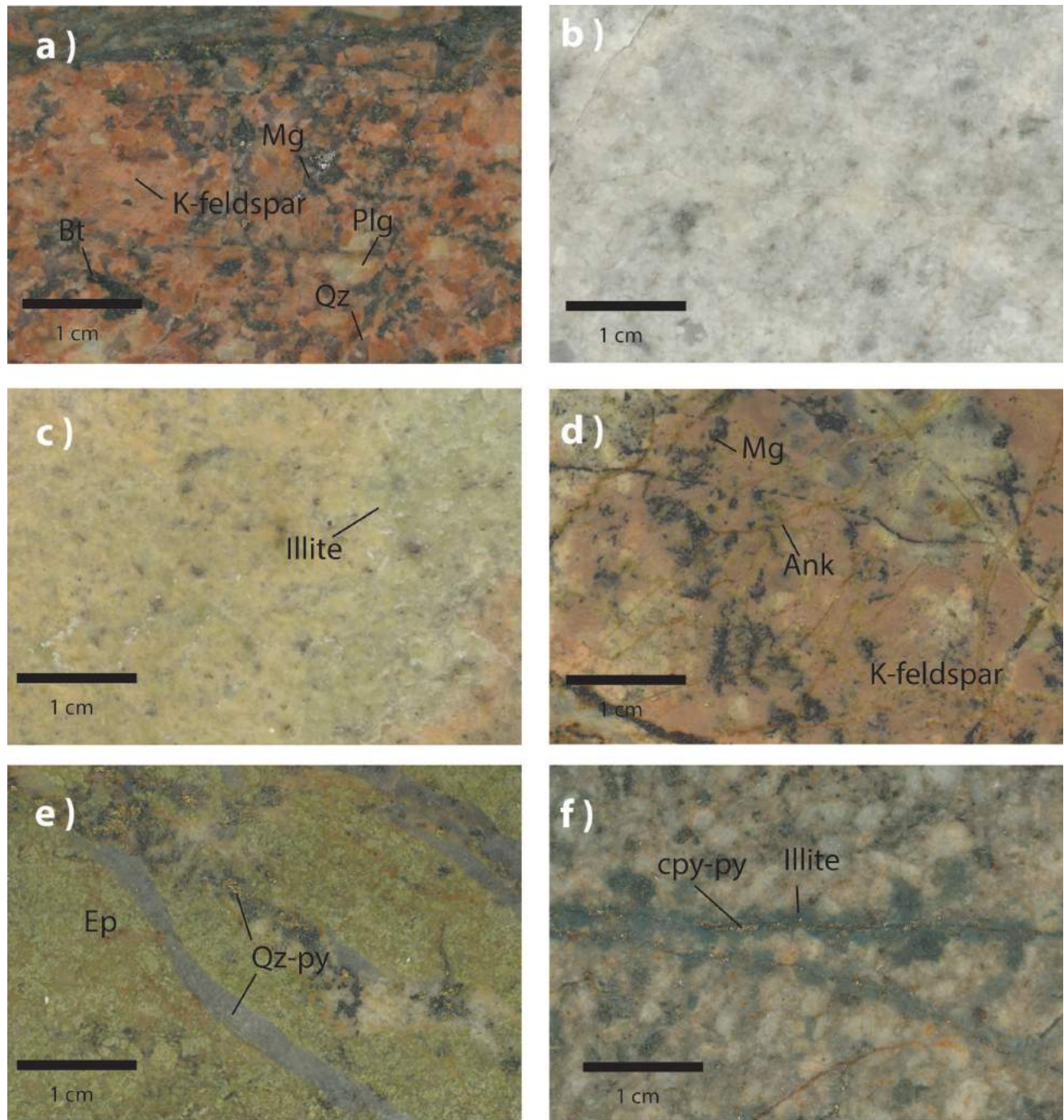


Figure 4. Alteration in the Southeast Zone (a, b, c) and Deerhorn (d, e, f) deposits (sample numbers represent drillhole numbers followed by depth): **a)** intense pervasive K-feldspar+biotite+magnetite alteration in coarse-grained quartz monzonite (SE11-62; 256.6 m); **b)** intense albite alteration of fine-grained quartz monzonite (SE11-36; 352.35 m); **c)** apple green illite alteration overprinting albite and K-feldspar+biotite+magnetite alteration in fine-grained quartz monzonite (SE10-18; 73.15 m); **d)** intense K-feldspar+biotite+magnetite alteration in the volcanic hostrock near the contact with monzonite A, with ankerite veins cutting the alteration (DH10-09; 202.85 m); **e)** epidote alteration halo to quartz-pyrite vein in the andesite volcanoclastic hostrock (DH10-09; 280.25 m); **f)** illite vein envelope of a chalcopyrite-pyrite stringer in monzonite D (DH10-09; 291.2 m). Abbreviations: Ank, ankerite; Bt, biotite; cpy, chalcopyrite; Ep, epidote; Mg, magnetite; Plg, plagioclase; py, pyrite; Qz, quartz.

Table 2. Description of alteration assemblages at the Deerhorn deposit, Woodjam property, central British Columbia.

Alteration assemblage	Style	Veinlets	Intensity	Sulphide mineralization	Distribution
K-feldspar+biotite+magnetite	Pervasive, K-feldspar affects the groundmass and replaces feldspar phenocrysts, biotite and magnetite replace mafic minerals	Magnetite stockwork, quartz-chalcopyrite-magnetite-hematite, quartz-chalcopyrite-pyrite(±molybdenite)	Very intense in monzonite A, moderate in monzonite D, very intense where the volcanic hostrock is in contact with monzonite A, weak in the distal volcanic hostrock	Main mineralization occurs with this alteration with average py:cpy:au ratios of monzonite A: 1:2:4, monzonite D: 2:1:0, volcanic host rock: 4:2:1	Throughout the deposit
Chlorite±epidote±pyrite(±magnetite)	Vein envelope, selective and vein controlled	Quartz-chlorite-magnetite±K-feldspar±sulphides	Weak in monzonites A and D, moderate to intense in volcanic hostrock.	Pyrite associated with this alteration	Throughout the deposit
Ankerite or calcite	Vein controlled	Pyrite-quartz±chlorite±carbonate±ankerite	Moderate to weak throughout all units	Barren	Ankerite in the northeast part of the section (DH10-09 and DH10-14); calcite in the centre and southwest part.
Illite	Vein envelope for Sulphide-epidote±hematite (±tourmaline), selective and fracture controlled	~	Very weak to strong when is fracture controlled; affects all units	Barren	Throughout the deposit

spar haloes also occur (Figure 5b). The timing relationship of these veins with magnetite-bearing veins is not known. Quartz±chalcopyrite±pyrite±molybdenite±anhydrite veins, with coarse quartz but without a K-feldspar halo (Figure 5c), cut quartz±sulphides±anhydrite veins with a K-feldspar halo; these last two types of veins do not occur with a frequency greater than four veins per metre. Pyrite±epidote±chlorite veins with epidote±hematite±illite haloes are the youngest veins that host pyrite with minor chalcopyrite and cut all earlier veins. Quartz±chalcopyrite±pyrite±molybdenite±anhydrite veins with and without K-feldspar haloes dominate areas with stronger K-feldspar+biotite+magnetite alteration but progressively become less abundant toward the margins of the deposit. Pyrite-epidote-chlorite veins occur most commonly at the margins of the deposit, and are associated with the intense chlorite±epidote±pyrite alteration assemblage of the host-rocks. They are rare to absent in the central parts of deposit. Pre- to synmineralization veins such as magnetite, quartz±magnetite±chalcopyrite and quartz±sulphides±anhydrite veins with and without K-feldspar haloes commonly occur in all quartz monzonite units but are less abundant in the K-feldspar porphyry unit. This unit is largely cut by late pyrite±epidote±chlorite veins. This relationship indicates that the K-feldspar porphyry unit is younger than the quartz monzonites and postdates at least part of the main phase of mineralization.

Deerhorn Deposit

In the Deerhorn deposit, early magnetite stockwork and Au-bearing quartz-magnetite±hematite±sulphide veins (Figure 5d; Scott, 2012) with banded texture commonly occur in monzonite A and the adjacent volcanic hostrock. Monzonite D cuts monzonite A and the early Au-bearing

quartz-magnetite-sulphide veins. Quartz±sulphide veins occur throughout all rock types and cut the early quartz-magnetite±sulphide veins (Figure 5d). Locally, quartz±sulphide veins have an illite overprint of a K-feldspar halo, which is interpreted as a later event (Figure 4f). Quartz-magnetite-chlorite-K-feldspar veins occur in the volcanic hostrock (hole DH11-33 in Figure 3b; Figure 5e); however, crosscutting relationships with the veins described above are not observed. Pyrite-quartz±hematite±epidote±tourmaline veins with a white illite halo occur throughout all rock units, cutting early veins and pyrite-chlorite±calcite±ankerite veins (Figure 5f). Late carbonate and hematite veins occur throughout all hostrocks including late mafic dikes. These observations indicate that pre- to synmineralization veins such as the Au-bearing quartz-magnetite±sulphide occur mainly in monzonite A and in the volcanic hostrock adjacent to it, whereas monzonite D is commonly cut by late veins.

Tables 3 and 4 summarize various vein types observed at the SEZ and Deerhorn deposits, and give their analogies with common vein types (i.e., M, A, B and D veins) in porphyry copper deposits (Gustafson and Hunt, 1975; Arancibia and Clark, 1996; Sillitoe, 2000, 2010).

Mineralization

Copper, gold and molybdenum mineralization in the Woodjam property are controlled by the rock type, alteration, density of veining and location (margins or central area) within the porphyry system. In the SEZ deposit, Cu occurs dominantly in chalcopyrite with subordinate bornite disseminated but more commonly in veins (Figure 5a-c). Molybdenite is observed mainly in veins (Figure 5b). Sulphide minerals occur in quartz veins and chalcopyrite±py-

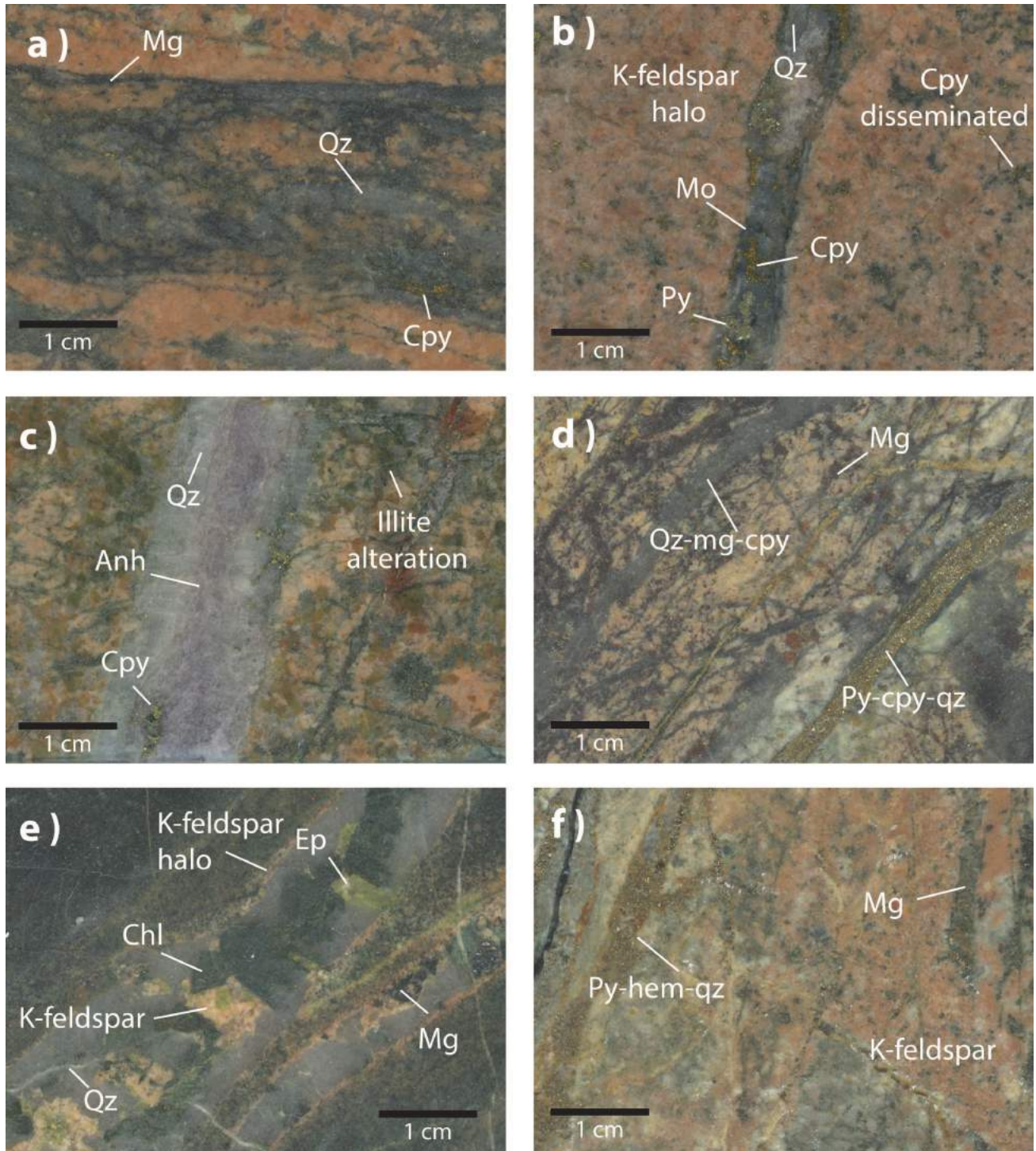


Figure 5. Examples of veining in the Southeast Zone (a, b, c) and Deerhorn (d, e, f) deposits, Woodjam property, central British Columbia (sample numbers represent drillhole numbers followed by depth): **a)** quartz-magnetite-chalcopyrite veining with very intense K-feldspar+biotite+magnetite alteration in coarse-grained quartz monzonite (SE11-62; 185.08 m); **b)** quartz-chalcopyrite-molybdenite-pyrite vein with a K-feldspar halo in the medium-grained quartz monzonite, disseminated chalcopyrite in a mafic mineral (SE11-59; 310.25 m); **c)** quartz-chalcopyrite-anhydrite centreline vein, with selective replacement of plagioclase by illite (SE11-36; 399 m); **d)** quartz-magnetite-chalcopyrite and magnetite veinlets are cut by a pyrite-chalcopyrite-quartz vein (DH12-39; 94.42 m); **e)** quartz-K-feldspar-magnetite-chlorite vein with a K-feldspar halo in the volcanoclastic sandstone (DH11-33; 248.2 m); **f)** K-feldspar vein-cut magnetite vein, which is itself cut by a pyrite-hematite-quartz vein (DH10-15; 210.35 m). Abbreviations: Anh, anhydrite; Chl, chlorite; Cpy, chalcopyrite; Ep, epidote; Mg, magnetite; Mo, molybdenite; Qz, quartz; Py, pyrite.

Table 3. Southeast Zone vein descriptions, Woodjam property, central British Columbia.

Vein type	Alteration halo	Texture and shape	Sulphides	Related pervasive alteration	Analogies with PCD vein types	Distribution
Magnetite	No halo	1–2 mm wide	No sulphides	Intense K-feldspar, biotite and magnetite	M veins	Rare, core of the deposit (hole SE11-62)
Quartz–sulphides± magnetite	K-feldspar	Banded veins with diffuse edges; 3 mm–1 cm wide	Chalcopyrite(±bornite)	Intense K-feldspar, biotite and magnetite	A veins	Core of the deposit (hole SE11-62)
Quartz± sulphides± anhydrite (±chlorite)	K-feldspar	Diffuse edges; 2 mm–20 cm wide; up to four veins per metre	Chalcopyrite± molybdenite±pyrite (±bornite), more molybdenite-chalcopyrite towards the center, but molybdenite is absent in the core of porphyry; more pyrite to the margins	K-feldspar, biotite and magnetite	A veins	Throughout central part of the system (holes SE11-36, SE11-59 and SE11-62)
Quartz± sulphides± anhydrite	No halo	Sharp edges; coarse-grained quartz, frequently stringer veins; 1–3 mm wide; up to four veins per metre	Chalcopyrite±pyrite±molybdenite	K-feldspar, biotite and magnetite	B veins	Throughout central part of the system
Sulphides± epidote±quartz	Epidote±hematite± white illite	Sharp edges; 1–4 mm wide	Pyrite with minor chalcopyrite	Epidote-chlorite-pyrite	D veins	Marginal and shallower area of the system
Carbonate	No halo	Sharp edges; 1–5 mm wide	No sulphides	Carbonate and hematite	~	Throughout the deposit

* PCD: porphyry copper deposits

rite stringer veins as fine-grained and anhedral grains, whereas disseminations in the hostrock are intimately related to mafic mineral sites. Areas of high Cu grades (~0.5%) are characterized by dense stockworks of thin veins with abundant disseminated chalcopyrite in the hostrock. Copper grades decrease with depth (to amounts less than 0.4%) and copper mineralization becomes more concentrated in quartz veins up to 2 cm wide with K-feld-

spar haloes. An increase in anhydrite is also observed. Gold mineralization (less than 1 ppm; rarely up to 4 ppm) may be related to banded dark quartz-magnetite-chalcopyrite veins that occur in the core of the porphyry deposit.

Sulphide zoning at the SEZ deposit consists of a chalcopyrite±bornite (±pyrite; hole SE11-62) assemblage in the core of the deposit, which changes upward and outward to chal-

Table 4. Deerhorn vein descriptions, Woodjam property, central British Columbia.

Vein type	Alteration halo	Texture and shape	Sulphides	Related pervasive alteration	Analogies with PCD vein types	Distribution
Magnetite	No halo	density up to 30% of the rock; 1–2 mm wide	No sulphides	Intense K-feldspar, biotite and magnetite	M veins	In monzonite A and volcanic hostrock in areas near the contact with the intrusive body
Quartz-magnetite± hematite± sulphides	K-feldspar	laminated veins with indistinct margins; up to a 70% of the rock; 3 mm–2 cm wide	Chalcopyrite-bornite	Intense K-feldspar, biotite and magnetite	A veins	In monzonite A and the volcanic hostrock in areas near the contact with the intrusive body
Quartz±sulphides	No halo	Sharp edges; 1–4 mm wide	Chalcopyrite-pyrite (in monzonite A); pyrite±chalcopyrite (±molybdenite; in monzonite D)	K-feldspar, biotite and magnetite	A veins	Monzonite A, monzonite D and the volcanic hostrock in areas near the contact with the intrusive body
Quartz–magnetite–chlorite±K-feldspar± sulphides	K-feldspar	Sharp edges; 4 mm–1 cm wide	Chalcopyrite-pyrite	Chlorite–magnetite–K-feldspar–epidote	A veins	Volcanic hostrock, mainly in hole DH11-33
Sulphide–epidote± hematite(±tourmaline)	White illite	Sharp edges; 2–5 mm wide	Pyrite	Pyrite-epidote-hematite-illite	D veins	Mainly in the volcanic host rock and in monzonite D
Pyrite-quartz±chlorite ±carbonate/ankerite	White illite	Sharp edges; 1–3 mm wide	Pyrite	Pyrite-chlorite-carbonate-illite	D vein	Monzonite A, monzonite D and volcanic hostrock; ankerite occurs northeast of the area
Carbonate-hematite-gypsum	No halo	1–5 mm wide	No sulphides	Carbonate and hematite	~	Throughout the whole deposit

* PCD: porphyry copper deposits

copyrite±molybdenite±pyrite (holes SE11-59 and SE11-36) and finally, a pyrite-dominated assemblage in the periphery of the deposit (holes SE10-18 and SE11-24). However, mineralization is not symmetric through the system. For example, the northeast area was intruded by the late or synmineralized K-feldspar porphyry intrusion in which pyrite is the dominant sulphide with Cu grading less than 0.4%.

Mineralization at the Deerhorn deposit differs from the SEZ deposit in that it has significantly higher Au grades associated with Cu mineralization (up to <1.5 ppm Au and <0.75% Cu). Mineralization is hosted dominantly in monzonite A (Figure 5d) and the adjacent volcanic hostrocks and occurs as disseminated in both the early quartz-magnetite-chalcopyrite veins and in later quartz-sulphide veins. Monzonite D hosts lower grades of Cu mineralization (~0.1–0.3% Cu) but does not host significant Au. Trace amounts of molybdenite have been observed in the later-stage quartz sulphide veins in monzonite D.

Discussion

The characteristics of the hostrock, alteration and mineralization of the Deerhorn and SEZ deposits were documented on the basis of field observations in order to understand their similarities, differences and possible genetic relationships.

The Southeast Zone deposit is hosted in texturally variable quartz monzonite intrusive rocks that are inferred to be part of the Takomkane batholith. Alteration is zoned from intense K-feldspar+biotite+magnetite in the centre, which becomes weaker toward the margins and is laterally surrounded by albite alteration at the margins of the deposit. Chlorite±epidote±pyrite alteration overprints the K-feldspar+biotite+magnetite alteration and is locally intense at the margins of the deposit, but is weak to absent in the core. Illite alteration commonly occurs at the margins and upper levels with fracture-controlled hematite alteration overprinting chlorite+epidote+pyrite alteration. Mineralization is zoned from chalcopyrite-bornite mineralization anomalous in Au (~0.2 ppm) to pyrite-dominated mineralization at the margins. However, the low abundance of quartz veining is not a typical feature of calcalkalic deposits.

The Deerhorn deposit is hosted in a series of narrow (<100 m) monzonite intrusions that have ‘pencil’ geometries. No modal quartz is observed in the volcanic hostrocks or the monzonite intrusions. The lack of modal quartz is a common characteristic of alkalic porphyry systems in BC (Lang et al., 1995). Alteration is characterized by intense K-feldspar+biotite+magnetite in monzonite A and adjacent volcanoclastic rocks and is moderate to weak in monzonite D. Potassium feldspar+biotite+magnetite alteration is overprinted by chlorite+epidote+hematite+pyrite alteration and a later white illite alteration that occurs as a halo

to tourmaline veins. The latest observed alteration stage comprises calcite+ankerite+pyrite. Mineralization is hosted in two vein stages: 1) a very dense laminated and sheeted network of quartz-magnetite-hematite-chalcopyrite veins that are strongly developed in monzonite A and the adjacent volcanic hostrocks and 2) later quartz-chalcopyrite-pyrite veins that crosscut all the hostrocks at the Deerhorn deposit, including monzonite D. The K-feldspar±biotite±magnetite alteration assemblage and the vein stages observed at the Deerhorn deposit are consistent with characteristics of Cu-Au calcalkalic porphyry systems (Sillitoe, 2000, 2010); however, the pencil-shaped intrusive hostrock lacking modal quartz is consistent with characteristics of Cu-Au alkalic porphyry systems (Holliday et al., 2002). These observations indicate that the Deerhorn deposit has characteristics of both alkalic and calcalkalic systems, similar to those at the Red Chris deposit in northwestern BC, where the hostrock is a quartz-poor monzonite and mineralization is hosted in banded quartz veins (Norris, 2011).

The close proximity as well as the similar alteration and vein stages of the SEZ and Deerhorn deposits suggest that they could be related and may represent a transition from the alkalic to calcalkalic environment. The next stage of this project will focus on the geochemistry and magmatic-hydrothermal evolution of these deposits in the Woodjam property, using detailed petrography and geochemical analyses.

Acknowledgments

Geoscience BC is acknowledged and thanked for the funding provided for this project. Gold Fields Canada is thanked for the funding and field support for the project. The entire staff of the Woodjam project, including J. Scott, M. McKenzie, S. Vanderkekhove, K. Rempel and M. Eckfeldt, are thanked for their support during fieldwork. T. Bissig, Mineral Deposit Research Unit, University of British Columbia, is thanked for review and comments on this paper.

References

- Arancibia, O.N. and Clark, A.H. (1996): Early magnetite-amphibole-plagioclase alteration-mineralization in the Island Copper porphyry copper-gold molybdenum deposit, British Columbia; *Economic Geology*, v. 91, p. 402–438.
- BC Geological Survey (2012): MINFILE BC mineral deposits database; BC Ministry of Energy, Mines and Natural Gas, URL <<http://minfile.ca/>> [November 2012].
- Casselman, M.J., McMillan, W.J. and Newman, K.M. (1995): Highland Valley porphyry copper deposits near Kamloops, British Columbia: a review and update with emphasis on the Valley deposit; *in* *Porphyry Deposits of the Northwestern Cordillera of North America*, T.G. Schroeter (ed.), Canadian Institute of Mining and Metallurgy, Special Volume 46, p. 161–191.

- Chamberlain, C.M., Jackson, M., Jago, C.P., Pass, H.E., Simpson, K.A., Cooke, D.R. and Tosdal, R.M. (2007): Toward an integrated model for alkalic porphyry copper deposits in British Columbia (NTS 039A, N; 104G); *in* Geological Fieldwork 2006, Geoscience BC, Report 2007-1, p. 259–274, URL <<http://www.empr.gov.bc.ca/Mining/Geoscience/PublicationsCatalogue/Fieldwork/Documents/26-Chamberlain.pdf>> [November 2012].
- Fraser, T.M., Stanley, C.R., Nikic, Z.T., Pesalj, R. and Gorc, D. (1995): The Mount Polley alkali porphyry copper-gold deposit, south-central British Columbia; *in* Porphyry Deposits of the Northwestern Cordillera of North America, T.G. Schroeter (ed.), Canadian Institute of Mining and Metallurgy, Special Volume, v. 46, p. 609–622.
- Gustafson, L.B. and Hunt, J.P. (1975): The porphyry copper deposit at El Salvador, Chile; *Economic Geology*, v. 70, no. 9, p. 857–312.
- Holliday, J.R., Wilson, A.J., Blevin, P.L., Tedder, I.J., Dunham, P.D. and Pfitzner, M. (2002): Porphyry gold-copper mineralization in the Cadia district, eastern Lachlan fold belt, New South Wales and its relationship to shoshonitic magmatism; *Mineralium Deposita*, v. 37, p. 100–116.
- Lang, J.R., Lueck, B., Mortensen, J.K., Russell, J.K., Stanley, C.R. and Thompson, J.M. (1995): Triassic-Jurassic silica undersaturated and silica-saturated alkalic intrusions in the Cordillera of British Columbia: implications for arc magmatism; *Geology*, v. 23, p. 451–454.
- Logan, J.M., Mihalynuk, R.M., Friedman, R.M. and Creaser, R.A. (2011): Age constraints of mineralization at the Brenda and Woodjam Cu–Mo±Au porphyry deposits—an early Jurassic calcalkaline event, south-central British Columbia; *in* Geological Fieldwork 2010, BC Ministry of Energy, Mines and Natural Gas, Paper 2011-1, p. 129–144, URL <http://www.empr.gov.bc.ca/Mining/Geoscience/PublicationsCatalogue/Fieldwork/Documents/2010/09_Logan_2010.pdf> [November 2012].
- McMillan, W.J., Thompson, J.F.H., Hart, C.J.R. and Johnston, S.T. (1995): Regional geological and tectonic setting of porphyry deposits in British Columbia and Yukon Territory; *in* Porphyry Deposits of the Northwestern Cordillera of North America, T.G. Schroeter (ed.), Canadian Institute of Mining, Metallurgy and Petroleum, Special Volume, v. 46, p. 40–57.
- Mihalynuk, M.G., Nelson, J. and Diakow, L.J. (1994): Cache Creek terrane entrapment: oroclinal paradox within the Canadian Cordillera; *Tectonics*, v. 19, p. 575–595.
- Monger, J. and Price, R. (2002): The Canadian Cordillera: geology and tectonic evolution; *Canadian Society of Exploration Geophysicists Recorder*, v. 27, no. 2, p. 17–36.
- Mortimer, N. (1987): The Nicola Group: Late Triassic and Early Jurassic subduction-related volcanism in British Columbia; *Canadian Journal of Earth Sciences*, v. 24, p. 2521–2536.
- Norris, J.R., Hart, C.J.R., Tosdal, R.M. and Rees, C. (2011): Magmatic evolution, mineralization and alteration of the Red Chris copper gold porphyry deposit, northwestern British Columbia (NTS 104H/12W); *in* Geoscience BC Summary of Activities 2010, Geoscience BC, Report 2011-1, p. 33–44.
- Panteleyev, A., Bailey, D.G., Bloodgood, M.A. and Hancock, K.D. (1996): Geology and mineral deposits of the Quesnel River–Horsefly map area, central Quesnel Trough, British Columbia; BC Ministry of Energy, Mines and Natural Gas, Bulletin 97, 156 p.
- Rainbow, A. (2010): Assessment report on 2010 activities on the Woodjam South property including soil sampling, surface rock sampling and diamond drilling; BC Ministry of Energy, Mines and Natural Gas, Assessment Report 32 958, 1260 p.
- Schiarizza, P., Bell, K. and Bayliss, S. (2009): Geology and mineral occurrences of the Murphy Lake area, south-central British Columbia (NTS 093A/03); *in* Geological Fieldwork 2008, BC Ministry of Energy, Mines and Natural Gas, Paper 2009-1, p. 169–188, URL <http://www.empr.gov.bc.ca/Mining/Geoscience/PublicationsCatalogue/Fieldwork/Documents/15_Schiarizza_2008.pdf> [November 2012].
- Scott, J. (2012): Geochemistry and Cu–Au mineral paragenesis of the Deerhorn prospect: Woodjam porphyry Cu–Au district, British Columbia, Canada; B.Sc. Honours thesis, University of British Columbia Okanagan, 120 p.
- Sherlock, R., Poos, S. and Trueman, A. (2012): National Instrument 43-101 technical report on 2011 activities on the Woodjam South property, Cariboo Mining Division, British Columbia, 194 p., URL <http://sedar.com/GetFile.do?lang=EN&docClass=24&issuerNo=00032460&fileName=/csfsprod/data132/filings/01934687/00000001/y%3A%5CWeb_Documents%5CRADAR%5CE3%5CE3CO0C24%5C23JL12137%5C120723WJSTR_jaj.pdf> [November 2012].
- Sillitoe, R.H. (2000): Gold-rich porphyry deposits: descriptive and genetic models and their role in exploration and discovery; *Reviews in Economic Geology*, v. 13, p. 315–345.
- Sillitoe R.H. (2010): Porphyry copper systems; *Economic Geology*, v. 105, p. 3–41.
- Vaca, S. (2012): Variability in the Nicola/Takla Group basalts and implications for alkali Cu/Au porphyry prospectivity in the Quesnel terrane, British Columbia, Canada; M.Sc. thesis, University of British Columbia, 163 p.

Burrell Creek Map Area: Setting of the Franklin Mining Camp, Southeastern British Columbia (NTS 082E/09)

T. Höy, Consultant, Sooke, BC, thoy@shaw.ca

Höy, T. (2013): Burrell Creek map area: setting of the Franklin mining camp, southeastern British Columbia (NTS 082E/09); in Geoscience BC Summary of Activities 2012, Geoscience BC, Report 2013-1, p. 91–102.

Introduction

The Burrell Creek project includes geological mapping and data compilation of a large part of the 1:50 000 scale Burrell Creek map area (NTS 82E/09), located in the Columbia Mountains of southeastern British Columbia (Figure 1). The project is a northward extension of the Deer Park (Höy, 2010; Höy and Jackaman, 2010) and Grand Forks (Höy and Jackaman, 2005) mapping projects, which focused on the potential and controls of Tertiary mineralization within the southern Monashee Mountains in the Pentiction (east half) map area (NTS 082E, east half). These projects recognized and defined a variety of base- and precious-metal occurrences that appear to be related to prominent north- and northwest-trending regional structures. The Burrell Creek project focused mainly on a mafic intrusive complex that hosts deposits in the historical Franklin mining camp, and recognized and mapped a similar deeper level intrusive complex to the east in the footwall of the Granby extensional fault. Dating of both these complexes, in progress through a contract with the University of British Columbia (UBC), may allow insights into role of Tertiary extension in the development of the camp and further controls on the displacement along a major Eocene extensional fault.

Project Objectives and Results

The project involves mainly geological mapping, at a scale of 1:20 000, of selected areas of the Burrell Creek map area. It also includes compilation in digital format of all regional geological and geophysical data, geochemical data collected under the National Geochemical Reconnaissance (NGR) program and the BC Regional Geochemical Survey (RGS), and update of the MINFILE BC database (BC Geological Survey, 2012b). This information will be combined to produce a 1:50 000 scale map of the Burrell Creek map area, as well as 1:20 000 scale maps of areas with higher

mineral potential suitable for directing and focusing mineral exploration.

An important focus of the project is mapping and evaluation of Tertiary faulting and magmatic activity, and their relationship to mineralization. Results are summarized in this paper and in published maps (Höy and Jackaman, 2010). A final 1:50 000 scale map will be released by Geoscience BC in early 2013.

Geological and Exploration History

The Burrell Creek map area (Figure 1) is part of the Kettle Valley area (NTS 082E, east half), which was mapped at a scale of 1 inch to 4 miles (approximately 1:253 000) by Little (1957). More recently, Tempelman-Kluit (1989) mapped and compiled the Pentiction area (NTS 082E) at a scale of 1:250 000, making only minor modifications in the eastern part in the Burrell Creek area. The geology of the two 1:50 000 areas to the south, Grand Forks and Deer Park, was recently published by Höy and Jackaman (2005, 2010), based on new mapping and on compilation of previous studies, most notably by Preto (1970), Tempelman-Kluit (1989), Acton et al. (2002) and Laberge and Pattison (2007). The Greenwood mining camp, located immediately west of the Grand Forks area, has been studied in considerable detail, initially by Little (1979) and more recently by Church (1986) and Fyles (1990). Mapping east of the Burrell Creek area includes the regional study of the Lardeau (west half) area by Little (1960) and, farther southeast, more detailed geological mapping of the Rossland and Nelson areas (Höy and Dunne, 2001, 2004). Recent geological mapping has focused on areas to the north (NTS 082L; Thompson, 2006) and several isolated areas in the western part of the Pentiction map area by the BC Geological Survey (Massey, 2006, 2007, 2010; Massey and Duffy, 2008; Massey et al., 2010).

Mineral exploration, focused largely in the south, dates back to the mid- to late 1800s, with discovery and development of rich gold and copper deposits in the Greenwood and Rossland mining camps, as well as the building of smelters in Greenwood, Grand Forks and Trail. This area, referred to as the Boundary district, continues to be actively explored by several junior exploration companies and, in the Republic district of Washington State, has had recent

Keywords: *geology, Grand Forks Gneiss Complex, Coryell syenite, Averill Plutonic Complex, Tenderloin Plutonic Complex, Granby fault, Kettle River fault, Eocene extensional faulting, Franklin mining camp, epithermal gold*

This publication is also available, free of charge, as colour digital files in Adobe Acrobat® PDF format from the Geoscience BC website: <http://www.geosciencebc.com/s/DataReleases.asp>.

gold production from Kinross Gold Corporation's Emmanuel Creek and Buckhorn deposits.

Mineralization in the Franklin mining camp, located in the southern part of the Burrell Creek map area, was discovered in the early 1900s (Drysdale, 1915). The only significant deposit in the camp, the Union mine, produced 122 555 tonnes grading 14.1 g/tonne Au and 353.4 g/tonne Ag, primarily in the early 1930s. The most recent exploration in the camp, included soil sampling, geological mapping and prospecting by Tuxedo Resources Ltd. in 2001–2004 (Caron, 2004) and rock sampling, trenching and limited diamond-drilling by Solitaire Minerals Inc. in 2004 (Caron, 2005).

Regional Geology

The Burrell Creek area is located on the northern extension of the Grand Forks Complex (Preto, 1970), one of a number of metamorphic core complexes in the southern Omineca Belt that appear to be related to Eocene faulting, extension and denudation (Tempelman-Kluit and Parkinson, 1986; Brown and Journeay, 1987; Parrish et al., 1988). The complex is bounded on the west by the west-dipping Granby fault and on the east by the east-dipping Kettle River fault. Normal movements on these faults were determined to be Early Tertiary, constrained by ages of intrusive rocks (Carr et al., 1987; Parrish et al., 1988). A variety of plutonic suites is recognized to the south and west of the Burrell Creek area

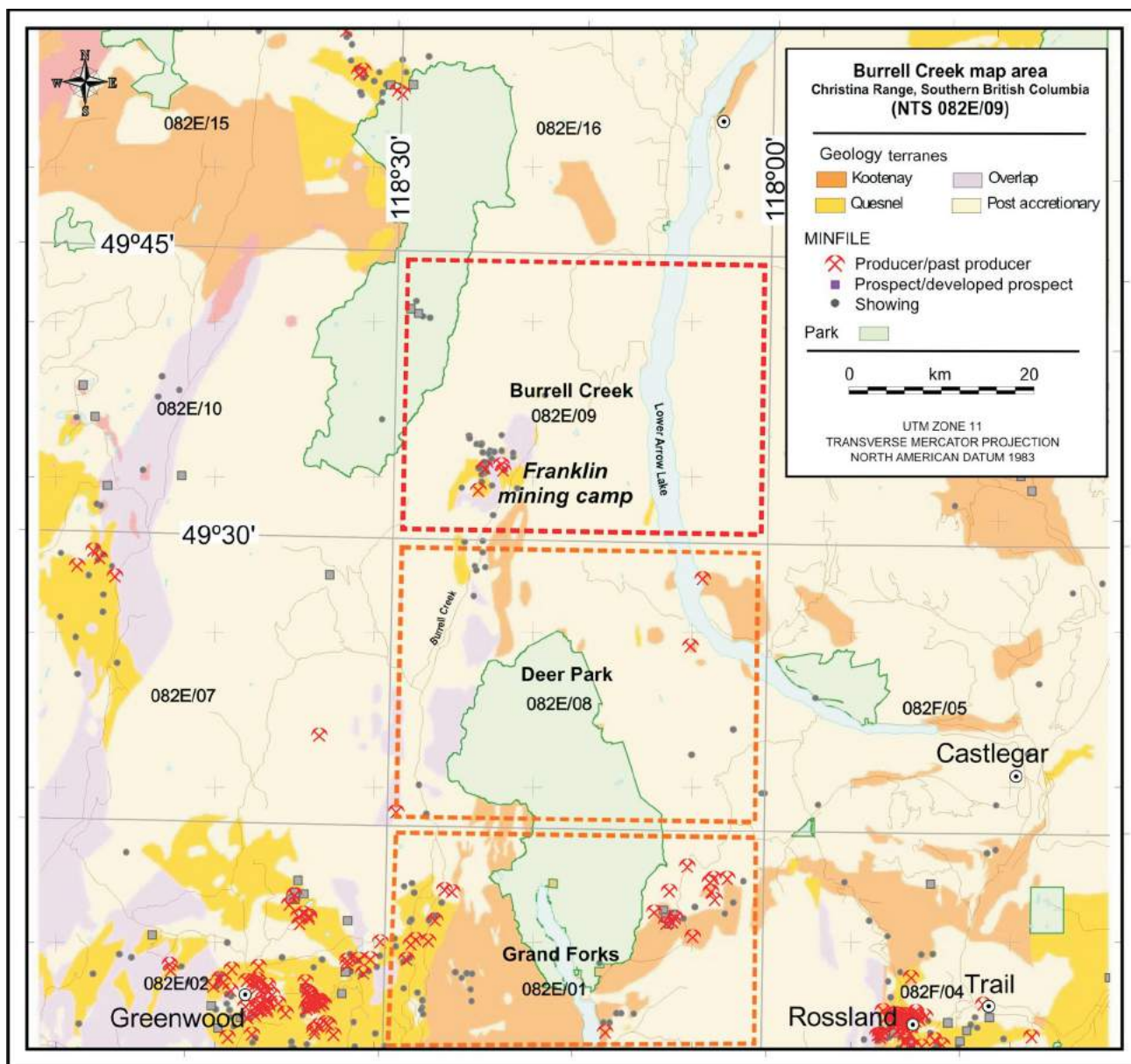


Figure 1. Locations of the 1:50 000 scale Burrell Creek map area (NTS 082E/09), two recently published maps to the south, BC MINFILE occurrences, mining camps and major lithological units in the southern Monashee Mountains and Okanagan Highlands of southeastern British Columbia. Modified from BC MapPlace (BC Geological Survey, 2012a).

(Little, 1957; Tempelman-Kluit, 1989), most notably Middle Jurassic 'Nelson' granodiorite, Cretaceous granite and Eocene 'Coryell' syenite.

Geology of the Burrell Creek Map Area

Introduction

The Burrell Creek map area is underlain mainly by Middle Jurassic, Cretaceous and Early Eocene intrusive rocks (Figure 2). In the vicinity of the Franklin mining camp, these intrude Late Paleozoic metasedimentary and metavolcanic rocks and are unconformably overlain by Eocene coarse-grained sedimentary rocks and volcanic rocks of the Kettle River and Marron formations. The structure of the area is dominated by north-trending, steep to relatively shallow dipping normal faults, including the inferred northern extensions of the Kettle River fault in the southeastern part of the area and the Granby fault that extends through the central part of the area to the northern limit of mapping. Virtually all known base- and precious-metal mineral occurrences are in the hangingwalls of these faults. The Union mine in the Franklin mining camp, the largest known metallic-mineral deposit in the area, produced silver, gold, lead and zinc from east-trending polymetallic veins until 1947, followed by heap leaching of tailings that continued to 1989.

Eocene Coryell Intrusions (Unit Ec)

The Coryell intrusions are a Middle Eocene, alkalic to sub-alkalic plutonic suite. They underlie a large part of the Burrell Creek map area, restricted mainly to the area between the Granby and Kettle River faults and north of a north-west-trending structural zone that includes the Franklin mining camp and a parallel fault, the Michaud Creek fault (Figure 2). The intrusions range from coarse-grained pink syenite with generally less than 10% biotite+hornblende to coarse-grained monzonite. Medium-grained and porphyritic phases are locally common, particularly in border zones, in exposures in the immediate hangingwall of the Granby fault and as suites of typically north-trending dikes.

Cretaceous Granite (Unit Kg)

Large exposures of granitic rock occur in the southern part of the Burrell Creek map area and form the axis of the mountain range in the northwestern part. These exposures are part of the Okanagan batholith, a large complex exposed throughout much of the Penticton map area to the west that Tempelman-Kluit (1989) indicated was "Cretaceous and/or Jurassic" in age. They are also similar to granitic rocks farther east, referred to by Little (1960) as the "Valhalla plutonic rocks" and interpreted to be Late Cretaceous by Parrish et al. (1988). They are often difficult to distinguish from granitic phases of the Nelson suite and differentiation of these two suites in the northwestern part of

the area requires more detailed work, including radiometric dating.

Exposures in the Burrell Creek area are mainly medium-grained leucocratic granite with minor (<10%) mafic content. Porphyritic phases, characterized by pink alkali feldspar phenocrysts, are less common. The granite is locally foliated and occasionally banded with pegmatite or more mafic phases.

The granite is typically fresh, although pegmatites, dikes, quartz veining and local brecciation with minor pyrite and jarosite alteration occur near contacts with both Coryell and Middle Jurassic intrusions.

Middle Jurassic Nelson Plutonic Suite (Unit Jgd)

Middle Jurassic granodiorite bodies occur throughout most of the area; unit Jgd includes, in the northern part, younger Cretaceous granite and, elsewhere, small stocks and dikes of Coryell syenite. 'Nelson' granodiorite has not been differentiated, comprising massive granodiorite, quartz diorite and, less commonly, granite. These phases range from massive and equigranular to porphyritic with large, subhedral, beige to pink feldspar phenocrysts in a medium- to coarse-grained granodiorite matrix. In the hangingwall of the Granby fault in the southern part of the map area, exposures are medium grained, more mafic and commonly veined and propylitically altered.

In the Franklin mining camp area, Nelson plutonic rocks intrude late Paleozoic basement metavolcanic and metasedimentary rocks and are unconformably overlain by conglomerate, grit and volcanic rocks of the Eocene Kettle River and Marron formations. As discussed below, their relationship to the Averill Plutonic Complex and associated mineralization is less clear.

Averill Plutonic Complex

Mineralization in the Franklin camp is spatially associated with the Averill Plutonic Complex, a suite of mafic alkalic intrusions that was originally interpreted to be Eocene (Drysedale, 1915) but is now considered to be Jurassic, based largely on a K-Ar date reported in Keep (1989). The complex has been studied in considerable detail by Keep (1989) and Keep and Russell (1988), and the following description is taken mainly from these papers.

The complex comprises five main units, ranging in composition from pyroxenite to syenite, which have been intruded by two dike swarms. The first four members of the suite include "pyroxenite, monzogabbro, monzodiorite and monzonite, and define a concentrically zoned intrusion with pyroxenite at the centre and monzonite at the edge. The fifth member, a syenite, was intruded through the centre of this

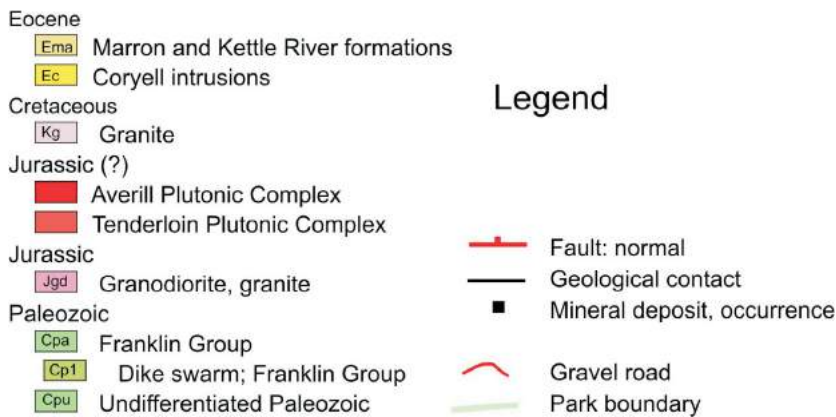
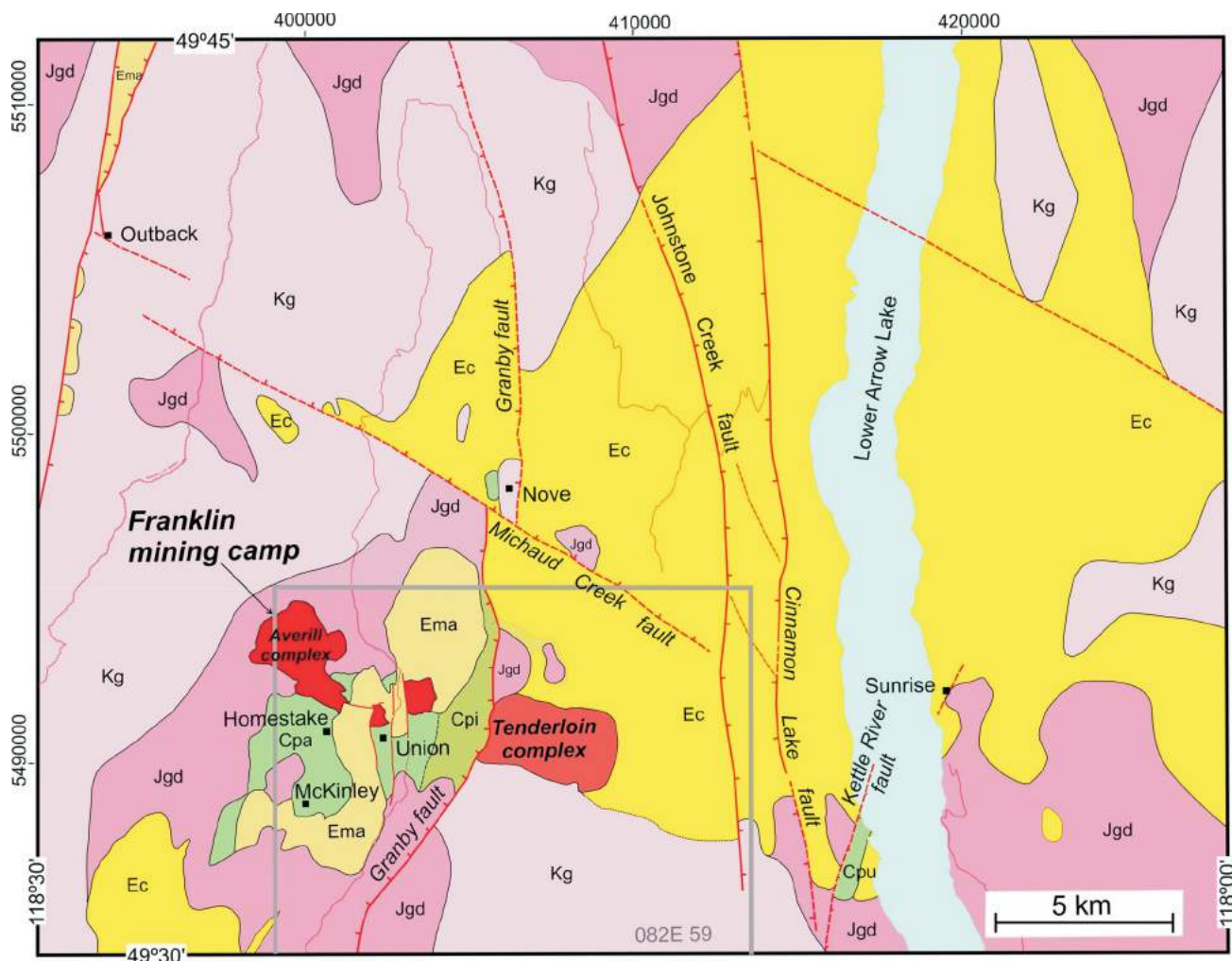


Figure 2. Geology of the Burrell Creek map area (NTS 082E/09), including data from Drysdale (1915), Little (1957), Keep (1989) and Tempelman-Kluit (1989), with selected mineral occurrences.

concentric zonation, causing brecciation of the pyroxenite and monzogabbro” (Keep, 1989).

The pyroxenite (unit Apx; Figure 3) is medium to coarse grained and black, and consists mainly of augite and biotite, with interstitial alkali feldspar and minor sphene and apatite. The mineralogy of the monzogabbro (unit Amg) is

similar to that of the pyroxenite, comprising mainly augite, with hornblende, biotite, alkali feldspar±plagioclase. Monzodiorite, the dominant phase in the complex (unit Amd), is intermediate in composition, comprising mainly augite, biotite, hornblende and alkali feldspar. Monzonite (unit Am), the outermost shell of the zoned Averill Complex, comprises mainly alkali feldspar and plagioclase, with intersti-

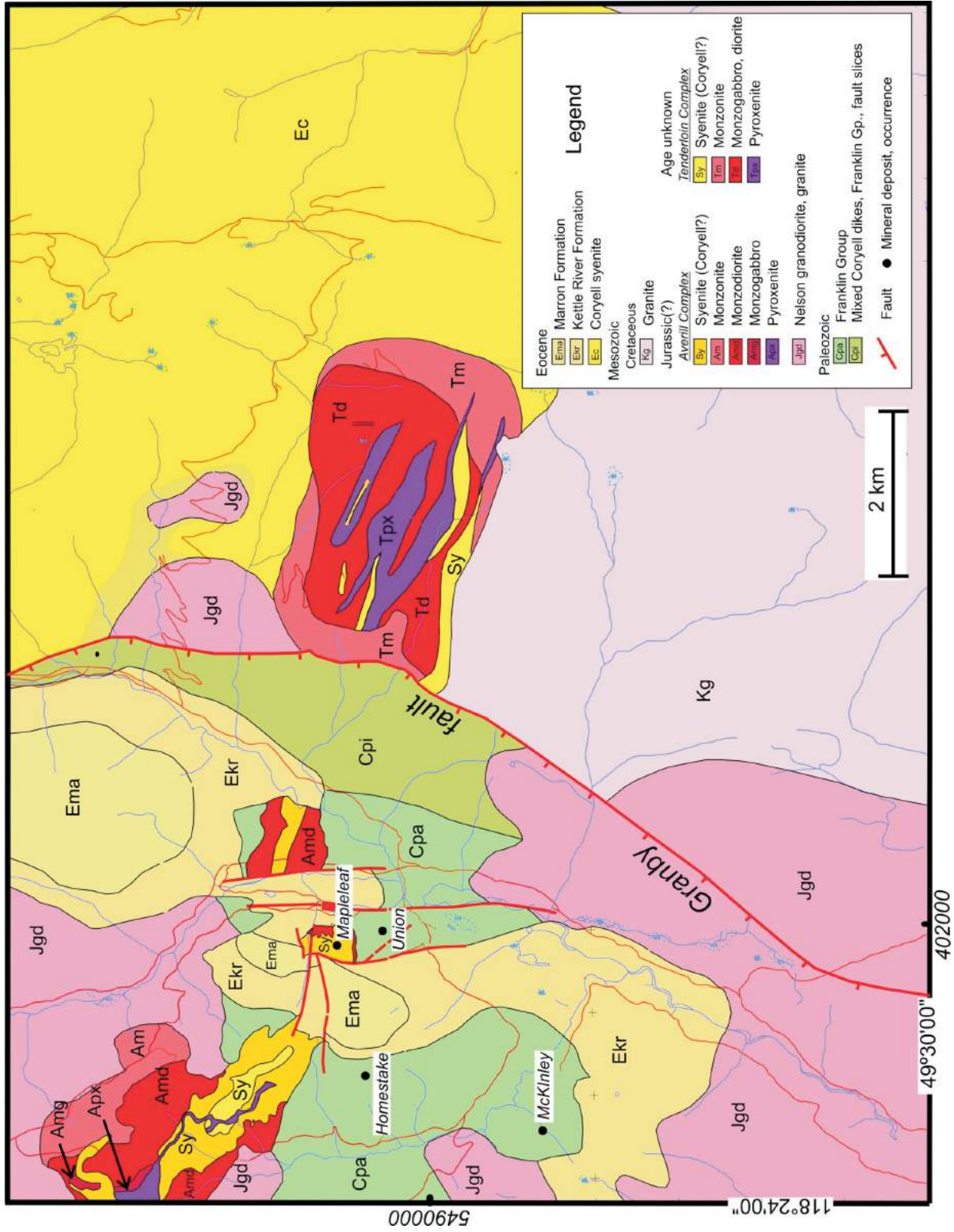


Figure 3. Geology of 1:20 000 scale TRIM map 082E/059 covering the Franklin mining camp, with data from Drysdale (1915), Keep (1989), Tempelman-Kluit (1989) and Caron (2004, 2005); location indicated by grey rectangle on Figure 2.

tial augite and biotite. Based on field, petrographic and whole-rock and trace-element data, Keep (1989) argued convincingly that these phases represent a cogenetic suite. The syenite (unit Sy), however, is distinctive in that it contains no plagioclase and clearly intruded the earlier phases. It is similar in composition to Coryell syenite, and hence may be part of that suite and not the Averill Complex.

Drysdale (1915), based on field relationships and their alkalic composition, proposed that rocks of the Averill Complex were Eocene in age, related to the Coryell Plutonic Suite. However, a sample of pyroxenite, taken from the base of a scree slope, returned a K-Ar date of 150 ± 5 Ma (unpublished data, UBC Geochronology Laboratory; cited in Keep, 1989), indicating a Jurassic age. To further constrain this age and those of other phases of the Averill Complex, five samples have been submitted to the UBC Geochronology Laboratory for Ar-Ar dating.

Tenderloin Plutonic Complex

A lithologically similar intrusive complex, located approximately 6 km east of the Averill Complex, has been mapped during the course of this study and named the 'Tenderloin Plutonic Complex' (Figure 2). Neither petrographic nor geochemical work has been done on it, and the following descriptions and nomenclature are based only on field observations. The complex is roughly concentric with an inner zone of pyroxenite and gabbro, surrounded by monzogabbro, diorite and monzonite (Figure 3). The intrusive complex trends west-northwest, particularly in the western and central parts; foliation and gneissosity within several phases, most notably the marginal monzonite, parallel this trend. Dikes of syenite parallel the west-northwest trend and these, based on crosscutting relationships and petrology, may be part of the Coryell suite. All phases are relatively fresh, with only minor alteration of augite to hornblende and chlorite.

The pyroxenite (unit Tpx) forms several east-northeast-trending lenses that appear to pinch out to the east near the margins of the complex. The pyroxenite is typically black, comprising mainly medium- to coarse-grained augite and biotite with up to 10% plagioclase (Figure 4). The monzogabbro and diorite (unit Td) appear to be gradational with the pyroxenite, containing mainly augite, biotite and up to approximately 50% plagioclase. The unit is coarse to medium grained and commonly cut by thin alkali feldspar veins (Figure 5). It forms the bulk of the Tenderloin Complex.

A marginal phase (unit Tm), comprising mainly monzonite but grading to quartz monzonite and monzodiorite, surrounds the more mafic phases of the Tenderloin Complex. It typically contains 10–25% mafic minerals, mainly augite, hornblende and biotite, in a matrix of plagioclase, minor alkali feldspar and occasional minor quartz. Exposures



Figure 4. Massive medium-grained pyroxenite of the Tenderloin Complex.

on the northwestern margin of the complex commonly show foliation textures and mineral segregations that are highly variable but generally approximately parallel to the margins of the intrusion and are assumed to be primary flow banding. Similar but north-trending fabrics occur within the monzonite unit on the eastern margin of the complex. In both localities, several syenite dikes, ranging from a few tens of centimetres to several metres thick, cut the monzonite, oriented parallel to the fabric.

Syenite (unit Sy) occurs as large east-trending dikes within the central and southern parts of the complex, cutting the more mafic phases; in eastern exposures, syenite dikes that cut monzonite trend more northerly parallel to the contact with the Coryell syenite. In the western exposures, large slabs of syenite, ranging from several to tens of metres thick, trend northerly; sheared contacts with the monzonite suggest that these are fault slabs related to the Granby fault.

The Tenderloin Complex has many similarities to the Averill Complex, including composition, zoning, its age relative to syenite and its west to northwest orientation (Figure 3). The Averill Complex is assumed to be Jurassic



Figure 5. Monzogabbro of the Tenderloin Complex, showing thin crosscutting alkali feldspar and plagioclase veins; width of main vein approximately 2 cm.

in age, based on a single 150 Ma K-Ar date on pyroxenite. The age of the Tenderloin Complex is not known, but five samples of monzogabbro and monzonite have been submitted to the Pacific Centre for Isotopic and Geochemical Research at UBC for Ar-Ar dating; these data and the new data from the Averill Complex will enable better comparisons between the two.

Late Paleozoic Succession (Unit CPa)

Metasedimentary and metavolcanic rocks, exposed in the Franklin camp area, comprise mafic volcanics, argillite, siltstone and minor limestone and chert. A number of veins and mineralized skarns in the camp are hosted by these rocks. Rocks of unit CPa are commonly tightly folded, silicified, fractured and veined, and cut by dikes of various ages. Farther east, in the immediate hangingwall of the Granby fault, these rocks (unit Cpi, Figures 2, 3) are intruded by numerous Coryell dikes that are locally sheared and intensely silicified or alkali feldspar altered.

These successions, named the Franklin Group by Drysdale (1915), have been correlated with the Carboniferous to Permian Anarchist Group and are similar to Paleozoic exposures described as Knob Hill in the Greenwood area (Church, 1986; Fyles, 1990; Massey, 2006) and rocks assigned to the Paleozoic Anarchist Group in the McKinney mining camp, located 40 km southwest of the Franklin camp (Massey and Duffy, 2008). However, Caron (2004) correlated the Franklin Group with the Triassic Brooklyn Formation in the Greenwood mining camp; until definite dating or rock geochemistry is done, a correlation with older Paleozoic rocks is assumed.

Eocene Kettle River Formation (Unit Ekr)

The Kettle River Formation comprises up to several hundred metres of conglomerate and feldspathic grit with rare plant fossil material and numerous sedimentary structures, including crossbedding, ripple marks and small scours (Drysdale, 1915). These structures and the coarse massive conglomerate facies indicate shallow-water and alluvial-fan deposition. Clasts and 'grit' within the formation were largely derived from the underlying Franklin Group but also include clasts derived from the Averill Complex (Caron, 2005) and from tuffaceous and flow rhyolite deposited contemporaneously with the sediments (Drysdale, 1915). The attitude of the Kettle River Formation is variable but generally dips to the northeast at angles up to 45°, indicating that some block faulting occurred either contemporaneously with or following deposition. It is overlain, locally unconformably, by andesitic and trachytic flows of the Marron Formation.

Eocene Marron Formation (Unit Ema)

The 'Midway volcanic group' caps Tenderloin Mountain and Mount McKinley mountains immediately north and

south of the Franklin camp area (Figure 3). The volcanic rocks vary in composition from alkalic basalt to trachyte, and range from well-banded basic tuff and blocky tephra to flows (Drysdale, 1915). They are correlated with the Marron Formation, which is exposed in grabens and depressions to the west in the Penticton map area (Tempelman-Kluit, 1989).

Structure

The structure of the Burrell Creek area is dominated by north- and northwest-trending normal faults that record a period of Tertiary extension in southern BC. These faults played a role in the distribution of both intrusive bodies and mineralization in the map area and in the Boundary district to the west and southwest. The Granby and Kettle River faults (Little, 1957; Preto, 1970) bound the high-grade Grand Forks Complex; these faults extend northward into the Deer Park area and the southern part of the Burrell Creek area (Tempelman-Kluit, 1989; Höy and Jackaman, 2010). Detailed structural and metamorphic studies of both hangingwall and footwall rocks suggest that depth contrasts reach approximately 5 km across both the Granby (Lalonde and Pattison, 2007) and Kettle River faults (Cubley and Pattison, 2009).

Granby Fault

The Granby fault is a west-dipping normal fault that, throughout most of its length, has truncated Coryell intrusive rocks in its hangingwall, and high-grade metamorphic rocks of the Grand Forks Complex in its footwall in the south and mainly Jurassic and Cretaceous intrusions farther north. In the southern part of the Burrell Creek area (Figure 2), late Paleozoic rocks of the Franklin Group, Middle Jurassic granodiorite and Tertiary sedimentary and volcanic rocks of the Kettle River and Marron formations occur in the hangingwall, with mainly Cretaceous granite, Coryell syenite and the Tenderloin Plutonic Complex in the footwall. Farther north, in the central part of the map area, Coryell rocks occur in the hangingwall, but these are typically finer grained, commonly porphyritic and cut by numerous dikes in contrast to the more massive and coarser grained syenite in the footwall. The fault is a high-level brittle structure, marked by brecciation, locally intense chloritic alteration and, east of the Franklin camp, numerous parallel splays that produce a wide zone of interlayered Coryell syenite, Paleozoic metavolcanic rocks and monzonite of the Tenderloin Complex.

The displacement along the fault in the Burrell Creek area is not known. Correlative Coryell rocks clearly show marked differences across the fault, with finer grained porphyritic phases, dikes and pervasive alteration in the hangingwall contrasting with coarser, more massive phases to the east. The fault is younger than the ca. 51 Ma Coryell syenite and

Middle Eocene Marron Formation volcanic rocks (Parrish et al., 1988; Carr and Parkinson, 1989).

Kettle River Fault

The Kettle River fault is shown on all regional maps as truncated by the Coryell intrusions in the central part of the Deer Park map area (Parrish et al., 1988; Tempelman-Kluit, 1989). Based on more recent studies, it has been projected northward through the Deer Park area into the southern part of the Burrell Creek map area (Höy and Jackaman, 2010). It is inferred to be exposed in the southeastern part of the area, where it juxtaposes Paleozoic metavolcanic and metasedimentary rocks in its hangingwall with Coryell and Middle Jurassic intrusive rocks in the footwall (Figure 2). On the east side of Lower Arrow Lake and on strike with the inferred trace of the fault is a zone of high-level shearing and brecciation associated with epithermal-style gold mineralization on the Sunrise property.

Johnstone Creek and Cinnamon Lake Faults

The Johnstone Creek and Cinnamon Lake faults, two newly recognized north-trending structures, were mapped in the southern part of the Burrell Creek area and projected northward the length of the map area along prominent topographic linears and truncation of map units (Figure 2). Both are late, post-Coryell, high-level brittle faults that are locally marked by brecciation, shearing and chloritic alteration. Normal displacement along these is restricted to a few hundred metres.

Northwest-Trending Structures

The Averill and Tenderloin complexes are on a west-northwest-trending 'structural zone' in the southern part of the Burrell Creek map area (Figure 2). The zone is marked by preferred orientations of intrusive bodies and the northern limit of a Cretaceous intrusion. The only exposures of Paleozoic rocks in the map area occur within this zone in the hangingwalls of the Granby and Kettle River faults, and the northerly orientation of the Granby fault is deflected to the northeast within the zone. The zone is inferred to be the locus of an older structural zone that controlled, in part, the distribution of intrusive complexes and mineralization in the Burrell Creek map area, as well as the distribution of intrusions and regional structures to the northwest in the Penticton map area. Although there is little evidence of large-scale Eocene faulting within the zone, several faults in the Franklin camp, with tens to a few hundred metres of offset, are recognized (Figure 3). In addition, approximately 5 km to the north, the northwest-trending Michaud Creek fault cuts Eocene Coryell intrusions.

The Michaud Creek fault is a north-dipping normal fault that trends northwesterly through the central part of the map area. It is marked by topographic linears and offset of Coryell, Middle Jurassic and Cretaceous intrusive rocks.

Veins of the Nove mineral occurrence (MINFILE 092ENE045) are in its immediate hangingwall, and the Sunrise occurrence (Kennedy, 2005) is located near the intersection of the northern extension of the Kettle River fault and the approximate southeastward projection of the Michaud Creek fault (Figure 2).

Mineralization

The focus of the present study is mainly on the structural controls and timing of mineralization in the Franklin mining camp and their implications for the regional distribution and controls of base- and precious-metal deposits in the eastern part of the Penticton map area. The Franklin camp is located in the southwestern part of the Burrell Creek map area, and several other vein occurrences are known throughout the remainder of the area. Mineralization in the camp, summarized below, is taken from detailed studies by Drysdale (1915) and from more recent provincial-government assessment reports, including Pinsent and Cannon (1988) and Caron (2004, 2005).

Drysdale (1915) and subsequent workers recognized three styles of mineralization in the camp; in addition, Caron (2004, 2005) recognized Eocene epithermal mineralization. The four styles are

- 1) small lenses of magnetite-, pyrrhotite-, chalcopyrite- and/or arsenopyrite-bearing skarns in altered and brecciated Franklin Group metavolcanic and metasedimentary rocks adjacent to Jurassic plutons and the Averill Complex;
- 2) minor platinum, palladium and silver associated with chalcopyrite in pyroxenite and syenite phases of the Averill Complex;
- 3) silver and/or gold mineralization, with or without base-metal mineralization, in silicified shears and faults; this style of mineralization characterizes the Union mine, the main producer in the camp; and
- 4) Eocene epithermal gold mineralization.

Several other areas of mineralization are known in the Burrell Creek map area. The Sunrise property is located on the east side of Lower Arrow Lake along the inferred northern projection of the Kettle River fault (Figure 2). It was discovered in 2004 during a regional prospecting program by Kootenay Gold Inc. (Kennedy, 2005). Mineralization comprises epithermal gold-quartz-chalcedony veins associated with minor pyrite and pyrrhotite in north-trending faults that cut Eocene syenite and Jurassic granodiorite. Mineralization is clearly syn to post Eocene, with veins cutting both Coryell syenite and late alkali feldspar porphyry dikes.

The Nove property occurs in the central part of the map area, immediately north of the Michaud Creek fault (Figure 2). Mineralization comprises anomalous gold and silver associated with minor chalcopyrite, bornite and galena in

veins along the north-trending sheared contact of Coryell syenite and a small Cretaceous(?) granitic stock (Wilkinson, 2001). Several other precious-metal occurrences, referred to as the Outback property (Bohme, 1991), are located on a parallel structure west-northwest of the Nove property. These comprise mainly epithermal gold mineralization related to a complex array of faults near the intersection of the northwest-trending structure and a north-trending Eocene extensional fault. The property is now within Granby Provincial Park.

A number of other small vein occurrences were discovered during the course of this regional mapping project. All comprise quartz veining associated with brecciation, pyrite and considerable limonitic alteration, and all occur along either the north- or northwest-trending faults.

Summary of the Geological History

The oldest rocks in the Burrell Creek area, the Franklin Group, comprise a package of mafic volcanic and sedimentary rocks that were deposited in Late Paleozoic time. These were intruded by mainly calcalkaline granodiorite of the Middle Jurassic Nelson plutonic suite. A variety of mineral deposits, including copper-gold veins in the Rosland camp, silver-lead-zinc veins in the Ymir and Nelson camps and skarn and vein deposits in the Greenwood camp, are related to intermediate to mafic phases of Middle Jurassic plutons. The Averill Plutonic Complex, and the Tenderloin Plutonic Complex to the east, were both emplaced along a strong west-northwest-trending linear, and vein and skarn mineralization was deposited in the higher levels of the Averill Complex and host Franklin Group.

Syenites of the Coryell suite were emplaced during a period of regional extension in Early Eocene time. Their broadly north-south orientation in the eastern half of the Penticton map area reflects east-west extension and emplacement along north-trending zones of structural weakness. On a more local scale, emplacement of Coryell plutons also appears to be controlled, in part, by the loci of earlier northwest-trending structures; the batholith in the Burrell Creek area is largely restricted to the area north of the 'Averill-Tenderloin' structural zone, and its contact with the Cretaceous granite follows this zone.

The west-northwest-trending Michaud Creek fault cuts the Coryell pluton in the central part of the map area, indicating that this trend remained a zone of crustal weakness throughout Eocene time. Tertiary epithermal precious-metal mineralization is preferentially located along this structure, most notably where it intersects prominent north-trending Tertiary extensional faults; for example, Outback mineralization occurs in the immediate hangingwall of the west splay of the Granby fault, the Nove occurrence is in the hangingwall of the Granby fault, and Sunrise is along the inferred extension of the Kettle River fault. Late, north-

trending, epithermal gold mineralization, recognized in the Granby camp, includes the White Bear occurrence (Caron, 2005). This style of mineralization contrasts markedly with deeper level vein and skarn mineralization of Jurassic(?) age, supporting reactivation of structures and repeated and superposed mineralizing events in the camp.

Summary and Discussion

The distribution of both Jurassic and Tertiary mineralization is controlled by two prominent structural trends: north-trending Eocene extensional faults and an earlier northwest-trending zone that localized mineralization in the Franklin camp and Eocene occurrences farther north.

Mineralization characteristic of the Franklin camp is restricted to the hangingwall of the Granby fault and is clearly related to higher levels in the mafic alkalic Averill Complex. A lithologically similar intrusion, the Tenderloin Complex of unknown age, is exposed at deeper structural levels in the footwall of the fault and is unmineralized.

Similar structural trends may have localized deposits elsewhere in the Penticton map area and farther east in the Slocan camp. Mineralization in the Deer Park area, south of the Burrell Creek map area, commonly occurs where north-trending structures are deflected to the northwest and silver-lead-zinc veins in the Slocan camp are located along west-trending faults above a major deflection in the north-trending Slocan Lake fault.

Many mineral camps and deposits in the eastern half of the Penticton map area are preferentially located in the hangingwalls of north-trending Eocene extensional faults. This preferred regional distribution is due, in part, to a genetic relationship to these faults, as exemplified in the Burrell Creek map area by Eocene epithermal-style gold mineralization, but also to the realization that hangingwall panels contain and expose higher intrusive levels and structures, both of which are more favourable settings for mineralization. Recognition and mapping of these major structural intersections will help direct and focus mineral exploration throughout the southern Monashee Mountains and the Okanagan Highlands of southeastern BC.

Acknowledgments

Geoscience BC is gratefully acknowledged for its financial support of this study. Kootenay Silver Inc. is thanked for allowing release of unpublished data on the Sunrise property. W. Jackaman is thanked for help in preparing base maps for this study, G. DeFields for her assistance in the field and L. Caron for discussions on the geology of the Franklin mining camp. The manuscript benefitted from reviews by D. Tempelman-Kluit, C. Sluggett of Geoscience BC and B. Davie of RnD Technical.

References

- Acton, S.L., Simony, P.S. and Heaman, L.M. (2002): Nature of the basement to Quesnel Terrane near Christina Lake, south-eastern British Columbia; *Canadian Journal of Earth Sciences*, v. 69, p. 65–78.
- BC Geological Survey (2012a): MapPlace GIS internet mapping system; BC Ministry of Energy, Mines and Natural Gas, URL <<http://www.MapPlace.ca>> [October 2012].
- BC Geological Survey (2012b): MINFILE BC mineral deposits database; BC Ministry of Energy, Mines and Natural Gas, URL <<http://minfile.ca>> [November 2012].
- Bohme, D.M. (1991): Diamond drilling report on the Outback claim group, Greenwood Mining Division; BC Ministry of Energy, Mines and Natural Gas, Assessment Report 21 916, 18 p., URL <http://aris.empr.gov.bc.ca/search.asp?mode=repsum&rep_no=21916> [November 2012].
- Brown, R.L. and Journeay, M. (1987): Tectonic denudation of the Shuswap metamorphic terrane of southeastern British Columbia; *Geology*, v. 15, p. 142–146.
- Caron, L. (2004): Assessment report on the Franklin property, Greenwood Mining Division: geology, geochemistry, trenching, diamond drilling; BC Ministry of Energy, Mines and Natural Gas, Assessment Report 27 328, 47 p., URL <http://aris.empr.gov.bc.ca/search.asp?mode=repsum&rep_no=27328> [November 2012].
- Caron, L. (2005): Assessment report on the 2004 exploration program: rock sampling, trenching, diamond drilling, Union property, Franklin camp, Greenwood Mining Division, British Columbia; BC Ministry of Energy, Mines and Natural Gas, Assessment Report 27 604, 37 p., URL <http://aris.empr.gov.bc.ca/search.asp?mode=repsum&rep_no=27604> [November 2012].
- Carr, S.D. and Parkinson, D.L. (1989): Eocene stratigraphy, age of the Coryell batholith, and extensional faults in the Granby valley, southern British Columbia; *Geological Survey of Canada, Paper 89-1E*, p. 79–87.
- Carr, S.D., Parrish, R.R. and Brown, R.L. (1987): Eocene structural development of the Valhalla complex, southeastern British Columbia; *Tectonics*, v. 6, p. 175–196.
- Church, B.N. (1986): Geological setting and mineralization in the Mount Attwood–Phoenix area of the Greenwood camp; BC Ministry of Energy, Mines and Natural Gas, Paper 1986-2, 65 p., URL <<http://www.empr.gov.bc.ca/Mining/Geoscience/PublicationsCatalogue/Papers/Pages/1986-2.aspx>> [November 2012].
- Cubley, J. and Pattison, D. (2009): Metamorphic contrast across the Kettle River fault, southeastern British Columbia, with implications for magnitude of fault displacement; *Geological Survey of Canada, Current Research 2009-9*, 19 p.
- Drysdale, C.W. (1915): Geology of the Franklin mining camp, southern British Columbia; *Geological Survey of Canada, Memoir 15*, 246 p.
- Fyles, J.T. (1990): Geology of the Greenwood–Grand Forks area, British Columbia; BC Ministry of Energy, Mines and Natural Gas, Open File 1990-25, 19 p., URL <<http://www.empr.gov.bc.ca/Mining/Geoscience/PublicationsCatalogue/OpenFiles/1990/Pages/1990-25.aspx>> [November 2012].
- Höy, T. (2010): Geology of the Deer Park map area, southeastern British Columbia (NTS 082E/08); *in* Geoscience BC Summary of Activities 2009, Geoscience BC Report 2010-1, p. 127–140.
- Höy, T. and Dunne, K.P.E. (2001): Metallogeny and mineral deposits of the Nelson-Rosland area, part II: the Early Jurassic Rossland Group, southeastern British Columbia; BC Ministry of Energy, Mines and Natural Gas, Bulletin 109, 195 p., URL <<http://www.empr.gov.bc.ca/Mining/Geoscience/PublicationsCatalogue/BulletinInformation/BulletinsAfter1940/Pages/Bulletin109.aspx>> [November 2012].
- Höy, T. and Dunne, K.P.E. (2004): Geology of the Nelson map sheet, British Columbia (NTS 082F/06); BC Ministry of Energy, Mines and Natural Gas, Geoscience Map 2004-2, scale 1:50 000, URL <<http://www.empr.gov.bc.ca/Mining/Geoscience/PublicationsCatalogue/Maps/GeoscienceMaps/Pages/2004-2.aspx>> [November 2012].
- Hoy, T. and Jackaman, W. (2005): Geology of the Grand Forks map sheet, British Columbia (NTS 082E/01); BC Ministry of Energy, Mines and Natural Gas, Geoscience Map 2005-2, scale 1:50 000, URL <<http://www.empr.gov.bc.ca/Mining/Geoscience/PublicationsCatalogue/Maps/GeoscienceMaps/Pages/2005-2.aspx>> [November 2012].
- Höy, T. and Jackaman, W. (2010): Geology of the Deer Park map sheet (NTS 082E/08); Geoscience BC, Map 2010-7-1, scale 1:50 000.
- Keep, M. (1989): The geology and petrology of the Averill alkaline complex, near Grand Forks, British Columbia; M.Sc. thesis, University of British Columbia, 110 p.
- Keep, M and Russell, J.K. (1988): Geology of the Averill plutonic complex, Franklin mining camp; *in* Geological Fieldwork 1987, BC Ministry of Energy, Mines and Natural Gas, Paper 1988-1, p. 49–53.
- Kennedy, C. (2005): Assessment report, rock geochemistry program, SR Property, Trail Creek Mining Division; BC Ministry of Energy, Mines and Natural Gas, Assessment Report 27 545, 13 p., URL <http://aris.empr.gov.bc.ca/search.asp?mode=repsum&rep_no=27545> [November 2012].
- Laberge, J.R. and Pattison, D.R.M. (2007): Geology of the western margin of the Grand Forks Complex: high grade Cretaceous metamorphism followed by early Tertiary extension on the Granby fault; *Canadian Journal of Earth Sciences*, v. 44, p. 199–208.
- Little, H.W. (1957): Kettle River, east half, Similkameen, Kootenay and Osoyoos districts, British Columbia; *Geological Survey of Canada, Map 6-1957*, scale 1:253 440, URL <ftp://ftp2.cits.rncan.gc.ca/pub/geott/ess_pubs/108/108451/gscprmap_6-1957_e_1957_mn01.pdf> [November 2012].
- Little, H.W. (1960): Nelson map area, west half, British Columbia; *Geological Survey of Canada, Memoir 308*, 205 p.
- Little, H.W. (1979): Geology of the Greenwood map area, British Columbia; *Geological Survey of Canada, Paper 79-29*, 37 p.
- Massey, N.W.D. (2006): Boundary project: reassessment of Paleozoic rock units of the Greenwood area (NTS 82E/02), southern British Columbia; *in* Geological Fieldwork 2005, BC Ministry of Energy, Mines and Natural Gas, Paper 2006-1, p. 99–107, URL <<http://www.empr.gov.bc.ca/Mining/Geoscience/PublicationsCatalogue/Fieldwork/Documents/2005/Paper10.pdf>> [November 12, 2012].
- Massey, N.W.D. (2007): Boundary project: Rock Creek area (NTS 082E/02W, 03E), southern British Columbia; *in* Geological Fieldwork 2006, BC Ministry of Energy, Mines and Natural Gas, Paper 2007-1, p. 117–128, URL <<http://www.empr.gov.bc.ca/Mining/Geoscience/Publications>>

- [Catalogue/Fieldwork/Documents/12-Massey.pdf](#)> [November 12, 2012].
- Massey, N.W.D. (2010): Boundary project: geochemistry of volcanic rocks of the Wallace Formation, Beaverdell area, south-central British Columbia; *in* Geological Fieldwork 2009, BC Ministry of Energy, Mines and Natural Gas, Paper 2010-1, p. 143–152, URL <http://www.empr.gov.bc.ca/Mining/Geoscience/PublicationsCatalogue/Fieldwork/Documents/2009/12_Massey_2009.pdf> [November 12, 2012].
- Massey, N.W.D. and Duffy, A. (2008): Boundary project: McKinney Creek (NTS 82E/03) and Beaverdell (NTS 82E/06E, 07W, 10W, 11W) areas, south-central British Columbia, *in* Geological Fieldwork 2007, BC Ministry of Energy, Mines and Natural Gas, Paper 2008-1, p. 87–102, URL <http://www.empr.gov.bc.ca/Mining/Geoscience/PublicationsCatalogue/Fieldwork/Documents/11-Massey_29606.pdf> [November 12, 2012].
- Massey, N.W.D., Gabites, J.E., Mortensen, J.K. and Ullrich, T.D. (2010): Boundary project: geochronology and geochemistry of Jurassic and Eocene intrusions, southern British Columbia (NTS 082E): *in* Geological Fieldwork 2009, BC Ministry of Energy, Mines and Natural Gas, Paper 2010-1, p. 127–142, URL <http://www.empr.gov.bc.ca/Mining/Geoscience/PublicationsCatalogue/Fieldwork/Documents/2009/11_Massey_2009.pdf> November 12, 2012].
- Parrish, R.R., Carr, S.D. and Parkinson, D.L. (1988): Eocene extensional tectonics and geochronology of the southern Omineca belt, British Columbia and Washington; *Tectonics*, v. 72, p. 181–212.
- Pinsent, R.H. and Cannon, R.W. (1988): Geological, geochemical and geophysical assessment report, Platinum Blonde property, Franklin Creek area, British Columbia; BC Ministry of Energy, Mines and Natural Gas, Assessment Report 17 273, 29 p., URL <http://aris.empr.gov.bc.ca/search.asp?mode=repsum&rep_no=17273> [November 12, 2012].
- Preto, V.A. (1970): Structure and petrology of the Grand Forks Group, British Columbia; Geological Survey of Canada, Paper 69-22, 80 p.
- Tempelman-Kluit, D.J. (1989): Geology, Penticton, west of the Sixth Meridian, British Columbia; Geological Survey of Canada, Map 1736A, scale 1:250 000.
- Tempelman-Kluit, D.J. and Parkinson, D. (1986): Extension across the Okanagan crustal shear in southern British Columbia; *Geology*, v. 14, p. 318–321.
- Thompson, R.I. (2006): Evolution of the ancestral Pacific margin, southern Canadian Cordillera: insights from new geologic maps; *in* Paleozoic Evolution and Metallogeny of Pericratonic Terranes at the Ancient Pacific Margin of North America, Canadian and Alaskan Cordillera; Geological Association of Canada, Special Paper 45, p. 433–482.
- Wilkinson, W.J. (2001): Prospecting assessment report on the JJ claims, Greenwood Mining Division; BC Ministry of Energy, Mines and Natural Gas, Assessment Report 26 613, 8 p., URL <http://aris.empr.gov.bc.ca/search.asp?mode=repsum&rep_no=26613> [November 2012].

Metamorphism and Structure of the Southern Kootenay Arc and Purcell Anticlinorium, Southeastern British Columbia (Parts of NTS 082F/02, /03, /06, /07)

E.R. Webster, University of Calgary, Calgary, AB, erwebste@ucalgary.ca

D.R.M. Pattison, University of Calgary, Calgary, AB

Webster, E.R. and Pattison, D.R.M. (2013): Metamorphism and structure of the southern Kootenay Arc and Purcell Anticlinorium, southeastern British Columbia (parts of NTS 082F/02, /03, /06, /07); in Geoscience BC Summary of Activities 2012, Geoscience BC, Report 2013-1, p. 103–118.

Introduction

This paper provides a summary of preliminary metamorphic, structural and geochronological work within the region between Nelson, Salmo and Creston in southeastern British Columbia. The aim of this study is to elucidate the complex tectonothermal history of the area as a means of putting the mineral deposits in a geological context. The results presented in this report are based on two field seasons.

Regional Geology

The geologically complex region of southeastern BC between Nelson, Salmo, Creston and the Canada–United States border (Figure 1) straddles the tectonic interface between the pericratonic metasedimentary and volcanic rocks of Quesnellia (Unterschutz et al., 2002) to the west, and distal marginal rocks of the ancestral North American margin (Monger et al., 1982) to the east. This tectonic juxtaposition, and subsequent episodes of magmatism, metamorphism and deformation, occurred during Cordilleran orogenesis in a time interval spanning the Jurassic to Eocene.

The primary structural-tectonic domains in the area are the Purcell Anticlinorium, Kootenay Arc and northernmost extension of the Priest River Complex (Figure 1). The Purcell Anticlinorium is a broad, Mesozoic, northerly plunging fold with extensive exposures of rift-related sedimentary rocks of the Proterozoic Windermere and Purcell supergroups (Price, 2000). The Kootenay Arc lies to the west of the Purcell Anticlinorium and is characterized by an increase in metamorphic grade and complexity of deformation, and a decrease in stratigraphic age (Warren, 1997).

The Priest River Complex (PRC) is a metamorphic core complex situated in northern Idaho that extends northward into southern BC. During the Eocene, it was partly ex-

humed by two normal fault systems, the west-dipping eastern Newport fault and the east-dipping Purcell Trench fault (Doughty and Price, 1999). The PRC consists of Mesoproterozoic Belt-Purcell rocks metamorphosed to middle–upper amphibolite facies, Archean basement gneisses and deformed Cretaceous intrusions. The northernmost expression of the PRC is upper-amphibolite metasedimentary rocks in the footwall of the Purcell Trench fault at the latitude of Creston (Figures 1, 2; Brown et al., 1995). The deformation and metamorphism associated with the PRC appears to gradually die out to the north.

The study area is situated mainly within deformed and metamorphosed Neoproterozoic sedimentary rocks of the Windermere Supergroup (a thick sequence of sandstone and conglomerate, interbedded with pelitic and carbonate layers), which unconformably overlie rocks of the Purcell Supergroup to the east. Unconformably overlying the Windermere Supergroup in the western part of the area are early Paleozoic coarse clastic and carbonate rocks (Figure 2).

Cutting through the study area are two major Eocene normal faults: the Purcell Trench fault (PTF; Daly, 1912; Kirkham and Ellis, 1926; Anderson, 1930; Rehrig et al., 1987; Doughty and Price, 2000) and the Midge Creek fault (MCF; Figure 2; Moynihan and Pattison, in press). These faults juxtapose rocks of contrasting metamorphic grades and mica cooling ages, and are discussed in more detail below.

Intrusions

The above deformed and metamorphosed sedimentary rocks are host to numerous granitoid intrusions that range in age from Middle Jurassic to Eocene and are part of larger intrusive suites extending across southeastern BC (Ghosh, 1995). There are two distinct suites of igneous rocks in the study area: an older, Jurassic ‘hornblende-biotite’ suite, characterized by hornblende and accessory titanite, and a younger, Cretaceous ‘two mica’ suite that is characterized by muscovite, biotite and accessory allanite. In addition, there are several small, Eocene syenite stocks. The Mine, Wall and Porcupine Creek are Middle Jurassic stocks (Fig-

Keywords: metamorphism, structure, tectonics, intrusions, deformation, Priest River Complex, Kootenay Arc, Purcell Anticlinorium

This publication is also available, free of charge, as colour digital files in Adobe Acrobat® PDF format from the Geoscience BC website: <http://www.geosciencebc.com/s/DataReleases.asp>.

ure 2, Table 1) that intruded the upper Proterozoic rocks of the Windermere Supergroup during regional deformation. Typically, they are medium- to coarse-grained granodiorite with rare megacrysts of potassium feldspar. These intru-

sions contain primary hornblende and biotite, and are therefore part of the 'hornblende-biotite' suite. Uranium-lead dates on zircon fractions from the Mine and Wall stocks yielded ages of 171 and 167 Ma, respectively (Archibald et

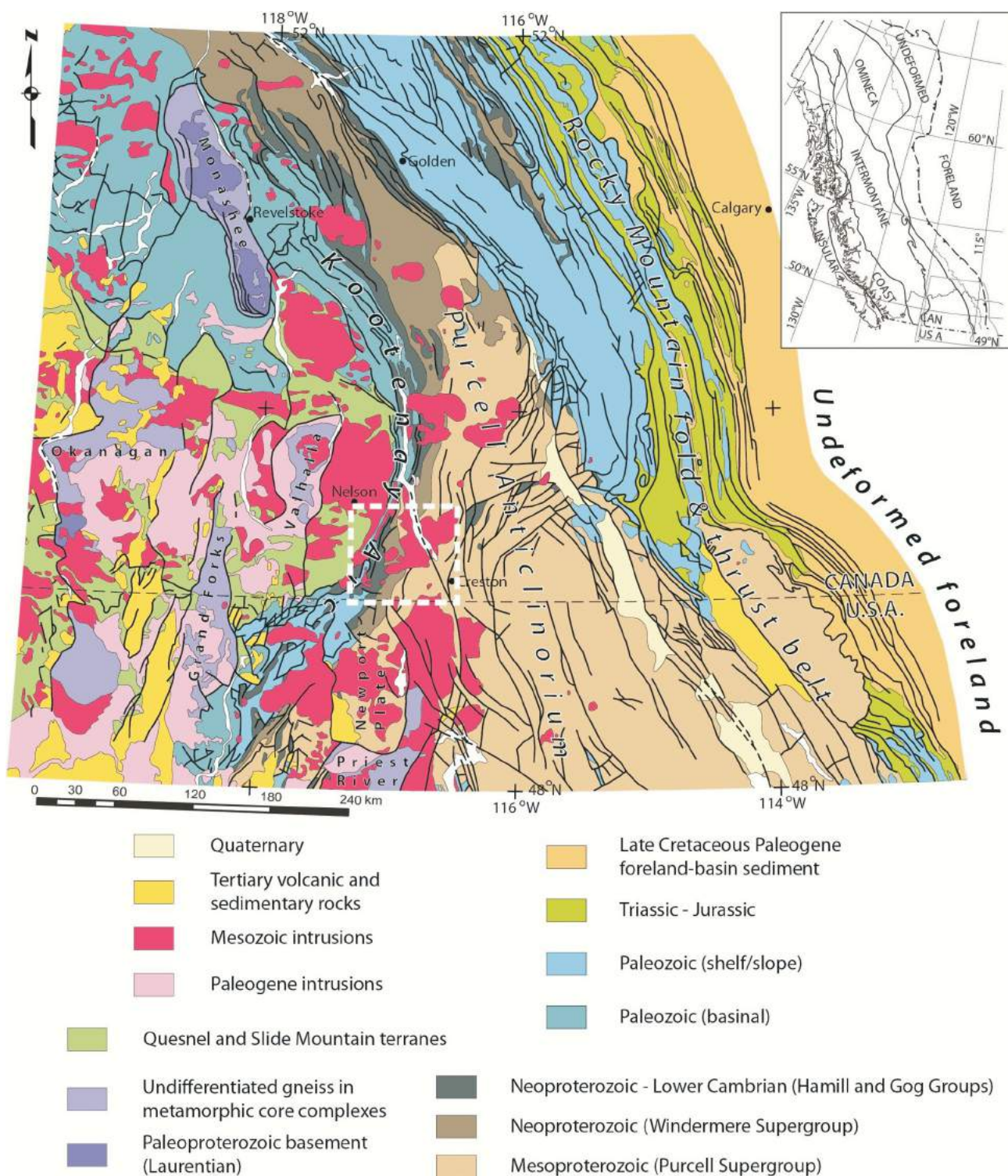


Figure 1. Regional geology of the southeastern Canadian Cordillera. Eocene core complexes are labeled on the map as Okanagan, Priest River, Grand Forks, Monashee and Valhalla. The study area is highlighted by the white dashed square. Map modified from Moynihan and Pattison (in press), originally after Wheeler and McFeely (1991).

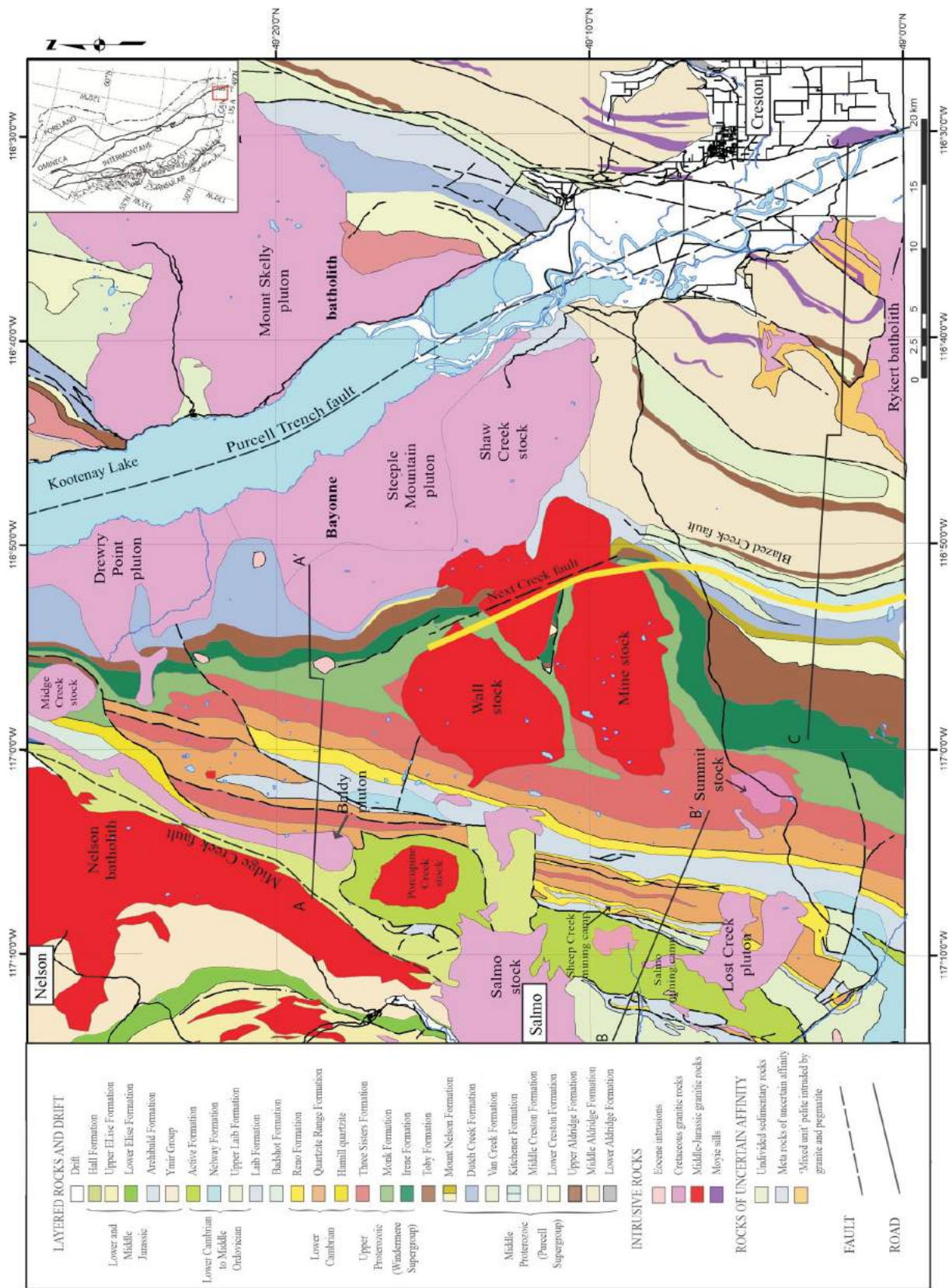


Figure 2. Regional geology of the study area, compiled from Reesor (1996), Höy and Dunne (1998), Glombick et al. (2010) and Paradis et al. (2009). The locations of the cross-sections in Figure 3 are shown. The eastern and western domains are separated by the thick yellow line. The rocks north of the Wall stock are within the northern domain. Inset modified after Wheeler and McFeely (1991).

Table 1. Summary of deformation, ages and dating methods of plutonic rocks in southeastern British Columbia.

Intrusion	Age		Dating method	Deformed	Domain	Reference
	Period	Ma				
Coryell	Eocene	52	K-Ar	No	Northern	Archibald et al., 1983
McGregor	Eocene	50	K-Ar	No	Northern	Archibald et al., 1983
Shaw Creek stock	Cretaceous	76	U-Pb	No	Eastern	Brown et al., 1999
Pegmatite, Highway 3	Cretaceous	83	U-Pb	Yes	Eastern	Brown et al., 1999
Emerald stock	Cretaceous	94	K-Ar	No	Western	Archibald et al., 1983
Rykert batholith	Cretaceous	94	U-Pb	Yes	Eastern	Brown et al., 1999
Steeple Mountain	Cretaceous	95	U-Pb	Partly	Eastern	Brown et al., 1999
Mount Skelly pluton	Cretaceous	99	K-Ar	No	Eastern	Archibald et al., 1983
Lost Creek pluton	Cretaceous	102	K-Ar	No	Western	Archibald et al., 1983
Summit stock	Cretaceous	102	K-Ar	No	Western	Archibald et al., 1983
Midge Creek stock	Cretaceous	111	U-Pb	Partly	Northern	Leclair et al., 1993
Baldy pluton	Cretaceous	117	U-Pb	Yes	Northern	Leclair et al., 1993
Corn Creek gneiss	Cretaceous	135	U-Pb	Yes	Eastern	Brown et al., 1999
West Creston gneiss	Cretaceous	135	U-Pb	Yes	Eastern	Brown et al., 1999
Porcupine Creek stock	Jurassic	157	K-Ar	?	Northern	Leech et al., 1963
Wall stock	Jurassic	167	U-Pb	Yes	Western	Archibald et al., 1983
Mine stock	Jurassic	171	U-Pb	Yes	Western	Archibald et al., 1983

al., 1983; Doughty et al., 1997). The Porcupine Creek stock has a 157 Ma K-Ar hornblende-cooling age. All three intrusions are therefore within the age range of the Nelson Suite (ca. 173–159 Ma; Ghosh, 1995; Table 1).

Cretaceous intrusions with ages of 117–73 Ma (Table 1) range in composition from diorite to granite and are typically leucocratic, medium to coarse grained and equigranular (Archibald et al., 1983). The Bayonne and Rykert batholiths are composite bodies with several phases of differing age and composition. The Bayonne batholith consists of the Mount Skelly pluton, the Shaw Creek stock and the Drewry Point and Steeple Mountain phases that range in age from 99 to 76 Ma. The Rykert batholith consists of the Search Lake, Shorty Peak, Klootch Mt., Ball Creek, Long Canyon and Hunt Creek intrusions, all of which are Cretaceous in age. The intrusive rocks in the study area are locally deformed depending on their spatial location and age (Table 1), as described in the next section. There are also two distinct suites of smaller Eocene intrusive rocks, the McGregor and the Coryell (Little, 1960). These are small, post-kinematic dikes and plugs of syenite and monzonite.

Structures

The structure of the rocks in the southern Kootenay Arc and western limb of the Purcell Anticlinorium is dominated by multiple folds from at least three periods of deformation, spanning the interval from mid-Mesozoic to Eocene (Fyles, 1964, 1967; Glover, 1978; Leclair, 1988; Brown et al., 1995). In general, there is an increase in structural complexity and intensity of deformation going from the southwestern corner of the study area to the east and north, corresponding to progressively deeper structural levels. An exception to this overall pattern is the abrupt change in the degree of deformation and metamorphism across the PTF and MCF. Due to the different episodes of deformation

throughout the study area, the structural observations have been split into western, northern and eastern domains, with initially no attempt to correlate between domains. In the following sections, the subscripts ‘W’, ‘N’ and ‘E’ will be used to refer to the western, northern and eastern domains, respectively. Relationships between structures in the different domains are discussed in a separate section.

Structural Observations—Western Domain

The earliest map-scale folds (F_{1W} : Phase 1 structures of MacDonald, 1970) in the western domain are the Laib syncline and Sheep Creek anticline, both of which are isoclinal folds that plunge from north-northeast to south-southwest and are inclined to the west (F_{1W} ; Figures 2, 3a, b). A well-developed subvertical cleavage (S_{1W}) is axial planar to the folds and is the dominant penetrative foliation (S_{1W}) in the western domain. Within semipelitic units, the cleavage (S_{1W}) is defined by chlorite, biotite and muscovite. At outcrop scale, F_{1W} folds are typically asymmetrical, upright, Z- and S-shaped isoclinal folds with an axial-planar foliation. These folds are best observed in carbonate layers of the Laib syncline and Sheep Creek anticline, as illustrated in Figure 4a. A shallowly plunging stretching lineation (L_{1W}) that parallels the fold axes is best observed in noncarbonate rocks, especially those rich in quartz and mica. A later crenulation is observed in more pelitic layers and is defined by a crinkling of the S_{1W} foliation. The fold axes of these small crenulations define a lineation (F_{2W}) that is subparallel to the trend and plunge of the F_{1W} fold axes.

Structural Observations—Northern Domain

The northern domain has a dominant, regional, north-northeast-striking structural trend that is the result of multiple periods of deformation. The deformed, metamorphosed sedimentary rocks in this domain are intruded by plutons of the Bayonne and Nelson suites (Figures 2, 3c), which helps

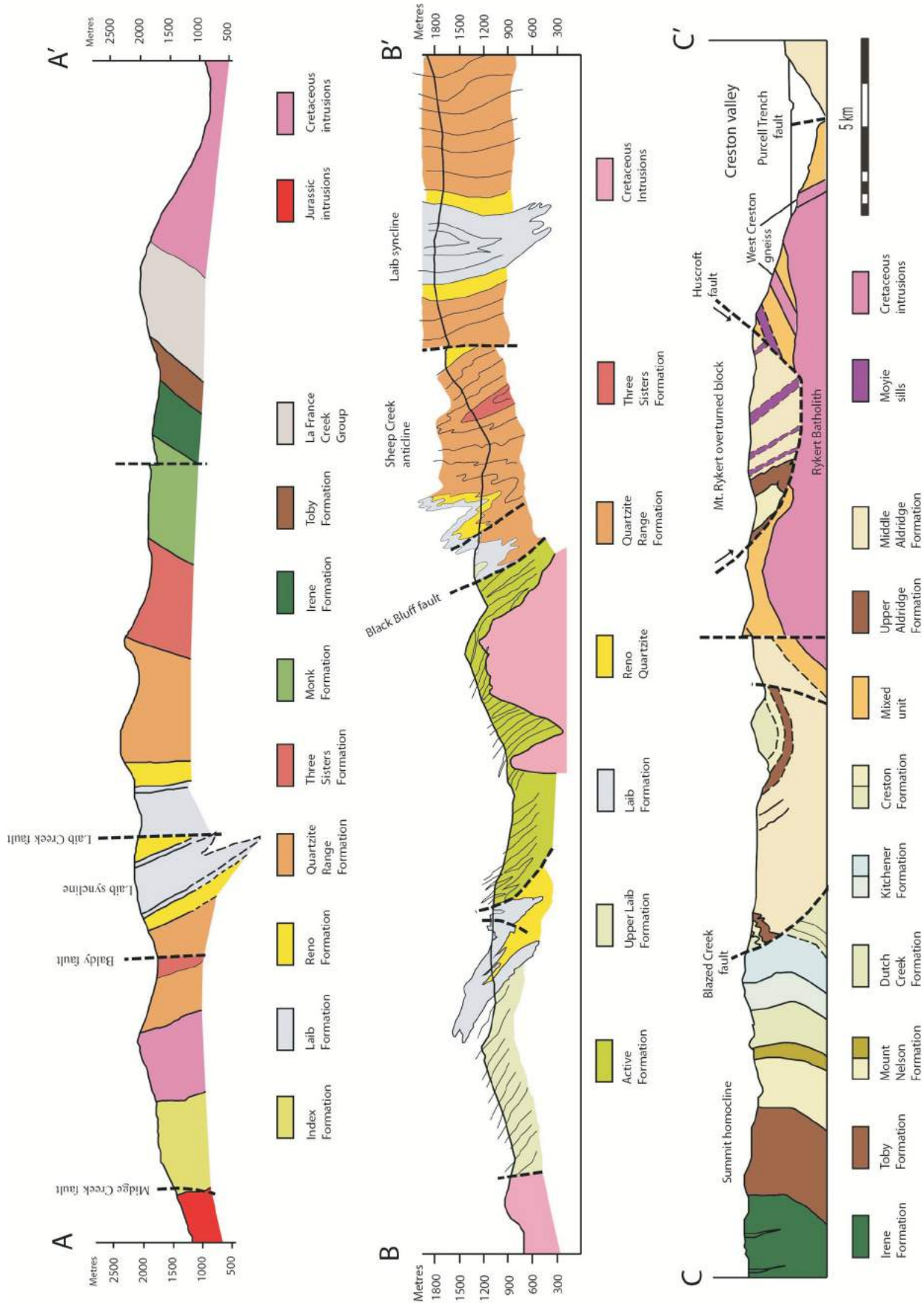


Figure 3. Vertical cross-sections from the study area. The lines of section are shown in Figure 2. Compiled from Leclair (1988 A-A'), Fyles and Hewlett (1959; B-B') and Brown et al. (1999; C-C').

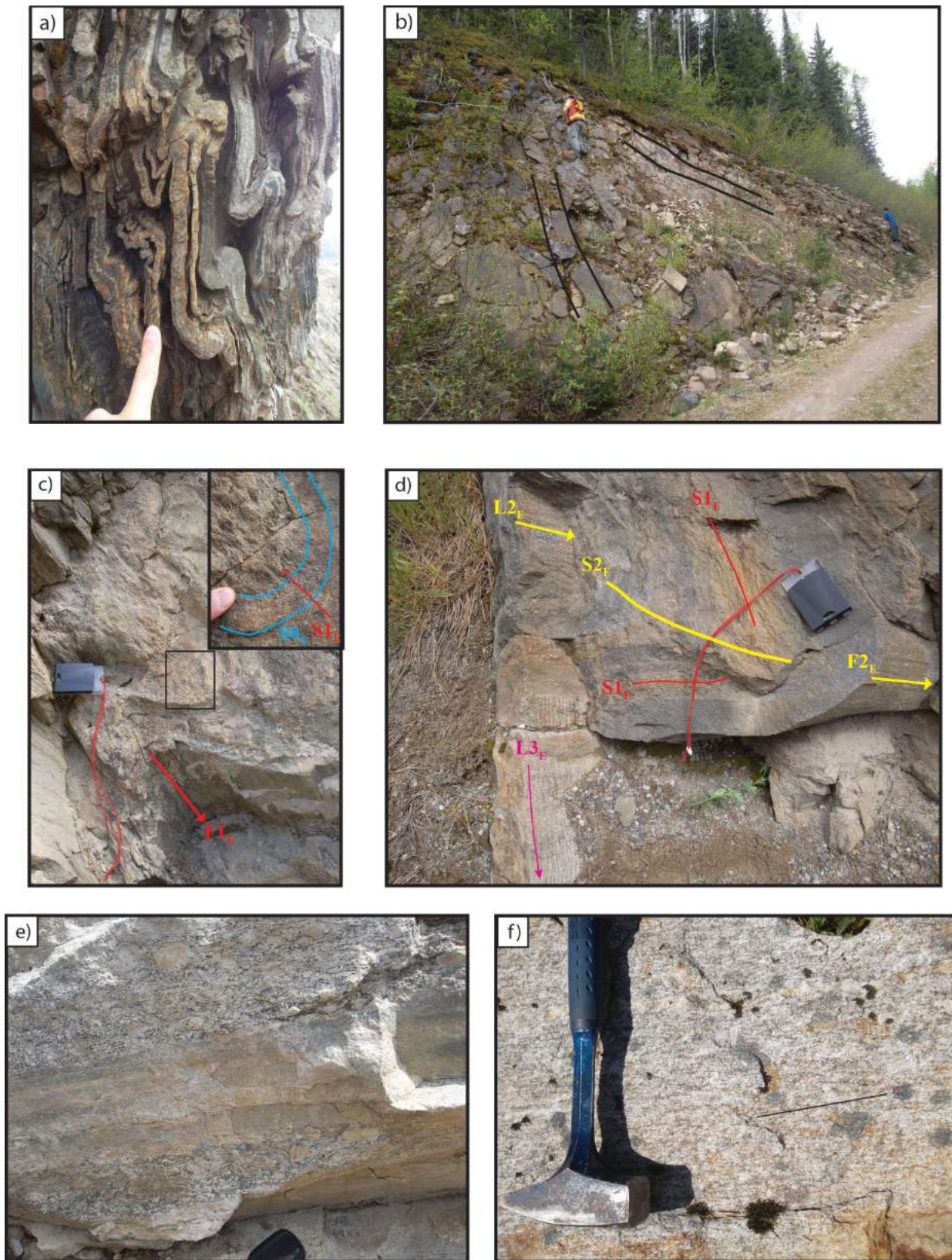


Figure 4. **a)** S-shaped F_{1W} folds in carbonate rocks of the Laib syncline. **b)** Large, inclined, outcrop-scale F_{2E} fold with a shallow northerly plunge. **c)** F_{1E} folds showing an axial-planar foliation. Inset highlights the axial-planar nature of the foliation. **d)** Gently plunging, recumbent F_{2E} fold with subhorizontal axial plane (S_{2E}). Steeply plunging crenulation lineation (L_{3E}). **e)** Example of the heterogeneous nature of the Rykert batholith with varying degrees of foliation development, mafic content and potassium feldspar megacryst size. **f)** Example of the Corn Creek gneiss with a shallowly plunging stretching lineation highlighted by the thin black line.

separate the timing of the deformation events. The dominant map-scale structures in the area are tight to isoclinal, upright to inclined, north-northeast- or south-southwest-plunging folds with subhorizontal axes (F_{1N} ; D_{1N} structures are D2 of Leclair, 1988 and Moynihan and Pattison, 2008). These folds are associated with a regionally penetrative, axial-planar cleavage (S_{1N}) that is generally subparallel to bedding (S_{0N}). The F_{1N} fold axes are parallel to a mineral and stretching lineation (L_{1N}) throughout this domain. This lineation becomes more pronounced with greater proximity to the PTF and MCF, as lower structural levels are exposed. The L_{1N} lineations are defined by rodding of quartz and feldspar in quartzite and in the Baldy pluton. Crenulations of the S_{1N} cleavage are observed in pelitic and semipelitic rocks throughout the northern domain and are locally strong enough to develop a crenulation cleavage (S_{2N}). The crenulation fold axes define a second lineation (L_{2N}) that is subparallel to the F_{1N} fold axes. A second crenulation sporadically crinkles S_{1N} at a high angle to the previous crenulation lineation (L_{2N}), defining a third lineation (L_{3N}) that trends east-northeast and plunges approximately 45° .

Structural Observations—Eastern Domain

The map pattern in the eastern domain is dominated by kilometre-scale, open to tight folds of the Belt-Purcell Supergroup (Figures 2, 3c; Brown et al., 1995). Field observations identified at least three phases of deformation in this domain. The earliest folds (F_{1E}) are upright to recumbent, isoclinal to open folds with an axial-planar schistosity (S_{1E} ; Figure 4c). The fold axes commonly have a gentle plunge to the north-northeast or south-southwest (Figure 4). A strong mineral and stretching lineation (L_{1E}) has developed in association with the F_{1E} folds. The lineation is more pronounced in pelitic units, in which micas have aligned parallel to the fold axes.

The F_{1E} folds and S_{1E} schistosity have been refolded by gently plunging, north-northeast- or south-southwest-plunging, upright to recumbent, open to tight folds (Figure 4b, d). These F_{2E} folds are the most prevalent outcrop-scale structures and form the dominant map-scale folds (Figures 2, 3c). The F_{2E} fold hinges are occasionally chevron shaped but are more commonly similar folds, with layering thickened in the hinge zone and thinned in the limbs. The axial planes to the second generation of folding generally dip moderately to the west-northwest and are locally strong enough to develop a second foliation (S_{2E}). A strong crenulation developed in conjunction with F_{2E} folds.

The D_2 structures are more pronounced at deeper structural levels in the footwall of large faults (PTF and MCF), as found by Moynihan and Pattison (2008) in the northern part of Kootenay Lake. This variation in structural intensity is also evident from east to west across the eastern domain. At

higher structural levels in the western portion of the eastern domain, F_{2E} folds are less well developed and have smaller wavelengths and amplitudes.

A third episode of deformation (D_{3E}) is observed throughout the eastern domain, manifested as a longer wavelength (centimetre-scale) crenulation and microfolding of micaeous layers. Locally, the crenulation is strong enough to develop a spaced cleavage. The fold axis of these crenulations defines a lineation with a moderate to steep plunge that is easily distinguishable from earlier structures.

Interface between Domains

The large F_{1W} folds of the Laib syncline and Sheep Creek anticline can be traced north from the western domain into the northern domain (Figures 2, 3). The same large structures observed in the west are the dominant structures found in the northern domain. The transition from higher structural levels and lower metamorphic grade in the west to deeper structural levels and higher metamorphic grade in the north appears to be gradual, occurring over several kilometres. The deepest structural levels are exposed in the footwall of the MCF and PTF (Figures 3a, 5), in which the regional metamorphic grade and intensity of deformation are highest.

The interface between the western and eastern domains is less clear. From west to east, there is a change to stratigraphically older rocks, an increase in structural complexity and an increase in metamorphic grade as the PTF is approached. Accompanying this change is a younging trend from west to east in muscovite and biotite $^{40}\text{Ar}/^{39}\text{Ar}$ cooling ages (Figure 5). The dashed yellow line on Figure 2 is an approximation of where there is a transition in cooling ages, from mid-Cretaceous (<100 Ma) to Middle Jurassic (>150 Ma). The current dataset does not have the spatial resolution to constrain the nature of the interface between the two domains. There does not appear to be any marked change in structural style or metamorphic grade where the change in cooling ages occurs. This will, however, be addressed with future petrological work.

Timing of Deformation

The age of deformation in each domain can be partly constrained by the crosscutting relationships and deformation features contained in igneous bodies of known age. In the western domain, the eastern limb of the Laib syncline is cut by the Middle Jurassic (167 Ma) Wall stock (Figure 2, Table 1), implying that the large map-scale folds (Laib syncline, Sheep Creek anticline) and associated D_{1W} are Jurassic features. Fabrics in the Mine and Wall stocks are parallel to the dominant foliation (S_{1W}) in the surrounding sedimentary rocks, indicating that D_{1W} continued to develop after the emplacement of the stocks. The same conclusions were drawn farther north in the central and northern parts of

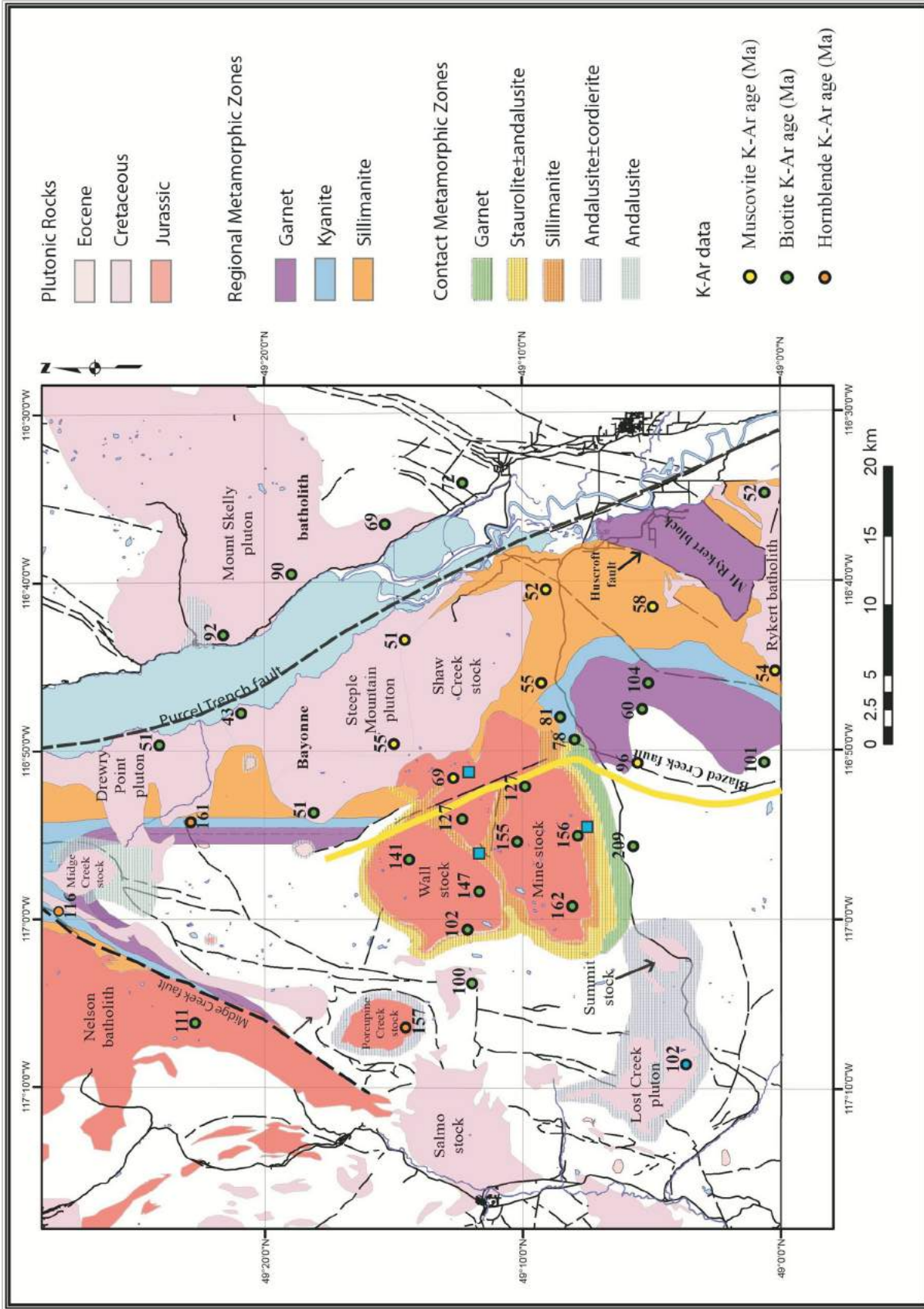


Figure 5. Metamorphic zones and plutonic rocks of the study area, compiled from Glover (1978), Archibald et al. (1983), Leclair (1988), Doughty et al. (1997) and new data. Areas with no shading are of low metamorphic grade. Blue squares are occurrences of kyanite away from the regional kyanite zone. K-Ar data compiled from Archibald et al. (1983), Leclair et al. (1993) and Glombick et al. (2010).

the Kootenay Arc (Warren, 1997). All of the deformation in the western domain has been overprinted by the contact aureole of the post-kinematic Summit stock and Lost Creek pluton (Archibald et al., 1984). Assuming the biotite-cooling age of these intrusions of 102 Ma (Table 1) is close to the emplacement age, it implies that D_{2W} deformation had ceased in the western domain by the mid-Cretaceous.

The Jurassic Sheep Creek anticline and Laib syncline can be traced north into the northern domain. The Cretaceous Baldy pluton ($117 \pm 4/-1$ Ma, U-Pb titanite; Leclair et al., 1993) is an elongate granodioritic body that is subparallel to the penetrative foliation (S_{1N}) and bedding, and is therefore interpreted to have intruded before or during D_{1N} deformation. The intrusion is foliated and has a strong mineral and stretching lineation (D_{1N}), parallel to those in the metamorphosed sedimentary rocks. This implies that the age of penetrative D_{1N} deformation in the northern domain is Cretaceous, considerably younger than the Jurassic structures in the western domain. A plausible explanation is that the earlier Jurassic structures that extend from the western to the northern domain were tightened in the northern domain during the Cretaceous. The Midge Creek stock (MCS) is a mid-Cretaceous intrusion (111 ± 4 Ma, U-Pb allanite; Leclair et al., 1993; Table 1) that crosscuts the regional structures. It is undeformed except at the northern tip (Figure 2), where the dominant foliation parallels the regional trend (Leclair, 1988). This implies that the MCS was intruded during the later stages of the penetrative deformation (D_{1N}), thus constraining the timing of D_{1N} .

The significance of the ages of the Baldy pluton and MCS is uncertain. There is no U-Pb zircon date for either of the intrusions (Leclair et al., 1993). The U-Pb dates for both of these intrusions are from titanite and allanite, and it is possible that either or both of these minerals either formed as metamorphic minerals or were reset during the Cretaceous because the ambient metamorphic temperature was above the closure temperature of these minerals (approximately 600°C). Because the age of these intrusions is critical to determining the age of the metamorphism and deformation in this area, new U-Pb analyses will be conducted.

The D_{1E} structures in the eastern domain appear to be younger than D_{1W} and D_{1N} structures in the western and northern domains. The primary evidence comes from two deformed gneissic bodies, the Corn Creek and West Creston gneisses (both 135 Ma; Table 1), and the deformed Rykert batholith (94 Ma; Brown et al., 1999; Figure 2). All three intrusions contain a penetrative, gently to moderately west-dipping mylonitic foliation and a shallow north-plunging stretching lineation. These are of the same orientation as those in the surrounding country rocks, and are therefore inferred to be younger than these igneous bodies (i.e., post ca. 94 Ma). Several deformed pegmatites occur within the schist of the Aldridge Formation along Highway 3 (Table 1). They lie

subparallel to, and are boudinaged within, S_{1W} but locally crosscut the foliation, suggesting emplacement broadly during D_{1E} . One pegmatite yielded an 81.7 ± 0.2 Ma U-Pb zircon date, interpreted to be its age of emplacement (Brown et al., 1999). The Shaw Creek stock has an emplacement age of 76 Ma (Figure 2; Brown et al., 1999) and crosscuts D_{1E} and the later D_{2E} structures. These events can therefore be constrained to the interval 94–76 Ma. The timing of D_{3E} is less well constrained and could be as young as Eocene.

In summary, the dominant deformation episodes in the three domains have different ages. The penetrative foliation and dominant folds are Middle Jurassic in the western domain, mid-Cretaceous in the northern domain and Late Cretaceous in the eastern domain. The dominant structures in all three domains have a similar north-northeast orientation, obscuring the relationships between the different periods of deformation and suggesting that earlier structures were overprinted and tightened by later structures in the northern and eastern domains. The nature of the interface between the Late Cretaceous structures in the east and the mid-Cretaceous structures in the north is not presently well understood and will be the focus of future work.

Metamorphism

The regional metamorphic grade in the study area is dominantly greenschist facies, apart from two discrete elongate domains of amphibolite-facies metamorphic rocks (Figure 5). In the northern part of the field area, the amphibolite-facies metamorphism forms a forked isograd pattern. The western fork is parallel to strike and is truncated by the Midge Creek fault. This fork is a continuation of the metamorphic high mapped north of the west arm of Kootenay Lake by Moynihan and Pattison (2008). The eastern fork transects the strike of the lithological units and is approximately parallel to the Purcell Trench fault in the northern part of the study area. This fork continues south into the United States and merges with amphibolite-facies metamorphism in the Priest River Complex. The two forks are separated by a large area of low metamorphic grade (Figure 5).

Contact aureoles have developed in proximity to a number of the intrusions and have distinct textures and mineral assemblages that make them distinguishable from the regional metamorphism. The metamorphic zones presented in this study are based on the distribution of metamorphic index minerals in pelitic rocks (Figure 5) and have been compiled from observations of this and previous studies (Glover, 1978; Archibald et al., 1983; Leclair, 1988; Doughty et al., 1997; Moynihan and Pattison, 2008).

Regional Metamorphism

Three regional amphibolite-facies metamorphic zones have been identified within the map area: garnet, kyanite and sillimanite. These metamorphic zones are typical of Barrovian metamorphism, with the highest metamorphic grade in the footwall of the PTF and MCF, and progressively lower grades with increasing distance from the fault zone. South of the Jurassic Mine and Wall stocks, the regional metamorphic zones are broad (Figure 5) but become progressively narrower to the north (Figure 5). The two belts of amphibolite-facies metamorphism converge in the vicinity of the Midge Creek stock. The map pattern shows that the regional metamorphic zones approximately parallel the PTF and MCF in the northern part of the field area but broaden and are less well defined south of the Mine and Wall stocks.

The MCF juxtaposes greenschist-facies phyllite of the Milford Group against sillimanite-zone schist in the footwall (Moynihan and Pattison, in press). There is also a large contrast in metamorphic grade across the PTF (Figure 5): pelite in the footwall has the mineral assemblage silliman-

ite±kyanite+garnet+muscovite+biotite+plagioclase+quartz+rutile, whereas pelite in the hangingwall has the assemblage biotite+muscovite+chlorite+albite+quartz (Figure 6). Based on these mineral assemblages, the contrast in peak metamorphic conditions across the fault is >2 kbar and >150°C (Figure 6).

One exception to the large temperature and pressure contrast across the PTF is an area of garnet-zone rocks in the hangingwall of the Huscroft fault (Figures 3c, 5), itself in the footwall of the PTF. These rocks are part of an overturned section of the Aldridge and Creston formations (Brown et al., 1995) and are thought to represent the overturned limb of a regional-scale fold. The upper-greenschist-facies rocks in the hangingwall of the Huscroft fault contrast with the sillimanite-zone rocks beneath the fault, implying a large amount of displacement on the fault. Because the PTF cuts the Huscroft fault, the throw on the PTF must be less than implied by the contrast in peak metamorphic assemblages across the PTF outside the Huscroft block. Further study of this matter is underway.

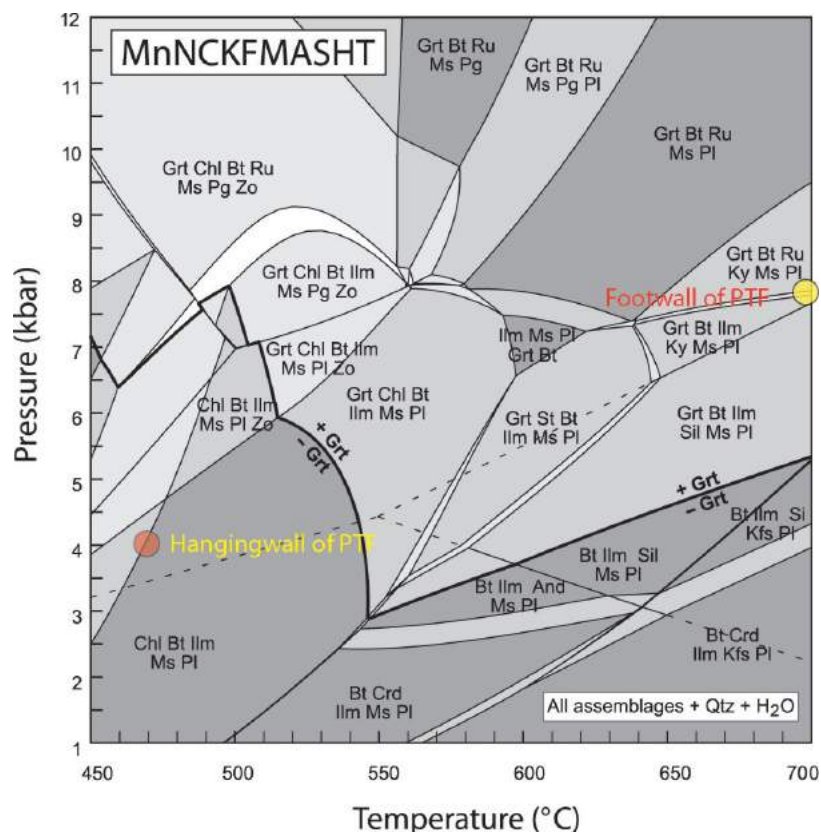


Figure 6. Section of an isochemical phase diagram for an average pelite composition from the Nelson area (modified from Pattison and Tinkham, 2009). The chemical system used to model the phase equilibria was MnNCKFMASHT (MnO-Na₂O-CaO-K₂O-FeO-MgO-Al₂O₃-SiO₂-H₂O-TiO₂, with C and P₂O₅ omitted from the whole-rock analysis, followed by projection from pyrrhotite). The yellow dot represents the stable mineral assemblage in the footwall of the PTF and the red dot represents the stable mineral assemblage in the hangingwall. Mineral abbreviations are from Kretz (1983).

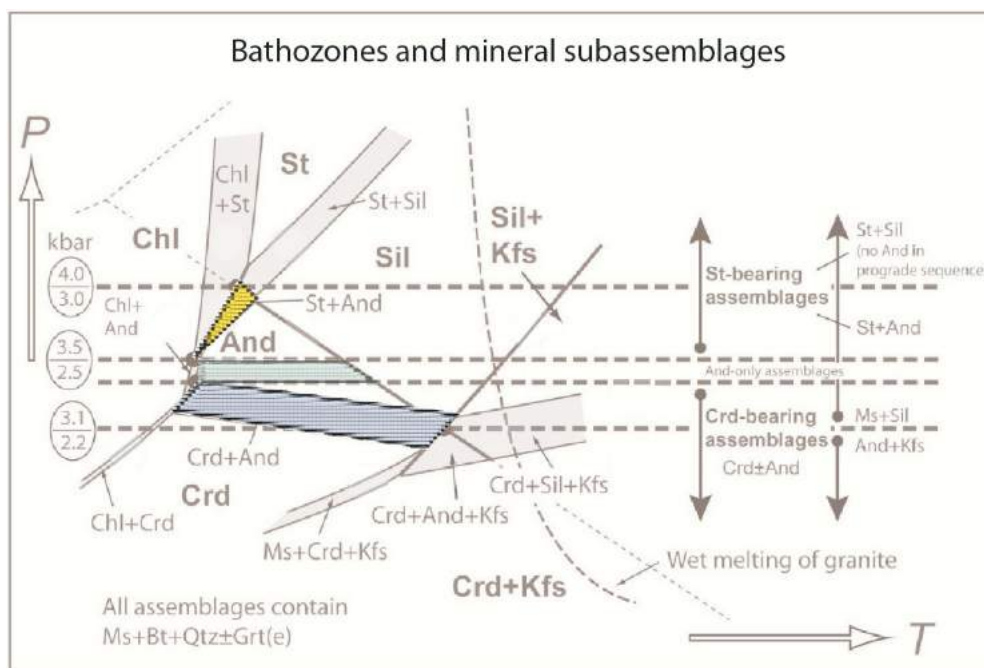


Figure 7. Schematic P-T phase diagram showing the relationship of mineral-assemblage domains to key subassemblages (modified from Pattison and Vogl, 2005). Contact aureoles from the field area are highlighted on the diagram with their corresponding colours. Yellow represents the stable mineral assemblage staurolite±andalusite and pressures of 3.5–4 kbar. Light green represents the stable mineral assemblage andalusite and pressures of 2.5–3.5 kbar. Blue represents the stable mineral assemblage cordierite+andalusite and pressures of 2.2–3.1 kbar. Mineral abbreviations are from Kretz (1983).

Contact Metamorphism

The study area has been intruded by numerous Jurassic and Cretaceous plutons (Figures 2, 5) that have imparted contact aureoles to the surrounding country rock. The contact aureole surrounding the Mine and Wall stocks is developed in regionally low-grade rocks of the Windermere Supergroup. The contact aureole is characterized by assemblages containing garnet, staurolite±andalusite and sillimanite. South of the intrusion, the contact aureole is well developed in pelitic rocks; however, along the western margin of the Mine and Wall stocks, where psammitic rocks predominate, the contact metamorphic zones are not observable. Within the contact aureole, several occurrences of kyanite have been identified that, from microstructural relations, postdate muscovite-rich pseudomorphs after andalusite (Figure 5). It is presently unclear if the kyanite is a result of contact metamorphism or later regional metamorphism; this will be the focus of future petrological work. Based on the abundant staurolite±andalusite assemblages, contact metamorphism associated with the Mine and Wall stocks occurred at 3.5–4 kbar (Figure 7, yellow domain). The Porcupine Creek stock (ca. 157 Ma, K-Ar hornblende age; Table 1) is situated 4 km northwest of the Wall stock and has a lower pressure (~3.0–3.5 kbar) contact aureole with cordierite+andalusite (Figures 5, 7), similar to the southern part of the Nelson batholith aureole (Pattison and Vogl, 2005).

The mid-Cretaceous, post-kinematic Lost Creek pluton (LCP) and Summit stock (SS; Table 1) have imparted the lower pressure contact aureoles on the surrounding low-grade country rocks. The mineral assemblage zonal sequence is cordierite, andalusite±cordierite and sillimanite±K-feldspar (Bjornson, 2012). New mapping (this study) and that of Bjornson (2012) illustrate that these metamorphic zones envelop both intrusions, with a metamorphic ‘high’ in the central domain between the two. Rocks in the contact aureole of the SS and LCP were metamorphosed at 2.2–3.2 kbar (Figure 7; Bjornson, 2012).

In summary, the Jurassic intrusions were emplaced at 3.5–4 kbar, which, for a pressure of 2.7 g/cc, corresponds to an 11–13 km emplacement depth, considerably deeper than the Cretaceous intrusions at 7–11 km. This implies approximately 5 km of aggregate exhumation between emplacement of the Jurassic intrusions and the Cretaceous intrusions.

⁴⁰K/⁴⁰Ar and ⁴⁰Ar/³⁹Ar Dating

Archibald et al. (1984) carried out a ⁴⁰K/⁴⁰Ar and ⁴⁰Ar/³⁹Ar study of the southern Kootenay Arc, including a significant part of this study area (Figure 5). They found early Paleogene cooling ages centred over the band of sillimanite-bearing rocks west of Kootenay Lake (Figures 2, 5). Older cooling ages occur across the PTF to the east and toward lower metamorphic grade to the west. The Eocene to

Cretaceous cooling ages are confined to within approximately 25 km of the PTF (Figure 5), based on the limited dataset of Archibald et al. (1983) and Brown et al. (1995). There appears to be a transition from Cretaceous to Jurassic cooling ages in the vicinity of the Blazed Creek fault, which marks approximately the boundary between the western and eastern structural domains. Mapping by Brown et al. (1995) and this study, however, found no evidence to suggest that there is a large fault in this area. Therefore, further work is planned to address the nature of the interface: fault, gradational or overprinting relationship. Little geochronological data exist for the northern part of the study area, so this area will be the focus of a further $^{40}\text{Ar}/^{39}\text{Ar}$ study.

Discussion

The observations presented above convey the complex structural, metamorphic and geochronological history of the study area, in which there are spatial variation in the grade of metamorphism, intensity of deformation and $^{40}\text{K}/^{40}\text{Ar}$ and $^{40}\text{Ar}/^{39}\text{Ar}$ cooling ages. Eocene extension and exhumation resulted in deeper structural levels, higher metamorphic grade and younger cooling ages being exposed in the footwall of the PTF and MCF. The following discussion is a preliminary synthesis of the geological history of the study area from the Middle Jurassic to the Early Eocene.

The earliest recorded metamorphism and deformation in the study area is restricted to the western domain; however, it likely affected the entire study area but was subsequently overprinted by later events. Regional peak-metamorphic conditions were attained during the Jurassic, broadly coeval with plutonism and deformation (D_{1W}). The well-developed staurolite±andalusite contact mineral assemblage developed around the Jurassic Mine and Wall stocks (Figure 5) implies emplacement depths of 11–13 km. The development of late kyanite implies either that, following the emplacement of these intrusions during the Middle Jurassic, they were deformed and buried to Barrovian metamorphic conditions, or that the kyanite developed in local bulk compositions at pressures and temperatures not significantly different from those of contact metamorphism (e.g., Pattison, 2001). Whatever interpretation is correct, these events must have occurred in the Jurassic because the igneous and metamorphic rocks in the area have Jurassic cooling ages. Following the Middle Jurassic, the western domain remained at higher structural levels while rocks at lower levels were intensely deformed and metamorphosed during the Cretaceous.

North of the west arm of Kootenay Lake, peak metamorphism and the dominant penetrative deformation has been constrained to the interval 143–124 Ma (Moynihan and Pattison, in press). The southern extension of this Early Cretaceous metamorphism and deformation is developed in the northern domain of this study area. In the northern

domain, the western flank of the amphibolite-facies metamorphism is cut by the MCF. The lower structural levels exposed in the footwall of the MCF are of much higher metamorphic grade than those in the hangingwall (Leclair et al., 1993; Moynihan and Pattison, in press). A similar trend was observed north of the study area, across the Gallagher fault (Moynihan and Pattison, 2008). Accepting the U-Pb ages for the late-synkinematic Baldy pluton and postkinematic Midge Creek stock as close to the intrusion age would support D_{1N} and peak metamorphism being mid-Cretaceous in age (Leclair et al., 1993; Moynihan and Pattison, in press).

Episodic magmatism continued through the mid-Cretaceous, with different phases of the Bayonne magmatic suite intruding the study area from approximately 100 to 76 Ma. The western domain was intruded by the postkinematic Lost Creek pluton and Summit stock ca. 102 Ma. The well-developed low-pressure cordierite+andalusite contact aureole around the intrusions constrains their emplacement level to 7–11 km depth in the crust. A similar cordierite+andalusite contact aureole can be found around the Mount Skelly pluton on the east side of Kootenay Lake, suggesting a similar emplacement level on the east side of the PTF at ca. 100 Ma.

Rocks in the amphibolite-facies metamorphic belt (Figure 5) in the eastern domain appear to have attained peak metamorphism during the Late Cretaceous, ca. 82 Ma (Brown et al., 1999). South of the Canada–United States border in the PRC, peak metamorphism occurred ca. 75 Ma (Doughty and Price, 1999). The regional metamorphic zones depicted on the west side of the PTF in Figure 5 suggest the presence of a continuous band of amphibolite-facies metamorphism from northern Idaho to the northern end of Kootenay Lake. However, there must be an interface between Early Cretaceous (ca. 145–125 Ma) amphibolite-facies metamorphism in the northern half of Kootenay Lake (Moynihan and Pattison, in press) and in the northern part of the study area, and Late Cretaceous amphibolite-facies metamorphism (ca. 94–76 Ma) extending from south of the border into the southern part of the study area. An 81.7 ± 0.2 Ma U-Pb monazite age, interpreted to be a metamorphic age in contrast to the 135 Ma zircon age from the Corn Creek gneiss (Brown et al., 1999), suggests that the Late Cretaceous metamorphism extends at least to the latitude of Creston. Future U-Pb monazite dating is planned to better constrain the interface between the two periods of metamorphism.

The Rykert batholith, the Corn Creek and West Creston gneisses (Table 1) and an 82 Ma pegmatite are deformed by the dominant penetrative foliation and lineation in the eastern domain, implying that D_{1E} is also Late Cretaceous, coeval with peak metamorphism. This area also experienced a strong D_{2E} deformation event, before the emplacement of

the Shaw Creek stock at 76 Ma, and a weak D_{3E} event, the timing of which is currently not well constrained. The area was then exhumed to higher structural levels in the early Eocene. This contrasts with what is observed in the west, where (D_{2W}) deformation had completely ceased prior to the emplacement of the LCP and SS, ca. 102 Ma. The nature of the boundary between the different structural, metamorphic and cooling histories of the eastern and western domains is unclear and will be the focus of future work.

During the early Eocene, Cretaceous amphibolite-facies metamorphism and deeper structural levels were exposed in the footwalls of the PTF and MCF. Although there is a significant difference in peak pressure and temperature across the PTF and MCF (Figure 6), caution must be exercised in attributing all of the contrast in peak P-T conditions to low-temperature movement along the PTF in the Eocene. Recent studies have shown that the displacement on large Eocene normal faults may be significantly less than previously thought (Gordon et al., 2008; Simony and Carr, 2011; Cubley and Pattison, in press), due to a two-stage exhumation process in which high-temperature exhumation is followed by low-temperature exhumation on the normal faults.

The Mt. Rykert block of lower grade metamorphic rocks, situated within the footwall of the PTF (Figure 5; Brown et al., 1995), is thought to be analogous to the Newport plate (Figure 1), within the Newport Fault system, south of the Canada–United States border (Doughty and Price, 2000). The lower grade domain of the Mt. Rykert block is probably an extensional klippe, riding on the original low-angle detachment (Figure 3), that was stranded when the steeper PTF developed (T. Doughty, pers. comm., 2012).

Mineral Deposits

A better understanding of the structural, magmatic, metamorphic and fluid events in the area allows for a more complete understanding of the genesis of mineral deposits in the area. The past-producing Pb-Zn and Mo-W deposits of the Salmo camp and the Au-Ag vein deposits of the Sheep Creek camp are situated within the western domain of the study area. The Pb-Zn deposits are carbonate-hosted, stratabound and stratiform lenticular concentrations that have been isoclinally folded (Paradis, 2007). Based on the observations of this study, the authors interpret these structures to be Jurassic D_{1W} structures.

A 50–75 km wide arcuate belt of Cretaceous intrusions, known as the Bayonne magmatic suite, extends from the Canada–United States border to north of Quesnel Lake, crosscutting through the study area. The Bayonne magmatic suite has been associated with Sn, W, W-Mo, U and Ag-Pb-Zn-Au deposits (Logan, 2002). The type of deposit varies depending on the emplacement depth of the intrusion (Lang and Baker, 2001). Relatively undeformed mid-Cre-

taceous intrusions that were emplaced at relatively shallow, higher structural levels are found throughout the western domain. These are host to the Mo-W mineralization in the Salmo camp, which the authors interpret to have overprinted the older Pb-Zn mineralization. Future work will be conducted to further elucidate on the source of their relationships.

Acknowledgments

This work was funded by a 2011 Geoscience BC grant to Pattison and Webster (1022684) and by Natural Sciences and Engineering Research Council (NSERC) Discovery Grant 037233 to Pattison. D. Moynihan, T. Doughty and S. Paradis provided insightful reviews that improved this paper. Thanks to J. Bjornson and C. Richardson for their excellent field assistance, and to B. Hamilton, J. Cubley, W. Matthews and P. Starr for additional help.

References

- Anderson, A.L. (1930): Geology and ore deposits of the Clark Fork district; Idaho Bureau of Mines and Geology, Bulletin 12, 132 p.
- Archibald, D.A., Glover, J.K., Price, R.A., Farrar, E. and Carmichael, D.M. (1983): Geochronology and tectonic implications of magmatism and metamorphism, southern Kootenay Arc and neighbouring regions, southeastern British Columbia, part 1: Jurassic to mid-Cretaceous; Canadian Journal of Earth Sciences, v. 20, no. 12, p. 1891–1913.
- Archibald, D.A., Krogh, T.E., Armstrong, R.L. and Farrar, E. (1984): Geochronology and tectonic implications of magmatism and metamorphism, southern Kootenay Arc and neighbouring regions, southeastern British Columbia, part 2: mid-Cretaceous to Eocene; Canadian Journal of Earth Sciences, v. 21, no. 5, p. 567–583.
- Bjornson, J. (2012): Contact metamorphism around the Lost Creek pluton and Summit Creek stock in the Summit Creek map area, southeastern British Columbia; B.Sc. thesis, University of Calgary, 66 p.
- Brown, D.A., Doughty, T.P., Glover, J.K., Archibald, D.A., David, D.W. and Pattison, D.R.M. (1999): Field trip guide and road log: Purcell Anticlinorium to the Kootenay Arc, southeastern British Columbia, Highway 3—Creston to Summit Pass and northern Priest River Complex, west of Creston; BC Ministry of Energy, Mines and Natural Gas, Information Circular 1999-2.
- Brown, D.A., Doughty, T.P. and Stinson, P. (1995): Geology and mineral occurrences of the Creston map area (82F/2); BC Ministry of Energy, Mines and Natural Gas, Open File 1995-15, 2 p., 1 map at 1:50 000 scale, URL <<http://www.empr.gov.bc.ca/Mining/Geoscience/PublicationsCatalogue/OpenFiles/1995/Documents/OF1995-15.pdf>> [November 13, 2012].
- Cubley, J.F. and Pattison, D.R.M. (in press): Metamorphism and exhumation of the Grand Forks Complex, southeastern British Columbia; Canadian Journal of Earth Sciences.
- Daly, R.A. (1912): Geology of the North American Cordillera at the 49th parallel; Geological Survey of Canada, Memoir 38, 856 p. and 17 maps at 1:63 360 scale.

- Doughty, P.T. and Price, R.A. (1999): Tectonic evolution of the Priest River Complex, northern Idaho and Washington: a re-appraisal of the Newport fault with new insights on metamorphic core complex formation; *Tectonics*, v. 18, p. 375–393.
- Doughty, P.T. and Price, R.A. (2000): Geology of the Purcell Trench rift valley and Sandpoint conglomerate: Eocene en échelon normal faulting and synrift sedimentation along the eastern flank of the Priest River metamorphic complex, northern Idaho; *Geological Society of America Bulletin*, v. 112, no. 9, p. 1356–1374.
- Doughty, P.T., Brown, D.A. and Archibald, D.A. (1997): Metamorphism of the Creston map area, southeastern British Columbia (82F/2); BC Ministry of Energy, Mines and Natural Gas, Open File 1997-5, 14 p. and 1 map at 1:50 000 scale, URL <<http://www.empr.gov.bc.ca/Mining/Geoscience/PublicationsCatalogue/OpenFiles/1997/Documents/OF1997-5.pdf>> [November 13, 2012].
- Fyles, J.T. and Hewlett, C.G. (1959): Stratigraphy and structure of the Salmo lead-zinc area; BC Ministry of Energy, Mines and Natural Gas, Bulletin 41, 162 p., URL <http://www.empr.gov.bc.ca/Mining/Geoscience/PublicationsCatalogue/BulletinInformation/BulletinsAfter1940/Documents/Bulletin_041.pdf> [November 13, 2012].
- Fyles, J.T. (1964): Geology of the Duncan Lake area, Lardeau District, British Columbia; BC Ministry of Mines, Energy and Natural Gas, Bulletin 49, 87 p., URL <<http://www.empr.gov.bc.ca/Mining/Geoscience/PublicationsCatalogue/BulletinInformation/BulletinsAfter1940/Pages/Bulletin49.aspx>> [November 13, 2012].
- Fyles, J.T. (1967): Geology of the Ainsworth-Kaslo area, British Columbia; BC Ministry of Energy, Mines and Natural Gas, Bulletin 53, 125 p., URL <<http://www.empr.gov.bc.ca/Mining/Geoscience/PublicationsCatalogue/BulletinInformation/BulletinsAfter1940/Pages/Bulletin53.aspx>> [November 13, 2012].
- Ghosh, D.K. (1995): U-Pb geochronology of Jurassic to early Tertiary granitic intrusives from the Nelson-Castlegar area, southeastern British Columbia, Canada; *Canadian Journal of Earth Sciences*, v. 32, no. 10, p. 1668–1680.
- Glombick, P., Brown, D.A. and MacLeod, R.F., compilers (2010): Geology, Creston, British Columbia; Geological Survey of Canada, Open File 6152, scale 1:50 000, URL <ftp://ftp2.cits.rncan.gc.ca/pub/geott/ess_pubs/261/261631/gscof_6152_e_2010_mn01.pdf> [November 13, 2012]. doi:10.4095/288925
- Glover, J.K. (1978): Geology of the Summit Creek area, southern Kootenay Arc, British Columbia; Ph.D. thesis, Queen's University, 144 p.
- Gordon, S.M., Whitney, D.L., Teyssier, C., Grove, M. and Dunlap, W.J. (2008): Timescales of migmatization, melt crystallization, and cooling in a Cordilleran gneiss dome: Valhalla complex, southeastern British Columbia; *Tectonics*, v. 27, p. 1–28.
- Höy, T. and Dunne, P.E.K. (1998): Geological compilation of the Trail map area, southeastern British Columbia (082F/3, 4, 5, 6); BC Ministry of Energy, Mines and Natural Gas, Geoscience Map 1998-1, scale 1:100 000, URL <<http://www.empr.gov.bc.ca/Mining/Geoscience/PublicationsCatalogue/Maps/GeoscienceMaps/Documents/GM1998-1-Trail.pdf>> [November 13, 2012].
- Kirkham, V.D. and Ellis, E.W. (1926): Geology and ore deposits of Boundary County, Idaho; Idaho Bureau of Mines and Geology, Bulletin 10, 78 p.
- Kretz, R. (1983): Symbols for rock-forming minerals; *American Mineralogist*, v. 68, p. 277–279.
- Lang, J.R. and Baker, T. (2001): Intrusion-related gold systems: the present level of understanding; *Mineralium Deposita*, v. 36, no. 6, p. 477–489.
- Leclair, A.D. (1988): Polyphase structural and metamorphic histories of the Midge Creek area, southeast British Columbia: implications for tectonic processes in the central Kootenay Arc; Ph.D. thesis, Queen's University, 264 p.
- Leclair, A.D., Parrish, R.R. and Archibald, D.A. (1993): Evidence for Cretaceous deformation in the Kootenay Arc on U-Pb and ⁴⁰Ar/³⁹Ar dating, southeastern British Columbia; *in* Current Research, Part A, Geological Survey of Canada, Paper 93-1A, p. 207–220.
- Leech, G.B., Lowdon, J.A., Stockwell, C.H. and Wanless, R.K. (1963): Age determinations and geological studies; Geological Survey of Canada, Paper 63-17, 140 p.
- Little, H.W. (1960): Nelson map-area, west half, British Columbia; Geological Survey of Canada, Memoir 308, 205 p.
- Logan, J.M. (2002): Intrusion-related gold mineral occurrences of the Bayonne magmatic belt; *in* Geological Fieldwork 2001, BC Ministry of Energy, Mines and Natural Gas, Paper 2002-1, p. 237–246, URL <<http://www.empr.gov.bc.ca/Mining/Geoscience/PublicationsCatalogue/Fieldwork/Documents/2001/17-JL-p237-246.pdf>> [November 13, 2012].
- MacDonald, A.S. (1970): Structural environment of the Salmo type lead-zinc deposits; State of Washington Department of Natural Resources, Division of Mines and Geology, Bulletin 61, p. 59–64.
- Miller, F.K. and Engels, J.C. (1975): Distribution and trends of discordant ages of plutonic rocks of northeastern Washington and northern Idaho; *Geological Society of America Bulletin*, v. 86, p. 517–528.
- Monger, J.W.H., Price, R.A. and Templeman-Kluit, D.J. (1982): Tectonic accretion and the origin of the two major metamorphic and plutonic belts in the Canadian Cordillera; *Geology*, v. 10, p. 70–75.
- Moynihan, D.P. and Pattison, D.R.M. (2008): Origin of the Kootenay Lake metamorphic high, southeastern British Columbia; *in* Geological Fieldwork 2007, Geoscience BC, Report 2008-1, p. 147–158, URL <<http://www.empr.gov.bc.ca/Mining/Geoscience/PublicationsCatalogue/Fieldwork/Documents/15-Moynihan14616.pdf>> [November 13, 2012].
- Moynihan, D.P. and Pattison, D.R.M. (in press): The Kootenay Lake metamorphic high: Early Cretaceous Barrovian metamorphism and Tertiary normal faulting in the central Kootenay Arc, southeastern British Columbia; *Canadian Journal of Earth Sciences*.
- Paradis, S. (2007): Carbonate-hosted Zn-Pb deposits in southern British Columbia—potential for Irish-type deposits; Geological Survey of Canada, Current Research 2007-A10, 7 p., URL <ftp://ftp2.cits.rncan.gc.ca/pub/geott/ess_pubs/224/224161/cr_2007_a10.pdf> [November 13, 2012]. doi:10.4095/224161
- Paradis, S., MacLeod, R.F. and Emperingham, R., compilers (2009): Bedrock geology, Salmo, British Columbia; Geological Survey of Canada, Open File 6048, scale 1:50 000, URL <ftp://ftp2.cits.rncan.gc.ca/pub/geott/ess_pubs/247/>

- [247443/gscof_6048_e_2009_mn01.pdf](#) [November 13, 2012]. doi:10.4095/247443
- Parrish, R.R., Carr, S.D. and Parkinson, D.L. (1988): Eocene extensional tectonics and geochronology of the southern Omineca belt, British Columbia and Washington; *Tectonics*, v. 7, no. 2, p. 181–212.
- Pattison, D.R.M. (2001): Instability of Al₂SiO₅ ‘triple point’ assemblages in muscovite+biotite+quartz-bearing metapelites, with implications; *American Mineralogist*, v. 86, p. 1414–1422.
- Pattison, D.R.M. and Tinkham, D.L. (2009): Interplay between equilibrium and kinetics in metamorphism of pelites in the Nelson aureole, British Columbia; *Journal of Metamorphic Geology*, v. 27, p. 249–279.
- Pattison, D.R.M. and Vogl, J.J. (2005): Contrasting sequences of metapelitic mineral-assemblages in the aureole of the tilted Nelson batholith, British Columbia: implications for phase equilibria and pressure determination in andalusite-sillimanite type settings; *Canadian Mineralogist*, v. 43, p. 51–88.
- Price, R.A. (2000): The southern Canadian Rockies: evolution of a foreland fold and thrust belt; Geological Association of Canada–Mineralogical Association of Canada, Joint Annual Meeting (GeoCanada 2000), Field Trip Guidebook 13, 246 p.
- Reesor, J.E. (1996): Geology, Kootenay Lake, British Columbia; Geological Survey of Canada, Map 1864A, scale 1:100 000, URL <ftp://ftp2.cits.nrcan.gc.ca/pub/geott/ess_pubs/207/207805/gscmap-a_1864a_e_1996_mg01.pdf> [November 13, 2012]. doi:10.4095/207805
- Rehrig, W.A., Reynolds, S.J. and Armstrong, R.L. (1987): A tectonic and geochronologic overview of the Priest River crystalline complex, northeastern Washington and northern Idaho; *in* Selected Papers on the Geology of Washington, J.E. Schuster (ed.), Washington Division of Geology and Earth Resources, Bulletin 77, p. 1–14.
- Simony, P.S. and Carr, S.D. (2011): Cretaceous to Eocene evolution of the southeastern Canadian Cordillera: continuity of Rocky Mountain thrust systems with zones of ‘in sequence’ mid-crustal flow; *Journal of Structural Geology*, v. 19, no. 6, p. 769–784.
- Unterschutz, J.L.E., Creaser, R.A., Erdmer, P., Thompson, R.I. and Daughtry, K.L. (2002): North American margin origin of Quesnel terrane strata in the southern Canadian Cordillera: inferences from geochemical and Nd isotopic characteristics of Triassic metasedimentary rocks; *Geological Society of America Bulletin*, v. 114, no. 4, p. 462–475.
- Warren, M.J. (1997): Crustal extension and subsequent crustal thickening along the Cordilleran margin of ancestral North America, western Purcell Mountains, southeastern British Columbia; Ph.D. thesis, Queen’s University, 361 p.
- Wheeler, J.O. and McFeely, P. (1991): Tectonic assemblage map of the Canadian Cordillera and adjacent parts of the United States of America; Geological Survey of Canada, Map 1712A, scale 1:2 000 000, URL <<http://geoscan.ess.nrcan.gc.ca/cgi-bin/starfinder/0?path=geoscan.download.fl&id=fastlink&pass=&format=FLDOWNLOAD&search=R=133549>> [November 13, 2012]. doi:10.4095/133549

The SEEK Project: Stimulating Exploration in the East Kootenays, Southeastern British Columbia (Parts of NTS 082F, G, J, K)

R.P. Hartlaub, Department of Mining and Mineral Exploration, British Columbia Institute of Technology, Burnaby, BC, Russell_hartlaub@bcit.ca

Hartlaub, R.P. (2013): The SEEK Project: Stimulating Exploration in the East Kootenays, southeastern British Columbia (parts of NTS 082F, G, J, K); in Geoscience BC Summary of Activities 2012, Geoscience BC, Report 2013-1, p.119-124.

Introduction

Geoscience BC, in partnership with the East Kootenay Chamber of Mines (EKCM), announced the launch of the SEEK (Stimulating Exploration in the East Kootenays) Project in November 2011. The goal of the SEEK Project is to increase economic activity related to mineral exploration in the Purcell Basin by acquiring, compiling and adding value to public and private sector mineral exploration information. The East Kootenay area in southeastern British Columbia has a long and successful history of mineral exploration and mining. The former Sullivan mine alone represented \$43 billion of production and sustained the economy of Kimberley and the East Kootenay area for almost 100 years.

A working group, composed of EKCM members and Geoscience BC staff, identified several main project activities, within the larger SEEK Project, focusing on the Purcell Basin (known as the Belt Basin in the United States; Figure 1). The first activity aims to categorize and add value to existing discoveries. This includes compiling the knowledge of local prospectors and exploration geologists, identifying high-interest mineral occurrences, and adding geological information that is not presently in the public record. A second activity focuses on the acquisition and dissemination of high value, historical, private sector, mineral exploration information, such as maps, core and core logs, and geochemical databases. To this end, Geoscience BC contributed funding to help support the development of a new EKCM core library. A third activity includes the acquisition, compilation and dissemination of public and private geophysical data. The final activity is the promotion of the mineral potential of the East Kootenay area. In particular, there is a need to highlight the key deposit types in the region and link up with current mineral exploration knowledge from the American side of the border. This paper reviews the geology and mineral potential of the East

Keywords: Purcell Basin, East Kootenay, SEDEX, Sullivan, Aldridge Formation, sediment-hosted copper, core library, MINFILE, geophysics, gravity

This publication is also available, free of charge, as colour digital files in Adobe Acrobat® PDF format from the Geoscience BC website: <http://www.geosciencebc.com/s/DataReleases.asp>.

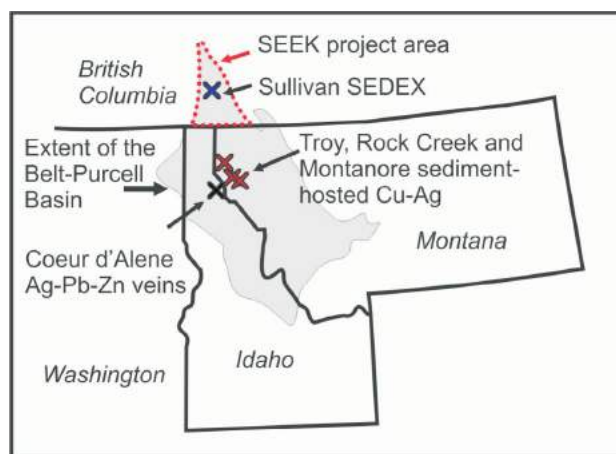


Figure 1. Approximate extent of the exposed Belt-Purcell Basin in British Columbia, Montana, Idaho and Washington (Purcell Basin in Canada and the Belt Basin in the United States). The locations of major mining areas discussed in the text are also included. Abbreviations: SEDEX, sedimentary exhalative; SEEK, Stimulating Exploration in the East Kootenays.

Kootenay area and highlights some results from the first year of the SEEK Project.

Regional Geology of the Purcell Basin

The seminal report by Höy (1993) provides a structural and stratigraphic framework for the Purcell Basin in southeastern BC. The oldest rocks of the Purcell Supergroup are exposed along the core and western margin of a north-northeast-trending large-scale anticlinorium. Regional compression during the Jurassic–Early Cretaceous and again during the Late Cretaceous–Paleocene transported the basin to the east and northeast (Price and Sears, 2000). The base of the Canadian portion of the basin, south and east of Cranbrook, contains ‘rift-fill’ turbidite rocks up to 12 km thick (Lydon, 2007). These turbidites make up the Aldridge Formation in Canada and the Prichard Formation in the United States. These turbidites are cut by the Moyie sills, a voluminous series of mafic intrusive rocks. These mafic magmas are believed to be syndepositional to the Aldridge Formation, and have a U-Pb crystallization age of 1468 ± 2 Ma (Anderson and Davis, 1995).

Overlying the Aldridge Formation, the Creston Formation (Ravalli Group in the United States) represents the begin-

ning of the upper shallow-water ‘rift-cover’ sequence. The Kitchener Formation is a distinctive horizon of carbonate rocks, which include oolitic limestone and dolomitic siltstone (Höy, 1993), and has been correlated with the Wallace, Empire and Helena formations in the United States (Winston, 1986). A recent study by Gardner and Johnston (2007) refined the stratigraphy of the upper Purcell Supergroup, those rocks lying above the Kitchener Formation. Maroon to green siltstone and argillite of the Van Creek Formation predates eruption of flood basalts of the Nicol Creek Formation, which have been indirectly dated at 1443 ± 7 Ma (Evans et al., 2000). An erosional unconformity locally separates the Nicol Creek Formation from overlying coarse clastic and stromatolitic carbonate rocks of the Sheppard Formation. The Sheppard Formation is, in turn, overlain in the northern Purcell Basin by shallow-water, fine-grained clastic rocks of the Dutch Creek, Gateway, Phillips and Roosville formations (Gardner and Johnston, 2007).

Metallogeny and Mineral Potential of Belt-Purcell Basin

The East Kootenays have a rich exploration history that is centred on the world class Sullivan Pb-Zn sedimentary exhalative (SEDEX) deposit (Figure 1). The Sullivan mine operated for nearly 100 years and exploration in the East Kootenay area has generally focused on discovering another SEDEX deposit in equivalent rocks. Whereas SEDEX mineralization remains an attractive exploration target, precious metal veins, sediment-hosted Cu and intrusion related porphyry or iron oxide copper gold (IOCG)-type deposits have recently gained more attention.

SEDEX Zn-Pb

The ‘rift-fill’ rocks of the Aldridge Formation host the Sullivan SEDEX Zn-Pb deposit and readers are directed to the wealth of information available on the subject (e.g., Lydon, 2000). The SEDEX deposit formed by deposition of sulphides on, or just below, the sea floor from hydrothermal fluids that were $>250^{\circ}\text{C}$ (Lydon, 2007). Tourmalinites and fragmental sedimentary bodies within the Aldridge Formation (Prichard Formation in the United States) are believed to represent the conduits and eruption breccias of mud volcanoes (Anderson and Höy, 2000). A study of BC MINFILE (BC Geological Survey, 2012) entries for strata of the Purcell Basin indicates that the Aldridge Formation has the largest number of showings, prospects and developed prospects. This is clearly related to the high mineral potential of these rocks and the clear focus on SEDEX mineral exploration. In 2012, an active SEDEX drill exploration program was carried out on the Findlay property through a MMG Limited joint venture with Eagle Plains Resources Ltd.

Precious Metal Veins (Ag-Pb-Zn and Au)

The largest economic concentration of Ag-Pb-Zn vein systems in the Belt-Purcell Basin lie within the Coeur d’Alene Mining District in Idaho (Figure 1). Mineralization is found as galena-sphalerite-tetrahedrite with variable amounts of quartz, carbonate, barite and/or iron oxides. In the Coeur d’Alene Mining District, Pb-Zn-rich veins formed during the Proterozoic, but the economically more important Ag-rich veins formed during the Cretaceous (Fleck et al., 2002). In BC, Pb-Zn-rich veins are Proterozoic and occur within the Aldridge Formation, and Ag-rich veins are Mesozoic and cut all units of the Purcell Basin (Païement et al., 2007). The St. Eugene deposit is the largest known Ag-Pb-Zn vein deposit on the Canadian side of the border (Joncas and Beaudoin, 2002). The discovery of boulders with massive sulphide galena during a field trip south of Cranbrook in 2012 is a testament to the potential for additional discoveries (Figure 2). In addition to Ag-Pb-Zn, numerous vein- and sediment-hosted Au occurrences also lie within the East Kootenay area. Recent exploration has focused on the ‘Kimberly gold trend’ near Cranbrook. Notable occurrences west of Cranbrook include the Zinger, Eddy and Dewdney trail properties of PJX Resources Inc. Major Pb-Zn, Ag-Pb-Zn and Au trends in the Purcell Basin are thought to be inherited from original Precambrian basement structures (McMechan, 2012).

Sediment-Hosted Cu Mineralization

The siliciclastic sedimentary rocks of the Belt-Purcell Basin were deposited in a relatively rapid period (Evans et al., 2000) leading to the formation of numerous sediment-hosted stratabound Cu-Ag occurrences in the quartzite-dominated Revett Formation (Creston Formation in BC; Hayes and Einaudi, 1986; Boleneus et al., 2005). These deposits, including the Troy, Rock Creek and Montanore, are all located in western Montana (Figure 1); however, evi-



Figure 2. A boulder of massive sulphide galena newly discovered in 2012 at the Spikes Great Adventure property, south of Cranbrook, British Columbia.

dence for sediment-hosted Cu mineralization has recently been identified in southeastern BC (Hartlaub, 2009; Hartlaub et al., 2011). Deposits in the Revett Formation can be viewed as their own subtype since the known deposits are hosted in quartz-rich sandstone. Unlike the redbed deposits, however, a reductant in the form of pyritic sandbodies, or possibly hydrocarbon fluids, is believed to have localized Cu and Ag mineralization (Boleneus et al., 2005; T. Hayes, pers. comm., 2008).

Intrusion-Related Mineral Occurrences

The Butte area of southwestern Montana is a major Cretaceous porphyry-epithermal-style polymetallic Cu district within the Belt-Purcell Basin. Cretaceous intrusions on the Canadian side of the border include the Reade Lake and Kiakho stocks (Höy, 1993), but significant porphyry-style mineralization has not been identified in this area. Cretaceous alkaline K-feldspar porphyritic plutons, termed the Howell Creek suite, occur along the eastern side of the Belt-Purcell Basin. These small hypabyssal and intrusive bodies are associated with low-grade, disseminated Au mineralization (Barnes, 2002). A 105.0 ± 2.5 Ma K-feldspar porphyritic syenite associated with polymetallic sediment-hosted mineralization occurs at Sheep Mountain, just west of Cranbrook (Hartlaub et al., 2011).

A significant number of Cu-polymetallic occurrences associated with mafic sills and dikes are found within the Cranbrook area. A large proportion of these showings occur where Moyie sills cut the middle Aldridge Formation. The Moyie sills have been interpreted to be roughly syndepositional, with crystallization occurring prior to lithification of the surrounding sediments (Höy, 1993). Although the Moyie sills are a voluminous component of the Aldridge Formation, there are a significant number of mafic sills and dikes that cut the Creston, Kitchener and Van Creek formations. These dikes have been postulated to be feeders to flood basalts of the Nicol Creek Formation. The King occurrence, located 8 km north of Cranbrook, is of particular interest. At this site, a number of roughly northeast-striking gabbroic intrusions cut carbonaceous fine-grained clastic rocks of the Kitchener Formation.

IOCG

Iron oxide breccia in the Iron Range, north of Creston, has been identified as a probable host of IOCG-type mineralization in the Belt-Purcell Basin (Galicki et al., 2012). Hematite-magnetite±chalcopyrite mineralization occurs along the Proterozoic Iron Range fault within the Aldridge Formation. In 2009, Eagle Plains Resources Ltd. reported a 7 m intercept grading 51.5 g/t (1.5 oz/ton) Au from the area (Eagle Plains Resources Ltd., 2009). Paleomagnetic age data support a possible linkage (Galicki et al., 2012) to intrusion-related mineralization of the mid-Cretaceous Bayonne plutonic suite (Logan, 2002).

The Idaho cobalt belt in southern Idaho has also been interpreted as possible IOCG-type mineralization based on the occurrence of high rare earth element (REE) and Y concentrations (Slack, 2006), although this belt has also been interpreted as an exhalative horizon (Nold, 1990). This belt is at least 64 km long and up to 10 km wide, centred on the Blackbird mine. In the Blackbird Mining District of Idaho, Co-Cu-Au deposits occur within banded siltite of the Mesoproterozoic Apple Creek Formation (Slack, 2006). At least 18 Co-Cu-Au deposits in this area are associated with metamorphosed mafic tuffs or volcanoclastic rocks, and typically occur within tourmaline-bearing chemical sediments (Nash and Hahn, 1989).

SEEK Project Activities and Deliverables 2011–2012

SEEK Project activities in 2011–2012 included

- providing support towards the establishment of a new EKCM core library,
- re-examining the MINFILE database and methods of collecting historical geoscience data, and
- completion of a ground geophysical gravity data compilation for the East Kootenay area.

The EKCM core library is being developed to archive a selection of historically important core from the region. The initial focus of this library is to collect, restore and catalogue core from the Sullivan SEDEX deposit and surrounding area. The contents of this library will be made available to individuals, companies and research institutions. Those engaging in mineral exploration in the area will be able to examine type sections of both mineralized and nonmineralized strata of the Purcell Basin (Figures 3, 4). Additional work will aim to maximize the effectiveness of this library by better identifying and documenting the location, orientation, quality and geological features of important core samples.



Figure 3. Core from the Sullivan deposit that will be organized and moved to the new East Kootenay Chamber of Mines core storage facility, southeastern British Columbia.



Figure 4. View of the new East Kootenay Chamber of Mines core storage facility, southeastern British Columbia. Core from the Sullivan Deeps and Vulcan projects have already been moved to the site. Older Sullivan deposit core boxes will require much more painstaking work to ensure the integrity and proper organization of the core prior to transport.

One of the key priorities of the SEEK Project is to compile the knowledge of local prospectors and exploration geologists, and identify high-interest mineral occurrences. An initial meeting with the BC Geological Survey (BCGS) was organized to discuss how to update the MINFILE database for the Purcell Basin. The SEEK Project team has decided to work with the BCGS and EKCM to publicize and help facilitate updates to the MINFILE Mineral Inventory for the East Kootenay area. In 2013, individuals and companies who are currently working in the East Kootenay area will be called upon to contribute to this project.

Compilation of historical geophysical data may prove to be one of the most challenging aspects of the SEEK Project. Ground geophysical gravity data has been demonstrated to be an excellent tool for the targeting of a variety of mineral deposit types. A project led by T. Sanders is focused on bringing together all of the existing ground gravity information into a single database. To do this, data from more than 2800 unique ground gravity stations are being compiled and reprocessed. This includes data from more than 25 publicly available assessment reports from the East Kootenay area, as well as pre-existing Geological Survey of Canada data. The database is designed so that future datasets can easily be added. The database, and a report detailing processing methods, was released on the Geoscience BC website in late 2012. A proposal to add new ground gravity survey stations to this database has been presented to Geoscience BC and is under consideration.

Acknowledgments

All funding for the SEEK Project has been provided by Geoscience BC. C. Kennedy and S. Kennedy are thanked for organizing an East Kootenay field trip. Constructive

and timely reviews of this paper were provided by R. Tafti and C. Sluggett.

References

- Anderson, H.E. and Davis, D.W. (1995): U-Pb geochronology of the Moyie sills, Purcell Supergroup, southeastern British Columbia: implications for the Mesoproterozoic geological history of the Purcell (Belt) Basin; *Canadian Journal of Earth Sciences*, v. 32, p. 1180–1193.
- Anderson, D. and Höy, T. (2000): Fragmental sedimentary rocks of the Aldridge Formation, Purcell Supergroup, British Columbia; *in* The Geological Environment of the Sullivan Deposit, British Columbia, J.W. Lydon, T. Höy, J.F. Slack and M. Knapp (ed.), Geological Association of Canada, Mineral Deposits Division, Special Publication No. 1, p. 259–271.
- Barnes, E.M. (2002): The Howell Creek suite, southeastern British Columbia: mid Cretaceous alkali intrusions and related gold deposition in the Canadian Cordillera; M.Sc. thesis, University of Alberta, 103 p.
- BC Geological Survey (2012): MINFILE BC mineral deposits database; BC Ministry of Energy, Mines and Natural Gas, URL <<http://minfile.ca/>> [September 2012].
- Boleneus, D.E., Appelgate, L.M., Stewart, J.H. and Zientek, M.L. (2005): Stratabound copper-silver deposits of the Mesoproterozoic Revett Formation, Montana and Idaho; United States Geological Survey, Scientific Investigations Report 2005–5231, 66 p.
- Eagle Plains Resources Ltd. (2009): Eagle Plains drills intersect high-grade gold at Iron Range; Eagle Plains Resources Ltd., press release, April 20, 2009, URL <http://www.eagleplains.bc.ca/news/09.04.20.EPL_drills_high_grade_gold_ironrange.asp> [November 2012].
- Evans, K.V., Aleinikoff, J.N., Obradovich, J.D. and Fanning, C.M. (2000): SHRIMP U-Pb geochronology of volcanic rocks, Belt Supergroup, western Montana: evidence for rapid deposition of sedimentary strata; *Canadian Journal of Earth Sciences*, v. 37, p. 1287–1300.
- Fleck, R.J., Criss, R.E., Eaton, G.F., Cleland, R.W., Wavra, C.S. and Bond, W.D. (2002): Age and origin of base and precious metal veins of the Coeur d'Alene Mining District, Idaho; *Economic Geology and the Bulletin of the Society of Economic Geologists*, v. 97, p. 23–42.
- Galicki, M., Marshall, D., Staples, R., Thorkelson, D., Downie, C., Gallagher, C., Enkin, R. and Davis, W. (2012): Iron oxide±Cu±Au deposits in the Iron Range, Purcell Basin, southeastern British Columbia; *Economic Geology*, v. 107, p. 1293–1301.
- Gardner, D.W. and Johnston, S.T. (2007): Sedimentology, correlation, and depositional environment of the upper Purcell Supergroup, northern Purcell Basin, southeastern British Columbia; Geological Survey of Canada, Current Research 2007-A6, 13 p.
- Hartlaub, R.P. (2009): Sediment-hosted stratabound copper-silver-cobalt potential of the Creston Formation, Purcell Supergroup, south-eastern British Columbia (parts of NTS 082G/03, /04, /05, /06, /12); *in* Geoscience BC Summary of Activities 2008, Geoscience BC, Report 2009-1, p. 123–132.
- Hartlaub, R.P., Davis, W.J. and Dunn, C.E. (2011): The characteristics, origin and exploration potential for sediment-hosted

- Cu±Ag mineralization in the Purcell Supergroup, Canada; Geoscience BC, Report 2011-16, 28 p.
- Hayes, T.S. and Einaudi, M.T. (1986): Genesis of the Spar Lake strata-bound copper-silver deposit, Montana: part I, controls inherited from sedimentation and pre-ore diagenesis; *Economic Geology*, v. 81, p. 1899–1931.
- Höy, T. (1993): Geology of the Purcell Supergroup in the Fernie west-half map area, southeastern British Columbia; BC Ministry of Energy, Mines and Natural Gas, Bulletin 84, 157 p.
- Joncas, I. and Beaudoin, G. (2002): The St. Eugene deposit, British Columbia: a metamorphosed Ag-Pb-Zn vein in Proterozoic Belt-Purcell rocks; *The Bulletin of the Society of Economic Geologists*, v. 97, p. 11–22.
- Logan, J.M. (2002): Intrusion-related gold mineral occurrences of the Bayonne Magmatic Belt; *in Geological Fieldwork 2001*, BC Ministry of Energy, Mines and Natural Gas, Paper 2002-1, p. 237–246.
- Lydon, J.W. (2000): A synopsis of the current understanding of the geological environment of the Sullivan deposit; *in The Geological Environment of the Sullivan Deposit*, British Columbia, J.W. Lydon, T. Höy, J.F. Slack and M. Knapp (ed.), Geological Association of Canada, Mineral Deposits Division, Special Publication No. 1, p. 12–31.
- Lydon, J.W. (2007): Geology and metallogeny of the Belt-Purcell Basin; *in Mineral Deposits of Canada: A Synthesis of Major Deposit Types, District Metallogeny, the Evolution of Geological Provinces and Exploration Methods*, W.D. Goodfellow (ed.), Geological Association of Canada, Mineral Deposits Division, Special Publication No. 5, p. 581–607.
- McMechan, M.E. (2012): Deep transverse basement structural control of mineral systems in the southeastern Canadian Cordillera; *Canadian Journal of Earth Sciences*, v. 49, p. 693–708.
- Nash, J.T. and Hahn, G.A. (1989): Stratabound Co-Cu deposits and mafic volcanoclastic rocks in the Blackbird Mining District, Lemhi County, Idaho; *in Sediment-Hosted Stratiform Copper Deposits*, R.W. Boyle, A.C. Brown, C.W. Jefferson, E.C. Jowett and R.V. Kirkham (ed.), Geological Association of Canada, Special Paper 36, p. 339–356.
- Nold, J.L. (1990): The Idaho cobalt belt, northwestern United States—a metamorphosed Proterozoic exhalative ore district; *Mineralium Deposita*, v. 25, p. 163–168.
- Paiement, J.-P., Beaudoin, G. and Paradis, S. (2007): Geological setting of Ag-Pb-Zn veins in the Purcell Basin, British Columbia; *Geological Survey of Canada, Current Research 2007-A4*, 10 p.
- Price, R.A. and Sears, J.W. (2000): A preliminary palinspastic map of the Mesoproterozoic Belt-Purcell Supergroup, Canada and USA: implications for the tectonic setting and structural evolution of the Purcell anticlinorium and the Sullivan deposit; *in The Geological Environment of the Sullivan Deposit*, British Columbia, J.W. Lydon, T. Höy, J.F. Slack and M.E. Knapp (ed.), Geological Association of Canada, Mineral Deposits Division, Special Publication No. 1, p. 61–81.
- Slack, J.F. (2006): High REE and Y concentrations in Co-Cu-Au ores of the Blackbird District, Idaho; *Economic Geology*, v. 101, p. 275–280.
- Winston, D. (1986): Stratigraphic correlation and nomenclature of the Middle Proterozoic Belt Supergroup, Montana, Idaho, and Washington; *in Belt Supergroup: A Guide to Proterozoic Rocks of Western Montana and Adjacent Areas*, Montana Bureau of Mines and Geology, Special Publication 94, p. 69–84.

Documentation and Assessment of Exploration Activities Generated by Geoscience BC Data Publications

S.A. Reichheld, Consultant, Sooke, BC, sa.reichheld@gmail.com

Reichheld, S.A. (2013): Documentation and assessment of exploration activities generated by Geoscience BC data publications; in Geoscience BC Summary of Activities 2012, Geoscience BC, Report 2013-1, p. 125–130.

Introduction

In 2007, Geoscience BC launched the QUEST (QUesnellia Exploration STrategy) Project in central British Columbia (Figure 1). It was aimed at stimulating exploration interest and investment in an underexplored region between Williams Lake and the District Municipality of Mackenzie, and to help diversify local forestry-based economies impacted by the mountain pine beetle infestation. Presently in its eighth year of operation as an industry-led, publicly funded organization, Geoscience BC is trying to track how successful it has been in positively impacting its target zones in early projects. The QUEST Project with its years of data is felt to be mature enough that it can now serve as the focus of an effective study of Geoscience BC's impacts in that region and by extension its potential effectiveness elsewhere in BC.

The purpose of this preliminary summary report is to lay out a framework for reviewing and/or assessing the impact of any public exploration initiative by synthesizing various information streams as they become available. Identifying which metrics to use and what timeframes to study are difficult to pin down, but in order to ensure that the methodology will be repeatable in the future, this study will use public sources of information.

At a grassroots level, the business of exploration, discovery and development is subject to reporting delays, confidentiality delays, commodity price fluctuations and other complications. The mine cycle of prospecting and exploration, discovery and advanced exploration, development and production, and finally reclamation, can easily take decades. As an initial study, this project will look past singular short-term gauges of success, such as mineral title acquisition, and look deeper into the temporal development of exploration opportunities, the impact of follow-up compilation studies funded by Geoscience BC and the effect the

Keywords: QUEST Project, mineral exploration, grassroots, public funding, assessment report, MINFILE, investment capital, data release

This publication is also available, free of charge, as colour digital files in Adobe Acrobat® PDF format from the Geoscience BC website: <http://www.geosciencebc.com/s/DataReleases.asp>.

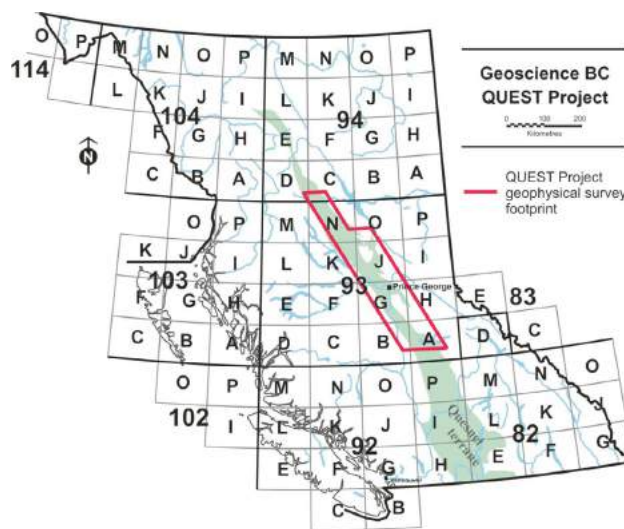


Figure 1. Location of Geoscience BC's QUEST (QUesnellia Exploration STrategy) Project geophysical survey footprint, central British Columbia. The Quesnel terrane, which was the focus of the project, is shaded in greenish-blue.

organization has had in attracting investment capital for private companies.

Geoscience BC QUEST Project

In May of 2007, Geoscience BC declared its intention to fund the QUEST Project, Geoscience BC's first major initiative since it was founded in 2005. Partnered with the Northern Development Initiative Trust, the QUEST Project was described initially as "... a \$5 million program of new geoscience data collection and compilation designed to stimulate exploration interest and investment in BC's interior, specifically in the highly prospective Quesnel Terrane, where the bedrock is obscured by glacial cover." (Anglin, 2008). The project activities originally consisted of geophysical surveys using airborne electromagnetic (EM) and airborne gravity techniques (Geotech Limited, 2008; Sander Geophysics Limited, 2008), geochemical sampling (Jackaman, 2008b) and reanalysis of archived samples (Jackaman, 2008a). Releasing the raw data throughout the following year (2008), Geoscience BC went a step further and funded a number of follow-up value-added projects, which were released in 2009 and 2010 as case studies that could serve as tools for the exploration community. These

included a case study of the Mount Milligan deposit using a z-axis tipper electromagnetic (ZTEM) and aeromagnetic survey (Geotech Limited, 2009), modelling of the various geophysical datasets (Phillips et al., 2009), a compilation and assessment of all available geochemical data (Barnett and Williams, 2009; Fraser and Hodgkinson, 2009), and review and revisions of BC Geological Survey (BCGS) Property File and MINFILE (Barlow et al., 2010; Owsiaci and Payie, 2010). As a result, companies have enjoyed a multi-year stream of announcements, field programs, data releases and added-value projects to help facilitate their efforts to raise capital, develop properties and create lasting connections with local communities.

Methodology

This preliminary paper is being drafted to ensure that all appropriate guidelines for documenting and reporting are considered, deemed beneficial and synthesized into a succinct, repeatable method. To create a quantifiable database summarizing the extent of development in exploration targets within the study area, the strengths and limitations of different reporting variables, such as land staking, assessment reports, press releases and company reports, will be examined. This is important in evaluating the actual or eventual impact of the QUEST Project since the progress of exploration targets can quickly become murky as companies change ownership, engage in joint ventures, adjust land inventory, shift focus to other properties or change exploration ideologies. As an initial study parameter, the research area will be bounded by the QUEST Project geophysical survey footprint (Figure 1) in order to test the value of a variety of parameters and ideas. For the final paper, the study area will be expanded to cover the greater QUEST project area, encompassing all geophysical, geochemical and value-added projects.

Acquiring data from public government-managed databases, private institutional reports and public company reports is subject to several time lags. The primary source of information will be assessment reports (BC Geological Survey, 2012a) which are, according to the Mines Act, technical assessment reports pertaining to geological, geophysical, geochemical, drilling and prospecting investigations. A qualified professional must compile the report for each property and it may be submitted for credit within the anniversary year of the actual fieldwork and, importantly for this project, will remain under confidential status for a period of one year from the date of the submission. As a result, there are significant time delays between fieldwork and public access to the data; e.g., an exploration project in the summer of 2011 may not become publicly available until 2013. Assessment reports include a number of important pieces of information for the purpose of this project, including location, previous work, key personnel, type of exploration, breakdown of expenditures and recommendations

for the future. Considering reporting and confidentiality restraints, this project will examine staking beginning after the initial announcement of the QUEST Project (May 14, 2007; Geoscience BC, 2007) and all available assessment reports published until the end of the 2010 calendar year.

A second source of information, in conjunction with assessment reports, are mineral titles from the government-run Mineral Titles Online (MTO; BC Geological Survey, 2012b). Mineral titles can be filed under one of three types, coal, mineral or placer, and as the bulk of research projects in the QUEST Project area have focused on the discovery of bedrock mineralization, only tenures classified as mineral will be used. Mineral titles and the total area of ground staked are important as revenue generators for the province, as indicators of interest in an area, and sources of information on who is staking land, which tenures are being renewed or held in inventory, and which areas have been transferred, shared or dropped.

The provincial mineral inventory database, MINFILE (BC Geological Survey, 2012c), is another publicly available source of geological, economic and exploration data used by industry for exploration strategies, geoscience research and resource potential. Recent attention has been given to updating MINFILE for the QUEST Project area (Owsiaci and Payie, 2010) and is another source that may be used for temporal investigations.

The cycle of announcement, fieldwork, data release and follow-up release is an important indicator of market responsiveness to Geoscience BC's efforts to encourage and stimulate industry growth, and when tied into ground staking, it is possible to see initially what information had the greatest impact, which companies took the most interest, which areas have maintained momentum and which areas have changed hands or seen little development.

Focusing on physical activities on the ground and development of exploration targets may be the major factor in determining long-term success in fostering a diversified economic community for central BC, but other factors need to be considered. A company's ability to generate investment capital each year is of fundamental importance and successfully tapping into capital markets depends on investor confidence, global economic developments, commodity price fluctuations, foreign competition and even shifts in interest to new areas. A review of company profiles, including share offerings, market prices and stock promotion, can provide a relative indication of continued investor interest in central BC. For publicly listed companies, the equity markets may be a good barometer of how well Geoscience BC projects attract follow-on development. Accelerated share trading in the stock markets may pinpoint heightened interest and presage a coming period of growth and expansion in the company's target area.

Results

The staking of new claims before and after the start of the QUEST Project is an example of an activity that can potentially show the impact of the project. In the QUEST Project geophysical survey footprint, the area of new claims staked (on previously unstaked or lapsed tenure ground) totalled 543 199 ha in 2006, this total rose to 1 307 126 ha in 2007 (BC Geological Survey, 2012b). Such increases in activity may be due to a combination of pre-emptive staking, online claim jumping, claim flipping, ground inventorying and new exploration targets; however, the size of the increase is suggestive and calls for further analysis. When filtering the numbers to include only those new claims with reports of work done on them and correlating them to important QUEST Project public releases, large spikes become evident (Figure 2). Total land tenure is an important aspect of provincial revenue in BC as the cost per hectare for new claims (throughout this time period) has been \$0.40/ha/year, increasing to \$4/ha/year and \$8/ha/year in subsequent years as the tenure is continually renewed. A practice of allowing a claim to lapse and immediately re-staking it was noticeable in some instances and needs consideration when examining the actual new land staked per year (Figure 3). While total land staked is valuable, it is the amount of land being explored and developed that will account for long-term benefits for BC.

For the reporting period after May 14, 2007 until the end of the 2010 calendar year, there were 294 assessment reports submitted on ground within the QUEST Project geophysical survey footprint (Figure 4). Fully 125 of these assessment reports were submitted by 37 unique operators on new ground staked by 44 unique owners. Of these tenure permits, 16 were joint ventures. Total reported expenditures for a range of exploration activities on new ground totalled \$5,139,335.36 for the May 14, 2007 to December 31, 2010 period. The relationship between tenure owner and operator was one of three combinations: one owner and operator, joint ventures with two owner-operators or independent owner and independent operator.

Categories of claim operator rise in scale from independent prospector up to major mining company and while some operating costs were covered by personal or private investments, the bulk of investments undoubtedly came from publicly reported channels (primary or secondary markets). Examples can be found in the mainstream media relating the QUEST Project to investment capital fundraising. An examination of available data should provide a reasonable ballpark of total dollars raised by operators for the QUEST Project area. Success in raising capital can be included in a discussion of the impact of the QUEST Project as well as provide estimates of company spending power and future activity within the region.

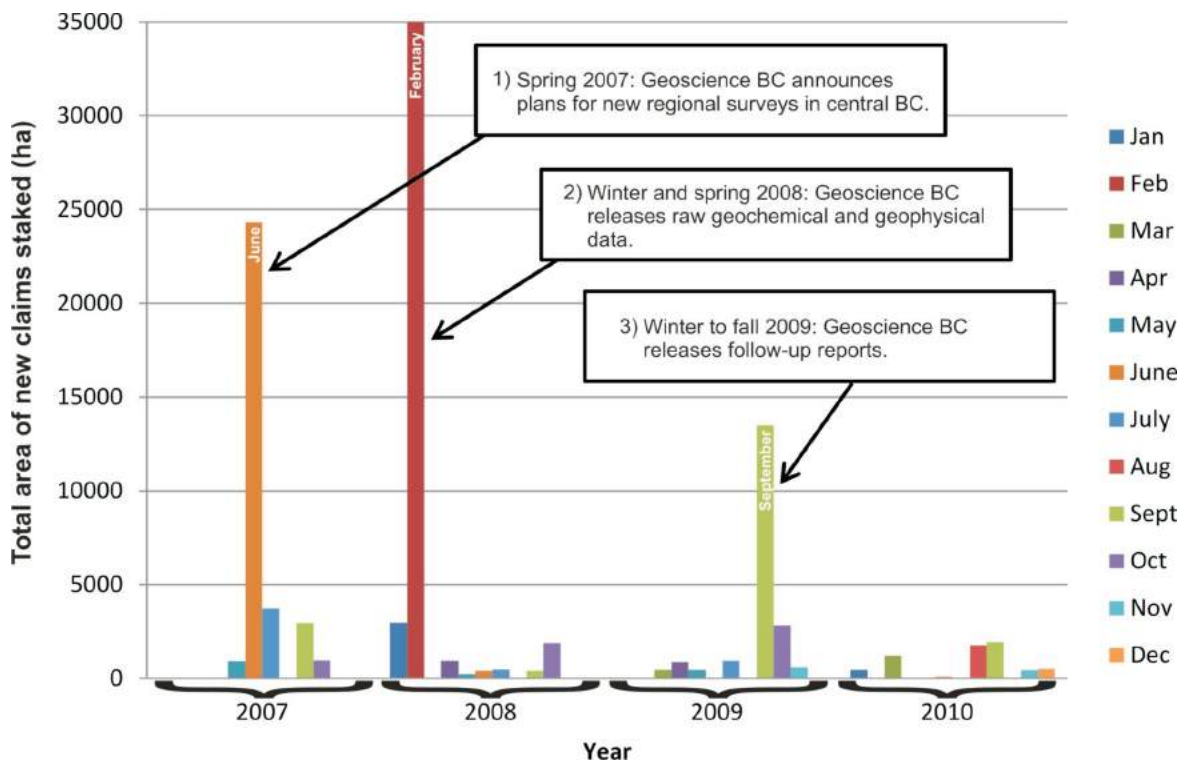


Figure 2. The number of new claims, within the QUEST Project geophysical survey footprint (central British Columbia), with reports of work done on them and the correlation to important QUEST Project public releases, 2007–2010.

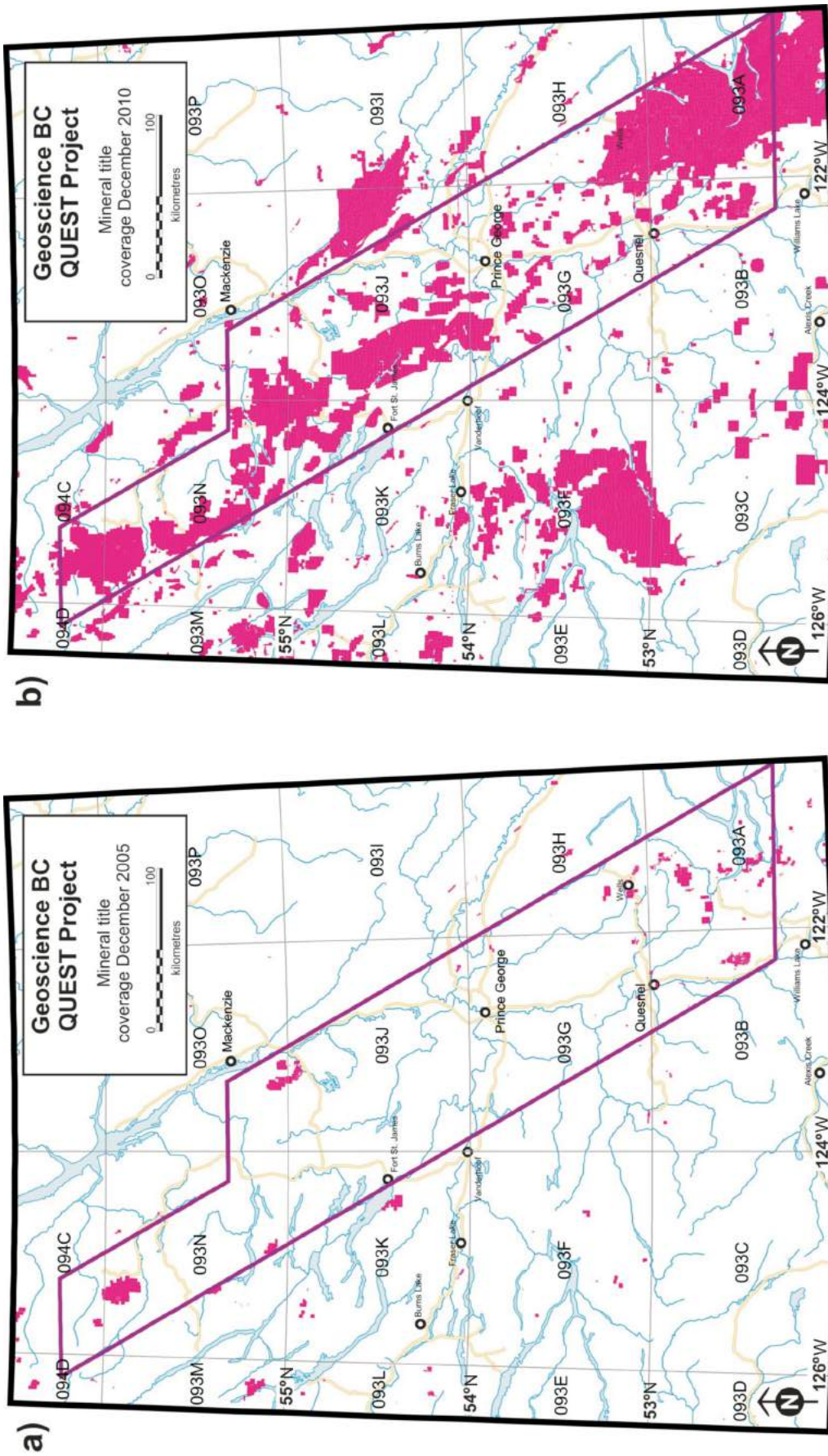


Figure 3. Maps showing the change in mineral title activity from a) 2005 to b) 2010 in the QUEST Project geophysical survey footprint and surrounding area, central British Columbia. Areas shaded in pink represent the coverage of mineral titles.

Summary

The methodology illustrated in this preliminary document will serve as the framework for the comprehensive report to follow, which will offer measures of performance built from a diverse sample of publicly available sources of information and synthesized into a quantifiable and repeatable method for evaluating the effectiveness of any publicly funded exploration initiative. It will bring to light insights into the success of the Geoscience BC QUEST Project model, and serve as a guide to expanded studies of Geoscience BC projects in the future. While this preliminary document is not all inclusive and guidelines and methods are still being considered in order to provide the best achievable product, it is strongly believed the methods have merit and will produce a multiplicity of valuable results and outcomes down the road. The maturity of the QUEST Project with its documented track record and availability of government provided information, press releases and company information makes it an ideal first case.

Acknowledgments

The author would like to thank Geoscience BC for funding this project as well as the BC Geological Survey, particularly A. Wilcox and P. Desjardins for their help in acquiring data. Special note should be given to W. Jackaman and D. Reichheld for their support and assistance in developing this project and editorial comments.

References

- Anglin, C.D. (2008): Foreward; *in* Geoscience BC Summary of Activities 2007, Geoscience BC, Report 2008-1, p. iii–vii, URL <http://www.geosciencebc.com/i/pdf/SummaryofActivities2007/SoA2007-PreliminaryPages_reduced.pdf> [October 2012].
- Barlow, N.D., Flower, K.E., Sweeney, S.B., Robinson, G.L. and Barlow, J.R. (2010): QUEST and QUEST-West Property File: analysis and integration of Property File's Industry File documents with British Columbia's MINFILE (NTS 093; 094A, B, C, D; 103I); *in* Geoscience BC Summary of Activities 2009, Geoscience BC, Report 2010-1, p. 175–188, URL <http://www.geosciencebc.com/i/pdf/SummaryofActivities2009/SoA2009_Barlow.pdf> [October 2012].
- Barnett, C.T. and Williams, P.M. (2009): Using geochemistry and neural networks to map geology under glacial cover; Geoscience BC, Report 2009-3, 27 p., URL <http://www.geosciencebc.com/i/project_data/QUESTdata/GBCReport2009-3/GBC_Report_2009-3.pdf> [October 2012].
- BC Geological Survey (2012a): ARIS assessment report indexing system; BC Ministry of Energy, Mines and Natural Gas, URL <<http://aris.empr.gov.bc.ca>> [October 2012].
- BC Geological Survey (2012b): Mineral Titles Online; BC Ministry of Energy, Mines and Natural Gas, URL <<http://www.empr.gov.bc.ca/Titles/MineralTitles/mto/Pages/default.aspx>> [October 2012].
- BC Geological Survey (2012c): MINFILE BC mineral deposits database; BC Ministry of Energy, Mines and Natural Gas, URL <<http://www.empr.gov.bc.ca/Mining/Geoscience/MINFILE/MINFILEproject/Pages/default.aspx>> [October 2012].
- Fraser, S.J. and Hodgkinson, J.H. (2009): An investigation using SiroSOM for the analysis of QUEST stream-sediment and lake-sediment geochemical data; Geoscience BC, Report 2009-14, 64 p., URL <http://www.geosciencebc.com/i/project_data/GBC_Report2009-14/GBC_Report_2009-14.pdf> [October 2012].
- Geoscience BC (2007): Geoscience BC planning for new regional surveys in central BC; Geoscience BC, press release, May 14, 2007, URL <http://www.geosciencebc.com/s/NewsReleases.asp?ReportID=358200&_Type=News&_Title=Geoscience-BC-Planning-For-New-Regional-Surveys-in-Central-BC> [October 2012].
- Geotech Limited (2008): Report on a helicopter-borne versatile time domain electromagnetic (VTEM) geophysical survey: QUEST Project, central British Columbia (NTS 93A, B, G, H, J, K, N, O & 94C, D); Geoscience BC, Report 2008-4, 35 p., URL <http://www.geosciencebc.com/i/project_data/QUESTdata/report/7042-GeoscienceBC_final.pdf> [October 2012].
- Geotech Limited (2009): Helicopter-borne Z-axis tipper electromagnetic (ZTEM) and aeromagnetic survey, Mt. Milligan test block; Geoscience BC, Report 2009-7, 51 p., URL <http://www.geosciencebc.com/i/project_data/GBC_Report2009-7/2009-7_Report.pdf> [October 2012].
- Jackaman, W. (2008a): QUEST Project sample reanalysis; Geoscience BC, Report 2008-3, 4 p., URL <http://www.geosciencebc.com/i/project_data/QUESTdata/GBCReport2008-3/2008-3_README.pdf> [October 2012].
- Jackaman, W. (2008b): Regional lake sediment and water geochemical data, northern Fraser Basin, central British Columbia (parts of NTS 093G, H, J, K, N & O); Geoscience BC, Report 2008-5, 446 p., URL <http://www.geosciencebc.com/i/project_data/QUESTdata/GBCReport2008-5/2008-5_Survey_Summary.pdf> [October 2012].
- Owsiacki, G. and Payie, G. (2010): MINFILE update of the QUEST project area, central British Columbia (parts of NTS 093A, B, G, H, J, K, N, O, 094C, D); *in* Geoscience BC Summary of Activities 2009, Geoscience BC, Report 2010-1, p. 189–202, URL <http://www.geosciencebc.com/i/pdf/SummaryofActivities2009/SoA2009_Owsiacki.pdf> [October 2012].
- Phillips, N., Nguyen, T.N.H. and Thomson, V. (2009): QUEST Project: 3D inversion modelling, integration, and visualization of airborne gravity, magnetic, and electromagnetic data, BC, Canada; Geoscience BC, Report 2009-15, 79 p., URL <http://www.geosciencebc.com/i/project_data/GBC_Report2009-15/Report/MiraAGIC_GeoscienceBC_QUEST_Geop_Modelling_Report_2009-15.pdf> [October 2012].
- Sander Geophysics Limited (2008): Airborne gravity survey, Quesnellia Region, British Columbia, 2008; Geoscience BC, Report 2008-8, 121 p., URL <http://www.geosciencebc.com/i/project_data/QUESTdata/GBCReport2008-8/Gravity_Technical_Report.pdf> [October 2012].

Creating a Regional Seismograph Network in Northeastern British Columbia to Study the Effect of Induced Seismicity from Unconventional Gas Completions (NTS 094C, G, I, O, P)

C.J. Salas, Geoscience BC, Vancouver, BC, salas@geosciencebc.com

D. Walker, BC Oil and Gas Commission, Victoria, BC

H. Kao, Pacific Geoscience Centre, Geological Survey of Canada, Victoria, BC

Salas, C.J., Walker, D. and Kao, H. (2013): Creating a regional seismograph network in northeastern British Columbia to study the effect of induced seismicity from unconventional gas completions (NTS 094C, G, I, O, P); in Geoscience BC Summary of Activities 2012, Geoscience BC, Report 2013-1, p. 131–134.

Introduction

Recently, geoscientists have applied their knowledge of rock mechanics and geophysics to develop shale gas reserves through multistage, high volume, hydraulic fracturing completions of horizontal wells and monitoring these completions with microseismic geophone arrays. Along with the routine microseismicity created by hydraulic fracturing, 250 low magnitude seismic events were triggered by fluid injection while hydraulic fracturing (fracking) in the Horn River Basin of northeastern British Columbia from April 2009 to December 2011. The BC Oil and Gas Commission (BCOGC) released a report on these events in August 2012, which noted that over 8000 high volume hydraulic fracturing completions have been performed in all of northeastern BC with no associated seismicity (BC Oil and Gas Commission, 2012). None of these events caused any injury, property damage or was found to pose any risk to public safety or the environment.

The BCOGC has recommended augmenting the Canadian National Seismograph Network (CNSN) to better track the effects of completions and induced seismicity. Enhancements to the seismograph network will increase the understanding of induced seismicity and its relationship to oil and gas operations, such as fracking and injection. Natural gas policy makers and regulators, the natural gas industry, communities and First Nations have a common interest in learning more about this issue to support the responsible development of BC's natural gas resources, and improving this seismograph array network is one step in increasing the understanding of this relationship.

A consortium headed by Geoscience BC, along with the Canadian Association of Petroleum Producers (CAPP),

Keywords: *seismicity, unconventional gas, seismograph, fracking, Horn River Basin*

This publication is also available, free of charge, as colour digital files in Adobe Acrobat® PDF format from the Geoscience BC website: <http://www.geosciencebc.com/s/DataReleases.asp>.

BCOGC and Natural Resources Canada (NRCAN), has initiated a project to add six seismograph stations to complement the two pre-existing CNSN stations. The state-of-the-art stations will provide the necessary data needed to further understand the relationship between multistage fracking and induced low magnitude events and ultimately aid in the responsible development of unconventional gas resources.

Background

During the period between April 2009 and December 2011, 38 low level seismic events were recorded by the CNSN's two stations near Hudson's Hope and Fort Nelson (Figure 1). The events ranged in magnitude between 2.2 and 3.8 on the Richter scale. The largest event (May 19, 2011) was felt on the surface although no damage or injuries were reported. The last seven events occurred during the period between December 8 and December 13, 2011. Prior to April 2009, the seismograph network had not detected any seismicity. The seismograph stations can detect events down to approximately 2.4 Richter, hence it was not possible to demonstrate whether smaller level events occurred during this time period. Seismic events in the range of 0.5–2.0 Richter are very common and are termed micro-earthquakes whereas those between 2.0–3.9 Richter are called minor earthquakes (United States Geological Survey, 2012). Those on the lower end of the range (i.e., 2.0 Richter) are rarely felt while those on the upper range (i.e., 3.9 Richter) are often felt but rarely cause damage.

The current CNSN has several technical limitations when used for the study of induced seismicity (BC Oil and Gas Commission, 2012). The first shortcoming is due to the limited station coverage, which results in a 5–10 km uncertainty on the epicentre's location while carrying an even larger uncertainty on the focal depth. Secondly, although the instruments minimum magnitude detection is approximately 2.4 Richter, calibration with an oil and gas industry-operated seismic array found that it had failed to detect 15 events >2.4 Richter during a two-month period. Hence, it is

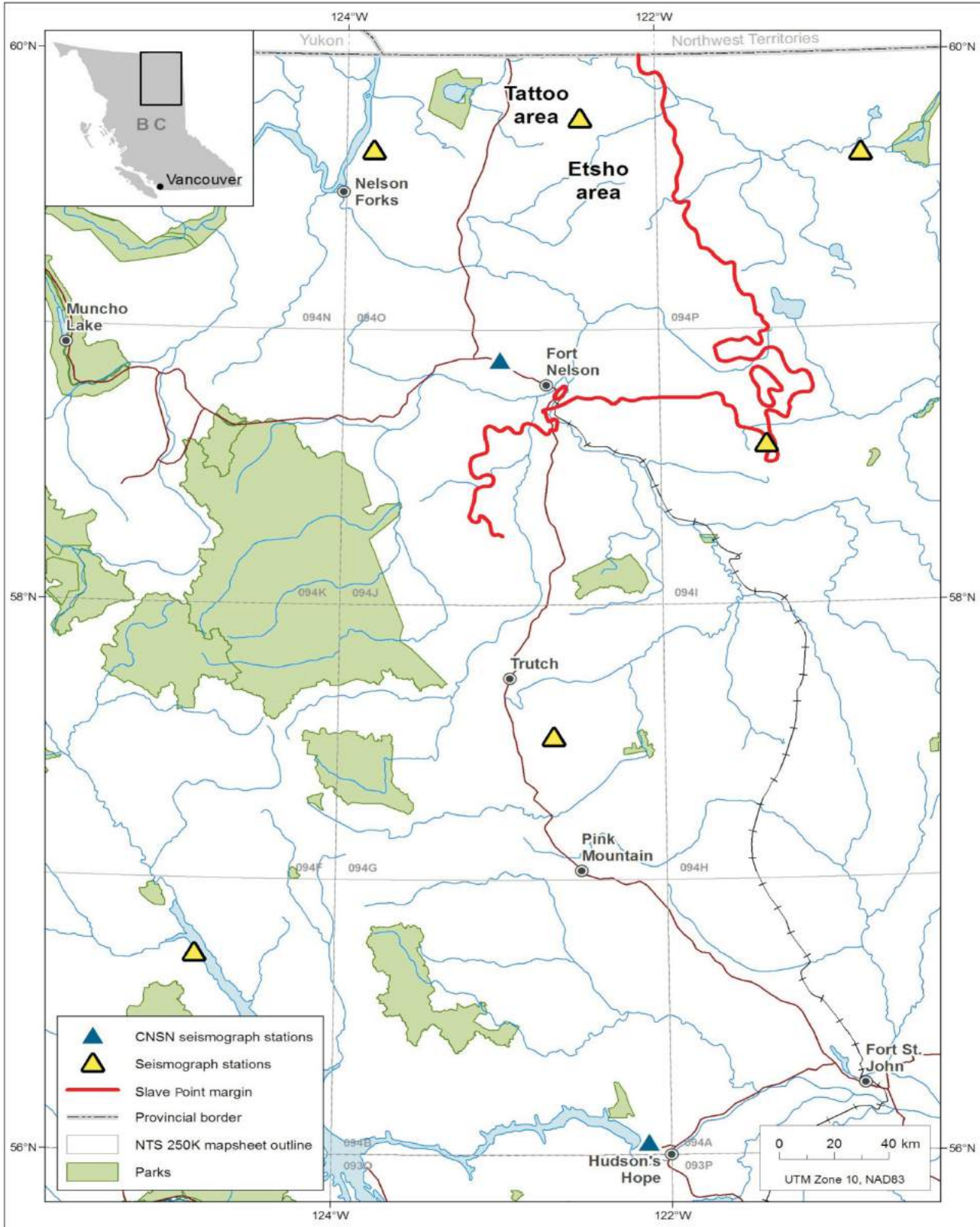


Figure 1. Map of northeastern British Columbia showing the locations of the two current Canadian National Seismograph Network (CNSN) seismograph stations and the site locations for the six Geoscience BC-led consortium seismograph stations.

likely that events in the 2.0–3.0 Richter range have been historically under reported.

Using CNSN's data, along with help from industry, NRCan, the University of BC and the Alberta Geological Survey (AGS), the BCOGC noted the low level seismic events were centred around the Etsho and Tattoo areas of northeastern BC (Figure 1). Additional dense array data provided by operators conducting completion operations captured an additional 212 anomalous seismic events (>2.0 Richter) in the greater Etsho area. The BCOGC's study concluded that these events were synchronous with completion operations and occurred at approximately the same depths as the fracturing stages. Furthermore, it was surmised that the anomalous induced seismicity seen over the period between April 2009 and December 2011 was the result of fault movement due to hydraulic fracturing.

The BCOGC report concluded with seven recommendations:

- 1) improve the accuracy of the CNSN in northeastern BC,
- 2) perform geological and seismic assessments to identify pre-existing faults,
- 3) establish procedures and requirements for induced seismicity monitoring reporting,
- 4) station ground motion sensors near selected northeastern BC communities to quantify the risk from ground motion,
- 5) the Commission will study the deployment of a portable dense seismograph array to selected locations where induced seismicity is anticipated or has occurred,
- 6) require the submission of microseismic reports to monitor hydraulic fracturing for containment of microfracturing and to identify existing faults, and
- 7) study the relationship between hydraulic fracturing parameters and seismicity.

Creation of a Consortium to Study Induced Seismicity in Northeastern BC

In response to the BCOGC's recommendations, a consortium was created between Geoscience BC, CAPP, BCOGC and NRCan to expand the CNSN in northeastern BC. The data collected will be analyzed, interpreted and published on Geoscience BC's website (www.geosciencebc.com). The project is managed by Geoscience BC and jointly funded by Geoscience BC and CAPP, with in-kind technical support provided by BCOGC and NRCan. A technical committee will be appointed by the partners to oversee the technical work. The budget for the research program is \$1.0 million over five years.

Technical Specifications and Interpretive Workflow

Six new seismographs will be installed throughout northeastern BC to augment the coverage of the CNSN (Figure 1). At four of the locations, the seismographs are mounted on screw-piled pads, set to a depth of approximately 10 m, at the site of 5 by 5 m pads, usually using pre-existing well pads. The other two seismographs are mounted directly on bedrock. The chosen seismographs are state-of-the-art Trillium 120PH broadband seismographs. They are solar powered and have very low power consumption. The seismographs will be installed, maintained and operated by Nanometrics Inc.

Once data has been received at the station, it is sent via satellite (a central site VSAT System) to NRCan's Pacific Geoscience Centre in Sidney, BC, where the data are processed by an Apollo server (a seismic-specific software package), which converts it to CNSN-compatible format. The data stream is then redirected to both the AGS and the Geological Survey of Canada where it is processed with data from the CNSN. Routine analysis is not in real time, unless the seismic event is >4.0 Richter, at which time it would be reported in real time. It is expected that there will be a 1–2 day delay between when the data arrives and the posted interpretation of the seismic event. The seismic events will be posted on the Earthquakes Canada (NRCan) website (<http://www.earthquakescanada.nrcan.gc.ca/recent/maps-cartes/index-eng.php>).

The stations are currently being permitted and installation is expected to begin by year-end. It is anticipated that the network will be operational in early 2013.

Acknowledgments

Geoscience BC would like to thank D. Molinski for putting the project together.

References

- BC Oil and Gas Commission (2012): Investigation of observed seismicity in the Horn River Basin; BC Oil and Gas Commission, Technical Report, 29 p., URL <<http://www.bcogc.ca/document.aspx?documentID=1270>> [August 2012].
- United States Geological Survey (2012): Earthquake facts and statistics; United States Geological Survey, URL <<http://earthquake.usgs.gov/earthquakes/eqarchives/year/eqstats.php>> [November 2012].

Developing a Water Monitoring Network in the Horn River Basin, Northeastern British Columbia (Parts of NTS 094I, J, O, P)

C.J. Salas, Geoscience BC, Vancouver, BC, salas@geosciencebc.com

D. Murray, Kerr Wood Leidal Associates Ltd., Victoria, BC

Salas, C.J. and Murray, D. (2013): Developing a water monitoring network in the Horn River Basin, northeastern British Columbia (parts of NTS 094I, J, O, P); in Geoscience BC Summary of Activities 2012, Geoscience BC, Report 2013-1, p. 135–138.

Introduction

As part of the Horn River Basin Aquifer Characterization Project, a three-year water study was initiated in the summer of 2011. The study objectives are to collect accurate water flow, water quality and climatic data for the key watersheds in the Horn River Basin, with the goal of providing the necessary data to support sustainable use of water for shale gas development. The project partners include Geoscience BC, First Nations, the Horn River Basin Producers Group, the BC Oil and Gas Commission, the BC Ministry of Energy, Mines and Natural Gas and the BC Ministry of Environment. The project manager, Kerr Wood Leidal Associates Ltd. (Kerr Wood Leidal), began planning seven hydrometric and three climate stations in the summer of 2011 and installed them in late spring 2012. Additionally, one of the hydrometric sites is being investigated for a program to monitor wetland groundwater. Water quality and benthic invertebrates are also being monitored.

Background

In 2008, Geoscience BC received \$5.7 million in funding from the BC Ministry of Energy, Mines and Natural Gas earmarked for oil and gas geoscience studies in northeastern British Columbia. The Horn River Basin covers an area of 11 000 km² in northeastern BC, much of it covered in muskeg, and spans 42 major watersheds. It also has a mean case estimate of 448 tcf of gas-in-place that is available to be produced (BC Ministry of Energy, Mines and Natural Gas and National Energy Board, 2010), making it one of the richest gas basins in North America. Unconventional gas development in the basin is water-intensive with an average well utilizing upwards of 80 000 m³ of water (Johnson, 2012) in their slickwater completions (i.e., a high volume of water with a low concentration of sand and friction re-

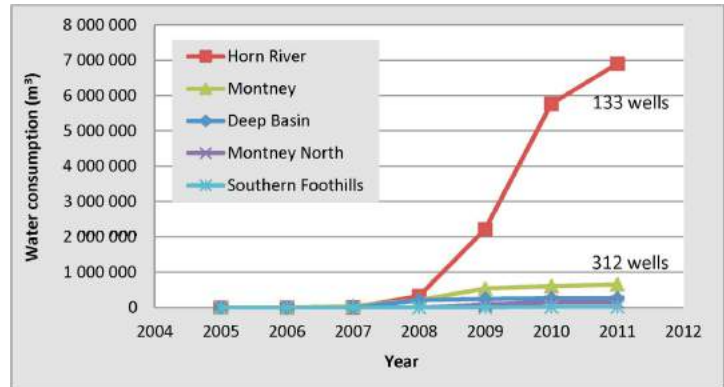


Figure 1. Yearly water utilization for various unconventional plays and areas in British Columbia. Reproduced with permission from Johnson (2012).

ducers). In 2011, a total of 133 wells used 7 million m³ of water from the basin for oil and gas activities (Figure 1).

The Horn River Basin Producers Group recognized the need for a water management plan that would enable sustainable and responsible development of unconventional gas in the Horn River Basin. In late 2008, the Horn River Basin Producers Group and Geoscience BC, with support from the BC Ministry of Energy, Mines and Natural Gas, initiated the Horn River Basin Aquifer Characterization Project, which would aid in responsible development of the gas resource. Phase 1 of the project entailed the study of deep saline aquifers. Geotechnical information gathered from Phase 1 can be used, not only for the identification of saline aquifers suitable for hydraulic fracturing (i.e., fracking), but also for disposal purposes. Phase 1 was managed by Petrel Robertson Consulting Ltd. and was completed by 2011 (Petrel Robertson Consulting Ltd., 2010).

A second phase of the project began soon afterward and comprises three components:

- 1) a pilot project managed by SkyTEM Canada Inc. to examine the applicability of airborne electromagnetic surveys for mapping near-surface groundwater;
- 2) the integration of new well data by Petrel Robertson Consulting Ltd. into the Phase 1 deep saline aquifer mapping project; and

Keywords: hydrometric station, climate station, Horn River Basin, slickwater, fracking, snow pillow

This publication is also available, free of charge, as colour digital files in Adobe Acrobat® PDF format from the Geoscience BC website: <http://www.geosciencebc.com/s/DataReleases.asp>.

- 3) a three-year regional surface-water study managed by Kerr Wood Leidal, which would focus on collecting data with respect to quality and quantity; the Fort Nelson and Acho Dene Koe First Nations would also partner by providing personnel that could be trained as water monitors.

Components 1 and 2 are now complete and final results are available (Petrel Robertson Consulting Ltd., 2012; SkyTEM Canada Inc., 2012). This paper focuses on the ongoing work of developing the water monitoring network.

Development of Water Monitoring Network

The objectives of the water monitoring network are four-fold:

- 1) to collect accurate water flow, water quality and climate data, which will allow the characterization of baseline conditions and provide better accuracy and reliability for water use;
- 2) to train two First Nations representatives in all aspects of water monitoring;
- 3) to aid and support the sustainable planning and use of water in unconventional gas development; and
- 4) to provide the necessary data needed for informed decisions by the Horn River Basin Producers Group and the BC Oil and Gas Commission.

The water monitoring network includes three main components: 1) hydrometric and climate monitoring; 2) water quality and biological monitoring; and 3) data management and reporting. Shallow muskeg groundwater–surface water interaction is also a secondary project component, which is currently being investigated.

Station Site Selection Process

Technical screening for the placement of the hydrometric and climate stations needed to evaluate not only watershed characteristics but also operational and logistical issues. Key aspects of the watershed that were addressed included the geography (mountains, escarpments, etc.), areal extent of the watershed, aspect, median elevation, stream order and percentage of wetland cover. Additional operational issues also taken into account included locations of pre-existing Water Survey of Canada, Environment Canada and BC Forest Service weather stations, or industry-operated hydrometric or climate gauges, First Nations traditional land use areas and the ability to obtain land tenure. The actual physical site selection accounted for logistical issues such as access, orientation and stream channel morphology. Once the draft sites were chosen, the Fort Nelson and Acho Dene Koe First Nations were informed and a review process was initiated. Input on the final site selection was also sought from stakeholders. In all, seven hydrometric stations and three climate stations were optimally located throughout the basin (Figure 2). The hydrometric

stations were operational in time for this season's freshet (April 2012) and the climate stations in June 2012.

Instrumentation

The typical data collection platform has three main components:

- 1) a solar-powered battery and its housing;
- 2) sensors, which gather water level and flow information; and
- 3) a data logger, which captures the information.

Telemetry equipment, which transmits the information via satellite in four of the units, allows for real-time observation of stream water level. This information will ultimately be used to create ratings curves (i.e., stage-discharge relationship) for the hydrometric stations over the three-year length of the project.

The climate stations are solar powered and collect information on temperature, humidity, barometric pressure, precipitation, solar radiation and wind direction and speed. The climate stations are outfitted with snow pillows, which allow the measurement of snowpack and/or snow water equivalent.

Biological Monitoring

The biological monitoring program captures baseline information on the ecosystem's health, the hydrology of the basin and climate. The end result will be a dataset that will allow industry, First Nations and communities to responsibly use the water resources.

Hydrological baseline information from the basin is made up of quantity and quality components. The quantity component is captured via the hydrometric stations, as discussed in the previous section, while water quality monitoring is accomplished through grab samples at the hydrometric sites, following BC Provincial Resource Information Standards Committee Hydrometric Standards quality assurance–quality control procedures and BC Water Quality Sample Guidelines. This program is being co-ordinated alongside Environment Canada to help increase baseline coverage. Two First Nations personnel have been trained as part of the water monitoring team that will perform water quality sampling and biological monitoring.

In order to assess the linkages between shallow groundwater, the wetland and local surface waters, one hydrometric station location is being selected as a possible muskeg (wetland) shallow groundwater monitoring site. Surficial geological mapping and reports by the Geological Survey of Canada, BC Ministry of Energy, Mines and Natural Gas (Levson et al., 2005; D. Huntley and A. Hickin, pers. comm., 2012) and Ducks Unlimited are being used to assess the merit of each site. The end result will be a better understanding of surface-groundwater interaction in the

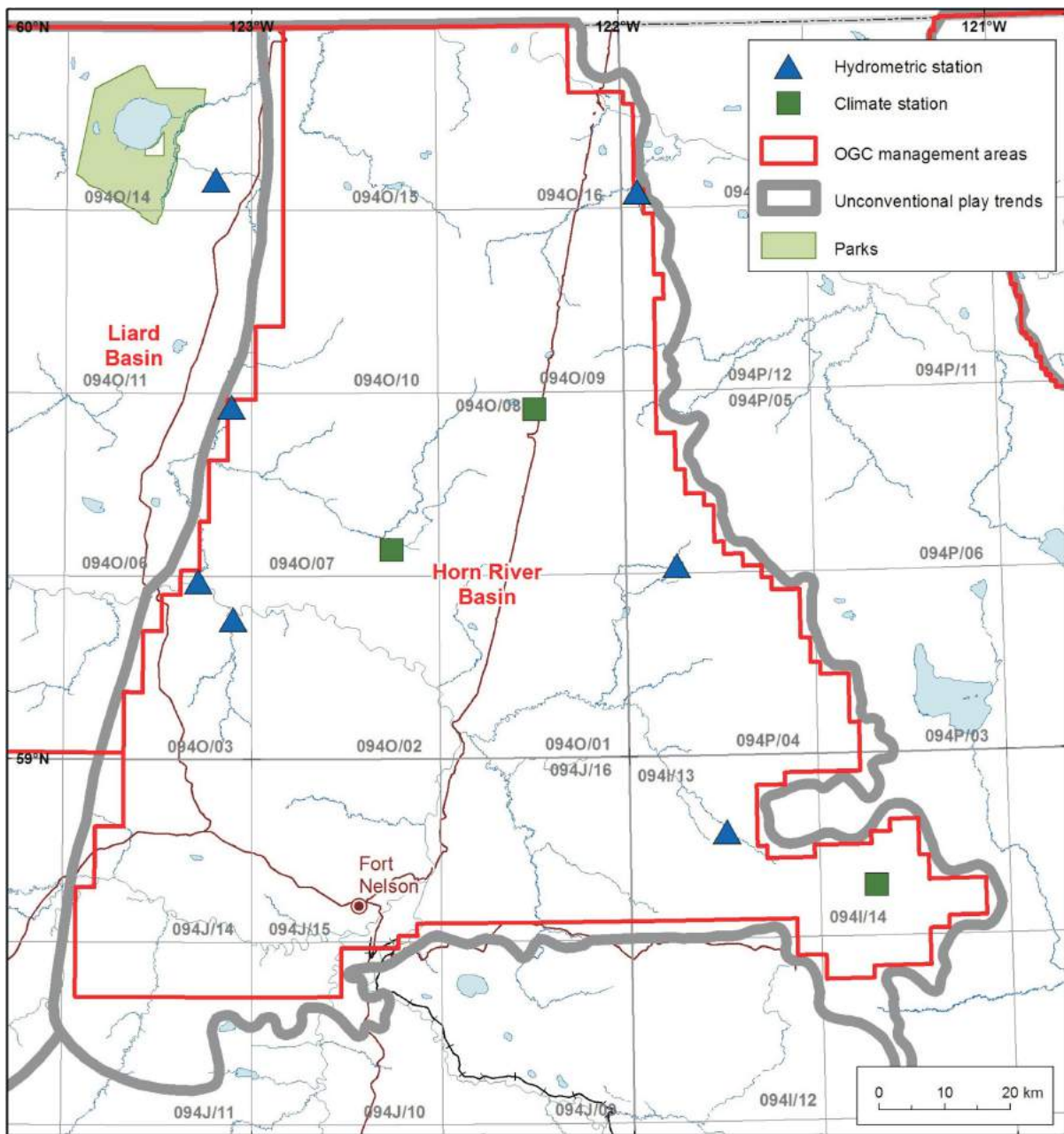


Figure 2. Location of Geoscience BC hydrometric and climate stations, Horn River Basin, northeastern British Columbia. Abbreviation: OGC, BC Oil and Gas Commission.

Horn River Basin, a critical piece of the puzzle when trying to devise responsible water management practices.

The biological monitoring of benthic invertebrates allows an assessment of the ecosystem’s health. It involves the comparison of benthic fauna at a reference site, which has minimal human activity, to a test site, where human impact is suspected. Reference sites are established in areas that are primarily undisturbed. Test sites are then established and samples taken are compared statistically to the reference site to determine cumulative impacts. The collection of this data has begun to provide a baseline for biological monitoring in the basin.

Continuing Work

The installation of the seven hydrometric and three climate stations will allow monitoring of environmental conditions for the three-year span of the project. The data gathered will not only allow a better definition of baseline water quality and quantity it will also provide valuable information necessary for the development of hydrological ratings curves, better understanding of surface water–groundwater interaction, and a more accurate determination of runoff, which can ultimately guide responsible resource development in the region.

References

- BC Ministry of Energy, Mines and Natural Gas and National Energy Board (2010): Ultimate potential for unconventional natural gas in northeastern British Columbia's Horn River Basin; BC Ministry of Energy, Mines and Natural Gas, Oil and Gas Reports 2011-1, 50 p, URL <http://www.empr.gov.bc.ca/OG/Documents/HornRiverEMA_2.pdf> [November 2012].
- Johnson, E. (2012): Water issues associated with hydraulic fracturing in northeast British Columbia; Unconventional Gas Technical Forum 2012, Victoria, April 3, 2012, presentation, 25 p., URL <<http://www.empr.gov.bc.ca/OG/oilandgas/petroleumgeology/UnconventionalGas/Documents/E%20Johnson.pdf>> [November 2012].
- Levson, V.M., Ferbey, T., Hickin, A., Bednarski, J., Smith, R., Demchuk, T., Trommelen, M., Kerr, B. and Chrush, A. (2005): Surficial geology and aggregate studies in the boreal plains of northeast British Columbia; *in* Summary of Activities 2005, BC Ministry of Energy, Mines and Natural Gas, p. 42–50, URL <http://www.empr.gov.bc.ca/OG/oilandgas/aggregates/Documents/Levson_et_al.pdf> [November 2012].
- Petrel Robertson Consulting Ltd. (2010): Horn River Basin Aquifer Characterization Project, geological report; Geoscience BC, Report 2010-11, 199 p., URL <http://geosciencebc.com/i/project_data/GBC_Report2010-11/HRB_Aquifer_Project_Report.pdf> [November 2012].
- Petrel Robertson Consulting Ltd. (2012): Horn River Basin Aquifer Characterization Project, phase 2: geological report; Geoscience BC, Report 2012-09, URL <<http://www.geosciencebc.com/s/Report2012-09.asp>> [November 2012].
- SkyTEM Canada Inc. (2012): Results from a pilot airborne electromagnetic survey, Horn River Basin, British Columbia; Geoscience BC, Report 2012-04, URL <<http://www.geosciencebc.com/s/Report2012-04.asp>> [November 2012].

Investigation of Land-Use Change and Groundwater–Surface Water Interaction in the Kiskatinaw River Watershed, Northeastern British Columbia (Parts of NTS 093P/01, /02, /07–/10)

G.C. Saha, Environmental Science and Engineering Program, University of Northern British Columbia, Prince George, BC

S.S. Paul, Environmental Science and Engineering Program, University of Northern British Columbia, Prince George, BC

J. Li, Environmental Science and Engineering Program, University of Northern British Columbia, Prince George, BC, li@unbc.ca

F. Hirshfield, Environmental Science and Engineering Program, University of Northern British Columbia, Prince George, BC

J. Sui, Environmental Science and Engineering Program, University of Northern British Columbia, Prince George, BC

Saha, G.C., Paul, S.S., Li, J., Hirshfield, F. and Sui, J. (2013): Investigation of land-use change and groundwater–surface water interaction in the Kiskatinaw River watershed, northeastern British Columbia (parts of NTS 093P/01, /02, /07–/10); in Geoscience BC Summary of Activities 2012, Geoscience BC, Report 2013-1, p. 139–148.

Introduction

The Kiskatinaw River watershed (KRW) comprises an environmentally critical riparian region that plays an essential role in the ecosystem of northern British Columbia. The Kiskatinaw River provides the water supply to the City of Dawson Creek, the Village of Pouce Coupe and thousands of rural residents of the Peace River Regional District. As a result, effective water-resources management within the KRW is of critical importance. However, water-resources management can be affected by a number of factors, such as the patterns of land-use change and the groundwater–surface water interaction.

On one hand, the major land-use practices in the KRW include agriculture, timber harvesting, wildlife and cattle grazing, oil-and-gas exploration, mineral-resources extraction and recreational parks (Dobson Engineering Ltd. and Urban Systems, 2003). As a world-class unconventional natural-gas reservoir, the Montney Shale gas play in the KRW is moving into the development-drilling stage. This shale-gas exploration, along with other human activities (e.g., removal of trees affected by mountain pine beetles, increasing agricultural activities) have resulted in a significant change in land-use practices. The changes of land use and land cover within the watershed may then change the

hydrological patterns and pose serious challenges for the community and many other water users.

On the other hand, groundwater and surface water are closely linked components in a hydrological system, and they can be frequently exchanged. During flooding season, surface water can recharge groundwater and raise the groundwater table; however, during drought season, groundwater is an important source of water to feed the river flow. Consequently, there is a pressing need to understand the pattern of land-use change and the groundwater–surface water interaction within KRW so that informed decisions can be made for effective water-resources management.

Remote sensing is a viable means of extracting land-use and land-cover data, and hence provides effective inventory and monitoring of land-use change (Ridd and Liu, 1998; Mas, 1999). The basic principle of using remote sensing in detection of land-use change is that the change in land cover causes change in radiance value of the object (Mas, 1999), which can then be captured by the comparison of temporally varied satellite images. In remote sensing, one of the widely used approaches for assessment of land-use change is digital-image classification, where pixels in satellite images are designated with real-world land cover-type information (Matinfar et al., 2007).

The conventional per-pixel–based image classification applies supervised or unsupervised statistical techniques by taking the spectral imagery information into account but ignoring the textural and contextual imagery information (Benz et al., 2004; Matinfar et al., 2007). The supervised

Keywords: *land-use change, groundwater–surface water interaction, Kiskatinaw River watershed*

This publication is also available, free of charge, as colour digital files in Adobe Acrobat® PDF format from the Geoscience BC website: <http://www.geosciencebc.com/s/DataReleases.asp>.

classification technique requires analyst-specified training data to classify image pixels and then group them into various land-use types, whereas the unsupervised technique is capable of classifying imagery without any prespecified training data.

In terms of groundwater–surface water interaction, different numerical methods have been applied by many researchers. For example, Hester and Doyle (2008) used several models (HEC-RAS, MODFLOW and MODPATH) to simulate coupled surface and subsurface hydraulics in a gaining stream (i.e., groundwater levels at both banks are higher than surface-water level in the stream). Hollander et al. (2009) applied a range of models (Catflow, CMF, Coup-Model, Hill-Vi, HYDRUS-2D, NetThales, SUMULAT, SWAT, TOPmodel and WaSiM-ETH) to assess groundwater–surface water interactions. van Roosmalen et al. (2009) used a DK model (i.e., the National Water Resource model for Denmark), based on the MIKE-SHE code (Refsgaard and Storm, 1995), to investigate groundwater–surface water interaction under changing climatic and land-use conditions. In addition to numerical models, various hydrograph separation methods have been used to quantify groundwater–surface water interaction. For example, Eckhardt (2005) developed a low-pass filtering technique on the hydrograph in order to separate base flow. Schilling (2009) used HYSEP, an automated base-flow separation method developed by Sloto and Crouse (1996), and the PART program, a United States Geological Survey (USGS) base-flow separation method (Rutledge, 1998), to quantify groundwater recharge. Gonzales et al. (2009) used a simple graphical approach to determine the end of direct runoff contribution, where the hydrograph was plotted on a semi-logarithmic scale and the groundwater recession curve was identified as a straight line.

Since very few studies have been conducted within the KRW to investigate land-use change and groundwater–surface water interaction, the objective of this study is to fill that gap. Land-use change within the KRW from 1984 to 2010 was captured using a remote-sensing technique, and the PART program was applied to separate groundwater contribution from stream-flow records within the basin. The groundwater contribution to stream flow was quantified on a monthly time scale for a five-year period from 2007 to 2011. The gridded surface–subsurface hydrological analysis (GSSHA; Downer, 2002) was also used to determine groundwater-flow direction in the KRW.

Study Area

The Kiskatinaw River watershed (KRW) is located in northeastern BC (Figure 1). The river has its source in the foothills of the Rocky Mountains, near Tumbler Ridge, and flows approximately 200 km north before joining the Peace River at the BC-Alberta border (Forest Practices Board,

2010). The watershed is a rain-dominated hydrological system, with peak flow occurring from late June to early July. It receives an average precipitation of 499 mm during the year, comprising 320 mm of rain and 179 mm of snow. The average annual flow rate is 10 m³/s, but it drops to 0.052 m³/s in January (Dobson Engineering Ltd. and Urban Systems, 2003). The significant variation in river flow is a challenging issue facing water-resources management within the KRW. In fact, water demand in the City of Dawson Creek has increased at an average rate of about 3.2% per year. As shown in Figure 1, the water-intake station for the city is located in Arras, and the KRW study area was divided into five major sub-basins, including Mainstem (433 km²), Brassey (208 km²), Halfmoon-Oetata (194 km²), East Kiskatinaw (996 km²) and West Kiskatinaw (1005 km²). The surficial geology map of the KRW (Figure 2) was digitized from Reimchen (1980). The major surficial deposits in the KRW are morainal deposits.

Methods

Detection of Land-Use Change

In this study, the advanced object-oriented classification technique was employed for capturing land-use change in the KRW, since its basic processing unit is image objects or segments containing several pixels instead of a single pixel. This technique has proven to be a better image-classifica-

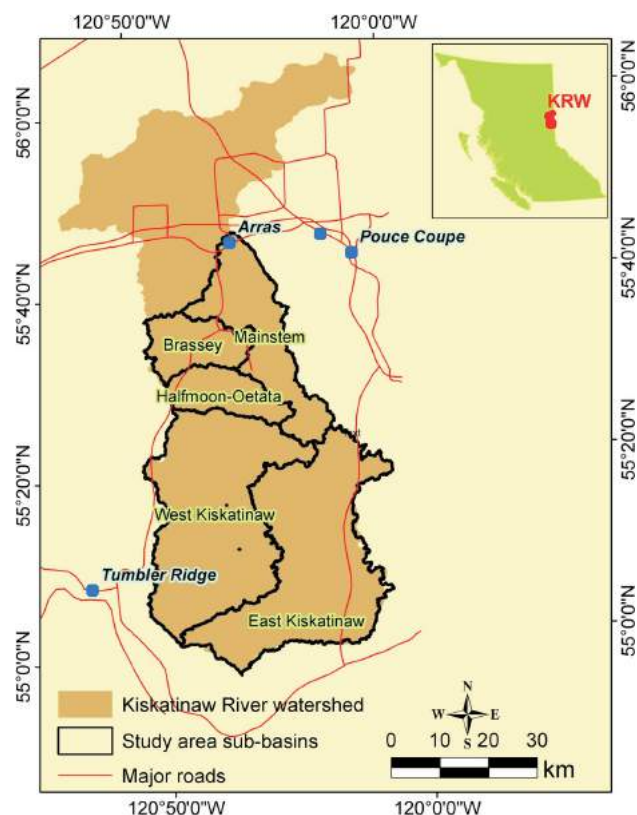


Figure 1. Major sub-basins in the Kiskatinaw River watershed study area. Communities are indicated by blue dots.

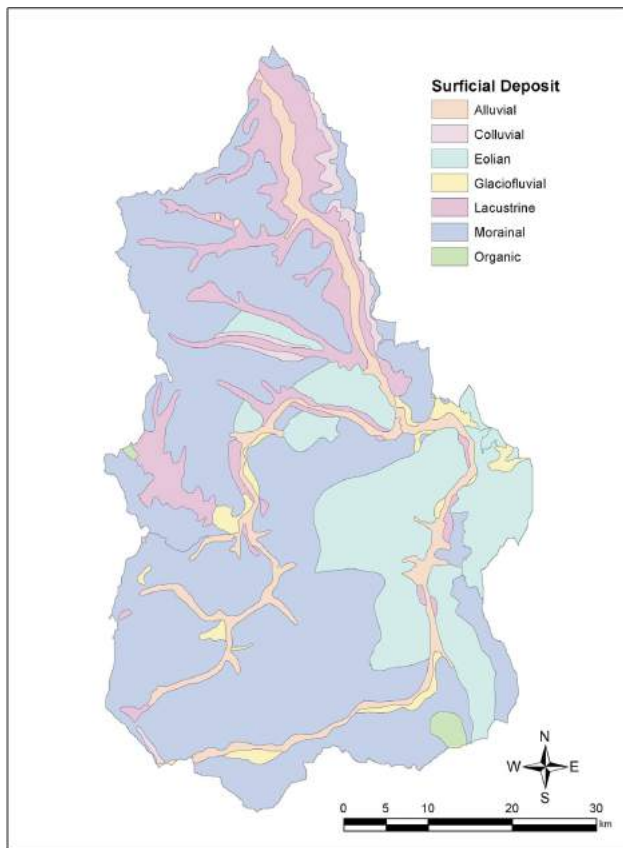


Figure 2. Surficial geology of the Kiskatinaw River watershed (after Reimchen, 1980).

tion method for detecting land-use change due to its meaningful statistics and textural calculation, and the close relation between real-world objects and image objects (Dorren et al., 2003; Matinfar et al., 2007). Landsat satellite imagery from 1984, 1999 and 2010 was used to map the land-use change. All of the imagery was downloaded from the USGS GloVis server. Table 1 lists the data description. After necessary preprocessing, including layer-stacking, georectification and mosaicing subsetting, the images were independently classified using an object-oriented algorithm to extract land-use feature classes. The IDRISI-selva software was used for the object-oriented classification, and PCI Geomatica, ArcGIS and Quantum GIS were used in different phases of the analysis.

The detailed procedure of image analysis can be summarized as follows:

1) Step 1: After downloading the appropriate satellite imagery, a single imagery file containing all the bands for each Landsat scene was prepared using the ‘transfer’ and ‘translate’ tools of PCI Geomatica. The two images were then mosaiced and the mosaiced image was cropped to the boundary of the KRW study area with the subsetting tool in PCI.

- 2) Step 2:** Digital classification was carried out using the IDRISI-selva tools. The first task was to generate the training class, using ground-truth field data, previous maps, higher resolution satellite imagery and airphotos, to enable the segment classifier to process the imagery. The next task was image segmentation followed by digital classification of the segments using the maximum likelihood algorithm to produce the object-oriented image classification.
- 3) Step 3:** An accuracy assessment of the segment classification output was carried out using the ‘accuracy assessment’ module in the IDRISI-selva software, which required a new set of ground-truth field data. Some tiny features consisting of only one or two pixels can be easily confused with other feature types in digital-image classification. The classified imagery was therefore manually edited using various GIS tools to ensure that such features were properly classified. The result was a complete land-use map of the study area for each of the three years.
- 4) Step 4:** Comparative analysis of the land-use maps for 1984, 1999 and 2010 generated statistics on land-use change and enabled prediction of future land-use change scenarios based on the present trend of change.

Investigation of Groundwater–Surface Water Interaction

In order to examine the interaction between groundwater and surface water, a groundwater-monitoring network was established in September 2010 by installing twenty-two piezometers equipped with Odyssey data loggers at eight sites in the KRW (Figure 3). At each site, a bank piezometer was installed on both right and left banks of the stream in addition to the in-stream piezometer. The piezometers, measuring 1.9 cm by 3.0 m (0.75 in. by 10 ft.) with 44 holes at one end along with a welded drive tip, were inserted at various depths, depending on site conditions, using hand auger, slide hammer and high-reach iron auger (Figure 4). In addition, three piezometers in the One Island Lake area and one piezometer in the Mainstem sub-basin of the KRW (Figure 1) equipped with data loggers were installed in the summer of 2011. Each Odyssey™ data logger (Dataflow Systems Pty. Ltd.) was calibrated using a three-point calibration method before being inserted in the piezometer and was set to record the groundwater level at 20 minute intervals. The surface-water levels and discharge at each study

Table 1. Description of satellite imagery used in the mapping of land-use change.

Remotely sensed data	Year	Spectral resolution	Spatial resolution
Landsat 4 5 TM	1984, 2010	Multispectral (Bands 1 5 and 7)	30 m
Landsat 7 ETM+	1999	Multispectral (Bands 1 5 and 7)	30 m

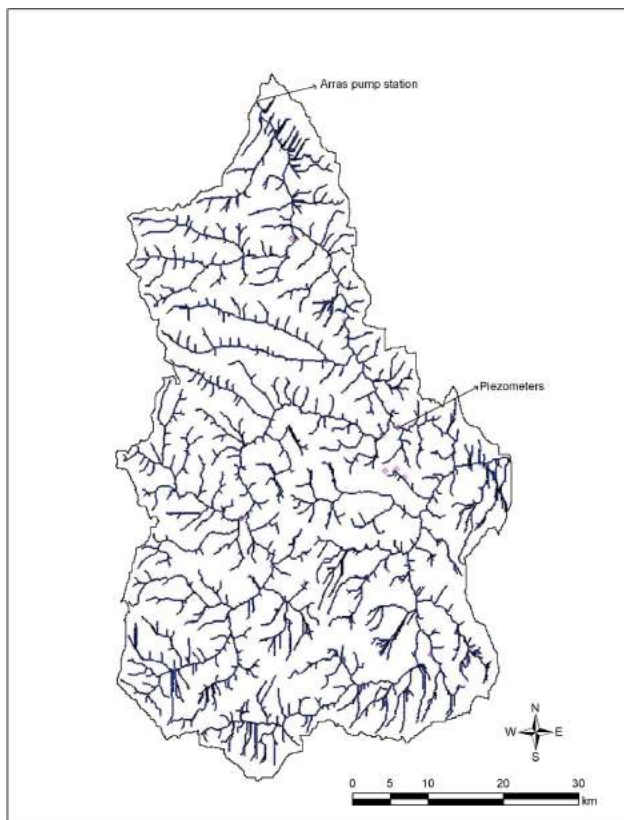


Figure 3. Study sites (red circles) with piezometers installed in the Kiskatinaw River watershed.

site were measured using staff gauges along with Odyssey capacitance data loggers and Sontek's FlowTracker® Acoustic Doppler Velocimeter. The cross-sections were completed in accordance with the British Columbia Hydro-metric Standards (BC Ministry of Environment, 2009).

Results

Land-Use Change in the Kiskatinaw River Watershed

The land-use maps for 1984 and 2010 (Figure 5a, b) include the following feature classes:

- **Cropland** – all cultivated agricultural land
- **Coniferous forest** – forested land dominated by trees that remain green throughout the year
- **Deciduous forest** – forested land dominated by trees that lose their leaves at the end of the frost-free season
- **Mixed forest** – forested land in which neither coniferous nor deciduous type dominates over the other
- **Planted or regrowth forest** – small plants of both coniferous and deciduous types that have regrown or been planted after forest fire, clear cutting or any other decay event; this class may also include some herb-shrubs, as they are hard to differentiate during digital-image classification using imagery of 30 m resolution;

- **Forest-fire lands** – only the 2010 land-use map has a forest-fire feature class, since a fire event occurred in the KRW in 2006
- **Cut block** – forest cut-block areas that have been cleared for timber or any other purpose; this class includes most of the gas development infrastructure, such as drilling pads
- **Pasture lands** – grassland kept for feeding livestock and also used for agriculture
- **Water** – water channels and lakes, but most of the rivers and creeks could not be captured by imagery of 30 m resolution
- **Wetland** – marshes and swamps (both nonforested and slightly forested) where the water table is at, near or above the ground surface for a significant part of the year
- **Built-up area** – land covered by human-built structures (e.g., houses, businesses, roads and industrial infrastructure); structures less than 30 m in width or length could not be included in the land-use maps because of the 30 m maximum spatial resolution of the imagery

From the land-use maps shown in Figure 5, the overall change may not be very conspicuous for the entire watershed, but changes for a particular land-use type within particular sub-watersheds are significant. Figure 6a presents



Figure 4. Stages of piezometer installation in the Mainstem sub-basin, Kiskatinaw River watershed.

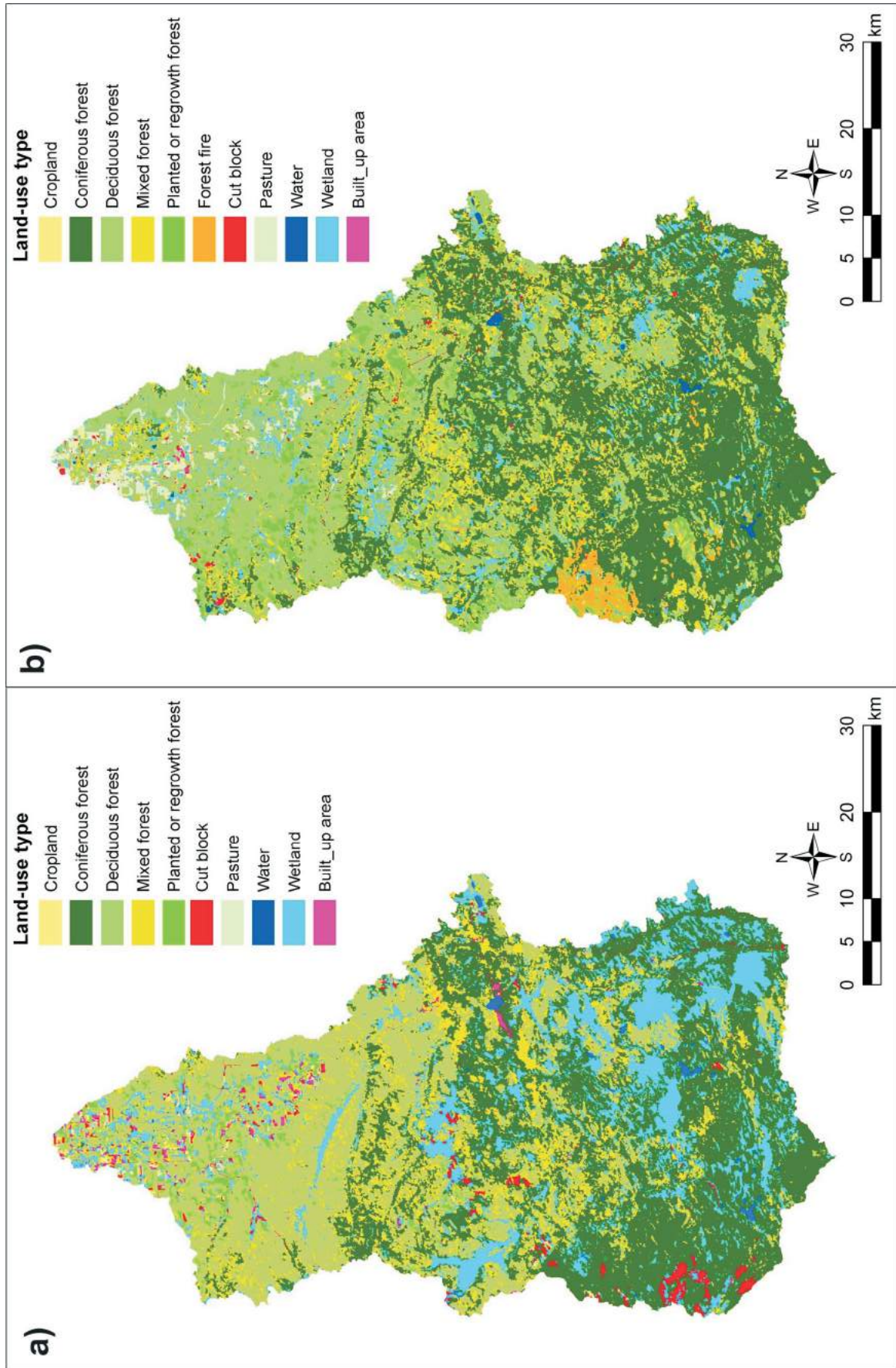


Figure 5. Land-use maps of the Kiskatinaw River watershed in **a)** 1984, and **b)** 2010.

the total area gained and lost for each land-use (LU) type between 1984 and 2010. In this figure, the area lost for a particular feature class was gained by other classes. For example, the substantial area of lost wetland (372 km²) between 1984 and 2010 might have been added to other forest-type features. The change in the area of forest type is more or less consistent, although a higher gain of 144 km² in the area of planted/regrowth forest has been noted. The significant gain (48 km²) in the area of forest fire refers to the ‘Hourglass Forest Fire’ in the KRW in 2006, which caused significant loss of forest stand in this watershed. The higher loss (21 km²) than gain (4 km²) in built-up area between 1984 and 2010 may be problematic and requires a review of the classification process. The probable cause of this is the low image quality in 1984 due to cloud cover over the study area, which caused uncertainty during the classification process. Figure 6b presents the net change for each land-use feature class between 1984 and 2010, with negative change in area indicating higher loss and positive change indicating higher gain of the land-use feature.

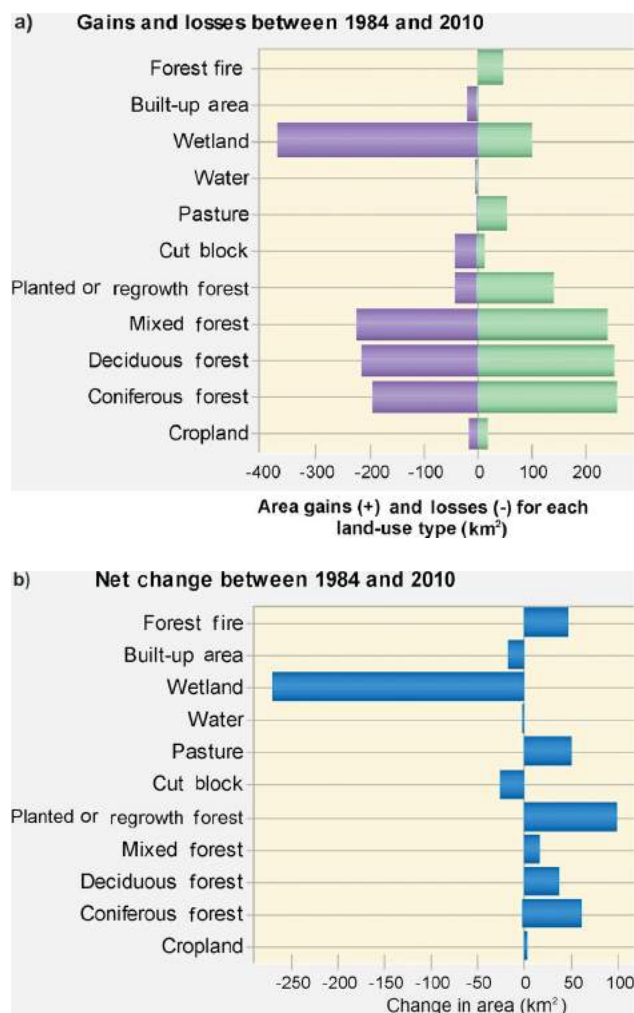


Figure 6. Land-use change between 1984 and 2010 in the Kiskatinaw River watershed: **(a)** total gains and losses for each land-use type, **(b)** net change in area for each land-use type.

Direction of Regional Groundwater Flow

The direction of regional groundwater flow in the KRW was determined using GSSHA software (Downer, 2002) and based on observed groundwater-level data collected from the groundwater-monitoring network. As can be seen in Figure 7, the groundwater-flow pattern in the KRW is a through-flow system (i.e., groundwater passing through the stream network).

Groundwater Contribution to Stream Flow

The PART base-flow separation program of the USGS was used in this study to quantify groundwater contribution to surface water. This program estimates daily base flow by considering it to be equal to stream flow on days that fit a requirement of antecedent recession, and then linearly interpolating it for other days in the record (Rutledge, 1998). Groundwater (base-flow) contribution to stream flow in the KRW was examined for the period January 2007 to December 2011 (Figure 8). It can be seen that groundwater contributes significantly to the stream flow and that this contribution varies with time. The monthly mean stream flow in the KRW is shown in Figure 9. Comparing Figures 8 and 9 shows that the annual base-flow index (i.e., annual groundwater contribution to river flow) increases when the annual mean stream flow decreases, and vice versa. Table 2 lists

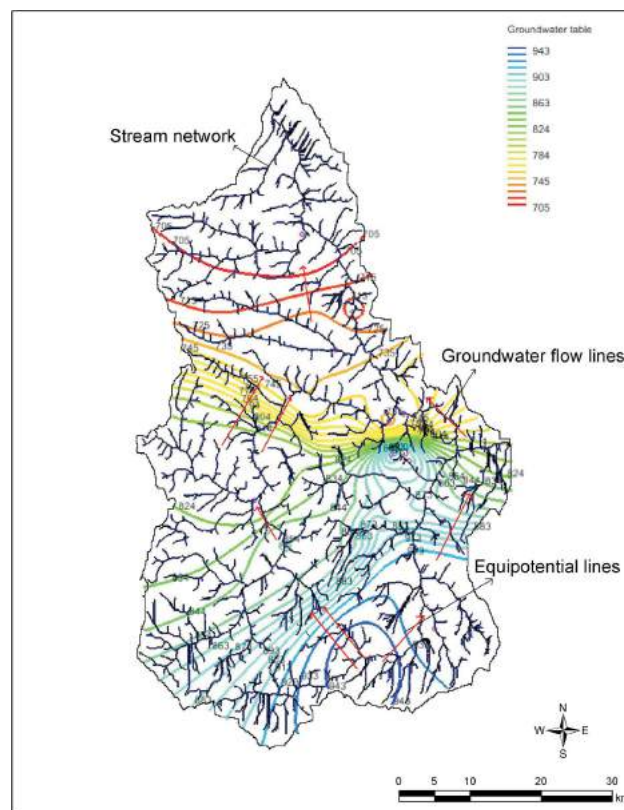


Figure 7. Groundwater table (m) in the Kiskatinaw River watershed.

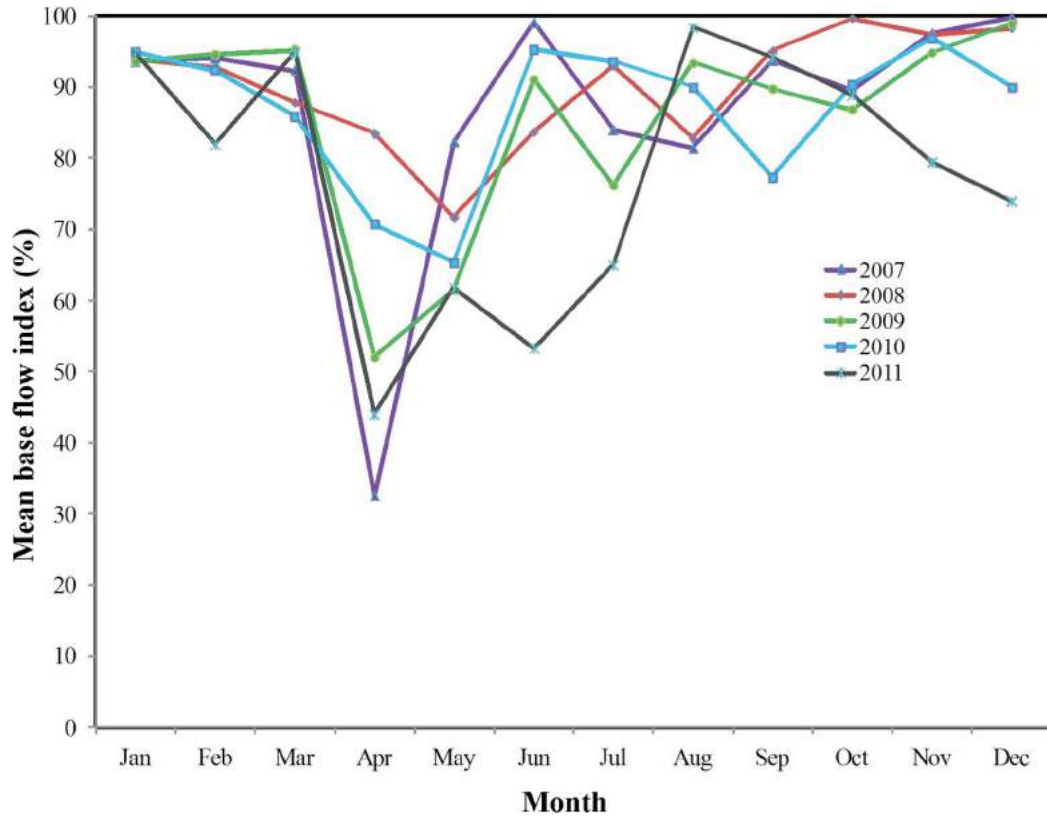


Figure 8. Base-flow index (groundwater contribution to river) in the Kiskatinaw River watershed.

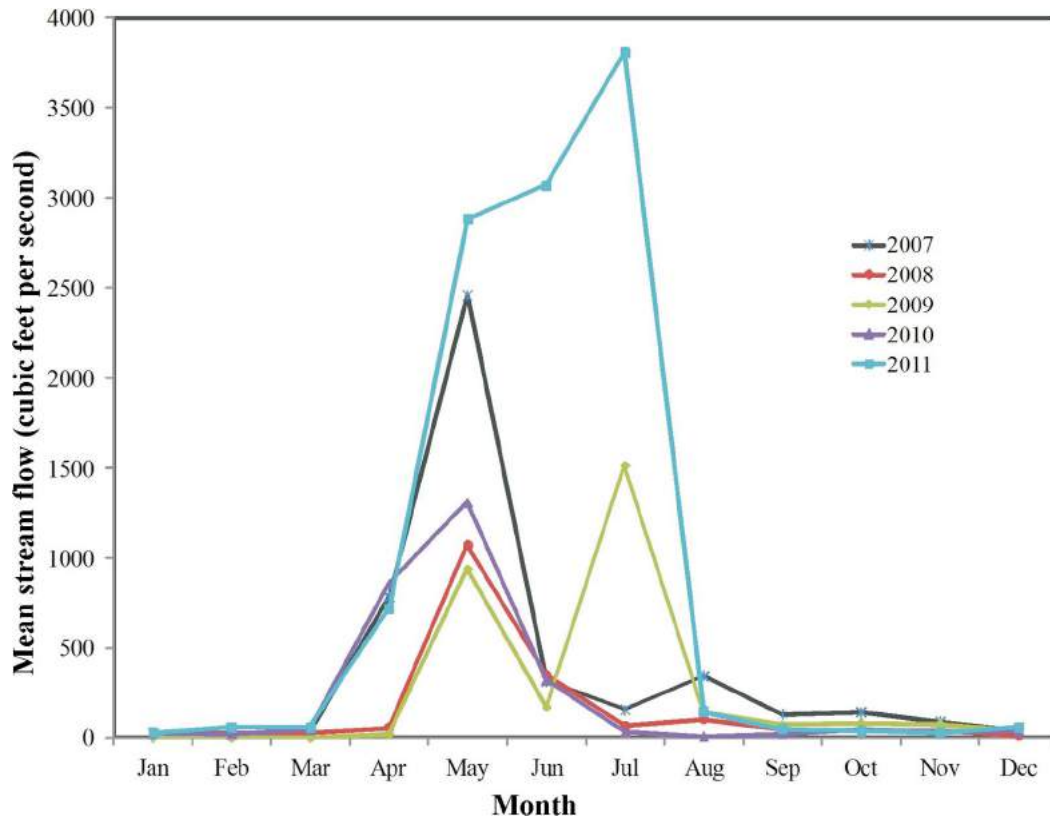


Figure 9. Monthly mean stream flow over time in the Kiskatinaw River watershed.

Table 2. Mean stream flow, mean base flow and base-flow index in the Kiskatinaw River watershed.

Year	Mean stream flow (cfs)	Mean base flow (cfs)	Base-flow Index (%)
2007	378.16	276.53	73.12
2008	156.09	117.27	75.13
2009	256.31	181.42	70.78
2010	230.01	163.1	70.91
2011	912.09	524.48	57.5

Abbreviation: cfs, cubic feet per second

the base-flow index in the KRW, with the highest index (75.13%) observed in the dry year (2008).

Conclusion

Land-use maps were generated by satellite-image analysis using remote-sensing and GIS tools to capture the land-use change dynamics within the Kiskatinaw River watershed (KRW). The gain and loss of 11 land-use features between 1984 and 2010 were quantified, and a significant land-use change was found for a number of features in the KRW. The digital-image classification has proven to be an effective method for land-use mapping, but some manual GIS editing was required to generate a more complete map because the Landsat imagery at 30 m spatial resolution was incapable of capturing features smaller than 30 m. Thus, a major part of the rivers and creeks, as well as the roads, could not be captured during the mapping effort.

The groundwater flow in the KRW was determined to be a through-flow system. Based on hydrograph separation results obtained using PART program, it was found that groundwater contributed a major part of the river flow in the KRW during the dry season and snowfall events. This contribution decreased during spring runoff and wet season, when surface runoff contributed a major part of the river flow. The annual base-flow index of the KRW increases when the annual mean stream flow decreases, and vice versa. Future work involves the development of a numerical model using gridded surface-subsurface hydrological analysis to quantify the combined impacts of land-use/land-cover and climate changes on groundwater-surface water interaction in the riparian zone of the KRW.

Acknowledgments

The authors gratefully acknowledge the funding support provided by Geoscience BC, Peace River Regional District, the City of Dawson Creek, EnCana Corporation and BP Canada Energy Co. The authors thank P. Caputa, C. van Geloven, R. Whiten and M. Maurer for their help with fieldwork and data collection. They are grateful to B. Chen at Memorial University of Newfoundland for reviewing this manuscript.

References

- BC Ministry of Environment (2009): Manual of British Columbia Hydrometric Standards; BC Ministry of Environment, v. 1, URL <[http://www.env.gov.bc.ca/fia/documents/Manual of British Columbia Hydrometric Standards V1.0, March 12, 2009.pdf](http://www.env.gov.bc.ca/fia/documents/Manual_of_British_Columbia_Hydrometric_Standards_V1.0_March_12_2009.pdf)> [November 21, 2012].
- Benz, U.C., Hofmann, P., Willhauck, G., Lingenfelder, I. and Heynen, M. (2004): Multi-resolution, object-oriented fuzzy analysis of remote sensing data for GIS-ready information; ISPRS Journal of Photogrammetry and Remote Sensing, v. 58, p. 239–258.
- Dobson Engineering Ltd. and Urban Systems Ltd. (2003): Kiskatinaw River Watershed Management Plan; unpublished report prepared for City of Dawson Creek, File 0714.0046.01, URL <<http://www.dawsoncreek.ca/cityhall/departments/water/watershed/background-watershed-management-plans/>> [November 21, 2012].
- Dorren, L.K., Maier, B. and Seijmonsbergen, A.C. (2003): Improved Landsat-based forest mapping in steep mountainous terrain using object-based classification; Forest Ecology and Management, v. 183, p. 31–46.
- Downer, C.W. (2002): Identification and modeling of important stream flow producing processes in watersheds; Ph.D. thesis, University of Connecticut, Storrs-Mansfield, Connecticut, 239 p.
- Eckhardt, K. (2005): How to construct recursive digital filters for base flow separation; Hydrological Processes, v. 19, p. 507–515.
- Forest Practices Board (2010): Audit of forestry, oil and gas and range activities in the Kiskatinaw river watershed; Forest Practices Board, URL <http://www.fpb.gov.bc.ca/ARC_121_Audit_of_Forestry_Oil_and_Gas_and_Range_Activities_in_the_Kiskatinaw_Watershed.htm> [November 21, 2012].
- Gonzales, A.L., Nonner, J., Heijckers, J. and Uhlenbrook, S. (2009): Comparison of different base flow separation methods in a lowland catchment; Hydrology and Earth System Sciences, v. 13, p. 2055–2068.
- Hester, E.T. and Doyle, M.W. (2008): In-stream geomorphic structures as drivers of hyporheic exchange; Water Resources Research, v. 44, W03417. doi:10.1029/2006WR005810
- Hollander, H.M., Blume, T., Bormann, H., Buytaert, W., Chirico, G.B., Exbrayat, J.F., Gustafsson, D., Holzel, H., Kraft, P., Stamm, C., Stoll, S., Bloschl, G. and Fluhler, H. (2009): Comparative predictions of discharge from an artificial catchment (Chicken Creek) using sparse data; Hydrology and Earth System Sciences, v. 13, p. 2069–2094.
- Mas, J.F. (1999): Monitoring land-cover changes: a comparison of change detection techniques; International Journal of Remote Sensing, v. 20, p. 139–152.
- Matinfar, H.R., Sarmadian, F., Panah, S.K.A. and Heck, R.J. (2007): Comparisons of object-oriented and pixel-based classification of land use/land cover types based on Landsat7, ETM+ spectral bands (case study: arid region of Iran); American-Eurasian Journal of Agriculture and Environmental Science, v. 2, p. 448–456.
- Refsgaard, J.C. and Storm, B. (1995): MIKE SHE; in Computer Models of Watershed Hydrology, V.P. Singh (ed.), Water Resources Publication, Highlands Ranch, Colorado, p. 809–846.

- Reimchen, T.H.F. (1980): Surficial geology, Dawson Creek, British Columbia; Geological Survey of Canada, Map 1467A, scale 1:250 000, URL <ftp://ftp2.cits.rncan.gc.ca/pub/geott/ess_pubs/120/120060/gscmap-a_1467a_e_1980_mn01.pdf> [November 21, 2012]. doi:10.4095/120060
- Ridd, K.M. and Liu, J. (1998): A comparison of four algorithms for change detection in urban environment; *Remote Sensing of Environment*, v. 63, p. 95–100.
- Rutledge, A.T. (1998): Computer programs for describing the recession of ground-water discharge and for estimating mean ground-water recharge and discharge from streamflow data—update; United States Geological Survey, Water-Resources Investigations Report 98-4148, 43 p.
- Schilling, K.E. (2009): Investigating local variation in groundwater recharge along a topographic gradient, Walnut Creek, Iowa, USA; *Hydrogeology Journal*, v. 17, no. 2, p. 397–407.
- Sloto, R.A. and Crouse, M.Y. (1996): HYSEP: a computer program for streamflow hydrograph separation and analysis; United States Geological Survey, Water-Resources Investigations Report 96-4040, 46 p.
- van Roosmalen, L., Sonnenborg, T.O. and Jensen, K.H. (2009): Impact of climate and land use change on the hydrology of a large-scale agricultural catchment; *Water Resources Research*, v. 45, W00A15. doi:10.1029/2007WR006760



Geoscience BC is an independent, not for profit society that works to attract mineral and oil and gas investment to British Columbia through collection and marketing of geoscience data.

Suite 440 – 890 West Pender Street
Vancouver BC V6C 1J9

info@geosciencebc.com
www.geosciencebc.com

Geoscience BC is funded through grants from the Provincial Government of British Columbia